Monographs on Statistics and Applied Probability 114

Introduction to Time Series Modeling

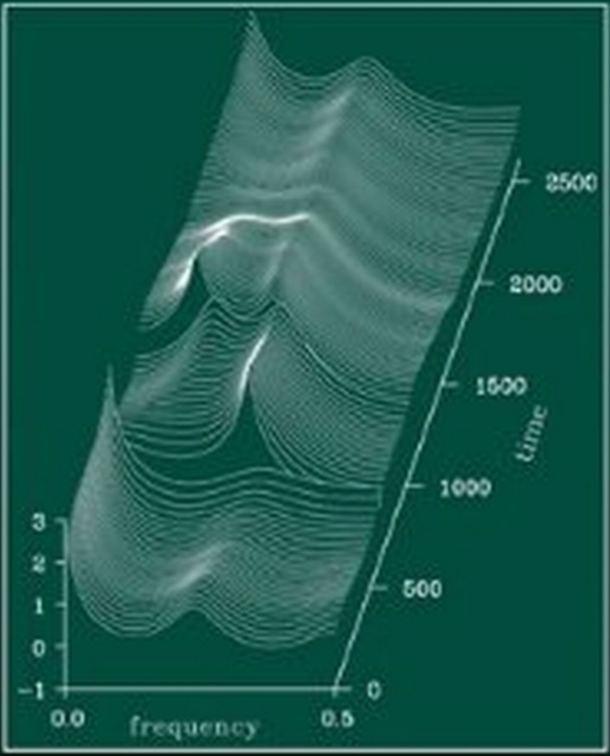

Genshiro Kitagawa

CRC Press
Taylor & Francis Group
A CHAPMAN & HALL BOOK

Introduction to Time Series Modeling

MONOGRAPHS ON STATISTICS AND APPLIED PROBABILITY

1 Stochastic Population Models in Ecology and Epidemiology *M.S. Barlett* (1960)
2 Queues *D.R. Cox and W.L. Smith* (1961)
3 Monte Carlo Methods *J.M. Hammersley and D.C. Handscomb* (1964)
4 The Statistical Analysis of Series of Events *D.R. Cox and P.A.W. Lewis* (1966)
5 Population Genetics *W.J. Ewens* (1969)
6 Probability, Statistics and Time *M.S. Barlett* (1975)
7 Statistical Inference *S.D. Silvey* (1975)
8 The Analysis of Contingency Tables *B.S. Everitt* (1977)
9 Multivariate Analysis in Behavioural Research *A.E. Maxwell* (1977)
10 Stochastic Abundance Models *S. Engen* (1978)
11 Some Basic Theory for Statistical Inference *E.J.G. Pitman* (1979)
12 Point Processes *D.R. Cox and V. Isham* (1980)
13 Identification of Outliers *D.M. Hawkins* (1980)
14 Optimal Design *S.D. Silvey* (1980)
15 Finite Mixture Distributions *B.S. Everitt and D.J. Hand* (1981)
16 Classification *A.D. Gordon* (1981)
17 Distribution-Free Statistical Methods, 2nd edition *J.S. Maritz* (1995)
18 Residuals and Influence in Regression *R.D. Cook and S. Weisberg* (1982)
19 Applications of Queueing Theory, 2nd edition *G.F. Newell* (1982)
20 Risk Theory, 3rd edition *R.E. Beard, T. Pentikäinen and E. Pesonen* (1984)
21 Analysis of Survival Data *D.R. Cox and D. Oakes* (1984)
22 An Introduction to Latent Variable Models *B.S. Everitt* (1984)
23 Bandit Problems *D.A. Berry and B. Fristedt* (1985)
24 Stochastic Modelling and Control *M.H.A. Davis and R. Vinter* (1985)
25 The Statistical Analysis of Composition Data *J. Aitchison* (1986)
26 Density Estimation for Statistics and Data Analysis *B.W. Silverman* (1986)
27 Regression Analysis with Applications *G.B. Wetherill* (1986)
28 Sequential Methods in Statistics, 3rd edition
G.B. Wetherill and K.D. Glazebrook (1986)
29 Tensor Methods in Statistics *P. McCullagh* (1987)
30 Transformation and Weighting in Regression
R.J. Carroll and D. Ruppert (1988)
31 Asymptotic Techniques for Use in Statistics
O.E. Bandorff-Nielsen and D.R. Cox (1989)
32 Analysis of Binary Data, 2nd edition *D.R. Cox and E.J. Snell* (1989)
33 Analysis of Infectious Disease Data *N.G. Becker* (1989)
34 Design and Analysis of Cross-Over Trials *B. Jones and M.G. Kenward* (1989)
35 Empirical Bayes Methods, 2nd edition *J.S. Maritz and T. Lwin* (1989)
36 Symmetric Multivariate and Related Distributions
K.T. Fang, S. Kotz and K.W. Ng (1990)
37 Generalized Linear Models, 2nd edition *P. McCullagh and J.A. Nelder* (1989)
38 Cyclic and Computer Generated Designs, 2nd edition
J.A. John and E.R. Williams (1995)
39 Analog Estimation Methods in Econometrics *C.F. Manski* (1988)
40 Subset Selection in Regression *A.J. Miller* (1990)
41 Analysis of Repeated Measures *M.J. Crowder and D.J. Hand* (1990)
42 Statistical Reasoning with Imprecise Probabilities *P. Walley* (1991)
43 Generalized Additive Models *T.J. Hastie and R.J. Tibshirani* (1990)

44 Inspection Errors for Attributes in Quality Control
N.L. Johnson, S. Kotz and X. Wu (1991)

45 The Analysis of Contingency Tables, 2nd edition *B.S. Everitt* (1992)

46 The Analysis of Quantal Response Data *B.J.T. Morgan* (1992)

47 Longitudinal Data with Serial Correlation—A State-Space Approach
R.H. Jones (1993)

48 Differential Geometry and Statistics *M.K. Murray and J.W. Rice* (1993)

49 Markov Models and Optimization *M.H.A. Davis* (1993)

50 Networks and Chaos—Statistical and Probabilistic Aspects
O.E. Barndorff-Nielsen, J.L. Jensen and W.S. Kendall (1993)

51 Number-Theoretic Methods in Statistics *K.-T. Fang and Y. Wang* (1994)

52 Inference and Asymptotics *O.E. Barndorff-Nielsen and D.R. Cox* (1994)

53 Practical Risk Theory for Actuaries
C.D. Daykin, T. Pentikäinen and M. Pesonen (1994)

54 Biplots *J.C. Gower and D.J. Hand* (1996)

55 Predictive Inference—An Introduction *S. Geisser* (1993)

56 Model-Free Curve Estimation *M.E. Tarter and M.D. Lock* (1993)

57 An Introduction to the Bootstrap *B. Efron and R.J. Tibshirani* (1993)

58 Nonparametric Regression and Generalized Linear Models
P.J. Green and B.W. Silverman (1994)

59 Multidimensional Scaling *T.F. Cox and M.A.A. Cox* (1994)

60 Kernel Smoothing *M.P. Wand and M.C. Jones* (1995)

61 Statistics for Long Memory Processes *J. Beran* (1995)

62 Nonlinear Models for Repeated Measurement Data
M. Davidian and D.M. Giltinan (1995)

63 Measurement Error in Nonlinear Models
R.J. Carroll, D. Rupert and L.A. Stefanski (1995)

64 Analyzing and Modeling Rank Data *J.J. Marden* (1995)

65 Time Series Models—In Econometrics, Finance and Other Fields
D.R. Cox, D.V. Hinkley and O.E. Barndorff-Nielsen (1996)

66 Local Polynomial Modeling and its Applications *J. Fan and I. Gijbels* (1996)

67 Multivariate Dependencies—Models, Analysis and Interpretation
D.R. Cox and N. Wermuth (1996)

68 Statistical Inference—Based on the Likelihood *A. Azzalini* (1996)

69 Bayes and Empirical Bayes Methods for Data Analysis
B.P. Carlin and T.A Louis (1996)

70 Hidden Markov and Other Models for Discrete-Valued Time Series
I.L. MacDonald and W. Zucchini (1997)

71 Statistical Evidence—A Likelihood Paradigm *R. Royall* (1997)

72 Analysis of Incomplete Multivariate Data *J.L. Schafer* (1997)

73 Multivariate Models and Dependence Concepts *H. Joe* (1997)

74 Theory of Sample Surveys *M.E. Thompson* (1997)

75 Retrial Queues *G. Falin and J.G.C. Templeton* (1997)

76 Theory of Dispersion Models *B. Jørgensen* (1997)

77 Mixed Poisson Processes *J. Grandell* (1997)

78 Variance Components Estimation—Mixed Models, Methodologies and Applications *P.S.R.S. Rao* (1997)

79 Bayesian Methods for Finite Population Sampling
G. Meeden and M. Ghosh (1997)

80 Stochastic Geometry—Likelihood and computation
O.E. Barndorff-Nielsen, W.S. Kendall and M.N.M. van Lieshout (1998)

81 Computer-Assisted Analysis of Mixtures and Applications—
Meta-analysis, Disease Mapping and Others *D. Böhning* (1999)

82 Classification, 2nd edition *A.D. Gordon* (1999)

83 Semimartingales and their Statistical Inference *B.L.S. Prakasa Rao* (1999)

84 Statistical Aspects of BSE and vCJD—Models for Epidemics
C.A. Donnelly and N.M. Ferguson (1999)

85 Set-Indexed Martingales *G. Ivanoff and E. Merzbach* (2000)

86 The Theory of the Design of Experiments *D.R. Cox and N. Reid* (2000)

87 Complex Stochastic Systems
O.E. Barndorff-Nielsen, D.R. Cox and C. Klüppelberg (2001)

88 Multidimensional Scaling, 2nd edition *T.F. Cox and M.A.A. Cox* (2001)

89 Algebraic Statistics—Computational Commutative Algebra in Statistics
G. Pistone, E. Riccomagno and H.P. Wynn (2001)

90 Analysis of Time Series Structure—SSA and Related Techniques
N. Golyandina, V. Nekrutkin and A.A. Zhigljavsky (2001)

91 Subjective Probability Models for Lifetimes
Fabio Spizzichino (2001)

92 Empirical Likelihood *Art B. Owen* (2001)

93 Statistics in the 21st Century
Adrian E. Raftery, Martin A. Tanner, and Martin T. Wells (2001)

94 Accelerated Life Models: Modeling and Statistical Analysis
Vilijandas Bagdonavicius and Mikhail Nikulin (2001)

95 Subset Selection in Regression, Second Edition *Alan Miller* (2002)

96 Topics in Modelling of Clustered Data
Marc Aerts, Helena Geys, Geert Molenberghs, and Louise M. Ryan (2002)

97 Components of Variance *D.R. Cox and P.J. Solomon* (2002)

98 Design and Analysis of Cross-Over Trials, 2nd Edition
Byron Jones and Michael G. Kenward (2003)

99 Extreme Values in Finance, Telecommunications, and the Environment
Bärbel Finkenstädt and Holger Rootzén (2003)

100 Statistical Inference and Simulation for Spatial Point Processes
Jesper Møller and Rasmus Plenge Waagepetersen (2004)

101 Hierarchical Modeling and Analysis for Spatial Data
Sudipto Banerjee, Bradley P. Carlin, and Alan E. Gelfand (2004)

102 Diagnostic Checks in Time Series *Wai Keung Li* (2004)

103 Stereology for Statisticians *Adrian Baddeley and Eva B. Vedel Jensen* (2004)

104 Gaussian Markov Random Fields: Theory and Applications
Håvard Rue and Leonhard Held (2005)

105 Measurement Error in Nonlinear Models: A Modern Perspective, Second Edition
Raymond J. Carroll, David Ruppert, Leonard A. Stefanski,
and Ciprian M. Crainiceanu (2006)

106 Generalized Linear Models with Random Effects: Unified Analysis via H-likelihood
Youngjo Lee, John A. Nelder, and Yudi Pawitan (2006)

107 Statistical Methods for Spatio-Temporal Systems
Bärbel Finkenstädt, Leonhard Held, and Valerie Isham (2007)

108 Nonlinear Time Series: Semiparametric and Nonparametric Methods
Jiti Gao (2007)

109 Missing Data in Longitudinal Studies: Strategies for Bayesian Modeling and Sensitivity Analysis
Michael J. Daniels and Joseph W. Hogan (2008)

110 Hidden Markov Models for Time Series: An Introduction Using R
Walter Zucchini and Iain L. MacDonald (2009)

111 ROC Curves for Continuous Data
Wojtek J. Krzanowski and David J. Hand (2009)

112 Antedependence Models for Longitudinal Data
Dale L. Zimmerman and Vicente A. Núñez-Antón (2009)

113 Mixed Effects Models for Complex Data
Lang Wu (2010)

114 Intoduction to Time Series Modeling
Genshiro Kitagawa (2010)

Monographs on Statistics and Applied Probability 114

Introduction to Time Series Modeling

Genshiro Kitagawa
Institute of Statistical Mathematics
Tokyo, Japan

CRC Press
Taylor & Francis Group
Boca Raton London New York

CRC Press is an imprint of the
Taylor & Francis Group, an **informa** business
A CHAPMAN & HALL BOOK

Chapman & Hall/CRC
Taylor & Francis Group
6000 Broken Sound Parkway NW, Suite 300
Boca Raton, FL 33487-2742

Printed in the United States of America on acid-free paper
10 9 8 7 6 5 4 3 2 1

International Standard Book Number: 978-1-58488-921-2 (Hardback)

This book contains information obtained from authentic and highly regarded sources. Reasonable efforts have been made to publish reliable data and information, but the author and publisher cannot assume responsibility for the validity of all materials or the consequences of their use. The authors and publishers have attempted to trace the copyright holders of all material reproduced in this publication and apologize to copyright holders if permission to publish in this form has not been obtained. If any copyright material has not been acknowledged please write and let us know so we may rectify in any future reprint.

Trademark Notice: Product or corporate names may be trademarks or registered trademarks, and are used only for identification and explanation without intent to infringe.

Visit the Taylor & Francis Web site at
http://www.taylorandfrancis.com

and the CRC Press Web site at
http://www.crcpress.com

To Hiro Akaike and Will Gersch

Preface

Because of rapid development of ICT (Information and Communication Technologies) and progress of globalization, the current societies have linked together in a complex manner at various levels, and there arose various difficult problems in economy, environment, health, safety, etc. Therefore, the elucidation, prediction, and control of such dynamic complex systems are very important subjects. On the other hand, in the statistical science, as a result of the development of the information criterion AIC, various methods of statistical modeling, in particular Bayes modeling, have been developed. Further, with the advent of massive large-scale database and fast parallel processors, many statistical models were developed and became in practical use.

This book aims at introducing and explaining basic methods of building models for time series. In time series modeling, we try to express the behavior of a certain phenomenon in relation to the past values of itself and other covariates. Since many important phenomena in statistical analysis are actually time series and the identification of conditional distribution of the phenomenon is an essential part of the statistical modeling, it is very important and useful to learn basic methods of time series modeling. In this book, many time series models and various tools for handling them are introduced.

The main feature of this book is to use the state space model as a generic tool for time series modeling. Three types of recursive filtering and smoothing methods, the Kalman filter, the non-Gaussian filter, and the sequential Monte Carlo filter, are presented as convenient tools for the state space models. Further, in this book, a unified approach to model evaluation is introduced based on the entropy maximization principle advocated by Dr. Akaike. Based on this unified approach, various methods of parameter estimation, such as the least squares method, the maximum likelihood method, the recursive estimation for the state space models, and the model selection by the information criterion AIC, are derived. After introducing standard stationary time series models, such as AR model and ARMA model, we present various nonstationary time series models, such as the locally stationary AR model, the trend model, the seasonal adjustment model, and the time-varying coefficient AR model and nonlinear non-Gaussian models. The simulation methods are also shown. The principal aim of the author will be achieved when readers succeed in building models for their own real-world problems.

This book is basically the translation of the book published in Japanese in 2005 from Iwanami Publishing Company. The first version was published in 1993 as a volume in Iwanami Computer Science Series. I would like to thank the Iwanami Publishing Company, in particular Mr. U. Yoshida, for allowing me to translate and publish in English.

I would like to acknowledge the many people who contributed to this book through collaborative research with the author. In particular, I would like to acknowledge with sincere thanks to Hirotugu Akaike and Will Gersch, from whom I have learned so many ideas and basis of time series modeling. Some of the models and estimation methods are developed during the process of cooperative research with Kohei Ohtsu, Tetsuo Takanami, and Norio Matsumoto. They also provided me with some of the data used in this book. I have greatly influenced through discussions with S. Konishi, D. F. Findley, H. Tong, K. Tanabe, Y. Sakamoto, M. Ishiguro, Y. Ogata, Y. Tamura, T. Higuchi, Y. Kawasaki, and S. Sato.

I am grateful to Prof. Subba Rao and two anonymous reviewers for their comments and suggestions that improved the original manuscript. I am also thankful to M. Oda for her help in preparing the manuscript of the English version. David Grubbs patiently encouraged and supported me throughout the preparation of this book. I express my sincere thanks to all of these people.

Genshiro Kitagawa

Tokyo, September 2009

List of Figures

List of Tables

Contents

Chapter 1

Introduction and Preparatory Analysis

In this chapter, various aspects of the classification of time series and the objectives of time series modeling considered in this book are discussed. There are various types of time series, and it is very important to find out the characteristics of a time series by carefully looking at graphs of the data before proceeding to the modeling and analysis phase. In the second half of the chapter, we shall consider various ways of pre-processing time series that will be applied before proceeding to time series modeling. Finally, the organization of the book is described.

1.1 Time Series Data

A record of phenomenon irregularly varying with time is called *time series*. As examples of time series, we may consider meteorological data such as atmospheric pressure, temperature, rainfall and the records of seismic waves; economic data such as stock prices and exchange rates; medical data such as electroencephalogram and electrocardiograms, and records of controlling cars, ships and aircraft.

As a first step in the analysis of a time series, it is important to carefully examine graphs of the data. These suggest various possibilities for the next step in the analysis, together with appropriate strategies for statistical modeling.

Figure 1.1 shows several typical time series that will be analyzed in subsequent chapters as numerical examples. The followings are the features of the time series depicted in Figures 1.1 (a)–(i).

Plot (a) shows a time series of the *yaw rate* of a ship under navigation in the Pacific Ocean, observed every second. The yaw rate fluctuates around 0 degrees per second, because the ship is under the control of course keeping system (offered by Prof. K. Ohtsu of Tokyo University of Marine Science and Technology).

Plot (b) shows a series of annual *sunspot number* (Wolfer sunspot number). Similar patterns of increase and decrease have been observed over a cycle approximately ten years in length.

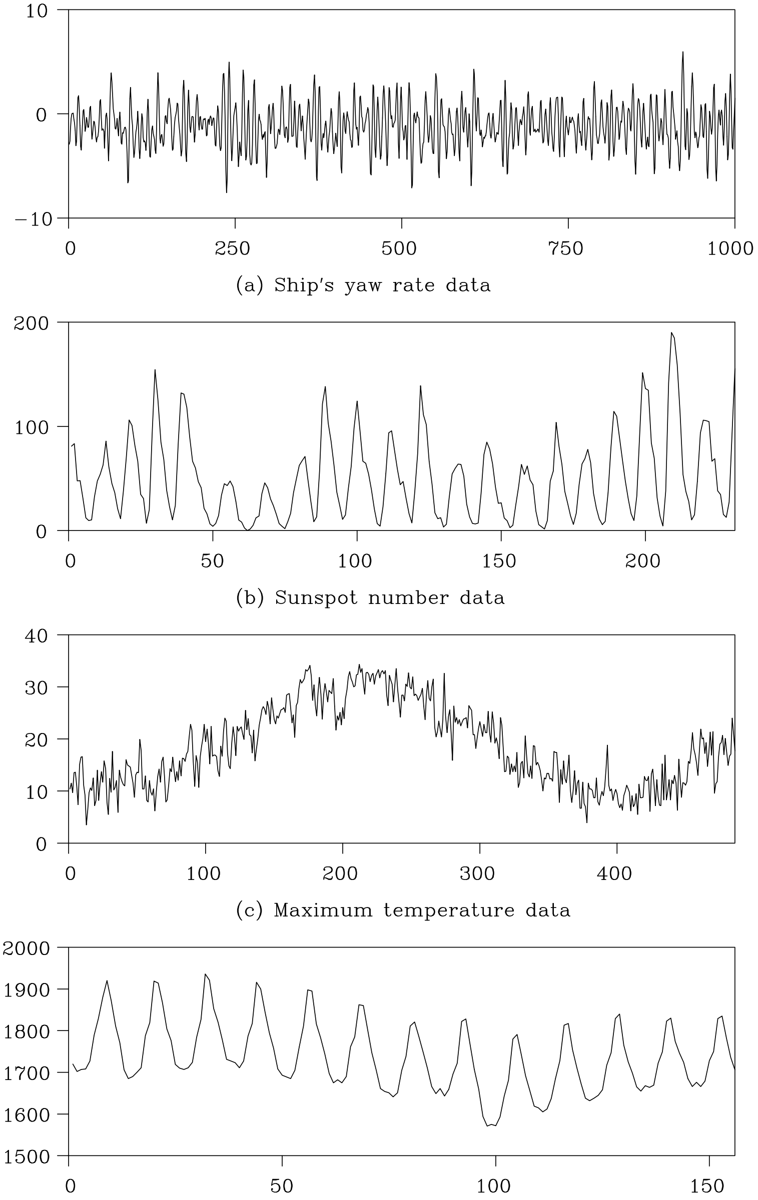

(a) Ship's yaw rate data

(b) Sunspot number data

(c) Maximum temperature data

(d) BLSALLFOOD data

Figure 1.1: *Examples of various time series.*

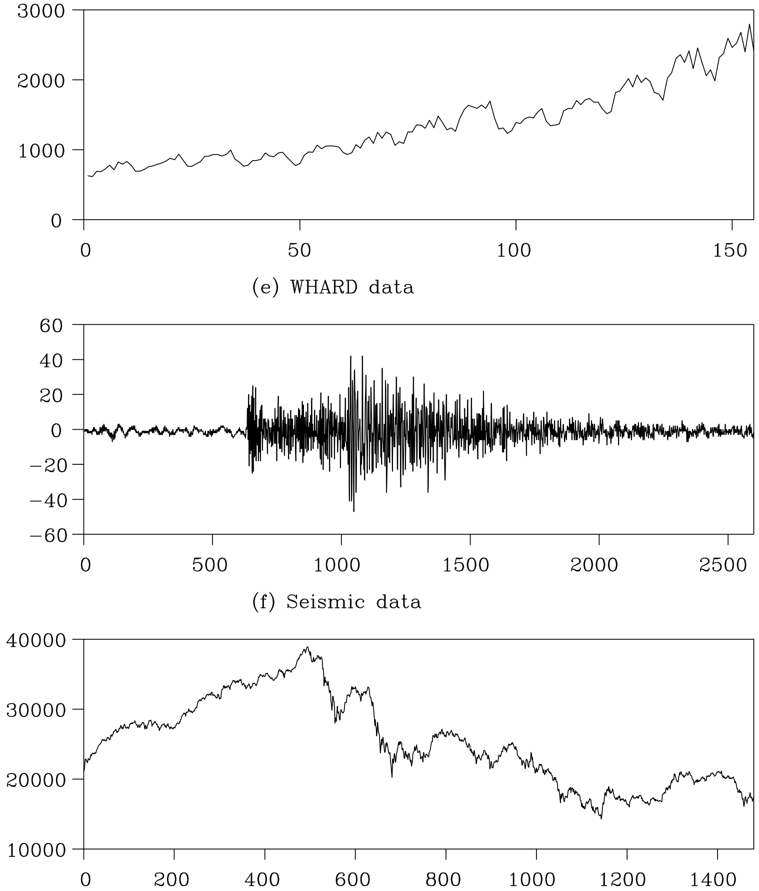

(e) WHARD data

(f) Seismic data

(g) Stock price index data

Figure 1.1: *Examples of various time series (continued).*

Plot (c) shows the daily *maximum temperatures* for Tokyo recorded for 16 months. Irregular fluctuations around the predominant annual period (trend) are seen (source: Tokyo District Meteorological Observatory).

Plot (d) shows the monthly time series of the number of workers engaged in food industries in the United States, called the *BLSALLFOOD data*. The data reveal typical features of economic time series that con-

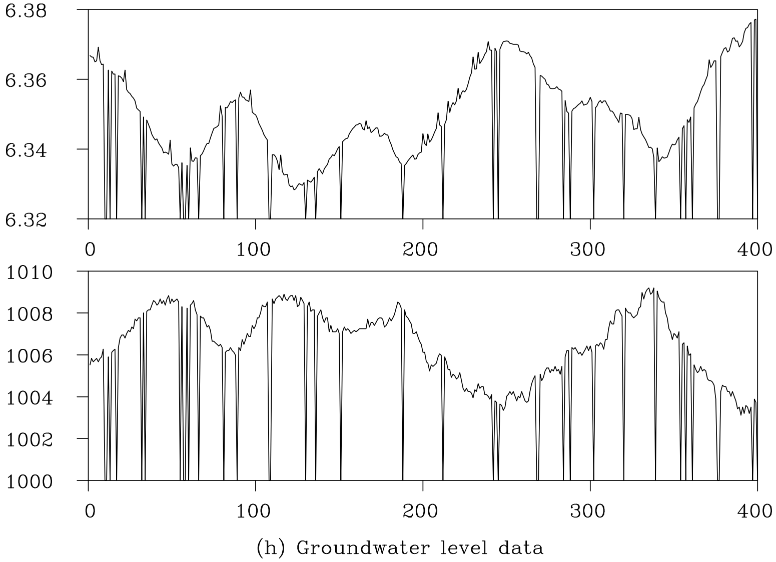

Figure 1.1: *Examples of various time series (continued).*

sists of trend and seasonal components. The trend component gradually varies and the seasonal component repeats a similar annual pattern (source: the U.S. Bureau of Labor Statistics (BLS)).

Plot (e) shows the monthly record of wholesale hardware data, called *WHARD data*. This time series reveals typical characteristics of economic data that increase at an almost fixed rate every year, such that the fluctuations around the trend gradually increase in magnitude over time (source: U.S. Bureau of Labor Statistics).

Plot (f) shows the time series of East-West components of *seismic waves*, recorded every 0.02 seconds. Because of the arrival of the P-wave (primary wave) and the S-wave (secondary wave), the variance of the series changed significantly. Moreover, it can be seen that not only the amplitude but also the frequency of the wave vary with time (Takanami (1991)).

Plot (g) depicts the daily closing values of the Japanese *stock price index*, Nikkei 225, quoted from January 4, 1988, to December 30, 1993. It reveals a monotone increase in values until the end of 1989, followed by a gradual decrease with large repetitive fluctuations after the Bubble crash in Japan in the 1990s. In the analysis of stock price data, we often

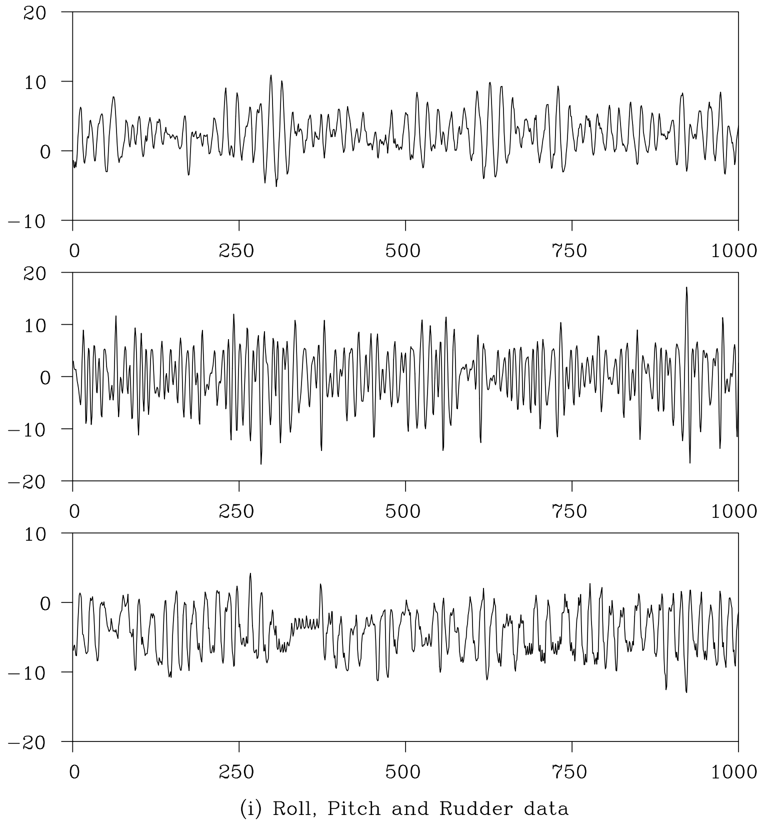

Figure 1.1: *Examples of various time series (continued).*

apply various analysis methods after taking the difference of the log-transformed data.

Plot (h) shows a bivariate time series of the *groundwater level* and the *atmospheric pressure* that were observed at 10-minute intervals at the observatory of the Tokai region, Japan, where a big earthquake was predicted to occur. A part of the time series that takes values on the horizontal axis, indicates missing observations, and some observations that significantly deviate upward might be considered as outliers that occurred due to malfunction of the observation device. To utilize the entire information contained in time series with many missing and outlying observations recorded over many years, it is necessary to develop a method that can be applied to data with such missing and outlying observations (offered by Dr. M. Takahashi and Dr. N. Matsumoto of National Institute of Advanced Industrial Science and Technology).

Plot (i) shows a multivariate time series of a ship's rolling, pitching and rudder angles recorded every second while navigating across the Pacific Ocean. As for the rolling and the rudder angles, both data show fluctuations over a cycle of approximately 16 seconds. On the other hand, the pitching angle varies over a shorter cycle of 10 seconds or less (offered by Prof. K. Ohtsu of Tokyo University of Marine Science and Technology).

1.2 Classification of Time Series

As has been shown in Figure 1.1, there is a wide variety of time series that can be classified into several categories from various viewpoints.

Continuous time series and discrete time series

Data continuously recorded, for example, by an analog device, are called *continuous* time series. On the other hand, data observed at certain intervals of time, such as the atmospheric pressure measured hourly, are called *discrete* time series.

There are two types of discrete time series; one where data observations are at *equally spaced intervals* and the other, where data observations are at *unequally spaced intervals*. Although the time series shown in Figure 1.1 are connected continuously by solid lines, they are all discrete time series. Hereafter in this book, we consider only discrete time series recorded at equally spaced intervals, because time series that we analyze on digital computers are usually discrete time series.

Univariate and multivariate time series

Time series consisting of a single observation at each time point as shown in Figures 1.1(a)–1.1(g) are called *univariate* time series. On the other hand, time series that are obtained by simultaneously recording two or more phenomena as the examples depicted in Figures 1.1(h)–1.1(i) are called *multivariate* time series. However, it may be difficult to distinguish between univariate and multivariate time series from their nature; rather the distinction is made from the analyst's viewpoint and by various other factors such as the measurement restriction and empirical or theoretical knowledge about the subject. From a statistical modeling point of view, variable selection itself is an important problem in time series analysis.

Stationary and nonstationary time series

A time series is a record of a phenomenon irregularly varying over time. In time series analysis, irregularly varying time series are generally expressed by stochastic models. In some cases, a random phenomenon can be considered as a realization of a stochastic model with a time-invariant structure. Such a time series is called a *stationary* time series. Figure 1.1(a) is a typical example of a stationary time series.

On the other hand, if the stochastic structure of a time series itself changes over time, it is called a *nonstationary* time series. As typical examples of nonstationary time series, consider the series in Figures 1.1(c), (d), (e) and 1.1(g). It can be seen that mean values change over time in Figures 1.1(c), (d), (e) and 1.1(g) and the fluctuation around the mean value changes over time in Figure 1.1(f).

Gaussian and non-Gaussian time series

When a distribution of a time series follows a normal distribution, the time series is called a *Gaussian* time series; otherwise, it is called a *non-Gaussian* time series. Most of the models considered in this book are Gaussian models, under the assumption that the time series follow Gaussian distributions.

As in the case of Figure 1.1(b), the pattern of the time series is occasionally asymmetric so that the marginal distribution cannot be considered as Gaussian. Even in such a situation, we may obtain an approximately Gaussian time series by an appropriate data transformation. This method will be introduced in Section 1.4 and Section 4.5.

Linear and nonlinear time series

A time series that is expressible as the output of a linear model is called a *linear* time series. In contrast, the output from a nonlinear model is called a *nonlinear* time series.

Missing observations and outliers

In time series modeling of real-world problems, we sometimes need to deal with *missing observations* and *outliers*. Some values of time series that have not been recorded for some reasons are called missing observations in the time series; see Figure 1.1(h). Outliers (outlying observations) might occur due to extraordinary behavior of the object, malfunction of the observation device or errors in recording. In the groundwater level data shown in Figure 1.1(h), some data jumping upward are considered to be outliers.

1.3 Objectives of Time Series Analysis

This book presents statistical modeling methods for time series. The objectives of *time series analysis* considered in this book are classified into four categories; description, modeling, prediction and signal extraction.

Description: This includes methods that effectively express or summarize the characteristics of time series. By drawing figures of time series or by computing basic descriptive statistics, such as sample autocorrelation functions, sample autocovariance functions and periodograms, we may capture essential characteristics of the time series and get a hint for time series modeling.

Modeling: In time series modeling, we capture the stochastic structure of time series by identifying an appropriate model. Since there are various types of time series, it is necessary to select an adequate model class and to estimate parameters included in the model, depending on the characteristics of the time series and the objective of the time series analysis.

Prediction: In the prediction of time series, based on the correlations over time and among the variables, we can estimate the future behavior of time series by using various information extracted from current and past observations. In particular, in this book, we shall consider methods of prediction and simulation based on the estimated time series models.

Signal extraction: In signal extraction problems, we extract essential signals or useful information from time series corresponding to the objective of the analysis. To achieve that purpose, it is important to build models based on the salient characteristics of the object and the purpose of the analysis.

1.4 Pre-processing of Time Series

For nonstationary time series, we sometimes perform pre-processing of the data before applying the analysis methods that are introduced later in this book. This section treats some methods of transforming nonstationary time series into approximately stationary time series. In Chapter 11 and thereinafter, however, we shall introduce various methods for modeling and analyzing nonstationary time series without pre-processing or stationalization.

1.4.1 Transformation of variables

Some types of time series obtained by counting numbers or by measuring a positive-valued process, such as the prices of goods and numbers of people illustrated in Figures 1.1(e) and 1.1(g), share the common characteristic that the variance of the series increases as the level of the series increases. For such a situation, we may construct a new series whose variance is almost time-invariant and whose noise distribution is closer to the normal distribution by using the log-transformation $z_n = \log y_n$ instead of the original series y_n.

A more general *Box-Cox transformation* (Box and Cox (1964)) includes the log-transformation as a special case and the automatic determination of its parameter will be considered later in Section 4.8. For time series y_n that take values in $(0,1)$ like probabilities or ratios of the occurrence of a certain phenomenon, we can obtain a time series z_n that takes a value in $(-\infty,\infty)$ by the logit transformation

$$z_n = \log\left(\frac{y_n}{1-y_n}\right). \tag{1.1}$$

In many cases, the distribution of the transformed time series z_n is less distorted than the original time series y_n, thus the modeling of the transformed series might be more tractable.

1.4.2 Differencing

When a time series y_n contains a trend as seen in Figures 1.1(c), (e) and (g), we might study the differenced series z_n defined by (Box and Jenkins (1970))

$$z_n = \Delta y_n = y_n - y_{n-1}. \tag{1.2}$$

This is motivated by the fact that, when y_n is a straight line expressed as $y_n = a + bn$, then the differenced series z_n becomes a constant as

$$z_n = \Delta y_n = b, \tag{1.3}$$

and the slope of the straight line can be removed.

Moreover, if y_n is a parabola and expressed by $y_n = a + bn + cn^2$, then the difference of z_n becomes a constant and a and b are removed as follows

$$\Delta z_n \quad = \quad z_n - z_{n-1}$$

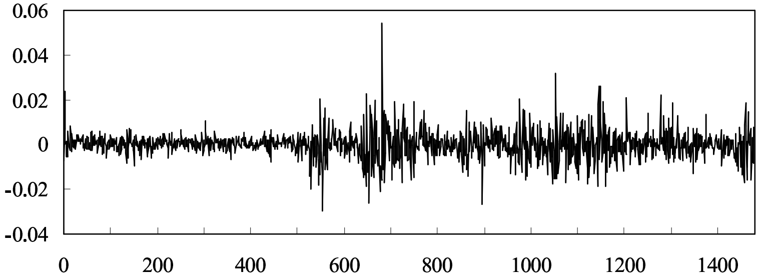

Figure 1.2: *Difference of the logarithm of the* Nikkei 225 *data.*

$$
\begin{aligned}
&= \Delta y_n - \Delta y_{n-1} \\
&= (b+2cn) - (b+2c(n-1)) \\
&= 2c. \qquad (1.4)
\end{aligned}
$$

When an annual cycle is observed in time series as shown in Figure 1.1(e), we might use the difference between the time series at the present time and one cycle before defined by

$$\Delta_p y_n = y_n - y_{n-p}. \qquad (1.5)$$

Figure 1.2 shows the difference of the logarithm $r_n = \log y_n - \log y_{n-1}$ of the Nikkei 225 data depicted in Figure 1.1(g), which is frequently utilized in the analysis of financial data in Japan. From Figure 1.2, it can be seen that the dispersion of the variation has changed abruptly around $n = 500$. We shall discuss this phenomenon in detail later in Sections 13.1 and 14.5.

1.4.3 Change from the previous month (quarter) and annual change

For economic time series as shown in Figure 1.1(e), we often consider a change from the previous month (or quarter) and an annual change of the original series y_n defined by

$$z_n = \frac{y_n}{y_{n-1}}, \qquad x_n = \frac{y_n}{y_{n-p}}. \qquad (1.6)$$

If the time series y_n is represented as the product of the trend T_n and the noise w_n as

$$y_n = T_n w_n, \qquad (1.7)$$

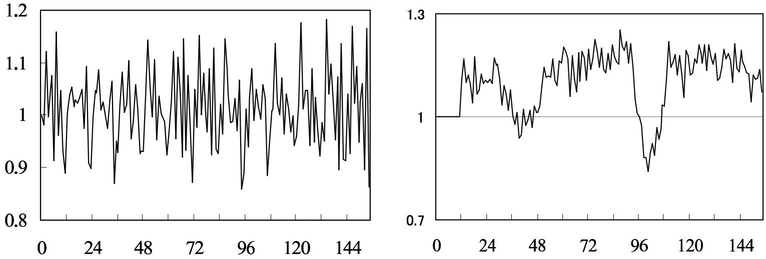

Figure 1.3 *Change from previous month and year-over-year change of WHARD data.*

and T_n evolves as $T_n = (1+\alpha)T_{n-1}$, where α is the growth rate, then the change from the previous month can be expressed by

$$z_n = \frac{y_n}{y_{n-1}} = \frac{T_n w_n}{T_{n-1} w_{n-1}} = (1+\alpha)\frac{w_n}{w_{n-1}}. \tag{1.8}$$

This means that, if the noise can be disregarded, the growth rate α can be determined by this transformation.

On the other hand, if y_n is represented as the product of a periodic function s_n with the cycle p and the noise w_n,

$$y_n = s_n \cdot w_n, \qquad s_n = s_{n-p} \tag{1.9}$$

then the annual changes x_n can be expressed by

$$x_n = \frac{y_n}{y_{n-p}} = \frac{s_n w_n}{s_{n-p} w_{n-p}} = \frac{w_n}{w_{n-p}}. \tag{1.10}$$

This suggests that the periodic function is removed by this transformation.

Figure 1.3 shows the change from the previous month and the annual change of the WHARD data shown in Figure 1.1(e). The trend component is removed by the change from the previous month. On the other hand, the annual periodic component is removed by the annual change. By means of this transformation, significant drops are revealed in the vicinity of $n = 40$ and $n = 100$.

1.4.4 Moving average

Constructing a moving average is a simple method for smoothing time series with random fluctuations. For a time series y_n, the $(2k+1)$-th term moving average of y_n is defined by

$$T_n = \frac{1}{2k+1}\sum_{j=-k}^{k} y_{n+j}. \tag{1.11}$$

When the original time series is represented by the sum of the straight line t_n and the noise w_n as

$$y_n = t_n + w_n, \quad t_n = a + bn, \tag{1.12}$$

where w_n is an independent noise with mean 0 and variance σ^2, then the moving average is given by

$$T_n = t_n + \frac{1}{2k+1}\sum_{j=-k}^{k} w_{n+j}. \tag{1.13}$$

Here, since the sum of the independent noises satisfies

$$\begin{aligned} E\left[\sum_{j=-k}^{k} w_{n+j}\right] &= \sum_{j=-k}^{k} E[w_{n+j}] = 0, \\ E\left[\left(\sum_{j=-k}^{k} w_{n+j}\right)^2\right] &= \sum_{j=-k}^{k} E\left[(w_{n+j})^2\right] = (2k+1)\sigma^2. \end{aligned} \tag{1.14}$$

Hence

$$\mathrm{Var}\left(\frac{1}{2k+1}\sum_{j=-k}^{k} w_{n+j}\right) = \frac{\sigma^2}{2k+1}. \tag{1.15}$$

This shows that the mean of the moving average T_n is the same as that of t_n, and the variance is reduced to $1/(2k+1)$ of the variance of noise term w_n.

Figure 1.4 shows the original maximum temperature data in Figure 1.1(c) and its moving averages for $k = 5, 17$ and 29. It can be seen that the moving averages yield smoother curves as k becomes larger.

In general, the weighted moving average is defined by

$$T_n = \sum_{j=-k}^{k} w_j y_{n-j}, \tag{1.16}$$

where the weights satisfy $\sum_{j=-k}^{k} w_j = 1$ and $w_j \geq 0$.

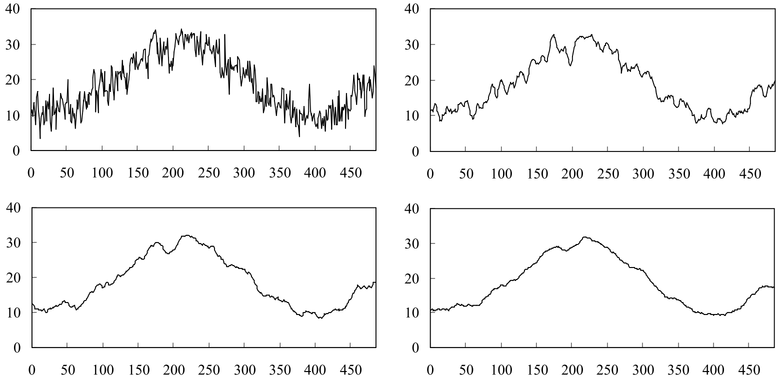

Figure 1.4 *Maximum temperature data and its moving average. Top left: original data, top right: moving average with $k = 5$, bottom left: $k = 17$, bottom right: $k = 29$.*

If we modify the definition of a moving average by using the median instead of the average, we obtain the $(2k+1)$-th term moving median that is defined by

$$T_n = \text{median}\,\{T_{n-k}, \cdots, T_n, \cdots, T_{n+k}\}. \qquad (1.17)$$

The moving median can detect a change in the trend more quickly than can the moving average.

1.5 Organization of This Book

The main aim of this book is to provide basic tools for modeling various time series that arise for real-world problems. Chapters 2 and 3 are basic chapters and introduce two descriptive approaches. In chapter 2, the autocovariance and autocorrelation functions are introduced as basic tools to describe univariate stationary time series. The cross-covariance and cross-correlation functions are also introduced for multivariate time series. In Chapter 3, the spectrum and the periodogram are introduced as basic tools for the frequency domain analysis of stationary time series. For the multivariate case, the cross spectrum and the power contribution are also introduced.

Chapters 4 and 5 discuss the basic methods for statistical modeling. In Chapter 4, typical probability distributions are introduced. Then, based on the entropy maximization principle, the likelihood function, the maximum likelihood method and the AIC criterion are derived. In Chapter 5, under the assumption of linearity and normality of the noise, the least squares method is derived as a convenient method for fitting various statistical models.

Chapters 6 to 8 are concerned with ARMA and AR models. In Chapter 6, the ARMA model is introduced and the impulse response function, the autocovariance function, partial autocorrelation coefficients, the power spectrum and characteristic roots are derived from the ARMA model. The multivariate AR model is also considered in this chapter and the cross-spectrum and power contribution are derived. The Yule-Walker method and the least squares method for fitting an AR model are shown in Chapter 7. In Chapter 8, the AR model is extended to the case where the time series is piecewise stationary and an application of the model to the automatic determination of the change point of a time series is given.

Chapter 9 introduces the state-space model as a unified way of expressing stationary and nonstationary time series models. The Kalman filter and smoother are shown to provide the conditional mean and variance of the unknown state vector, given the observations. It is also shown that we can get a unified method for prediction, interpolation and parameter estimation by using the state-space model and the Kalman filter.

Chapters 10 to 13 show examples of the application of the state-space model. In Chapter 10, the exact maximum likelihood method for the ARMA model is shown. The trend models are introduced in Chapter 11. In Chapter 12, the seasonal adjustment model is introduced to decompose seasonal time series into several components such as the trend and seasonal components. Chapter 13 is concerned with the modeling of nonstationarity in the variance and covariance. Time-varying coefficient AR models are introduced and applied to the estimation of a changing spectrum.

Chapters 14 and 15 are concerned with nonlinear non-Gaussian state-space models. In Chapter 14, the non-Gaussian state-space model is introduced and a non-Gaussian filter and smoother are derived for state estimation. Applications to the detection of sudden changes of the trend component and other examples are presented. In Chapter 15, the Monte Carlo filter and smoother are introduced as a very flexible method of filtering and smoothing for very general nonlinear non-Gaussian models.

Chapter 16 shows methods for generating various random numbers and time series that follow an arbitrarily specified time series model.

Algorithms for nonlinear optimization and the Monte Calro filter/smoother and the derivations of the Levinson's algorithm and the Kalman filter are shown in Appendices.

Problems

1. What is necessary to consider when discretizing a continuous time series?
2. Give an example of a non-Gaussian time series and describe its characteristics.
3. (1) Obtain the inverse transformation of the logit transformation (1.1).
   (2) Find a transformation from (a,b) to $(-\infty,\infty)$ and find its inverse.
4. Describe the problem in constructing a stationary time series from a nonstationary time series by differencing.
5. Describe the problem in removing cyclic components by annual changes.
6. (1) Show that if the true trend is a straight line, then the mean value does not change for the three-term moving average, and that the variance becomes $1/3$ of the observed data variance.
   (2) Discuss the differences between the characteristics of the moving average filter and the moving median filter.

Chapter 2

The Covariance Function

In this chapter, the covariance and correlation functions are presented as basic methods to represent stationary time series. The autocovariance function is a tool to represent the relation between past and present values of time series and the cross-covariance function is to express the relation between two time series. These covariance functions are used to capture features of time series to estimate the spectrum and to build time series models.

2.1 The Distribution of Time Series and Stationarity

The *mean* and the *variance* of data are frequently used as basic statistics to capture characteristics of random phenomena. A histogram is used to represent rough features of the data distribution. Therefore, by obtaining the mean, the variance and the histogram, it is expected to capture some aspects or features of the data.

Accordingly, we shall investigate whether these statistics are useful for the analysis of time series. The upper plots (a) and (b) in Figure 2.1 illustrate the histograms of the two time series (a) a ship's yaw rate and (i) the ship's rolling as shown in Figure 1.1. However, although the time series in plot (a) of Figure 1.1 is apparently different from that in plot (i) of Figure 1.1, the histogram shown in Figure 2.1 (a) is quite similar to that shown in (b) of Figure 2.1. This means that histograms cannot capture some aspects of the characteristics of the time series that are visually apparent.

Figures 2.1 (c) and (d) are *scatterplots* obtained by putting y_{n-2} on the horizontal axis and y_n on the vertical axis, for the yaw rate and the ship's roll data, respectively. Similarly, Figures 2.1(e) and (f) show scatterplots obtained by putting y_{n-4} on the horizontal axis, again with the time series as before. The scatterplot in (c) shows that the data are distributed evenly within a circle in the vicinity of the origin and this indicates that, in the case of the yaw rate, there is little correlation between y_n and y_{n-2}.

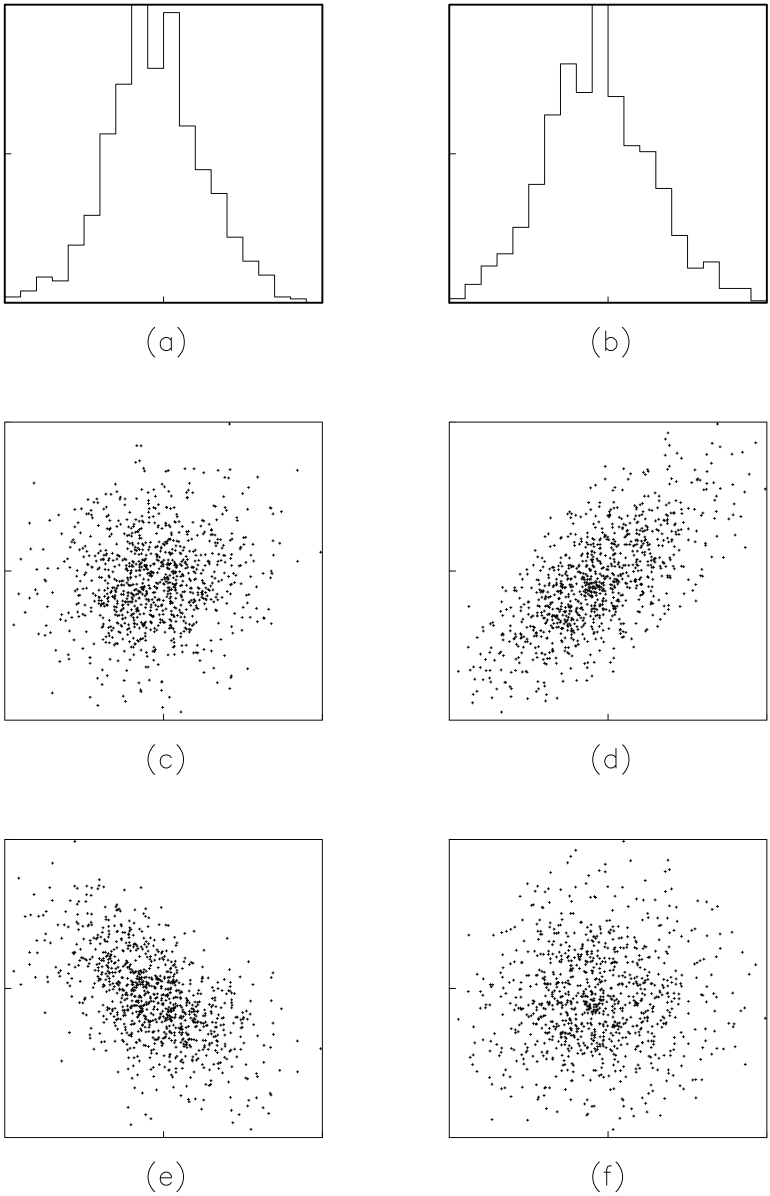

Figure 2.1: *Histograms and scatterplots of the yaw rate and rolling of a ship.*

On the other hand, the scatterplot shown in (d) are concentrated in a neighborhood of a straight line with positive slope, indicating that y_n has significant positive correlation with y_{n-2}. However, for the scatterplot (e), a negative linear relation is seen, and that indicates a negative correlation between y_n and y_{n-4} such a correlation is not evident at all for the plot (f).

These examples show that, in the analysis of time series, it is not possible to capture the essential features of time series by the marginal distribution of y_n that is obtained by ignoring the time series structure. Consequently, it is necessary to consider not only the distribution of y_n but also the joint distribution of y_n and y_{n-1}, y_n and y_{n-2}, and in general y_n and y_{n-k}. The properties of these joint distributions can be concisely expressed by the use of covariance and correlation coefficients of y_n and y_{n-k}.

Given a time series $y_1, \cdots, y_N$, the expectation of the time series y_n is defined by

$$\mu_n = \mathrm{E}(y_n) \tag{2.1}$$

and is called the *mean value function*. Here $\mathrm{E}(y)$ denotes the expectation with respect to the distribution of y. The covariance of a time series at two different times y_n and y_{n-k} is defined by

$$\mathrm{Cov}(y_n, y_{n-k}) = \mathrm{E}\{(y_n - \mu_n)(y_{n-k} - \mu_{n-k})\} \tag{2.2}$$

and is called the *autocovariance* of the time series y_n (Box and Jenkins (1970), Brockwell and Davis (1991)). For $k = 0$, we obtain the variance of the time series at time n, $\mathrm{Var}(y_n)$.

In this chapter, we consider the case when the mean, the variance, and the covariance do not change over time n. That is, we assume that for an arbitrary integer ℓ, it holds that

$$\begin{aligned} \mathrm{E}(y_n) &= \mathrm{E}(y_{n-\ell}) \\ \mathrm{Var}(y_n) &= \mathrm{Var}(y_{n-\ell}) \\ \mathrm{Cov}(y_n, y_m) &= \mathrm{Cov}(y_{n-\ell}, y_{m-\ell}). \end{aligned} \tag{2.3}$$

A time series with these properties is called *weakly stationary* or *covariance stationary*. In Chapter 8 and later, sophisticated models are introduced for the analysis of general nonstationary time series for which the mean and the covariance change with time.

If the data are distributed as a normal (Gaussian) distribution, the characteristics of the distribution are completely determined by the mean, the variance and the covariance. However, such an assumption does not hold for many actual data. In such a situation, it is recommended to draw a histogram of the data. The histogram might reveal a difference in the distributions even though the two sets of data have the same mean and variance.

Therefore, the features of a time series cannot always be captured completely only by the mean, the variance and the covariance function. In general, it is necessary to examine the *joint probability density function* of the time series $y_1,\cdots,y_N$, i.e., $f(y_1,\cdots,y_N)$. For that purpose, it is sufficient to specify the joint probability density function $f(y_{i_1},\cdots,y_{i_k})$ of $y_{i_1},\cdots,y_{i_k}$ for arbitrary integers k and arbitrary time points satisfying $i_1 < i_2 < \cdots < i_k$.

In particular, when this joint distribution is a k-variate normal distribution, the time series is called a *Gaussian time series*. The features of a Gaussian time series can be completely captured by the mean vector and the variance-covariance matrix.

When the distribution of a certain time series is invariant with respect to a time shift and the probability distribution does not change with time, the time series is called *strongly stationary*. Namely, a time series is called strongly stationary, if its distribution function satisfies the following relation

$$f(y_{i_1},\cdots,y_{i_k}) = f(y_{i_1-\ell},\cdots,y_{i_k-\ell}), \tag{2.4}$$

for an arbitrary time shift ℓ and arbitrary time points $i_1,\cdots,i_k$.

As noted above, the properties of Gaussian distributions are completely specified by the mean, the variance and the covariance. Therefore, for Gaussian time series, weak stationarity is equivalent to strong stationarity.

2.2 The Autocovariance Function of Stationary Time Series

Under the assumption of stationarity, the mean value function μ_n of a time series becomes a constant and does not depend on time n. Therefore, for a stationary time series, it can be expressed as

$$\mu = \mathrm{E}(y_n), \tag{2.5}$$

where μ is called the *mean* of the time series y_n. Further, the covariance of y_n and y_{n-k}, $\mathrm{Cov}(y_n,y_{n-k})$, becomes a value that depends only on the time difference k . Therefore, it can be expressed as

$$C_k = \mathrm{Cov}(y_n,y_{n-k}) = \mathrm{E}\{(y_n-\mu)(y_{n-k}-\mu)\}, \tag{2.6}$$

and it is called the *autocovariance function* of the stationary time series (Box and Jenkins (1970), Brockwell and Davis (1991), Shumway and Stoffer (2000)). Here, k is called the *lag* or the time lag. When $k = 0$, the autocovariance function is equal to the variance of y_n. The autocovariance function is an even function, i.e., $C_\ell = C_{-\ell}$, and it satisfies the inequality $|C_k| \leq C_0$.

The correlation coefficient between y_n and y_{n-k} is given by

$$R_k = \frac{\mathrm{Cov}(y_n, y_{n-k})}{\sqrt{\mathrm{Var}(y_n)\mathrm{Var}(y_{n-k})}}, \tag{2.7}$$

and by regarding it as a function of lag k, it is called the *autocorrelation function*.

For a stationary time series, since it is the case that

$$\mathrm{Var}(y_n) = \mathrm{Var}(y_{n-k}) = C_0, \tag{2.8}$$

the autocorrelation function is easily obtained from the autocovariance function as

$$R_k = \frac{C_k}{C_0}. \tag{2.9}$$

Example (White noise) When a time series y_n is a realization of an uncorrelated random variable with autocovariance function

$$C_k = \begin{cases} \sigma^2 & k = 0 \\ 0 & k \neq 0, \end{cases} \tag{2.10}$$

it is called a *white noise* with variance σ^2. Obviously, the autocorrelation function of a white noise is given by $R_0 = 1$, $R_k = 0$ for $k = \pm 1, \pm 2 \ldots$.

2.3 Estimation of the Autocovariance and Autocorrelation Functions

When a stationary time series $\{y_1, \cdots, y_N\}$ is given, the mean μ, the autocovariance function C_k and the autocorrelation function R_k are estimated by

$$\hat{\mu} = \frac{1}{N}\sum_{n=1}^{N} y_n \tag{2.11}$$

$$\hat{C}_k = \frac{1}{N}\sum_{n=k+1}^{N} (y_n - \hat{\mu})(y_{n-k} - \hat{\mu}) \tag{2.12}$$

$$\hat{R}_k = \frac{\hat{C}_k}{\hat{C}_0}, \tag{2.13}$$

respectively. Here $\hat{\mu}$ is called the *sample mean*, $\hat{C}_k$ is the *sample autocovariance function*, and $\hat{R}_k$ is the *sample autocorrelation function*.

For Gaussian process, the variance of the sample autocorrelation $\hat{R}_k$ is given approximately by (Bartlett (1948), Box and Jenkins (1970))

$$\mathrm{var}(\hat{R}_k) \sim \frac{1}{N} \sum_{j=-\infty}^{\infty} \left\{ R_j^2 + R_{j-k}R_{j+k} - 4R_k R_j R_{j-k} + 2R_j^2 R_k^2 \right\}. \quad (2.14)$$

Therefore, for time series for which all the autocorrelations R_j are zero for $j > m$ for some m, the variance of $\hat{R}_k$, $k > m$ is given by

$$\mathrm{var}(\hat{R}_k) \sim \frac{1}{N} \sum_{j=-\infty}^{\infty} R_j^2 = \frac{1}{N}\left(1 + 2\sum_{j=1}^{\infty} R_j^2\right). \quad (2.15)$$

In particular, for a white noise sequence with $R_k = 0$ for $k > 0$, the approximate expression is simply given by

$$\mathrm{var}(\hat{R}_k) \sim \frac{1}{N}. \quad (2.16)$$

This can be used for the test of whiteness of the time series. For example, the standard error of $\hat{R}_k$ is 0.1, 0.032 and 0.01 for $N = 100$, 1000 and 10,000, respectively.

Example (Autocorrelation functions of time series) Figure 2.2 shows the sample autocorrelation functions of the time series shown in the Figure 1.1 (a) – (f). In the case of the stationary time series of plot (a) of Figure 2.2, the peaks of the sample autocorrelation function rapidly decay to 0 with a cyclic fluctuation of period 8 or 9 as the lag increases. In the plot (b), the autocorrelation function of the log-transformed series is illustrated, because the original data reveal significant asymmetry. The peaks of the sample autocorrelation function repeatedly appear at an almost 10-year cycle corresponding to the approximate 10-year cycle of the sunspot data, and the amplitude of the sample autocorrelation gradually decreases as the lag increases. The amplitude of the sample autocorrelation function in plot (c) shows extremely slow decay, because a smooth annual trend is seen in Figure 1 (c). These distinct features are common to most nonstationary time series with a drifting mean value.

For the economic time series of plot (d), a one-year cycle in the sample autocorrelation function is seen corresponding to the annual cycle of the time series. However, the amplitude of the sample autocorrelation function decreases more slowly than those of (b) because of the presence of a trend in the time series. For the economic time series of plot (e), the

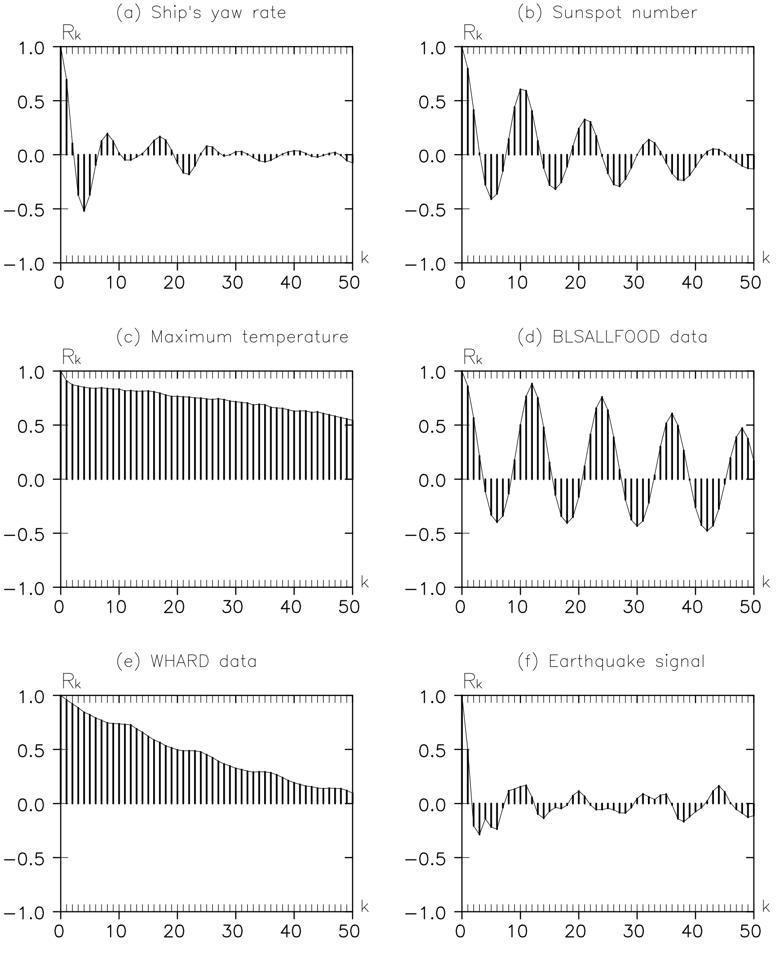

Figure 2.2: *Sample autocorrelation functions.*

value of the data increases over time and the amplitude grows along with it. Therefore, the data have been log-transformed prior to computing the sample autocorrelation function. For the earthquake data of plot (f), the fluctuation of the sample autocorrelation function continues for a considerably long time with an approximate 10-second cycle after a sudden reduction in the amplitude.

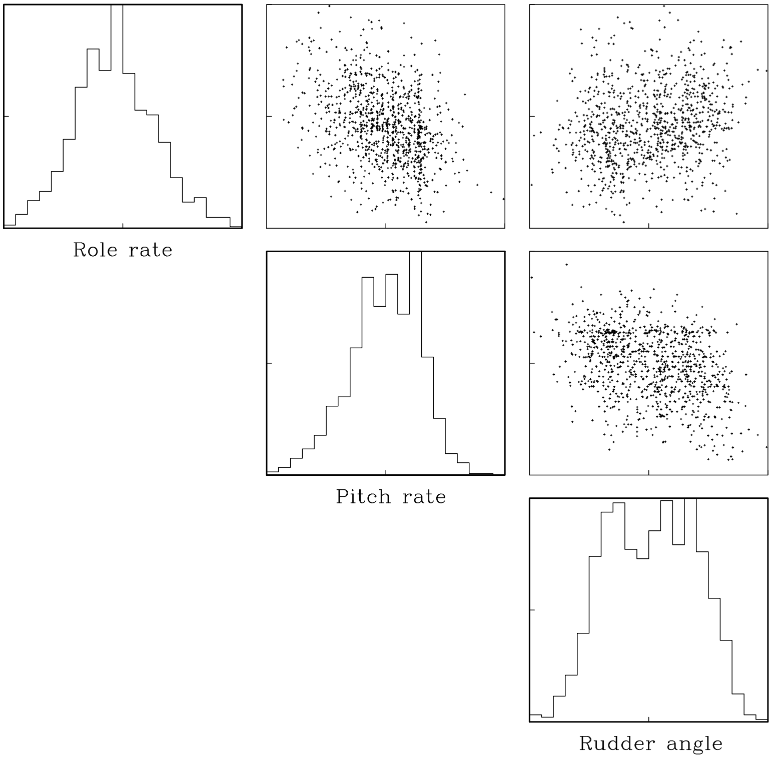

Figure 2.3: *Histograms and scatterplots of ship's data.*

2.4 Multivariate Time Series and Scatterplots

Simultaneous records of random phenomena fluctuating over time are called *multivariate time series.* An ℓ-variate time series is expressed as $y_n = (y_n(1),\cdots,y_n(\ell))^T$, where $y_n(j)$, $j = 1,\cdots,\ell$, is the j-th time series at time n. Here v^T denotes the transpose of the vector v.

The characteristics of a univariate time series are expressed by the autocovariance function and the autocorrelation function. For multivariate time series, it is necessary to consider the relation between different variables.

As stated in the previous chapter, the first approach to time series analysis is illustrating them with graphs. In the case of a multivariate time series $y_n = (y_n(1),\cdots,y_n(\ell))^T$, the relation among the variables can be understood by examining the *scatterplot.* The scatterplot of the time series $y_n(i)$ versus $y_n(j)$ is obtained by plotting the point $(y_n(i),\ y_n(j))$ on the 2-dimensional plane with $y_n(i)$ shown on the horizontal axis and $y_n(j)$ on the vertical axis.

Example In Figure 2.3, off-diagonal plots show the scatterplots of the 3-variate ship's data (roll rate, pitch rate and rudder angle) that are shown in Figure 1.1 (i), and the diagonal plots show histograms of the time series $y_n(1), y_n(2)$ and $y_n(3)$.

Negative relations between two variables can be seen in the scatterplots of the roll rate and the pitch rate and also of the roll rate and the rudder angle. On the other hand, the scatterplot of the roll rate and the rudder angle are scattered over the whole region, which indicates that the simultaneous correlation is negligible between these two variables.

Figure 2.4 shows the histograms and the scatterplot of the groundwater level data and the barometric pressure shown in Figure 1.1 (h). In the scatterplot, we see that the data points are concentrated near the diagonal of negative inclination. From the figures, we can see that the variation in the groundwater level corresponds closely to the variation in the barometric pressure.

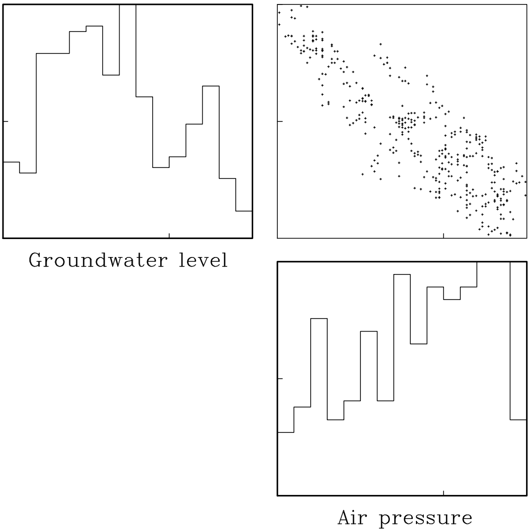

Figure 2.4 *Histograms and scatterplot of the groundwater level and barometric pressure data.*

As shown in the above examples, the relationships between two variables can be observed in the scatterplots. As was the situation with univariate time series, the relationship is not limited to the simultaneous case. For multivariate time series, we have to consider the relations between variables of y_n and y_{n-k}, i.e., $y_n(i)$ and $y_{n-k}(j)$.

Therefore, to consider the relations among the multivariate time series, it is necessary to examine the scatterplots of $y_n(i)$ and $y_{n-k}(j)$ for all combinations of i, j, and k. To express such relations between variables with time delay, we use the cross-covariance and cross-correlation functions that will be introduced in Section 2.5.

2.5 Cross-Covariance Function and Cross-Correlation Function

Univariate time series are characterized by the basic statistics, i.e., the mean, the autocovariance function and the autocorrelation function. Similarly, the mean vector, the cross-covariance function, and the cross-correlation function are used to characterize the multivariate time series $y_n = (y_n(1), \cdots, y_n(\ell))^T$.

The mean of the i-th time series $y_n(i)$ is defined by

$$\mu(i) = \mathrm{E}\{y_n(i)\}, \tag{2.17}$$

where $\mu = (\mu(1), \cdots, \mu(\ell))^T$ is called the *mean vector* of the multivariate time series y_n.

The covariance between the time series, $y_n(i)$, and the time series with time lag k, $y_{n-k}(j)$ is defined by

$$\begin{aligned} C_k(i,j) &= \mathrm{Cov}\big(y_n(i), y_{n-k}(j)\big) \\ &= \mathrm{E}\Big\{\big(y_n(i)-\mu(i)\big)\big(y_{n-k}(j)-\mu(j)\big)^T\Big\}, \end{aligned} \tag{2.18}$$

where the $\ell \times \ell$ matrix

$$C_k = \begin{bmatrix} C_k(1,1) & \cdots & C_k(1,\ell) \\ \vdots & \ddots & \vdots \\ C_k(\ell,1) & \cdots & C_k(\ell,\ell) \end{bmatrix} \tag{2.19}$$

is called the cross-covariance matrix of lag k (Box and Jenkins (1970), Akaike and Nakagawa (1989), Brockwell and Davis (1991)).

Considering C_k, $k = 0, 1, 2, \cdots$, as a function of lag k, it is called a *cross-covariance function*. Here, the diagonal element $C_k(i,i)$ of the cross-covariance function is the autocovariance function of the i-th time series $y_n(i)$.

The correlation coefficient between $y_n(i)$ and $y_{n-k}(j)$ is defined by

$$\begin{aligned} R_k(i,j) &= \mathrm{Cor}(y_n(i), y_{n-k}(j)) \\ &= \frac{C_k(i,j)}{\sqrt{C_0(i,i)C_0(j,j)}}, \end{aligned} \tag{2.20}$$

and the $\ell \times \ell$ matrix

$$R_k = \begin{bmatrix} R_k(1,1) & \cdots & R_k(1,\ell) \\ \vdots & \ddots & \vdots \\ R_k(\ell,1) & \cdots & R_k(\ell,\ell) \end{bmatrix} \tag{2.21}$$

is called the *cross-correlation function*.

The autocovariance function and the autocorrelation function are even functions and satisfy $C_{-k} = C_k$ and $R_{-k} = R_k$. For the multivariate time series, however, the cross-covariance function and the cross-correlation function do not have these symmetries in general. However, the relations

$$C_{-k} = C_k^T, \qquad R_{-k} = R_k^T \tag{2.22}$$

do hold, so that it is sufficient to consider C_k and R_k only for $k \geq 0$.

When the multivariate time series $\{y_1(j), \cdots, y_N(j)\}$, $j = 1, \cdots, \ell$, of length N are considered, estimates of the mean $\mu(i)$, the cross-covariance function $C_k(i,j)$, and the cross-correlation function $R_k(i,j)$ are obtained by

$$\hat{\mu}(i) = \frac{1}{N}\sum_{n=1}^{N} y_n(i) \tag{2.23}$$

$$\hat{C}_k(i,j) = \frac{1}{N}\sum_{n=k+1}^{N} (y_n(i) - \hat{\mu}(i))(y_{n-k}(j) - \hat{\mu}(j)) \tag{2.24}$$

$$\hat{R}_k(i,j) = \frac{\hat{C}_k(i,j)}{\sqrt{\hat{C}_0(i,i)\hat{C}_0(j,j)}}. \tag{2.25}$$

Here, the ℓ-dimensional vector $\hat{\mu} = \left(\hat{\mu}(1), \ldots \hat{\mu}(\ell)\right)^T$ is called the *sample mean vector*, the $\ell \times \ell$ matrix $\hat{C}_k = \left(\hat{C}_k(i,j)\right)$ and $\hat{R}_k = \left(\hat{R}_k(i,j)\right)$, $k = 0, 1, \ldots, i = 1, \ldots \ell, j = 1, \ldots \ell$, are called the *sample cross-covariance function* and the *sample cross-correlation function*, respectively.

Example (Ship data) Figure 2.5 shows the sample cross-correlation

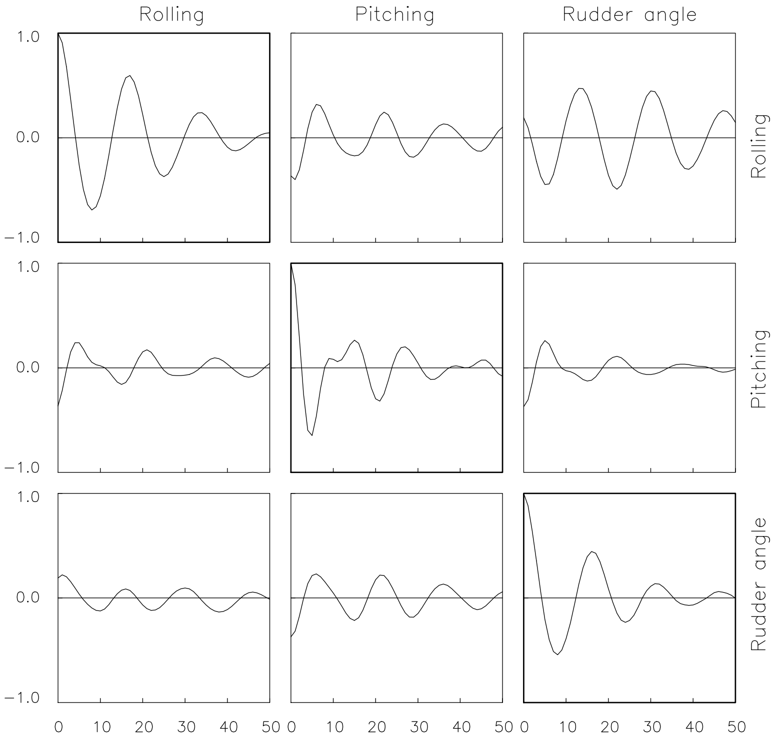

Figure 2.5 *Autocorrelation functions and cross-correlation functions of ship's data.*

function of the ship's data consisting of roll rate, pitch rate and rudder angle as shown in Figure 1.1 (i). The graph in the i-th row and the j-th column shows the correlation function $R_k(i,j)$, $k = 0,\cdots,50$. Therefore, the three plots with bold frames on the diagonal of Figure 2.5 show the autocorrelation function $R_k(i,i)$ and other six plots show the cross-correlation function $R_k(i,j)$.

From these figures, it can be seen that the roll rate and the rudder angle fluctuate somewhat periodically. On the other hand, the autocorrelation function of the pitch rate is complicated. Furthermore, the figures indicate a strong correlation between the roll rate and the rudder angle, because the autocorrelation function of the roll rate is similar to that of the rudder angle and the cross-correlation $R_k(1,3)$ between the rudder angle and the roll rate is very high.

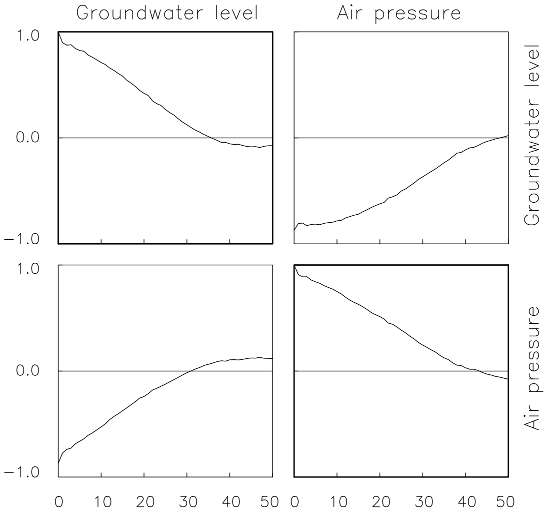

Figure 2.6 *Autocorrelation functions and cross-correlation functions of the groundwater level and barometric pressure data.*

Example (Grandwater level data) Figure 2.6 shows the cross-correlation function between the groundwater level data and the barometric pressure data illustrated in Figure 1.1(h). A very strong correlation between the two variables is seen.

Problems

1. Show that a weakly stationary Gaussian time series is strongly stationary.
2. Is a strongly stationary time series weakly stationary?
3. Show that the autocovariance function of a stationary time series is an even function.
4. Obtain the autocovariance function of a time series that satisfies $y_n = v_n - cv_{n-1}$, where $|c| < 1$ and v_n is a white noise with mean 0 and variance 1.
5. Assuming that $C_0, C_1, \ldots,$ is the autocovariance function of a station-

ary time series, show that the matrix

$$C = \begin{bmatrix} C_0 & C_1 & \cdots & C_{k-1} \\ C_1 & C_0 & \ddots & \vdots \\ \vdots & \ddots & \ddots & C_1 \\ C_{k-1} & \cdots & C_1 & C_0 \end{bmatrix}$$

is positive semi-definite.

6.(1) What is the expected value of the sample autocovariance function $\hat{C}_k$?

(2) Discuss the reason that the sum is divided by N, not by $N-k$, in the definition of the sample autocovariance function.

7.(1) Assuming that the time series is a Gaussian white noise, obtain the distributions of $\hat{C}_k$ and $\hat{R}_k$.

(2) Using the results of (1), consider a method for checking whether or not a time series is white.

Chapter 3

The Power Spectrum and the Periodogram

In this section, the spectral analysis method is introduced as a basic tool for stationary time series analysis. By means of spectral analysis, we can capture the characteristics of time series by decomposing time series into trigonometric functions at each frequency and by representing the features with the strength of each periodic component. The subjects discussed here will lead to the definition of the power spectrum and the periodogram of time series, computational methods, variance reduction and smoothing methods. Moreover, an efficient method of computing periodograms is presented using fast Fourier transforms (FFT). The readers interested in the spectral analysis of time series are referred to Brillinger (1974), Bloomfied (1976), Akaike and Nakagawa (1989) and Brockwell and Davis (1991).

3.1 The Power Spectrum

If the autocovariance function C_k rapidly decreases as the lag k increases and satisfies

$$\sum_{k=-\infty}^{\infty} |C_k| < \infty,$$

we can define the *Fourier transform* of C_k.

The function defined on the frequency $-1/2 \leq f \leq 1/2$,

$$p(f) = \sum_{k=-\infty}^{\infty} C_k e^{-2\pi i k f}, \tag{3.1}$$

is called the *power spectral density function* or simply the *power spectrum*.

Since the autocovariance function is an even function and satisfies $C_k = C_{-k}$, the power spectrum can also be expressed as

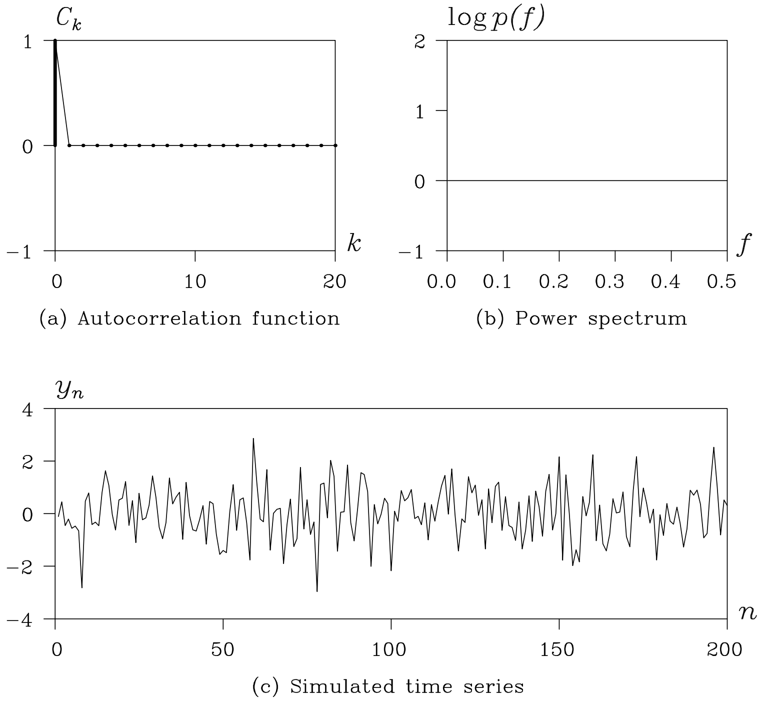

(a) Autocorrelation function

(b) Power spectrum

(c) Simulated time series

Figure 3.1 *Autocorrelation function, power spectrum, and realization of a white noise with variance* $\sigma^2 = 1$.

$$
\begin{aligned}
p(f) &= \sum_{k=-\infty}^{\infty} C_k \cos(2\pi k f) - i \sum_{k=-\infty}^{\infty} C_k \sin(2\pi k f) \\
&= \sum_{k=-\infty}^{\infty} C_k \cos 2\pi k f = C_0 + 2\sum_{k=1}^{\infty} C_k \cos 2\pi k f. \qquad (3.2)
\end{aligned}
$$

The power spectrum represents a time series in terms of trigonometric functions with various frequencies and expresses the characteristics of a time series by the magnitudes of these cyclic components. On the other hand, if a power spectrum is given, then the autocovariance function can be obtained via the inverse Fourier transform

$$
C_k = \int_{-\frac{1}{2}}^{\frac{1}{2}} p(f) e^{2\pi i k f} df = \int_{-\frac{1}{2}}^{\frac{1}{2}} p(f) \cos 2\pi k f \, df. \qquad (3.3)
$$

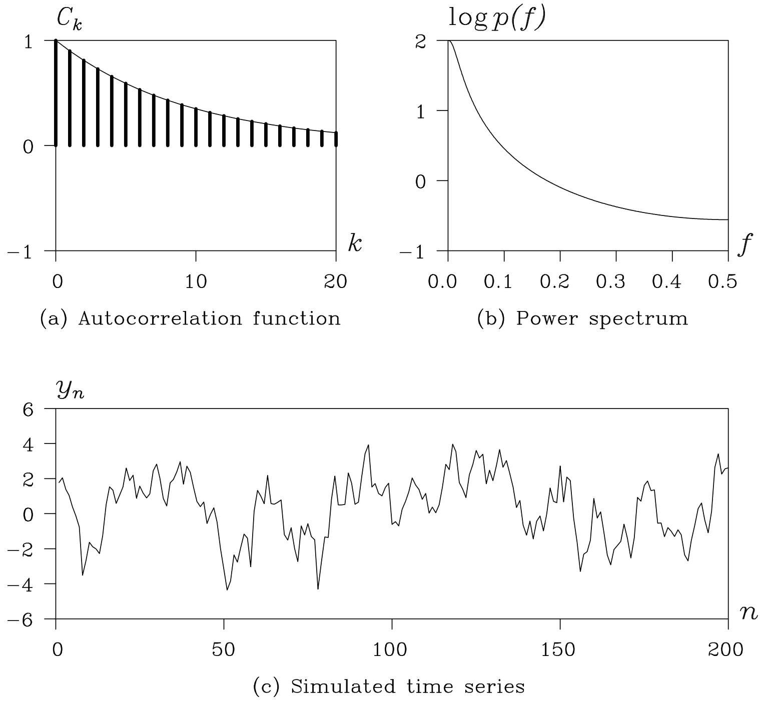

Figure 3.2 *Autocorrelation function, power spectrum, and realization of a first-order AR model with $a = 0.9$.*

Example (The power spectrum of white noise) The autocovariance function of a *white noise* is given by $C_0 = \sigma^2$ and $C_k = 0$ for $k \neq 0$. Therefore, the power spectrum of a white noise becomes

$$p(f) = \sum_{k=-\infty}^{\infty} C_k \cos 2\pi k f = C_0 = \sigma^2, \tag{3.4}$$

taking a constant value for any frequency f. It means that a white noise contains cyclic components of various frequencies with the same magnitude. Plots (a), (b) and (c) in Figure 3.1 show the autocorrelation function and the power spectrum of a white noise with variance $\sigma^2 = 1$ and realizations of white noise generated by the simulation. The simulation method for a time series from an assumed model will be introduced later in Chapter 16.

Example (Power spectrum of an AR model) Assume that w_n is a

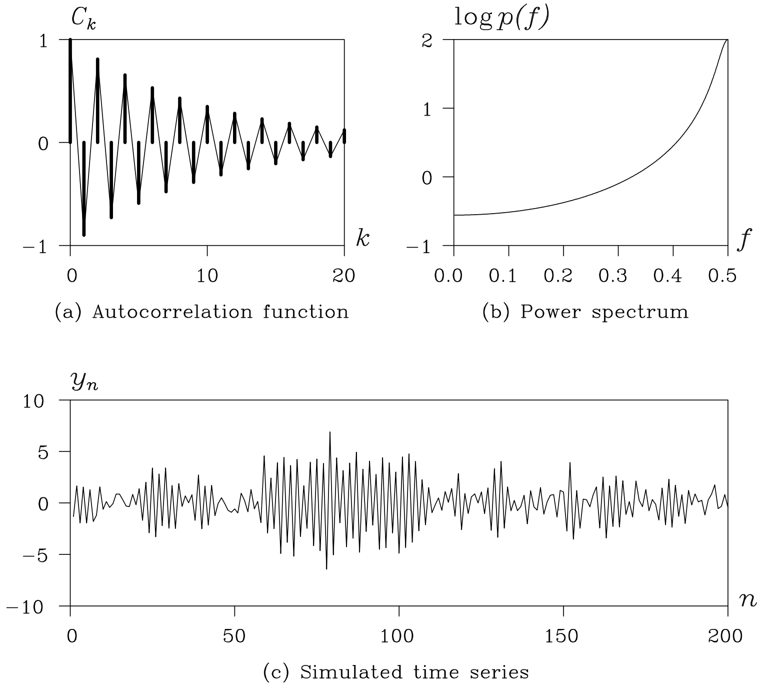

Figure 3.3 *Autocorrelation function, power spectrum, and realization of a first-order AR model with a* $= -0.9$.

white noise with variance σ^2. If a time series is generated by a first-order autoregressive model $y_n = ay_{n-1} + w_n$, the autocovariance function is given by $C_k = \sigma^2(1-a^2)^{-1}a^{|k|}$ and then the power spectrum of this time series can be evaluated as

$$p(f) = \frac{\sigma^2}{|1-ae^{-2\pi if}|^2} = \frac{\sigma^2}{1-2a\cos 2\pi f + a^2}. \tag{3.5}$$

Plots (a), (b) and (c) of Figure 3.2 show the autocorrelation function, the power spectrum and the realization, which were generated by the simulation for a first autoregressive model with $a = 0.9$. Similarly, Figure 3.3 shows the case of a first-order autoregressive model with a negative coefficient $a = -0.9$. The autocorrelation function is very wiggly, and unlike the case of positive coefficient, the power spectrum is an increasing function of the frequency f.

If a time series follows a second-order AR model $y_n = a_1y_{n-1} +$

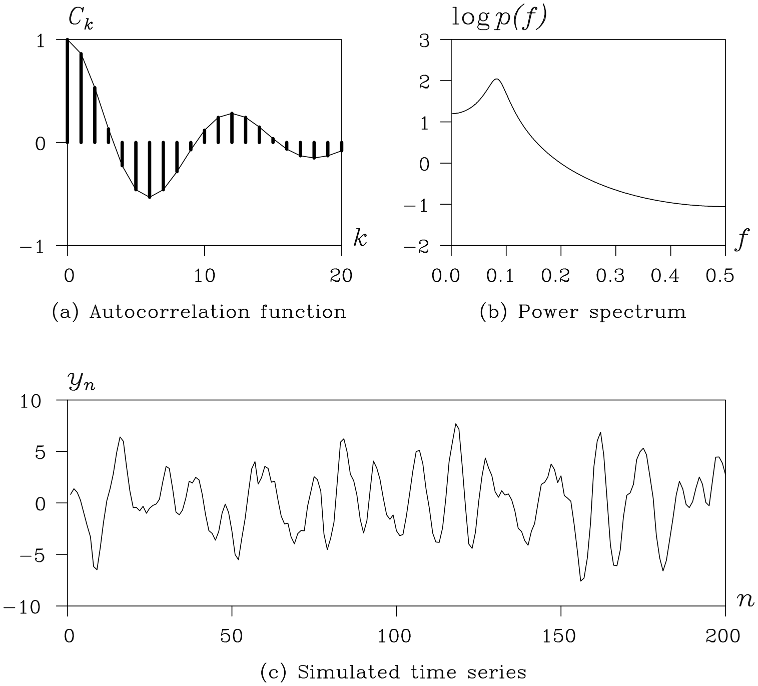

(a) Autocorrelation function

(b) Power spectrum

(c) Simulated time series

Figure 3.4 *Autocorrelation function, power spectrum, and realization of a second-order AR model with* $a_1 = 0.9\sqrt{3}$ *and* $a_2 = -0.81$.

$a_2 y_{n-2} + w_n$, the autocorrelation function satisfies

$$R_1 = \frac{a_1}{1-a_2}, \qquad R_k = a_1 R_{k-1} + a_2 R_{k-2}, \tag{3.6}$$

and the power spectrum can be evaluated as

$$\begin{aligned} p(f) &= \frac{\sigma^2}{|1 - a_1 e^{-2\pi i f} - a_2 e^{-4\pi i f}|^2} \\ &= \frac{\sigma^2}{1 - 2a_1(1-a_2)\cos 2\pi f - 2a_2 \cos 4\pi f + a_1^2 + a_2^2}. \end{aligned} \tag{3.7}$$

Figure 3.4 shows (a) the autocorrelation function, (b) the power spectrum and (c) a realization, which were generated by the simulation for a second-order AR model with $a_1 = 0.9\sqrt{3}$ and $a_2 = -0.81$. The autocorrelation function is oscillatory, and the power spectrum has a peak around at $f = 0.1$.

3.2 The Periodogram

Given a time series $y_1, \cdots, y_N$, the *periodogram* is defined by

$$p_j = \sum_{k=-N+1}^{N-1} \hat{C}_k e^{-2\pi i k f_j} = \hat{C}_0 + 2\sum_{k=1}^{N-1} \hat{C}_k \cos 2\pi k f_j, \tag{3.8}$$

where the sample autocovariance function $\hat{C}_k$ is substituted for the autocovariance function C_k of equations (3.1) and (3.2).

In the definition of the periodogram, we consider only the natural frequencies defined by $f_j = j/N, j = 0, \cdots, [N/2]$. Here $[N/2]$ denotes the maximum integer, which does not exceed $N/2$. An extension of the periodogram

$$\hat{p}(f) = \sum_{k=-N+1}^{N-1} \hat{C}_k e^{-2\pi i k f}, \qquad -0.5 \le f \le 0.5, \tag{3.9}$$

obtained by extending the domain to the continuous interval $[0, 1/2]$ is called the *sample spectrum.*

In other words, the periodogram is obtained from the sample spectrum by restricting its domain to the natural frequencies. Corresponding to the relations of (3.3), the following relation holds between the sample spectrum and the sample autocovariance function,

$$\hat{C}_k = \int_{-\frac{1}{2}}^{\frac{1}{2}} \hat{p}(f) e^{2\pi i k f} df, \qquad k = 0, \cdots, N-1. \tag{3.10}$$

Example (Periodograms) Figure 3.5 shows the periodograms of the univariate time series corresponding to Figures 1.1 (a)–(f). Note that the vertical axis here has a logarithmic scale.

Plot (a) shows the periodogram of the ship's yaw rate. A fairly strong periodic component with an approximate 10-second period, i.e., $f = 0.1$, is observed.

Plot (b) shows the periodogram of the annual sunspot number series. A strong periodic component with an approximate 10-year period $(f = 0.1)$ is shown. However, because of the strong variation, other periodic components cannot be clearly seen.

In the periodogram of the maximum temperature data shown in plot (c), there is no apparent periodicity.

In the periodogram of the BLSALLFOOD data shown in plot (d), a sharp peak is seen at the frequency $f = 1/12$ corresponding to the

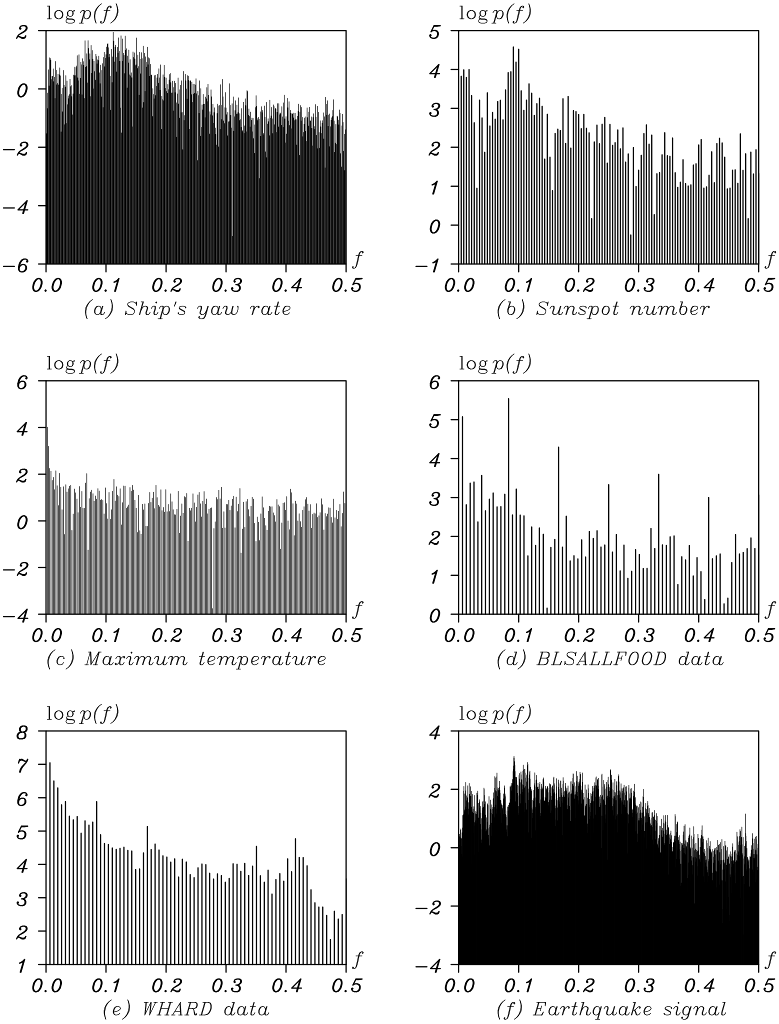

(a) Ship's yaw rate

(b) Sunspot number

(c) Maximum temperature

(d) BLSALLFOOD data

(e) WHARD data

(f) Earthquake signal

Figure 3.5: *Periodograms of the data of Figure 1.1 (on a logarithmic scale).*

seasonal components. The frequencies of the other four peaks are integer multiples of the frequency of the main peak and are considered to be the higher harmonics of the nonlinear waveform.

Similar peaks can be seen in the WHARD data shown in plot (e), but they are not as significant as the ones shown in plot (d).

The periodogram of seismic wave data of plot (f) shows two plateaus around $f = 0.1$ and $f = 0.25$, and sharp peaks are seen at $f = 0.07$ and $f = 0.1$.

We note the properties of the periodogram hereafter. The periodogram and the sample spectrum are asymptotically unbiased and satisfy

$$\lim_{N\to\infty} \mathrm{E}\{\hat{p}(f)\} = p(f) = \sum_{k=-\infty}^{\infty} C_k \cos 2\pi k f. \tag{3.11}$$

This means that at each frequency f, the expectation of the sample spectrum converges to the true spectrum as the number of data points increases. However, it does not imply the consistency of $\hat{p}(f)$, that is, the sample spectrum $\hat{p}(f)$ does not necessarily converge to $p(f)$ as the number of data points increases. Actually,

$$\frac{2\hat{p}(f_1)}{p(f_1)}, \ldots, \frac{2\hat{p}(f_{[\frac{N}{2}]-1})}{p(f_{[\frac{N}{2}]-1})}, \tag{3.12}$$

independently follow the χ^2 distribution with two degrees of freedom, and $\hat{p}(0)/p(0)$ and $\hat{p}(0.5)/p(0.5)$ follow the χ^2 distribution with one degree of freedom. Therefore, the variance of the periodogram is constant, independent of the sample size N. Thus the periodogram cannot be a consistent estimator.

Example (Sample autocorrelation functions and periodograms) Figures 3.6 (a) and (b) show the sample autocorrelation function and the periodogram, respectively, of the realizations of white noise with a sample size $N = 200$, which are generated similarly to Figure 3.1(c). Sample autocorrelations are close to zero and are almost contained in the confidence interval $[-200^{-1/2}, 200^{-1/2}] \simeq [-0.07, 0.07]$. The theoretical spectrum of the white noise is a constant, $\log p(f) \equiv 0$ in this case. However, the periodogram fluctuates sharply, indicating that it cannot be a good estimate of the spectrum.

Figures 3.6 (c)–(f) show the sample autocorrelation functions and the periodogram of realizations of white noise with sample sizes 800 and 3200. The sample autocorrelations $\hat{C}_k$ converge to the true value C_k as the

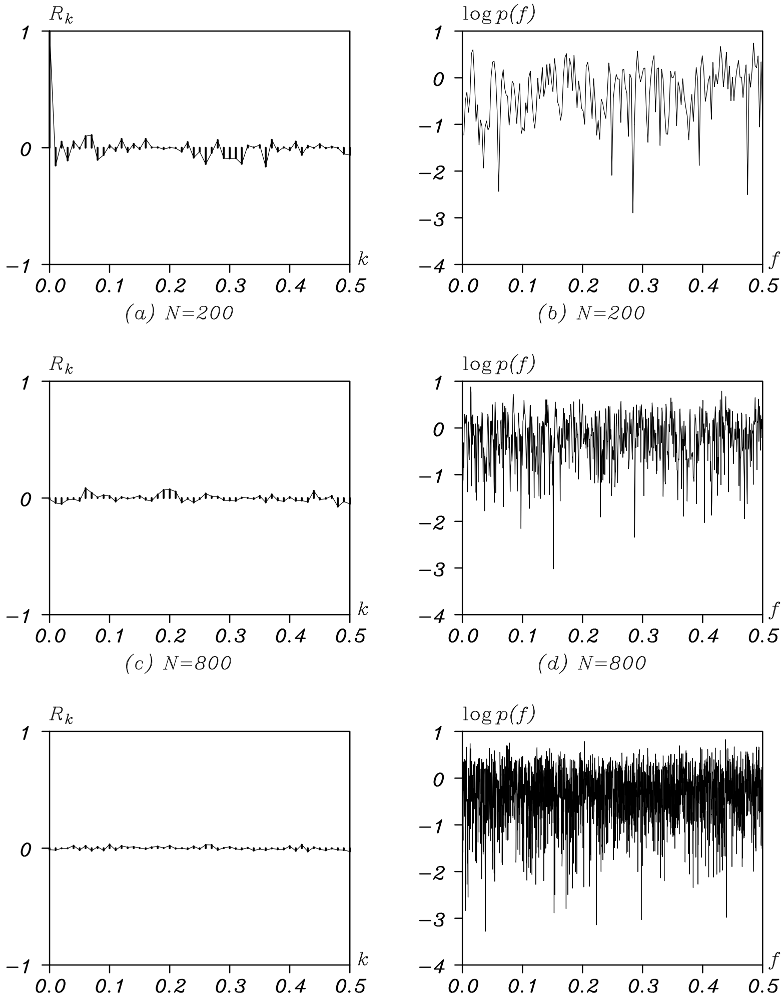

(a) N=200 (b) N=200

(c) N=800 (d) N=800

(e) N=3200 (f) N=3200

Figure 3.6 *Sample autocorrelation functions and periodograms in a logarithmic scale: sample sizes $n = 200, 800, 3200$.*

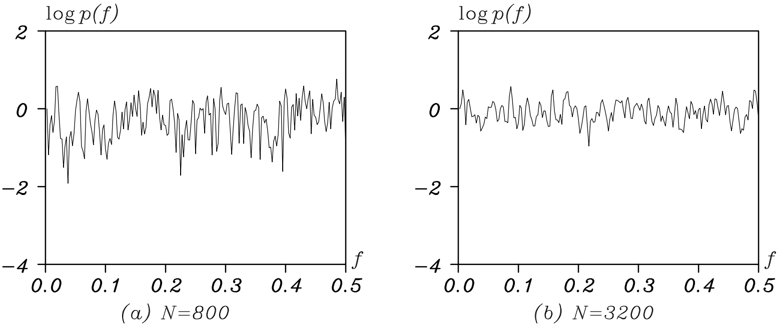

Figure 3.7: *Raw spectra of a white noise.*

data length increases. On the other hand, the amount of variation in the periodogram does not decrease even when the data length increases and the frequency of the variation increases in proportion to N. This suggests that the sample spectrum will never converge to the true spectrum, even if the data length increases without limit. This reflects the fact that the sample spectrum is not a consistent estimator of the spectrum.

3.3 Averaging and Smoothing of the Periodogram

In this section, we shall consider a method of obtaining an estimator that converges to the true spectrum as n increases. Instead of (3.8), define p_j by

$$p_j = \hat{C}_0 + 2\sum_{k=1}^{L-1} \hat{C}_k \cos 2\pi k f_j, \tag{3.13}$$

for the frequencies $f_j = j/2L$ for $j = 0,\cdots,L$, where L is an arbitrary integer.

The p_j defined in this way is called the *raw spectrum*. Figures 3.7 (a) and (b) show the raw spectrum p_j for the data shown in Figures 3.6 (c) and (e), respectively, setting $L = 200$. In this case, the range of vertical variation decreases as the number of data points increases. This suggests that, by using a fixed lag L, the raw spectrum p_j defined by (3.13) converges to the true spectrum.

In the definition of the periodogram (3.8), the sample autocovariances are necessary up to the lag $N-1$. However, by just using a fixed number, $L-1$, of autocovariances, the raw spectrum converges to the

Table 3.1 *Variances of the periodogram and the logarithm of the periodogram obtained from (3.8) and (3.14).*

Data length N	200	800	3200
p_j by (3.8)	1.006	0.998	1.010
p_j by (3.14)	1.006	0.250	0.061
$\log p_j$ by (3.8)	0.318	0.309	0.315
$\log p_j$ by (3.14)	0.318	0.053	0.012

true spectrum as the number of data points (i.e., N) increases. On the assumption that the number of data points N increases according to $N=\ell L$, $\ell = 1,2,\cdots$, computing the raw spectrum with the maximum lag $L-1$ is equivalent to applying the following procedures.

Firstly, divide the time series $y_1,\cdots,y_n$ into N/L sub-series of length L, $y_j^{(i)},\cdots,y_L^{(i)}$, $i=1,\cdots,N/L$, namely, $y_j^{(i)} \equiv y_{(i-1)L+j}$, and a periodogram $p_j^{(i)}$, $j=0,\cdots,[L/2]$ is obtained from each sub-series for $i=1,\cdots,N/L$. After calculating the periodogram $p_j^{(i)}$, $j=0,\cdots,[L/2]; i=1,\cdots,N/L$, the *averaged periodogram* is obtained by averaging the N/L estimates for each $j=0,\cdots,[L/2]$,

$$p_j = \frac{L}{N}\sum_{i=1}^{N/L} p_j^{(i)}. \tag{3.14}$$

By this procedure, the variance of $p_j^{(i)}$ does not change, even if the number of data points, N, increases as $\ell, 2\ell,\cdots,L\ell$. However, since p_j is obtained as the mean of ℓ periodograms, $p_j^{(i)}$, $i=1,\cdots,\ell$, the variance of p_j becomes $1/\ell$ of the variance of $p_j^{(i)}$. Therefore, the variance of p_j converges to 0 as the number of data points N, or ℓ increases to infinity.

Table 3.1 shows the variances of the periodogram and the logarithm of the periodogram obtained using Eqs. (3.8) and (3.14), respectively. The variances of the periodogram obtained by Eq. (3.8) do not change as the number of data points increases. Note that the theoretical variances of the periodogram and the log-periodogram are 1 and $\pi^2/6(\log 10)^2$, respectively. However, those obtained by (3.14) are inversely proportional to the data length. The reduction in the variances is also seen for the logarithm of the periodogram. In this case, the variances are reduced even faster.

Table 3.2: *Hanning and Hamming windows.*

Window	m	W_0	W_1
Hanning	1	0.50	0.25
Hamming	1	0.54	0.23

Summarizing the above argument, although the periodogram does not converge to the true spectrum with the increase in the number of data points, we can obtain an estimate of the spectrum that converges to the true spectrum by fixing the maximum lag, L, in computing the Fourier transform (3.13).

Here, note that the raw spectrum of (3.13) does not exactly agree with the averaged periodogram (3.14), and sometimes it might happen that $p_j < 0$. To prevent this situation and to guarantee the positivity of p_j, we need to compute p_j by (3.14). However, in actual computation, the raw spectrum is smoothed by using the *spectral window*. That is, for a given spectral window W_i, $i = 0, \pm 1, \cdots, \pm m$, an estimate of the spectrum is obtained by

$$\hat{p}_j = \sum_{i=-m}^{m} W_i p_{j-i}, \qquad j = 0, 1, \cdots, [L/2], \tag{3.15}$$

where $p_{-j} = p_j$ and $p_{[L/2]+i} = p_{[L/2]-i}$. By properly selecting a spectral window, we can obtain an optimal estimate of the spectrum that is always positive and with smaller variance. Table 3.2 shows some typical spectral windows. Note that they are symmetric, $W_{-i} = W_i$, and also satisfy $W_i > 0$ to guarantee that $\hat{p}_j > 0$.

Example (Smoothed periodograms) Figure 3.8 shows the smoothed periodograms obtained by putting $L = 2\sqrt{N}$ and applying the Hanning window to the data shown in Figure 3.5. When the number of data points is large, as occurs in Figures 3.8 (a) and (f), the fluctuations become fairly small, so that reasonable estimates of the spectrum are obtained. However, in Figures 3.8 (d) and (e), the line spectra corresponding to the annual cycle become unclear due to the smoothing operation, although they can be clearly detected by the original periodogram as shown in Figure 3.5. We need to make a compromise between the smoothness of the estimate and sensitivity to the presence of significant peaks. This problem can be solved by efficient use of time series models as will be shown in Chapter 6.

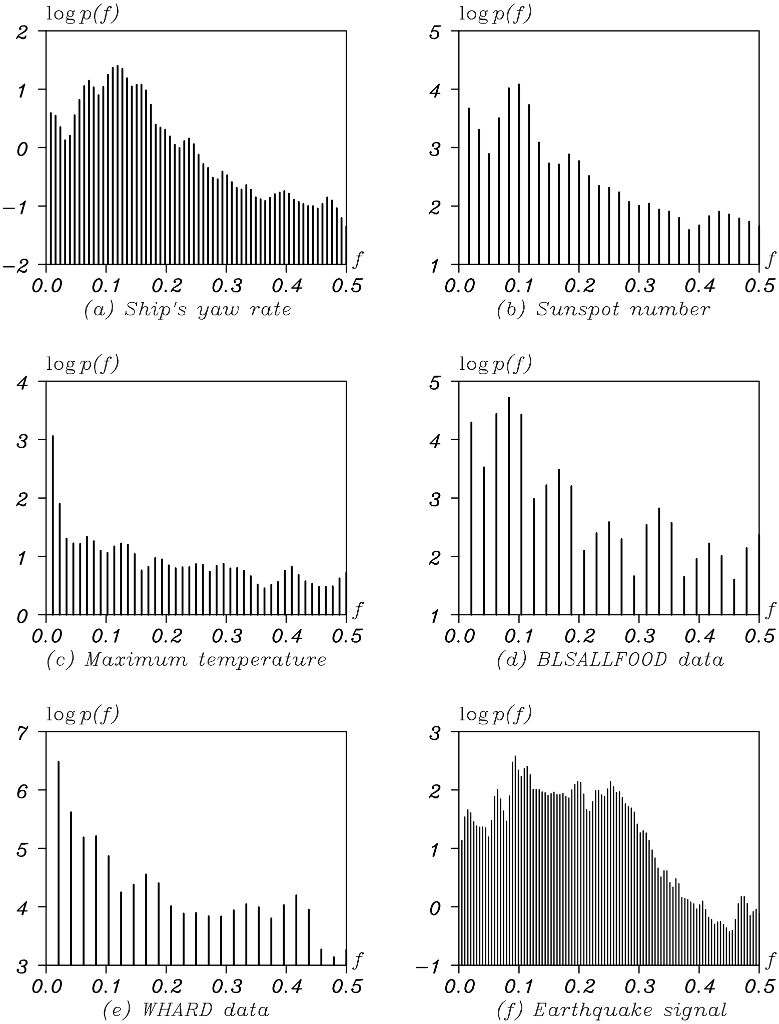

Figure 3.8 *Smoothed periodograms of the data shown in Figure 1.1. Horizontal axis: frequency f, vertical axis: periodogram on a logarithmic scale,* $\log p(f)$.

3.4 Computational Method of Periodogram

The Görtzel method is known to be an effective method of calculating Fourier transforms exactly. If the Fourier cosine transform and the Fourier sine transform of the series $x_0, \cdots, x_{L-1}$ are computed directly,

$$X_c(f) = \sum_{n=0}^{L-1} x_n \cos(2\pi n f), \quad X_s(f) = \sum_{n=0}^{L-1} x_n \sin(2\pi n f),$$

L additions and multiplications and L evaluations of trigonometric functions are necessary for each calculation.

However, by adopting the Görtzel method, based on the additive theorem for trigonometric functions, to compute the Fourier transform $X_c(f)$ and $X_s(f)$, we only need to evaluate the trigonometric functions twice, i.e., $\cos 2\pi f$ and $\sin 2\pi f$. This algorithm is based on the following properties of the trigonometric functions. If we put $a_0 = 0$, $a_1 = 1$ and generate $a_2, \cdots, a_{L-1}$ by $a_n = 2a_{n-1}\cos 2\pi f - a_{n-2}$, then $\sin 2\pi n f$ and $\cos 2\pi n f$ can be obtained by

$$\sin 2\pi n f = a_n \sin 2\pi f, \quad \cos 2\pi n f = a_n \cos 2\pi f - a_{n-1},$$

respectively.

3.5 Computation of the Periodogram by Fast Fourier Transform

As noted in the last section, the periodogram is obtained from the discrete Fourier transform of the sample autocovariance function. In general, N^2 addition and multiplication operations are necessary to calculate the discrete Fourier transform of a series of length N. Consequently, it takes a long time to compute the discrete Fourier transform when N is very large.

On the other hand, the fast Fourier transform (FFT) provides us with a very efficient algorithm. If the number of data points is of the form $N = p^\ell$, then this method requires approximately $Np\ell$ necessary operations, thus reducing the number of necessary operations by a factor of $Np\ell/N^2 = p\ell/N$. For instance, when $N = 1024 = 2^{10}$ (or $N = 4096 = 2^{12}$), the number of necessary operations is reduced by a factor of approximately $1/50$ (or $1/170$).

However, if we calculate the periodogram by the formula (3.8), i.e., the Fourier transform of the sample autocovariance function, $N^2/2$ operations are required to obtain the sample autocovariance function $\hat{C}_k$, $k = 0, \cdots, N-1$. Therefore, it might be more efficient to apply the FFT algorithm directly to the time series to obtain the periodogram. The Fourier transform, X_j, of a time series $y_1, \cdots, y_N$ is obtained by

$$\begin{aligned} X_j &= \sum_{n=1}^{N} y_n e^{-2\pi i(n-1)j/N} \\ &= \sum_{n=1}^{N} y_n \cos\frac{2\pi(n-1)j}{N} - i\sum_{n=1}^{N} y_n \sin\frac{2\pi(n-1)j}{N} \\ &\equiv \mathrm{FC}_j - i\,\mathrm{FS}_j, \end{aligned} \tag{3.16}$$

for $j = 0, \cdots, N/L$.

Then the periodogram is obtained by

$$p_j = \frac{|X_j|^2}{N} = \frac{1}{N}\left|\sum_{n=1}^{N} y_n e^{-2\pi i(n-1)j/N}\right|^2 = \frac{\mathrm{FC}_j^2 + \mathrm{FS}_j^2}{N}. \tag{3.17}$$

It can be easily confirmed that the periodogram (3.17) agrees with the periodogram obtained using the original definition (3.8). In particular, when the length of the time series is $N = 2^\ell$ for some integer ℓ, the FFT is readily calculable.

For a time series of general length, i.e., not expressible in the form of $N = 2^\ell$, we might use the prime number factorization: $N = p_1^{\ell_1} \times \cdots \times p_m^{\ell_m}$. An alternative simple way of computing the periodogram by means of the FFT algorithm is to apply the FFT after modifying the time series by adding $(2^\ell - N)$ zeros behind the data, to make it of length $N' = 2^\ell$. By this method, we can obtain the same value for the sample spectrum that is calculated by equation (3.13) for the frequencies $f_j = j/N'$, $j = 0, \cdots, N'/2$.

It should be noted here that we can compute the Fourier transform for arbitrary frequencies f by using the original definition (3.13). However, if the data length is N, the frequencies of the periodogram obtained by the FFT algorithm are limited to $f_k = k/N$.

Therefore, if $N \neq 2^\ell$, the periodogram obtained using the FFT is evaluated at different frequencies from those of the periodogram obtained directly, using the definition in Section 3.2. These differences are not very crucial when the true spectrum is continuous. However, if the true spectrum contains line spectra or sharp peaks, the two methods might yield quite different results.

Figure 3.9 (a) shows the realizations of the model that has two line

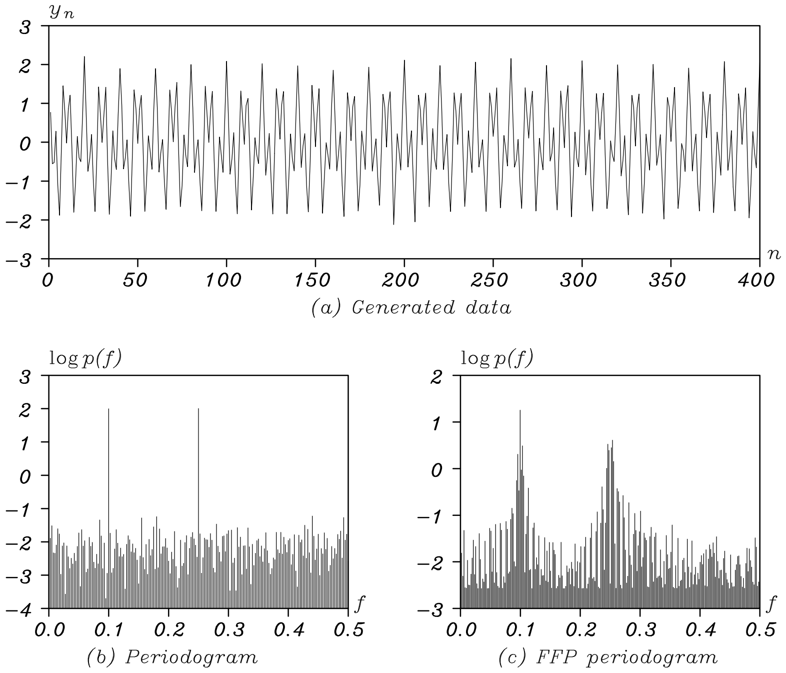

Figure 3.9 *Data with line spectrum and its periodograms obtained by (3.8) and by FFT after adding 112 zeros.*

spectra defined by

$$y_n = \cos\frac{2\pi n}{10} + \cos\frac{2\pi n}{4} + w_n, \tag{3.18}$$

where $N = 400$ and $w_n \sim N(0, 0.01)$. Figure 3.9 (b) shows the periodogram obtained from the data $y_1, \cdots, y_{400}$ for which two line spectra are seen at the frequencies $f = 0.05$ and $f = 0.0125$ corresponding to the two trigonometric functions of (3.18). For other frequencies that correspond to the white noise w_n, the periodogram fluctuates around at a certain level.

On the other hand, Figure 3.9 (c) shows the periodogram obtained by using the FFT after generating the data with $N' = 512 = 2^9$ by adding 112 zeros behind $y_1, \cdots, y_{400}$. In this case, the periodogram (c) looks quite different from the periodogram (b), because the frequencies to be calculated for the periodogram (c) have deviated from the position of the line spectrum.

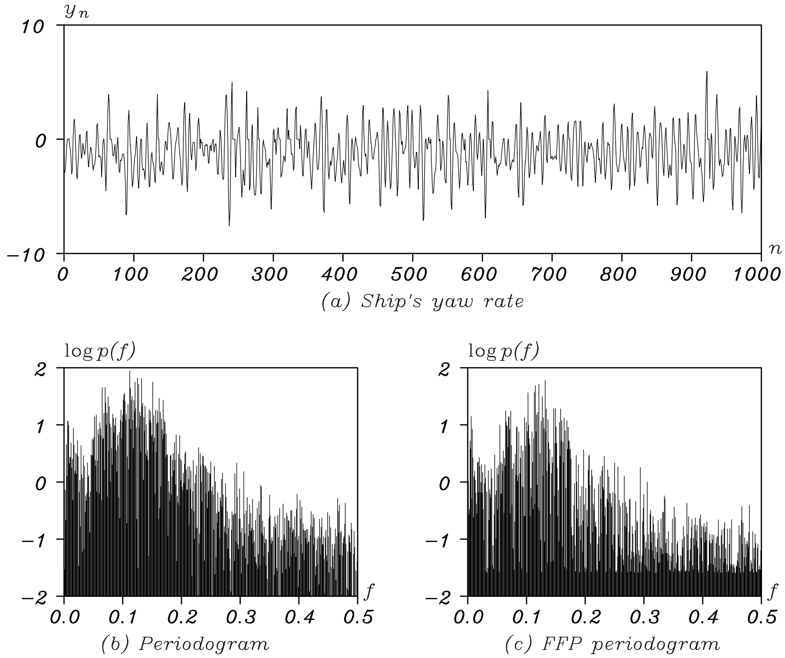

(a) Ship's yaw rate

(b) Periodogram

(c) FFP periodogram

Figure 3.10: *Yaw rate data, periodogram and FFT spectrum.*

Figure 3.10 (a) duplicates the ship's yaw rate data shown in Figure 1.1 (a). Plots (b) and (c) show the periodograms obtained using the original definition and the FFT, respectively. This example shows that, if the spectrum is continuous and does not contain any line spectra, the periodogram obtained by using FFT after adding zeros behind the data is similar to the periodogram obtained using the original definition.

Problems

1. Verify equation (3.2), that the power spectrum can be expressed using a cosine function.
2. Using the results of Equation 4 of Chapter 2, obtain the power spectrum of the time series $y_n = v_n - cv_{n-1}$, when v_n is a white noise with mean 0 and variance 1.

3. If the autocovariance function is given by $C_k = \sigma^2(1-a^2)^{-1}a^{|k|}$, verify that the power spectrum can be obtained using equation (3.5).
4. Show that the power spectrum of the time series (3.8) is given by (3.17).
5. Show the asymptotic unbiasedness of the sample spectrum, i.e., that $\lim_{n\to\infty} E\,[\,\hat{p}(f)\,] = p(f)$.

Chapter 4

Statistical Modeling

In the statistical analysis of time series, measurements of a phenomenon with uncertainty are considered to be the realization of a random variable that follows a certain probability distribution. Time series models and statistical models, in general, are built to specify this probability distribution based on data. In this chapter, a basic criterion is introduced for evaluating the closeness between the true probability distribution and the probability distribution specified by a model. Based on this criterion, we can derive a unified approach for building statistical models including the maximum likelihood method and the information criterion, AIC (Akaike (1973,1974), Sakamoto et al. (1986) and Konishi and Kitagawa (2008)).

4.1 Probability Distributions and Statistical Models

Given a *random variable* Y, the probability that the event $Y \le y$ occurs, $\text{Prob}(Y \le y)$ can be defined for all real numbers $y \in R$. Considering this to be a function of y, the function of y defined by

$$G(y) = \text{Prob}(Y \le y) \tag{4.1}$$

is called the *probability distribution function* (or *distribution function*) of the random variable Y.

Random variables used in time series analysis are usually *continuous*, and their distribution functions are expressible in integral form

$$G(y) = \int_{-\infty}^{y} g(t)dt, \tag{4.2}$$

with a function that satisfies $g(t) \ge 0$ for $-\infty < t < \infty$. Here, $g(x)$ is called a *density function*. On the other hand, if the distribution function or the density function is given, the probability that the random variable Y satisfies $a < Y \le b$ for arbitrary $a < b$ is obtained by

$$G(b) - G(a) = \int_{a}^{b} g(x)dx. \tag{4.3}$$

In statistical analysis, various distributions are used to model characteristics of the data. Typical density functions are as follows:

(a) **Normal distribution (Gaussian distribution).** The distribution with density function

$$g(x) = \frac{1}{\sqrt{2\pi\sigma^2}} \exp\left\{ -\frac{(x-\mu)^2}{2\sigma^2} \right\}, \qquad -\infty < x < \infty \tag{4.4}$$

is called a *normal distribution*, or a *Gaussian distribution*, and is denoted by $N(\mu, \sigma^2)$. The mean and variance are given by μ and σ^2, respectively. $N(0,1)$ is called the standard normal distribution.

(b) **Cauchy distribution.** The distribution with density function

$$g(x) = \frac{\tau}{\pi\{(x-\mu)^2 + \tau^2\}}, \qquad -\infty < x < \infty \tag{4.5}$$

is called a *Cauchy distribution.* μ and τ^2 are called the location parameter and the dispersion parameter, respectively. Note that the square root of dispersion parameter, τ, is called the scale parameter.

(c) **Pearson family of distributions.** The distribution with density function

$$g(x) = \frac{c}{\{(x-\mu)^2 + \tau^2\}^b}, \qquad -\infty < x < \infty \tag{4.6}$$

is called the *Pearson family of distributions* with central parameter μ, dispersion parameter τ^2 and shape parameter b. The value c is a normalizing constant given by $c = \tau^{2b-1}\Gamma(b)/(\Gamma(b-\frac{1}{2})\Gamma(\frac{1}{2}))$. This distribution agrees with the Cauchy distribution for $b = 1$. Moreover, if $b = (k+1)/2$ with a positive integer k, it is called the *t-distribution* with k degrees of freedom.

(d) **Exponential distribution.** The distribution with density function

$$g(x) = \begin{cases} \lambda e^{-\lambda x} & \text{for } x \geq 0 \\ 0 & \text{for } x < 0 \end{cases} \tag{4.7}$$

is called the exponential distribution. The mean and variance are given by λ^{-1} and λ^{-2}, respectively.

(e) χ^2 **distribution (chi-square distribution).**
The distribution with density function

$$g(x) = \begin{cases} \dfrac{1}{2^{k/2}\Gamma(\frac{k}{2})} e^{-\frac{x}{2}} x^{\frac{k}{2}-1} & \text{for } x \geq 0 \\ 0 & \text{for } x < 0 \end{cases} \tag{4.8}$$

is called the χ^2 *distribution* with k degrees of freedom. Especially, for $k=2$, it becomes an exponential distribution. The sum of the square of k Gaussian random variables follows the χ^2 distribution with k degrees of freedom.

(f) **Double exponential distribution.** The distribution with density function

$$g(x) = e^{x-e^x} \tag{4.9}$$

is called the *double exponential distribution*. The logarithm of the exponential random variable follows the double exponential distribution.

(g) **Uniform distribution.** The distribution with density function

$$g(x) = \begin{cases} (b-a)^{-1}, & \text{for } a \le x < b \\ 0, & \text{otherwise} \end{cases} \tag{4.10}$$

is called the *uniform distribution* over $[a,b)$.

Example Figure 4.1 shows the density functions defined in (a)–(f) above. By the simulation methods to be discussed in Chapter 16, data $y_1,\cdots,y_N$ can be generated that take various values according to the density function. The generated data are called *realizations* of the random variable. Figure 4.2 shows examples of realizations with the sample size $N=20$ for the distributions of (a)–(c) and (f) above.

If a probability distribution or a density function is given, we can generate data that follow the distribution. On the other hand, in statistical analysis, when data $y_1,\cdots,y_N$ have been obtained, they are considered to be realizations of a random variable Y. That is, we assume a random variable Y underlying the data, and when we obtain the data, we consider them as realizations of that random variable. Here, the density function $g(y)$ defining the random variable is called the *true model*. Since this true model is usually unknown for us, given a set of data, it is necessary to estimate the probability distribution that generates the data. For example, we estimate the density function shown in Figure 4.1 from the data shown in Figure 4.2. Here, the density function estimated from data is called a *statistical model* and is denoted by $f(y)$.

In ordinary statistical analysis, the probability distribution is sufficient to characterize the data, whereas for time series data, we have to consider the joint distribution $f(y_1,\cdots,y_N)$ as shown in Chapter 2. In

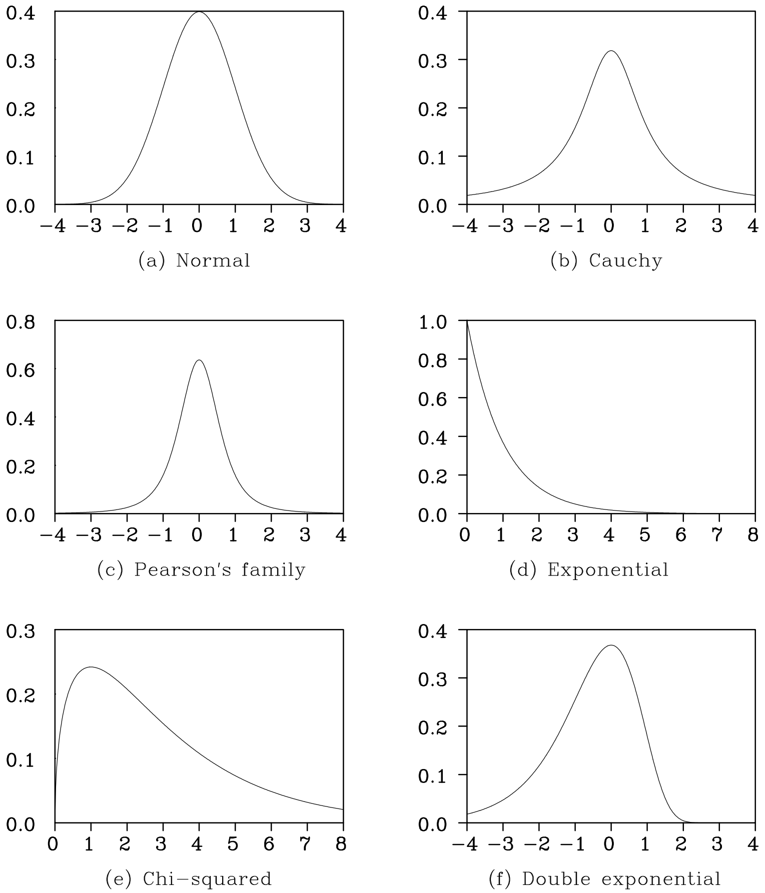

(a) Normal

(b) Cauchy

(c) Pearson's family

(d) Exponential

(e) Chi−squared

(f) Double exponential

Figure 4.1: *Density functions of various probability distributions.*

Chapter 2, we characterized the time series $y_1, \cdots, y_N$ using the sample mean $\hat{\mu}$ and the sample autocovariance function $\hat{C}_k$. The implicit assumption behind this is that the N dimensional vector $y = (y_1, \cdots, y_N)^T$ follows a multidimensional normal distribution with mean vector $\hat{\mu} =$

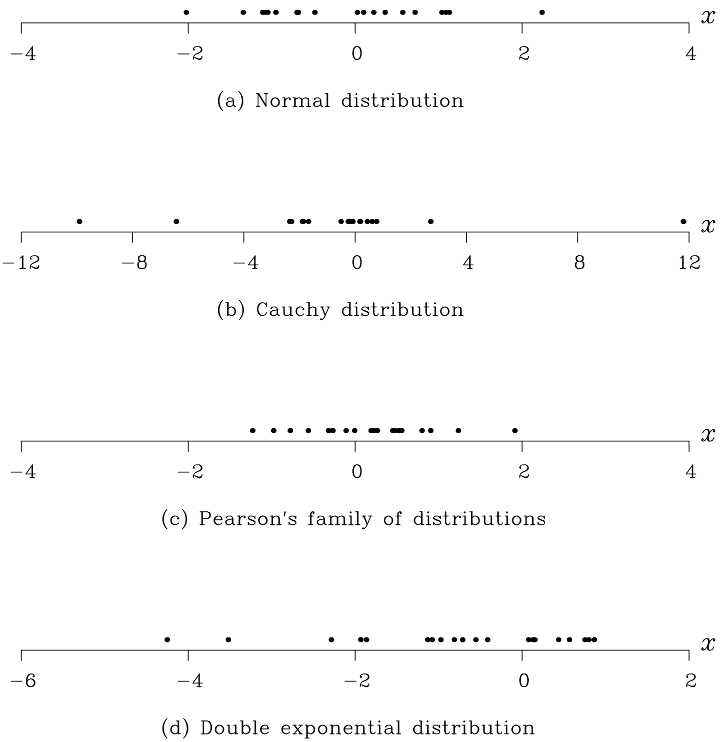

(a) Normal distribution

(b) Cauchy distribution

(c) Pearson's family of distributions

(d) Double exponential distribution

Figure 4.2: *Realizations of various probability distributions.*

$(\hat{\mu}, \cdots, \hat{\mu})^T$ and variance covariance matrix

$$\hat{C} = \begin{bmatrix} \hat{C}_0 & \hat{C}_1 & \cdots & \hat{C}_{N-1} \\ \hat{C}_1 & \hat{C}_0 & \cdots & \hat{C}_{N-2} \\ \vdots & \vdots & \ddots & \vdots \\ \hat{C}_{N-1} & \hat{C}_{N-2} & \cdots & \hat{C}_0 \end{bmatrix}. \tag{4.11}$$

This model can express an arbitrary Gaussian stationary time series very flexibly. However, it does not achieve an efficient compression of the information contained in the data since it requires the estimation of $N+1$ unknown parameters, $\hat{C}_0, \cdots, \hat{C}_{N-1}$ and $\hat{\mu}$, from N observations. On the other hand, stationary time series models that will be discussed in Chapter 5 and later can express the covariance matrix of (4.11) using only a small number of parameters.

4.2 K-L Information and the Entropy Maximization Principle

It is assumed that a true model generating the data is $g(y)$ and that $f(y)$ is an approximating statistical model. In statistical modeling, we aim at building a model $f(y)$ that is "close" to the true model $g(x)$. To achieve this, it is necessary to define a criterion to evaluate the goodness of the model $f(y)$ objectively.

In this book, we use the *Kullback-Leibler information* (hereinafter, abbreviated as *K-L information* (Kullback and Leibler (1951)))

$$I(g;f) = \mathrm{E}_Y \log\left\{\frac{g(Y)}{f(Y)}\right\} = \int_{-\infty}^{\infty} \log\left\{\frac{g(y)}{f(y)}\right\} g(y)dy \qquad (4.12)$$

as a criterion. Here, E_Y denotes the expectation with respect to the true density function $g(y)$ and the last expression in (4.12) applies to a model with a continuous probability distribution. This K-L information has the following properties:

$$\begin{array}{llcll} \text{(i)} & I(g;f) & \geq & 0 & \\ \text{(ii)} & I(g;f) & = & 0 \quad \Longleftrightarrow & g(y) = f(y). \end{array} \qquad (4.13)$$

The negative of the K-L information, $B(g;f) = -I(g;f)$, is called the generalized (or Boltzmann) entropy. When n realizations are obtained from the model distribution $f(y)$, the entropy is approximately $1/N$ of the logarithm of the probability that the relative frequency distribution coincides with the true distribution $g(y)$. Therefore, we can say that the smaller the value of the K-L information, the closer the probability distribution $f(y)$ is to the true distribution $g(y)$. Statistical models approximate the true distribution $g(y)$ based on the data $y_1,\cdots,y_N$, whose goodness of approximation can be evaluated by the K-L information, $I(g;f)$. In statistical modeling, the strategy of constructing a model so as to maximize the entropy $B(g;f) = -I(g;f)$ is referred to as the *entropy maximization principle* (Akaike (1977)).

Example (Kullback-Leibler information of a normal distribution model) Consider the case where both the true model, $g(y)$, and the approximate model, $f(y)$, are normal distributions defined by

$$g(y|\mu,\sigma^2) \quad = \quad \frac{1}{\sqrt{2\pi\sigma^2}} \exp\left\{-\frac{(y-\mu)^2}{2\sigma^2}\right\}$$

$$f(y|\xi,\tau^2) \;=\; \frac{1}{\sqrt{2\pi\tau^2}}\exp\left\{-\frac{(y-\xi)^2}{2\tau^2}\right\}. \tag{4.14}$$

In this case, since the following holds:

$$\log\left\{\frac{g(y)}{f(y)}\right\} = \frac{1}{2}\left\{\log\frac{\tau^2}{\sigma^2} - \frac{(y-\mu)^2}{\sigma^2} + \frac{(y-\xi)^2}{\tau^2}\right\}, \tag{4.15}$$

the K-L information is

$$\begin{aligned} I(g;f) &= \mathrm{E}_Y \log\left\{\frac{g(Y)}{f(Y)}\right\} \\ &= \frac{1}{2}\left\{\log\frac{\tau^2}{\sigma^2} - \frac{\mathrm{E}_Y(Y-\mu)^2}{\sigma^2} + \frac{\mathrm{E}_Y(Y-\xi)^2}{\tau^2}\right\} \\ &= \frac{1}{2}\left\{\log\frac{\tau^2}{\sigma^2} - 1 + \frac{\sigma^2+(\mu-\xi)^2}{\tau^2}\right\}. \end{aligned} \tag{4.16}$$

If the true distribution $g(y)$ is the standard normal distribution, $N(0,1)$, and the model $f(x)$ is $N(0.1, 1.5)$, then the K-L information can be easily evaluated as $I(g;f) = (\log 1.5 - 1 + 1.01/1.5)/2 = 0.03940$.

Similar to the above example, the K-L information $I(g;f)$ is easily calculated, if both g and f are normal distributions. However, for the combination of general distributions g and f, it is not always possible to compute $I(g;f)$ analytically. Therefore, in general, to obtain the K-L information, we need to resort to numerical computation. To illustrate the accuracy of numerical computation, Table 4.1 shows the K-L information with respect to two density functions $g(y)$ and $f(y)$ obtained by numerical integration over $[x_0, x_k]$ using the trapezoidal rule

$$\hat{I}(g\,;f) = \frac{\Delta x}{2}\sum_{i=1}^{k}\{h(x_i)+h(x_{i-1})\}, \tag{4.17}$$

where k is the number of nodes and

$$\begin{aligned} x_0 &= -x_k, \\ x_i &= x_0 + (x_k - x_0)\frac{i}{k} && (4.18) \\ h(x) &= g(x)\log\frac{g(x)}{f(x)} && (4.19) \\ \Delta x &= \frac{x_k - x_0}{k}\,. \end{aligned}$$

Table 4.1 *K-L information for various values of x_n and k. (g: normal distribution and f: normal distribution)*

x_k	k	Δx	$\hat{I}(g\,;f)$	$\hat{G}(x_k)$
4.0	8	1.000	0.03974041	0.99986319
4.0	16	0.500	0.03962097	0.99991550
4.0	32	0.250	0.03958692	0.99993116
4.0	64	0.125	0.03957812	0.99993527
6.0	12	1.000	0.03939929	1.00000000
6.0	24	0.500	0.03939924	1.00000000
6.0	48	0.250	0.03939924	1.00000000
6.0	96	0.125	0.03939923	1.00000000
8.0	16	1.000	0.03939926	1.00000000
8.0	32	0.500	0.03939922	1.00000000
8.0	64	0.250	0.03939922	1.00000000
8.0	128	0.125	0.03939922	1.00000000

Table 4.1 shows the numerically obtained K-L information $\hat{I}(g\ f)$ and the $\hat{G}(x_k)$, obtained by integrating the density function $g(y)$ from $-x_k$ to x_k, for x_0 = 4, 6 and 8, and k = 8, 16, 32 and 64. It can be seen from Table 4.1 that if x_0 is set sufficiently large, a surprisingly good approximation is obtained even with such small values of k as $k = 16$ or $\Delta x = 0.5$. This is because we assume that $g(y)$ follows a normal distribution, and it vanishes to 0 very rapidly as $|x|$ becomes large. When a density function is used for $g(y)$ whose convergence is slower than that of the normal distribution, the accuracy of numerical integration can be judged by checking whether $\hat{G}(x_k)$ is close to one.

Table 4.2 shows the K-L information obtained by the numerical integration when $g(y)$ is assumed to be the standard normal distribution, and $f(y)$ is assumed to be the standard Cauchy distribution with $\mu = 0$ and $\tau^2 = 1$. It can be seen that even with a large Δx, such as 0.5, we can get very good approximations of $\hat{I}(g;f)$, obtained by using a smaller Δx, and $\hat{G}(x_k)$ is 1 even for $\Delta x = 0.5$.

4.3 Estimation of the K-L Information and Log-Likelihood

Though the K-L information was introduced as a criterion for the goodness of fit of a statistical model in the previous section, it is rarely used

Table 4.2 *Numerical integration for K-L information with various values of k when $g(y)$ is the standard normal distribution and $f(y)$ is a Cauchy distribution.*

x_k	k	Δx	$\hat{I}(g\,,f)$	$\hat{G}(x_k)$
8.0	16	1.000	0.25620181	1.00000001
8.0	32	0.500	0.25924202	1.00000000
8.0	64	0.250	0.25924453	1.00000000
8.0	128	0.125	0.25924453	1.00000000

directly to evaluate an actual statistical model except for the case of a Monte Carlo experiment for which the true distribution is known. In actual statistical analysis, the true distribution is unknown and thus the K-L information cannot be calculated. In an actual situation, the data $y_1,\cdots,y_N$ are obtained instead of the true distribution $g(y)$. Hereinafter we consider the method of estimating the K-L information of the model $f(y)$ by assuming that the data $y_1,\cdots,y_N$ are independently observed from $g(y)$ (Sakamoto et al. (1986) and Konishi and Kitagawa (2008)).

According to the entropy maximization principle, the best model can be obtained by finding the model that maximizes $B(g;f)$ or minimizes $I(g;f)$. As a first step, the K-L information can be decomposed into two terms as

$$I(g;f) = \mathrm{E}_Y \log g(Y) - \mathrm{E}_Y \log f(Y). \tag{4.20}$$

Although the first term on the right-hand side of equation (4.20) cannot be computed unless the true distribution $g(y)$ is given, it can be ignored because it is a constant, independent of the model $f(y)$. Therefore, a model that maximizes the second term on the right-hand side signifies a good model. This second term is called *expected log-likelihood*. For a continuous model with density function $f(y)$, it is expressible as

$$\mathrm{E}_Y \log f(Y) = \int \log f(y) g(y) dy. \tag{4.21}$$

The expected log-likelihood also cannot be directly calculated when the true model $g(y)$ is unknown. However, because data y_n is generated according to the density function $g(y)$, due to the *law of large numbers*, it is the case that

$$\frac{1}{N}\sum_{n=1}^{N} \log f(y_n) \longrightarrow \mathrm{E}_Y \log f(Y), \tag{4.22}$$

as the number of data points goes to infinity, i.e., $N \rightarrow \infty$.

Therefore, by maximizing the left term, $\sum_{n=1}^{N} \log f(y_n)$, instead of the original criterion $I(g;f)$, we can approximately maximize the entropy. When the observations are obtained independently, N times the term on the left-hand side of (4.22) is called the *log-likelihood*, and it is given by

$$\ell = \sum_{n=1}^{N} \log f(y_n). \tag{4.23}$$

The quantity obtained by taking the exponential of ℓ,

$$L = \prod_{n=1}^{N} f(y_n) \tag{4.24}$$

is called the *likelihood*.

For models used in time series analysis, the assumption that the observations are obtained independently, does not usually hold. For such a general situation, the likelihood is defined by using the joint distribution of $y_1, \cdots, y_N$ as

$$L = f(y_1, \cdots, y_N). \tag{4.25}$$

Equation (4.25) is a natural extension of (4.24), because it reduces to (4.24) when independence of the observations is assumed. In this case, the log-likelihood is obtained by

$$\ell = \log L = \log f(y_1, \cdots, y_N). \tag{4.26}$$

4.4 Estimation of Parameters by the Maximum Likelihood Method

If a model contains a parameter θ and its distribution can be expressed as $f(y) = f(y|\,\theta\,)$, the log-likelihood ℓ can be considered as a function of the parameter θ. Therefore, by expressing the parameter θ explicitly,

$$\ell(\theta) = \begin{cases} \sum_{n=1}^{N} \log f(y_n|\,\theta\,), & \text{for independent data} \\ \log f(y_1, \cdots, y_N|\,\theta\,), & \text{otherwise} \end{cases} \tag{4.27}$$

is called the *log-likelihood function* of θ.

Since the log-likelihood function $\ell(\theta)$ evaluates the goodness of fit of the model specified by the parameter θ, by selecting θ so as to maximize $\ell(\theta)$, we can determine the optimal value of the parameter of the parametric model, $f(y|\,\theta\,)$. The parameter estimation method derived by maximizing the likelihood function or the log-likelihood function is referred to as the *maximum likelihood method*. The parameter estimated by the method of maximum likelihood is called the *maximum likelihood estimate* and is denoted by $\hat{\theta}$.

Under some regularity conditions, the maximum likelihood estimate has the following properties (Huber (1967) and Konishi and Kitagawa (2008)):

(i) The maximum likelihood estimator $\hat{\theta}$ converges in probability to θ_0 as sample size $N \to \infty$.

(ii) (Central limit theorem) The distribution of $\sqrt{N}(\hat{\theta}-\theta_0)$ converges in law to the normal distribution with the mean vector 0 and the variance covariance matrix $J^{-1}IJ$ as $N \to \infty$, i.e.,

$$\sqrt{N}(\hat{\theta}-\theta_0) \to N(0, J^{-1}IJ), \tag{4.28}$$

where I and J are the *Fisher information matrix* and the negative of the expected Hessian with respect to $\hat{\theta}$ defined by

$$\begin{aligned} I &\equiv \mathrm{E}_Y\left\{\frac{\partial}{\partial\theta}\log f(Y|\theta_0)\right\}\left\{\frac{\partial}{\partial\theta}\log f(Y|\theta_0)\right\}^T, & (4.29)\\ J &\equiv -\mathrm{E}_Y\left\{\frac{\partial^2}{\partial\theta\partial\theta^T}\log f(Y|\theta_0)\right\}. & (4.30)\end{aligned}$$

Example (Maximum likelihood estimate of the mean of the normal distribution model) Consider a normal distribution model with mean μ and variance 1

$$f(y|\mu) = \frac{1}{\sqrt{2\pi}}\exp\left\{-\frac{(y-\mu)^2}{2}\right\}, \tag{4.31}$$

and estimate the mean parameter μ by the maximum likelihood method. Given N observations, $y_1, \cdots, y_N$, the log-likelihood function is given by

$$\ell(\mu) = -\frac{N}{2}\log 2\pi - \frac{1}{2}\sum_{n=1}^{N}(y_n-\mu)^2. \tag{4.32}$$

To maximize the log-likelihood $\ell(\mu)$, it suffices to find μ that minimizes

$$S(\mu) = \sum_{n=1}^{N}(y_n-\mu)^2. \tag{4.33}$$

By equating the first derivative of $S(\mu)$ to zero, we obtain

$$\hat{\mu} = \frac{1}{N}\sum_{n=1}^{N} y_n. \tag{4.34}$$

A method of estimating the parameters of a model by minimizing the sum of squares such as (4.30) is called the *least squares method*.

A general method of solving the least squares problem will be described in Chapter 5. For a normal distribution model, the maximum likelihood estimates of the parameters often coincide with the least squares estimates and can be solved analytically. However, the likelihood or the log-likelihood functions of a time series model is very complicated in general, and it is not possible to obtain maximum likelihood estimates or even their approximate values analytically except for some models such as the AR model in Chapter 7 and the polynomial trend model in Chapter 11.

In general, the maximum likelihood estimate of the parameter θ of a time series model is obtained by using a *numerical optimization* algorithm based on the *quasi-Newton method* described in Appendix A. According to this method, using the value $\ell(\theta)$ of the log-likelihood and the first derivative $\partial\ell/\partial\theta$ for a given parameter θ, the maximizer of $\ell(\theta)$ is automatically estimated by repeating

$$\theta_k = \theta_{k-1} + \lambda_k H_{k-1}^{-1}\frac{\partial\ell}{\partial\theta}, \tag{4.35}$$

where θ_0 is an initial estimate of the parameter. The step width λ_k and the inverse matrix H_{k-1}^{-1} of the Hessian matrix are automatically obtained by the algorithm.

Example (Maximum likelihood estimate of the Cauchy distribution model) Assume that ten observations are given as follows.

−1.10	−0.40	−0.20	−0.02	0.02
0.71	1.35	1.46	1.74	3.89

The log-likelihood of the Cauchy distribution model

$$f(y|\mu,\tau^2) = \frac{1}{\pi}\frac{\tau}{(y-\mu)^2+\tau^2,} \tag{4.36}$$

is obtained by

$$\ell(\mu,\tau^2) = 5\log\tau^2 - 10\log\pi - \sum_{n=1}^{10}\log\{(y_n-\mu)^2+\tau^2\}. \tag{4.37}$$

Table 4.3 *Estimation of the parameters of the Cauchy distribution by the quasi-Newton method.*

k	μ	τ^2	log-likelihood	$\partial\ell/\partial\mu$	$\partial\ell/\partial\tau^2$
0	0.00000	1.00000	−19.1901	2.10968	−0.92404
1	0.38588	0.83098	−18.7140	−0.21335	−0.48655
2	0.34795	0.62966	−18.6536	−0.35810	0.06627
3	0.26819	0.60826	−18.6396	0.00320	−0.01210
4	0.26752	0.60521	−18.6395	0.00000	−0.00002
5	0.26752	0.60520	−18.6395	0.00000	0.00000

The first derivatives of the log-likelihood with respect to the parameter $\theta = (\mu, \tau^2)^T$ are given by

$$\frac{\partial \ell}{\partial \mu} = 2\sum_{n=1}^{10} \frac{y_n - \mu}{(y_n-\mu)^2 + \tau^2} \tag{4.38}$$

$$\frac{\partial \ell}{\partial \tau^2} = \frac{5}{\tau^2} - \sum_{n=1}^{10} \frac{1}{(y_n-\mu)^2 + \tau^2}. \tag{4.39}$$

Table 4.3 summarizes the optimization process for obtaining the maximum likelihood estimate of the parameters of the Cauchy distribution when the initial vector is set to $\theta_0 = (0,1)^T$. The absolute values of $\partial\ell/\partial\mu$ and $\partial\ell/\partial\tau^2$ decrease rapidly, and the maximum likelihood estimate is obtained with five recursions.

As noted in the above example, when the log-likelihood and the first derivatives are obtained analytically, the maximum likelihood estimate of the parameter of the model can be obtained by using a numerical optimization method. However, in time series modeling, it is difficult to obtain the first derivative of the log-likelihood, because for many time series models, the log-likelihood function is in a very complicated form. For many time series models, the log-likelihood is evaluated numerically, using a Kalman filter. Even in such cases, the maximum likelihood estimate can be obtained by using the first derivative computed by numerical differentiation of the log-likelihood. Table 4.4 shows the result of optimization by this method using the log-likelihood only. The results are almost identical with Table 4.2, and the recursion terminates in a smaller number of iterations.

Table 4.4 *Estimation of the parameters of the Cauchy distribution by a quasi-Newton method that uses numerical differentiation.*

k	μ	τ^2	log-likelihood	$\partial\ell/\partial\mu$	$\partial\ell/\partial\tau^2$
0	0.00000	1.00000	-19.1901	2.10967	-0.92404
1	0.38588	0.83098	-18.7140	-0.21335	-0.48655
2	0.34795	0.62966	-18.6536	-0.35810	0.06627
3	0.26819	0.60826	-18.6396	0.00320	-0.01210
4	0.26752	0.60521	-18.6395	0.00000	-0.00000

4.5 AIC (Akaike Information Criterion)

It has been established that the log-likelihood is a natural estimator of the expected log-likelihood and that the maximum likelihood method can be used for estimation of the parameters of the model. Similarly, if there are several candidate parametric models, it seems natural to estimate the parameters by the maximum likelihood method, and then find the best model by comparing the values of the maximum log-likelihood $\ell(\hat{\theta})$. However, the maximum log-likelihood is not directly available for comparisons among several parametric models, because of bias. That is, for the model with the maximum likelihood estimate $\hat{\theta}$, the maximum log-likelihood $(N^{-1}\ell(\hat{\theta})$ has a positive bias as an estimator of $\mathrm{E}_Y \log f(Y|\hat{\theta})$ (see Figure 4.3 and Konishi and Kitagawa (2008)).

This bias is caused by using the same data twice for the estimation of the parameters of the model and also for the estimation of the expected log-likelihood for evaluation of the model.

The bias of $N^{-1}\ell(\hat{\theta}) \equiv N^{-1}\sum_{n=1}^{N} \log f(y_n|\hat{\theta})$ as an estimate of $\mathrm{E}_Y \log f(Y|\hat{\theta})$ is given by

$$C \equiv \mathrm{E}_X \left\{ \mathrm{E}_Y \log f(Y|\hat{\theta}) - N^{-1} \sum_{n=1}^{N} \log f(y_n|\hat{\theta}) \right\}. \tag{4.40}$$

Note here that the maximum likelihood estimate $\hat{\theta}$ depends on the sample X and can be expressed as $\hat{\theta}(X)$. And the expectation E_X is taken with respect to X.

Then, correcting the maximum log-likelihood $\ell(\hat{\theta})$ for the bias C, $N^{-1}\ell(\hat{\theta}) + C$ becomes an unbiased estimate of the expected log-likelihood $E_Y \log f(Y|\hat{\theta})$. Here, as will be shown later, since the bias is evaluated as $C = -N^{-1}k$, we obtain the *Akaike Information Criterion*

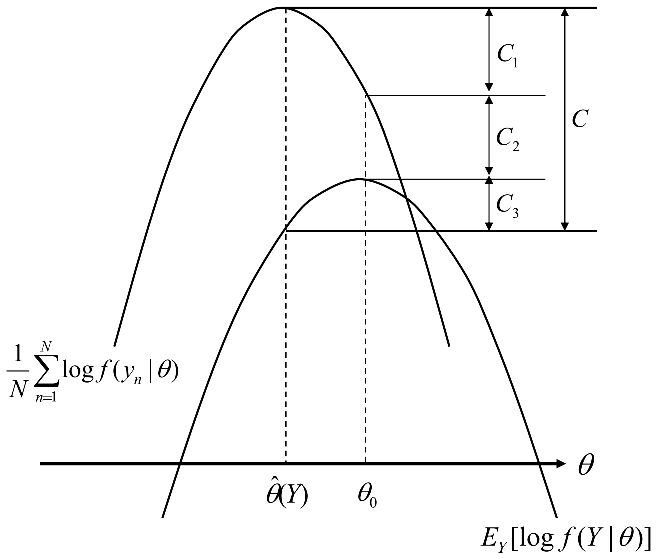
C_1
C_2
C_3
C
$\frac{1}{N}\sum_{n=1}^{N}\log f(y_n \mid \theta)$
θ
$\hat{\theta}(Y)$
θ_0
$E_Y[\log f(Y \mid \theta)]$

Figure 4.3 *Difference between the expected log-likelihood and the log-likelihood.*

(AIC)

$$\begin{aligned} \text{AIC} &= -2\,\ell(\hat{\theta}) + 2\,k \\ &= -2\,(\text{maximum log-likelihood}) \\ &\quad + 2\,(\text{number of parameters}). \end{aligned} \tag{4.41}$$

In this book, AIC is used as a criterion for model selection (Akaike (1973,1974), Sakamoto et al. (1986) and Konishi and Kitagawa (2008)).

Hereinafter, a brief derivation of the AIC will be shown in this section. Readers who are not interested in the model selection criterion itself may skip this part. For more details and other criteria, such as BIC and GIC, the readers are referred to Konishi and Kitagawa (2008).

Here, it is assumed that the true distribution is $f(y)$, the model distribution is $g(y)$ and the maximum likelihood estimate of the parameter θ based on data $X = (x_1, \cdots, x_N)$ is denoted by $\hat{\theta} \equiv \hat{\theta}(X)$. On the other hand, the parameter θ_0 that maximizes the expected log-likelihood

$\mathrm{E}_Y \log f(Y|\theta)$ is called the true parameter. Then, θ_0 satisfies

$$\frac{\partial}{\partial\theta}\mathrm{E}_Y \log f(Y|\theta_0) = 0.$$

On the other hand, since $\hat{\theta}$ maximizes the log-likelihood function $\ell(\theta) = \sum_{n=1}^{N} \log f(x_n|\theta)$, the following equation holds.

$$\frac{\partial}{\partial\theta}\sum_{n=1}^{N} \log f(x_n|\hat{\theta}) = 0.$$

Here, the terms in (4.37) can be decomposed into three terms (see Figure 4.3).

$$\begin{aligned} C &= \mathrm{E}_X\left\{\mathrm{E}_Y \log f(Y|\hat{\theta}) - \mathrm{E}_Y \log f(Y|\theta_0)\right\} \\ &\quad + \mathrm{E}_X\left\{\mathrm{E}_Y \log f(Y|\theta_0) - N^{-1}\sum_{n=1}^{N}\log f(x_n|\theta_0)\right\} \\ &\quad + \mathrm{E}_X\left\{N^{-1}\sum_{n=1}^{N}\log f(x_n|\theta_0) - N^{-1}\sum_{n=1}^{N}\log f(x_n|\hat{\theta})\right\} \\ &\equiv C_1 + C_2 + C_3. \end{aligned} \tag{4.42}$$

4.5.1 *Evaluation of C_1*

Consider the Taylor series expansion around θ_0 of the expected log-likelihood $\mathrm{E}_Y \log f(Y|\hat{\theta})$ of the model specified by the maximum likelihood estimate up to the second order. Exchanging the order of the differentiation and the expectation, we have

$$\begin{aligned} \mathrm{E}_Y \log f(Y|\hat{\theta}) &\approx \mathrm{E}_Y \log f(Y|\theta_0) + \left\{\frac{\partial}{\partial\theta}\mathrm{E}_Y \log f(Y|\theta_0)\right\}(\hat{\theta}-\theta_0) \\ &\quad + \frac{1}{2}(\hat{\theta}-\theta_0)^T\left\{\frac{\partial^2}{\partial\theta\partial\theta^T}\mathrm{E}_Y \log f(Y|\theta_0)\right\}(\hat{\theta}-\theta_0) \\ &= \mathrm{E}_Y \log f(Y|\theta_0) - \frac{1}{2}(\hat{\theta}-\theta_0)^T J(\hat{\theta}-\theta_0). \end{aligned}$$

Here, I and J are the Fisher information matrix and the negative of the expected Hessian defined by (4.29) and (4.30), respectively.

Then, according to the central limit theorem (4.28), $\sqrt{N}\big(\,(\hat{\theta}-\theta_0\big)$ follows a normal distribution with mean 0 and the variance-covariance matrix $J^{-1}IJ^{-1}$. Therefore, by taking the expectation with respect to X, it follows that

$$\mathrm{E}_X(\hat{\theta}-\theta_0)^T J(\hat{\theta}-\theta_0) \;=\; \frac{1}{N}\mathrm{trace}\left\{IJ^{-1}\right\} \;\approx\; \frac{k}{N} \tag{4.43}$$

where k is the dimension of the matrix I. Note that, if there exists θ_0 such that $g(y) = f(y|\theta_0)$, it follows that $J = I$, and trace $\left\{IJ^{-1}\right\} = k$ (Konishi and Kitagawa (2008)). Thus, we have an approximation to C_1 :

$$C_1 \equiv \mathrm{E}_X\left\{\mathrm{E}_Y \log f(Y|\hat{\theta}) - E_Y \log f(Y|\theta_0)\right\} \;\approx\; -\frac{k}{2N}. \tag{4.44}$$

4.5.2 *Evaluation of C_3*

By the Taylor series expansion of $N^{-1}\sum_{n=1}^{N}\log f(x_n|\theta_0)$ around $\hat{\theta}$, it follows that

$$\begin{aligned}\frac{1}{N}\sum_{n=1}^{N}&\log f(x_n|\theta_0)\\ &\approx\; \frac{1}{N}\sum_{n=1}^{N}\log f(x_n|\hat{\theta}) + \frac{1}{N}\sum_{n=1}^{N}\frac{\partial}{\partial\theta}\log f(x_n|\hat{\theta})(\theta_0-\hat{\theta})\\ &\quad +\frac{1}{2}(\theta_0-\hat{\theta})^T\left\{\frac{1}{N}\sum_{n=1}^{N}\frac{\partial^2}{\partial\theta\partial\theta^T}\log f(x_n|\hat{\theta})\right\}(\theta_0-\hat{\theta}).\end{aligned} \tag{4.45}$$

Since $\hat{\theta}$ is the maximum likelihood estimate, the second term on the right-hand side becomes 0. Moreover, according to the law of large numbers, if $N \to \infty$, it is the case that

$$\frac{1}{N}\sum_{n=1}^{N}\frac{\partial^2}{\partial\theta\partial\theta^T}\log f(x_n|\hat{\theta}) \longrightarrow \mathrm{E}_Y\left\{\frac{\partial^2}{\partial\theta\partial\theta^T}\log f(Y|\theta_0)\right\} = -J, \tag{4.46}$$

and we have

$$\frac{1}{N}\sum_{n=1}^{N}\log f(x_n|\theta_0) \approx \frac{1}{N}\sum_{n=1}^{N}\log f(x_n|\hat{\theta}) - \frac{1}{2}(\theta_0-\hat{\theta})^T J(\theta_0-\hat{\theta}).$$

Therefore, similarly to (4.44), by taking the expectation of both sides, we have the approximation

$$C_3 = \mathrm{E}_X\left\{\frac{1}{N}\sum_{n=1}^{N}\log f(x_n|\theta_0) - \frac{1}{N}\sum_{n=1}^{N}\log f(x_n|\hat{\theta})\right\} \;\approx\; -\frac{k}{2N}. \tag{4.47}$$

4.5.3 Evaluation of C_2

Since the expectation of $\log f(x_n|\theta_0)$ becomes the expected log-likelihood for any fixed θ_0, we have

$$C_2 = \mathrm{E}_X \left\{ \mathrm{E}_Y \log f(Y|\theta_0) - \frac{1}{N}\sum_{n=1}^{N} \log f(x_n|\theta_0) \right\} = 0. \tag{4.48}$$

4.5.4 Evaluation of C and AIC

By summing up the three expressions (4.44), (4.47) and (4.48), we have the approximation

$$C = \mathrm{E}_X \left\{ \mathrm{E}_Y \log f(Y|\hat{\theta}) - \frac{1}{N}\sum_{n=1}^{N} \log f(x_n|\hat{\theta}) \right\} \approx -\frac{k}{N}, \tag{4.49}$$

and this shows that $N^{-1}\ell(\hat{\theta})$ is larger than $\mathrm{E}_Y \log f(Y|\hat{\theta})$ by k/N on average.

Therefore, it can be seen that

$$N^{-1}\ell(\hat{\theta}) + C \approx N^{-1}\left(\ell(\hat{\theta}) - k\right) \tag{4.50}$$

is an approximately unbiased estimator of the expected log-likelihood $\mathrm{E}_Y \log f(Y|\hat{\theta})$ of the maximum likelihood model. The AIC is defined by multiplying (4.46) by $-2N$, i.e.,

$$\begin{aligned} \mathrm{AIC} &= -2\,\ell(\hat{\theta}) \;+\; 2\,k \\ &= -2\,(\text{maximum log-likelihood}) \\ &\quad +2\,(\text{number of parameters}). \end{aligned} \tag{4.51}$$

Because minimizing the AIC is approximately equivalent to minimizing the K-L information, an approximately optimal model is obtained by selecting the model that minimizes AIC. A reasonable and automatic model selection thus becomes possible by using this AIC.

4.6 Transformation of Data

When we draw graphs of positive valued processes, such as the number of occurrences of a certain event, the number of people or the amount of sales, we may find that the variance increases together with an increase in the mean value or the distribution is highly skewed. It is difficult to

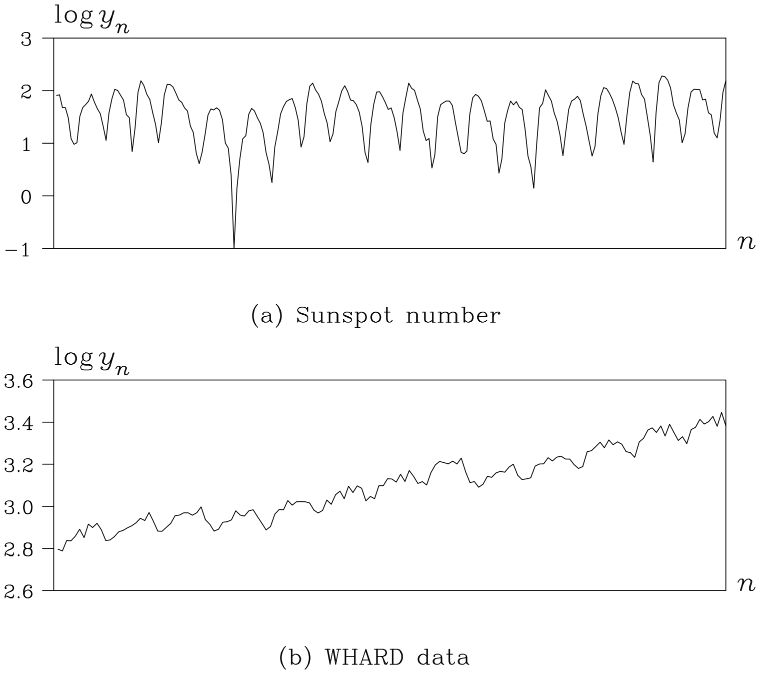

(a) Sunspot number

(b) WHARD data

Figure 4.4 *Log-transformation of the sunspot number data and the WHARD data.*

analyze such data using a simple model since the characteristics of the data change with its level and the distribution is significantly different from the normal distribution, unless we use the nonstationary models described in Chapters 11, 12 and 13, or the non-Gaussian models in Chapters 14 and 15.

Even in those cases, the variance of the log-transformed series $z_n = \log y_n$ might become almost uniform and its marginal distribution might be reasonably approximated by a normal distribution. In Figure 4.4, it can be seen that the highly skewed sunspot number data shown in plot (b) of Figure 1.1 become almost symmetric after log-transformation. Moreover, the WHARD data shown in the plot (e) of Figure 1.1 can be transformed to a series with approximately constant variance after log-transformation, though the variance of the original time series increases gradually with time.

The *Box-Cox transformation* is well known as a generic data transformation (Box and Cox (1964)), which includes the log-transformation as a special case

$$z_n = \begin{cases} \lambda^{-1}(y_n^\lambda - 1), & \text{if } \lambda \neq 0 \\ \log y_n, & \text{if } \lambda = 0. \end{cases} \tag{4.52}$$

Ignoring a constant term, the Box-Cox transformation yields the logarithm of the original series for $\lambda = 0$, the inverse for $\lambda = -1$ and the square root for $\lambda = 0.5$. In addition, it agrees with the original data for $\lambda = 1$. Applying the information criterion AIC to the Box-Cox transformation, we can determine the best parameter λ of the Box-Cox transformation (Konishi and Kitagawa (2008)). On the assumption that the density function of the data $z_n = h(y_n)$ obtained by the Box-Cox transformation of data y_n is given by $f(z)$, then the density function of y_n is obtained by

$$g(y) = \left| \frac{dh}{dy} \right| f(h(y)). \tag{4.53}$$

Here, $|dh/dy|$ is called the *Jacobian* of the transform. The equation (4.53) implies that a model for the transformed series automatically determines a model for the original data. For instance, assume that the values of AICs of the normal distribution models fitted to the original data y_n and transformed data z_n are evaluated as AIC_y and AIC_z, respectively. Then, it can be judged which, the original data or the transformed data, is closer to a normal distribution by comparing the values of

$$\text{AIC}_z' = \text{AIC}_z - 2\sum_{i=1}^{N} \log \left| \frac{dh}{dy} \right|_{y=y_i} \tag{4.54}$$

with AIC_y.

Namely, it will be considered that the original data are better than the transformed data, if $\text{AIC}_y < \text{AIC}_z'$, and the transformed data are better, if $\text{AIC}_y > \text{AIC}_z'$. Further, by finding a value that minimizes AIC_z', the optimal value λ of the Box-Cox transformation can be selected. However, in actual time series modeling, we usually fit various time series models to the Box-Cox transformation of the data. Therefore, in such a situation, it is necessary to correct the AIC of the time series model with the Jacobian of the Box-Cox transformation.

Table 4.5: *Various Box-Cox transforms and their AICs.*

λ	AIC	λ	AIC	λ	AIC
-1.0	2365.12	-0.2	2355.45	0.6	2370.74
-0.8	2360.46	0.0	2356.89	0.8	2378.55
-0.6	2357.27	0.2	2359.90	1.0	2387.94
-0.4	2355.59	0.4	2364.52		

Example (Box-Cox transformation of the sunspot number data) Table 4.5 shows the results of applying the Box-Cox transformation with various values of λ to the sunspot number data of Figure 1.1(b). In this case, it can be seen that the transformation with $\lambda = -0.2$, that is, $z_n = y_n^{-1/5}$ is the best Box-Cox transformation.

Problems

1. Given n integers $\{m_1, \ldots, m_n\}$, obtain the maximum likelihood estimate $\hat{\lambda}$ of the Poisson distribution model $f(m|\lambda) = e^{-\lambda}\lambda^m/m!$.
2. Given two sets of data $\{x_1, \ldots, x_n\}$ and $\{y_1, \ldots, y_m\}$ that follow normal distributions,

   (1) Assuming that the variances are the same, show a method of checking whether the means are identical by using the AIC.

   (2) Assuming that the means are the same, show a method of checking whether the variances are identical by using the AIC.
3. Given data $\{y_1, \ldots, y_n\}$, consider a method of deciding whether a Gaussian model or a Cauchy model is better by using the AIC.
4. In tossing a coin n times, a head occurred m times.

   (1) Obtain the probability of the occurrence of a head.

   (2) Consider a method of deciding whether this is a fair coin, based on the AIC.
5. Assume that the true density function is $g(y)$ and the model is $f(y|\theta)$. If there exists θ_0 such that $g(y) = f(y|\theta_0)$, show that $J = I$.
6. Obtain the density function of y when $z = \log y$ follows a Gaussian distribution $N(\mu, \sigma^2)$.

Chapter 5

The Least Squares Method

For many regression models and time series models that assume normality of the noise distribution, least squares estimates may often coincide with or provide good approximations to the maximum likelihood estimates of the unknown parameters. This chapter explains the Householder transformation as a convenient method to obtain least squares estimates of regression models (Golub (1965), Sakamoto et al. (1986)). With this method, we can obtain precise estimates of the coefficients of the model and perform order selection or variable selection based on the information criterion AIC quite efficiently.

5.1 Regression Models and the Least Squares Method

On the assumption that y_n is the objective variable and $x_{n1},\cdots,x_{nm}$ are the explanatory variables, a model that expresses the variation of y_n by the linear combination of the explanatory variables

$$y_n = \sum_{i=1}^{m} a_i x_{ni} + \varepsilon_n, \tag{5.1}$$

is called a *regression model*. Here, a_i is called the *regression coefficient* of the explanatory variable x_{ni} and the number of explanatory variables m is called the *order* of the model. Moreover, ε_n, a portion of the variation of y_n that cannot be explained by the variation of the explanatory variables is called the *residual*, and it is assumed to be an independent random variable that follows a normal distribution with mean 0 and variance σ^2.

Defining the N dimensional vector y and the $N \times m$ matrix Z as

$$y = \begin{bmatrix} y_1 \\ y_2 \\ \vdots \\ y_N \end{bmatrix}, \qquad Z = \begin{bmatrix} x_{11} & \cdots & x_{1m} \\ x_{21} & \cdots & x_{2m} \\ \vdots & & \vdots \\ x_{N1} & \cdots & x_{Nm} \end{bmatrix}, \tag{5.2}$$

the regression model can be concisely expressed by the matrix-vector representation

$$y = Za + \varepsilon. \tag{5.3}$$

The vector y and the matrix Z are called the vector of objective variables and the matrix of explanatory variables (or design matrix), respectively. $a = (a_1, \cdots, a_m)^T$ is a vector of regression coefficients, and $\varepsilon = (\varepsilon_1, \cdots, \varepsilon_N)^T$ is a vector of residuals. The regression model (5.1) contains the regression coefficients $a_1, \cdots, a_m$, and the variance σ^2 as parameters, and we can combine these as a vector of parameters, $\theta = (a_1, \cdots, a_m, \sigma^2)^T$.

When N independent observations $\{y_n, x_{n1}, \cdots, x_{nm}\}$, $n = 1, \cdots, N$, are given, the likelihood and log-likelihood of the regression model become functions of θ, and are given by

$$\begin{aligned} L(\theta) &= \prod_{n=1}^{N} p(y_n | \theta, x_{n1}, \cdots, x_{nm}) & (5.4) \\ \ell(\theta) &= \sum_{n=1}^{N} \log p(y_n | \theta, x_{n1}, \cdots, x_{nm}), & (5.5) \end{aligned}$$

respectively. Here, from equation (5.1), each term of the right-hand side of the above equations can be expressed as

$$p(y_n | \theta, x_{n1}, \cdots, x_{nm}) = \frac{1}{\sqrt{2\pi\sigma^2}} \exp\left\{ -\frac{1}{2\sigma^2} \left(y_n - \sum_{i=1}^{m} a_i x_{ni} \right)^2 \right\}, \tag{5.6}$$

$$\log p(y_n | \theta, x_{n1}, \cdots, x_{nm}) = -\frac{1}{2} \log 2\pi\sigma^2 - \frac{1}{2\sigma^2} \left(y_n - \sum_{i=1}^{m} a_i x_{ni} \right)^2, \tag{5.7}$$

and the log-likelihood function is given by

$$\ell(\theta) = -\frac{N}{2} \log 2\pi\sigma^2 - \frac{1}{2\sigma^2} \sum_{n=1}^{N} \left(y_n - \sum_{i=1}^{m} a_i x_{ni} \right)^2. \tag{5.8}$$

The maximum likelihood estimate $\hat{\theta} = (\hat{a}_1, \cdots, \hat{a}_m, \hat{\sigma}^2)^T$ of the parameter θ can be obtained by finding the value of θ that maximizes the log-likelihood function $\ell(\theta)$. Given any set of regression coefficients $a_1, \cdots, a_m$, the maximum likelihood estimate of σ^2 can be obtained by solving the normal equation

$$\frac{\partial \ell(\theta)}{\partial \sigma^2} = -\frac{N}{2\sigma^2} + \frac{1}{2(\sigma^2)^2} \sum_{n=1}^{N} \left(y_n - \sum_{i=1}^{m} a_i x_{ni} \right)^2 = 0. \tag{5.9}$$

Therefore, σ^2 can be easily obtained as

$$\hat{\sigma}^2 = \frac{1}{N}\sum_{n=1}^{N}\left(y_n - \sum_{i=1}^{m} a_i x_{ni}\right)^2. \tag{5.10}$$

Then, substituting this into (5.8), the log-likelihood becomes a function of the regression coefficients $a_1, \cdots, a_m$ and is given by

$$\ell(a_1, \cdots, a_m) = -\frac{N}{2}\log 2\pi\hat{\sigma}^2 - \frac{N}{2}. \tag{5.11}$$

Since the logarithm is a monotone increasing function, the regression coefficients $a_1, \cdots, a_m$ that maximize the log-likelihood (5.11) are obtained by minimizing the variance $\hat{\sigma}^2$ in (5.10). Thus, it can be seen that the maximum likelihood estimates with respect to the parameters of the regression model could be obtained by the least squares method.

5.2 The Least Squares Method Based on the Householder Transformation

As shown in the previous section, the maximum likelihood estimates of the regression coefficients of linear regression models can be obtained by the *least squares method* that minimizes (5.10). Here, using the matrix-vector notation of (5.2) and (5.3), the residual sum of squares can be simply expressed as

$$\sum_{n=1}^{N}\left(y_n - \sum_{i=1}^{m} a_i x_{ni}\right)^2 = \|y - Za\|_N^2 \quad = \quad \|\varepsilon\|_N^2, \tag{5.12}$$

where $\|y\|_N$ denotes the Euclidean norm of the N dimensional vector y. The well-known derivation of the least squares method is to set the partial derivative of $||y - Za\|_N^2$ in (5.12) with respect to the parameter a equal to zero, which results in the normal equation $Z^T y = Z^T Za$. Then, solving this equation, we obtain the least squares estimates of a by $\hat{a} = (Z^T Z)^{-1} Z^T y$.

However, in actual computation, it is convenient to use the following method based on orthogonal transformation, since it can yield accurate estimates and it is suited for various kinds of modeling operations (Golub (1965), Sakamoto et al. (1986)).

For any $N \times N$ orthogonal matrix U, the norm of the vector $y - Za$ is unchanged, even if it is transformed by U. Namely, we have that

$$||y - Za\,||_N^2 = \|U(y - Za)\|_N^2 = \|Uy - UZa\|_N^2, \tag{5.13}$$

and this implies that the vector a that minimizes $||Uy - UZa||_N^2$ is identical to the one that minimizes $||y - Za||_N^2$. Therefore, to obtain the least squares estimates of a, we can first apply an orthogonal transformation to make UZ an adequate form and then find a vector a that minimizes (5.13).

The least squares method based on (5.13) can be realized very efficiently by using a *Householder transformation* as follows (Golub (1965), Sakamoto et al. (1986)). First, define an $N \times (m+1)$ matrix

$$X = [\,Z|y\,], \tag{5.14}$$

by augmenting with the vector of objective variables y to the right of the matrix of the explanatory variables Z.

Applying a suitable Householder transformation U to the matrix X, it can be transformed to an upper triangular matrix S as

$$UX = S = \begin{bmatrix} s_{11} & \cdots & s_{1m} & s_{1,m+1} \\ & \ddots & \vdots & \vdots \\ & & s_{mm} & s_{m,m+1} \\ & & & s_{m+1,m+1} \\ & \mathrm{O} & & \end{bmatrix}. \tag{5.15}$$

Here, since the first m rows and the $(m+1)$-th rows of S correspond to UZ and Uy in equation (5.13), respectively, we have that

$$\begin{aligned} ||Uy - UZa||_N^2 &= \left\| \begin{bmatrix} s_{1,m+1} \\ \vdots \\ s_{m,m+1} \\ s_{m+1,m+1} \\ 0 \\ \vdots \\ 0 \end{bmatrix} - \begin{bmatrix} s_{11} & \cdots & s_{1m} \\ & \ddots & \vdots \\ & & s_{mm} \\ & \mathrm{O} & \\ & & \end{bmatrix} \begin{bmatrix} a_1 \\ \vdots \\ a_m \end{bmatrix} \right\|_N^2 \\ &= \left\| \begin{bmatrix} s_{1,m+1} \\ \vdots \\ s_{m,m+1} \end{bmatrix} - \begin{bmatrix} s_{11} & \cdots & s_{1m} \\ & \ddots & \vdots \\ \mathrm{O} & & s_{mm} \end{bmatrix} \begin{bmatrix} a_1 \\ \vdots \\ a_m \end{bmatrix} \right\|_m^2 + s_{m+1,m+1}^2 \end{aligned} \tag{5.16}$$

It should be noted that the second term $s_{m+1,m+1}^2$ on the right-hand side of (5.16) does not depend on the value of a and takes a constant value. Therefore, the least squares estimate is obtained by finding the vector $a = (a_1, \cdots, a_m)^T$ that attains the minimum of the first term, namely 0. This shows that the least squares estimate of a is obtained as the solution to the linear equation

$$\begin{bmatrix} s_{11} & \cdots & s_{1m} \\ & \ddots & \vdots \\ \text{O} & & s_{mm} \end{bmatrix} \begin{bmatrix} a_1 \\ \vdots \\ a_m \end{bmatrix} = \begin{bmatrix} s_{1,m+1} \\ \vdots \\ s_{m,m+1} \end{bmatrix}. \tag{5.17}$$

The linear equation (5.17) can be easily solved by backward substitution, because the matrix on the left-hand side is in upper triangular form. That is, we can obtain $a = (a_1, \cdots, a_m)^T$ by

$$\begin{aligned} \hat{a}_m &= \frac{s_{m,m+1}}{s_{mm}} && (5.18) \\ \hat{a}_i &= \frac{(s_{i,m+1} - s_{i,i+1}\hat{a}_{i+1} - \cdots - s_{i,m}\hat{a}_m)}{s_{ii}}, \quad i = m-1, \cdots, 1. \end{aligned}$$

Further, since $s^2_{m+1,m+1}$ is the sum of squares of the residual vector, the least squares estimate of the residual variance σ^2 of the regression model with order m is obtained by

$$\hat{\sigma}^2_m = \frac{s^2_{m+1,m+1}}{N}. \tag{5.19}$$

5.3 Selection of Order by AIC

By substituting the estimate of the residual variance obtained from (5.19) into (5.11), the maximum log-likelihood becomes

$$\ell(\hat{\theta}) = -\frac{N}{2}\log\left(2\pi\hat{\sigma}^2_m\right) - \frac{N}{2}. \tag{5.20}$$

The regression model with order m has $m+1$ parameters, $a_1, \cdots, a_m$ and σ^2. Therefore, the AIC of the regression model with order m is given by

$$\begin{aligned} \text{AIC}_m &= -2\,\ell(\hat{\theta}) + 2\,(\text{number of parameters}) \\ &= N(\log\left(2\pi\hat{\sigma}^2_m\right) + 1) + 2\,(m+1). \end{aligned} \tag{5.21}$$

If the upper triangular matrix S in (5.15) is given, not only the regression model with order m, but also all regression models with order less than m can be obtained. That is, for $j \le m$, the estimate of the residual variance and the AIC of the regression model with j explanatory variables, $x_{n1},\cdots,x_{nj}$,

$$y_n = \sum_{i=1}^{j} a_i x_{ni} + \varepsilon_n, \tag{5.22}$$

are obtained by (Sakamoto et al. (1986))

$$\begin{aligned} \hat{\sigma}_j^2 &= \frac{1}{N}\sum_{i=j+1}^{m+1} s_{i,m+1}^2 \\ \mathrm{AIC}_j &= N(\log 2\pi\hat{\sigma}_j^2 + 1) + 2\,(j+1). \end{aligned} \tag{5.23}$$

The least squares estimates of the regression coefficients can be obtained by solving the linear equation by backward substitution,

$$\begin{bmatrix} s_{11} & \cdots & s_{1j} \\ & \ddots & \vdots \\ & & s_{jj} \end{bmatrix} \begin{bmatrix} a_1 \\ \vdots \\ a_j \end{bmatrix} = \begin{bmatrix} s_{1,m+1} \\ \vdots \\ s_{j,m+1} \end{bmatrix}. \tag{5.24}$$

To perform *order selection* using the AIC, we need to compute $\mathrm{AIC}_0,\cdots,\mathrm{AIC}_m$ by (5.23), and to look for the order that achieves the smallest value. Here we note that once the upper triangular matrix S is obtained, the AICs of the regression models of all orders can be immediately computed by (5.23) without estimating the regression coefficients. Therefore, the estimation of the regression coefficients by (5.24) is necessary only for the model with the order that attains the minimum value of the AIC.

Example (Trigonometric regression model) Table 5.1 summarizes the residual variances and the AICs when trigonometric regression models with various orders

$$y_n = a + \sum_{j=1}^{m} b_j \sin(j\omega n) + \sum_{j=1}^{\ell} c_j \cos(j\omega n) + \varepsilon_n, \tag{5.25}$$

are fitted to the maximum temperature data shown in Figure 1.1(c). Here, ℓ is either m or $m-1$. The numbers in the right-most column in the Table 5.1 show the differences of the AICs from the minimum AIC value. The explanatory variables were assumed to be adopted in the order of $\{1,\ \sin\omega n,\ \cos\omega n,\ \cdots,\ \sin k\omega n,\ \cos k\omega n\}$. Therefore, the parameter vector of the model with the highest order becomes $\theta = (a,\ b_1,\ c_1,\ \cdots,b_k,\ c_k)^T$. The number of regression coefficients is $p = 2m$

Table 5.1 *Residual variances and AICs of regression models of various orders. p: number of regression coefficients of the model, $\hat{\sigma}_p^2$: residual variance, D-AIC: difference of AIC*

p	$\hat{\sigma}_p^2$	AIC	D-AIC	p	$\hat{\sigma}_p^2$	AIC	D-AIC
0	402.62	4298.23	1861.17	11	9.04	2475.06	38.00
1	60.09	3375.76	938.69	12	8.71	2459.04	21.98
2	44.54	3232.23	795.17	13	8.70	2460.84	23.78
3	9.29	2475.54	35.48	14	8.64	2459.36	22.30
4	9.29	2474.31	37.25	15	8.64	2461.00	23.94
5	9.28	2476.14	39.08	16	8.42	2450.71	13.65
6	9.28	2477.94	40.87	17	8.40	2451.57	14.51
7	9.27	2479.23	42.16	18	8.24	2443.98	6.92
8	9.27	2481.22	44.16	19	8.10	2437.80	0.74
9	9.26	2483.08	46.02	20	8.05	2437.06	0.00
10	9.04	2473.11	36.05	21	8.05	2438.65	1.58

for $\ell = m-1$ and $p = 2m+1$ for $\ell = m$. The model with the highest order $k = 10$ has 21 explanatory variables. Since a strong annual cycle was seen in this data, it was assumed that $\omega = 2\pi/365$. Table 5.1 shows the AIC of the model with 20 explanatory variables, that is, composed of a constant term, 10 sine components and 9 cosine components attains the minimum. Figure 5.1 shows the original data and the regression curve obtained using this model.

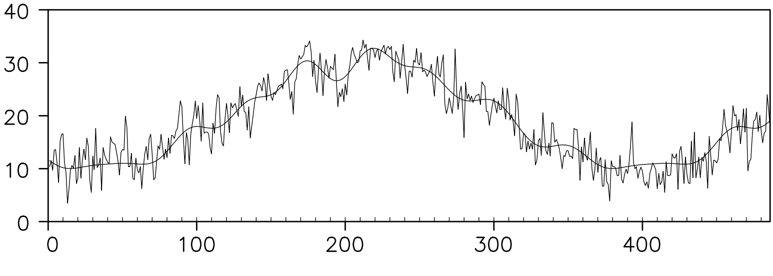

Figure 5.1 *Original data and the minimum AIC regression curve for the maximum temperature data.*

5.4 Addition of Data and Successive Householder Reduction

Utilizing the properties of orthogonal transformations, it is easily possible to update the model by addition of data (Kitagawa and Akaike (1978)). In the case of fitting a regression model to a huge data set, if we try to store the matrix of (5.14), then the memory of the computer might become overloaded, thus making execution impossible.

Even in this case, repeated application of the method introduced in this section yields the upper triangular matrix in (5.13). That is, if our computer has a memory sufficient to store the area of the $L \times (m+1)$ matrix (here, $L > m+1$), then the upper triangular matrix S can be obtained by dividing the data into several sub-data-sets with data length less than or equal to $L-m-1$.

Assuming that an upper triangular matrix S has already been obtained from N sets of data $\{y_n, x_{n1}, \cdots, x_{nm}\}$, $n = 1, \cdots, N$, we could effectively obtain a regression model from the matrix S, as shown in section (5.15). Here, we assume that M new sets of data $\{y_n, x_{n1}, \cdots, x_{nm}\}$, $n = N+1, \cdots, N+M$, are obtained. Then, in order to fit a regression model to the entire $N+M$ sets of data, we have to construct the $(N+M) \times (m+1)$ matrix

$$X_1 = \begin{bmatrix} x_{11} & \cdots & x_{1m} & y_1 \\ \vdots & \ddots & \vdots & \vdots \\ x_{N+M,1} & \cdots & x_{N+M,m} & y_{N+M} \end{bmatrix} \tag{5.26}$$

instead of (5.14) and then transform this into an upper triangular matrix by a Householder transformation $S' = U'X_1$. Inconveniently, this method cannot utilize the results of the computation for the previous data sets, and we need a large storage area for preparing the $(N+M) \times (m+1)$ matrix X_1.

Since the Householder transformation is an orthogonal transformation, it can be shown that the same matrix as S' can be obtained by building an $(M+m+1) \times (m+1)$ matrix by argumenting an $M \times (m+1)$ matrix under the triangular matrix (5.15), thus:

$$X_2 = \begin{bmatrix} s_{11} & \cdots & s_{1m} & s_{1,m+1} \\ & \ddots & \vdots & \vdots \\ & & s_{mm} & s_{m,m+1} \\ \text{O} & & & s_{m+1,m+1} \\ x_{N+1,1} & \cdots & x_{N+1,m} & y_{N+1} \\ \vdots & \ddots & \vdots & \vdots \\ x_{N+M,1} & \cdots & x_{N+M,m} & y_{N+M} \end{bmatrix}, \tag{5.27}$$

and reducing it to an upper triangular matrix by a Householder transformation.

Therefore, to perform a Householder transformation of data length longer than L, we first obtain an upper triangular matrix S by putting $N = L$, and then repeat the update of S by adding $M = L - m - 1$ data elements.

On the other hand, if the upper triangular matrix S_2 has already been obtained from a new data set $\{y_n, x_{n1}, \cdots, x_{nm}\}$, $n = N+1, \cdots, N+M$, then we define a $2(m+1) \times (m+1)$ matrix by

$$X_3 = \begin{bmatrix} S_1 \\ S_2 \end{bmatrix}, \tag{5.28}$$

and by reducing it to upper triangular form, we can obtain the same matrix as S'.

For $M \gg m$, since the number of rows of the matrix X_3 is smaller than the number of rows of X_1 and X_2, the amount of computation for the Householder transformation of X_3 is significantly less than that required for the other methods. This method will be used in Chapter 8 to fit a locally stationary AR model.

5.5 Variable Selection by AIC

In Section 5.3, the method of selection of the order for the model by AIC was explained. However, in that section, it was implicitly assumed that the order of adopting the explanatory variables was provided beforehand, and only a model of the form

$$y_n = \sum_{i=1}^{j} a_i x_{ni} + \varepsilon_n \tag{5.29}$$

was considered.

This method of selecting variables is quite natural for the autoregressive model shown in Section 6.1 and the polynomial regression model shown in Section 11.1. However, with respect to a multivariate regression model and multivariate time series models, the order of adopting variables as explanatory variables is not generally provided beforehand. Assuming that $(\ell_1, \cdots, \ell_m)$ is an index vector that indicates the order of adopting the explanatory variables, the optimal model could be selected among models of the form

$$y_n = \sum_{i=1}^{j} a_{\ell_i} x_{n,\ell_i} + \varepsilon_n. \tag{5.30}$$

In this case, even if the order j is provided, there are ${}_m\mathrm{C}_j$ different models, depending on the index vector. Such a model is called a *subset regression model*. To fit subset regression models with explanatory variables in the order of $(\ell_1,\cdots,\ell_m)$, transform the upper triangular matrix S to the matrix T that consists of $m+1$ column vectors with the numbers of non-zero elements given by $j_1,\cdots,j_m$, respectively, by the Householder transformation. Here, $j_1,\cdots,j_m$ is the inverse function of the index vector $(\ell_1,\cdots,\ell_m)$, satisfying $\ell_{j_i}=i$.

Example For the case of $m=4$ and $(\ell_1,\ell_2,\ell_3,\ell_4)=(2,4,3,1)$, it becomes $(j_1,\cdots,j_m)=(4,1,3,2)$ and the matrix T is given by

$$T=\begin{bmatrix} t_{11} & t_{12} & t_{13} & t_{14} & t_{15} \\ t_{21} & 0 & t_{23} & t_{24} & t_{25} \\ t_{31} & 0 & t_{33} & 0 & t_{35} \\ t_{41} & 0 & 0 & 0 & t_{45} \\ 0 & 0 & 0 & 0 & t_{55} \end{bmatrix}. \tag{5.31}$$

Then, the residual variance and the AIC of the model that uses the j explanatory variables $\{x_{nl_1},\cdots,x_{nl_j}\}$ are given by

$$\begin{aligned} \hat{\sigma}^2(\ell_1,\cdots,\ell_j) &= \frac{1}{N}\sum_{i=j+1}^{m+1} t_{i,m+1}^2 \\ \mathrm{AIC}(\ell_1,\cdots,\ell_j) &= N\log 2\pi\hat{\sigma}^2(\ell_1,\cdots,\ell_j)+N+2\,(j+1). \end{aligned} \tag{5.32}$$

Regression coefficients are then obtained by solving the linear equation

$$\begin{bmatrix} t_{1,\ell_1} & \cdots & t_{1,\ell_j} \\ & \ddots & \vdots \\ \mathrm{O} & & t_{j,\ell_j} \end{bmatrix}\begin{bmatrix} a_{\ell_1} \\ \vdots \\ a_{\ell_j} \end{bmatrix}=\begin{bmatrix} t_{1,m+1} \\ \vdots \\ t_{j,m+1} \end{bmatrix} \tag{5.33}$$

by backward substitution.

However, in actual computation, it is not necessary to exchange the order of explanatory variables and reduce the matrix to upper triangular form. We can easily obtain them from the upper triangular matrix T of (5.31) by the following backward substitution:

$$\begin{aligned} \hat{a}_{\ell_j} &= t_{j,\ell_j}^{-1}t_{j,m+1} \qquad (5.34) \\ \hat{a}_{\ell_i} &= t_{i,\ell_i}^{-1}(t_{i,m+1}-t_{i,\ell_i+1}\hat{a}_{\ell_i+1}-\cdots-t_{i,\ell_j}\hat{a}_{\ell_j}), \qquad i=j-1,\cdots,1. \end{aligned}$$

Problems

1. Obtain the AIC when the variance σ^2 is known in the regression model in (5.1).

2. Assume that N pairs of data $\{x_1, y_1\}, \ldots, \{x_N, y_N\}$ are given.

   (1) Obtain the least squares estimates $\hat{a}$ and $\hat{b}$ of the second-order polynomial regression model $y_n = ax_n^2 + bx_n + \varepsilon_n$ that passes through the origin.

   (2) Obtain a second-order polynomial regression model that passes through the origin and the point $(c, 0)$, and consider how to obtain the least squares estimate of the model.

Chapter 6

Analysis of Time Series Using ARMA Models

The features of time series can be concisely described using time series models. In this chapter, we consider methods for obtaining the impulse response function, the autocovariance function, the partial autocorrelation (PARCOR), the power spectrum and the roots of the characteristic equation from the univariate ARMA model (Box and Jenkins (1970), Brockwell and Davis (1991), Shumway and Stoffer (2000)). The relations between the AR coefficients and the PARCORs are also shown. Further, methods of obtaining the cross spectrum and the relative power contribution based on the multivariate AR model are presented.

6.1 ARMA Model

A model that expresses a time series y_n as a linear combination of past observations y_{n-i} and white noise v_{n-i} is called an *autoregressive moving average model* (ARMA model),

$$y_n = \sum_{i=1}^{m} a_i y_{n-i} + v_n - \sum_{i=1}^{\ell} b_i v_{n-i}. \tag{6.1}$$

Here, m and a_i are called the *autoregressive order* and the *autoregressive coefficient* (AR coefficient), respectively. Similarly, ℓ and b_i denote the *moving average order* and the *moving average coefficient* (MA coefficient), respectively. The AR order and the MA order (m, ℓ) taken together are called the ARMA order. Further, we assume that v_n is a white noise that follows a normal distribution with mean 0 and variance σ^2 and is independent of the past time series y_{n-i}. That is, v_n satisfies

$$\begin{array}{lcll} \mathrm{E}(v_n) & = & 0, & \\ \mathrm{E}(v_n^2) & = & \sigma^2, & \\ \mathrm{E}(v_n v_m) & = & 0, & \text{for } n \neq m \\ \mathrm{E}(v_n y_m) & = & 0, & \text{for } n > m. \end{array} \tag{6.2}$$

A time series y_n that follows an ARMA model is called an ARMA process. In practical terms, the most important model is an *AR model* (autoregressive model) of order m that expresses the time series as a linear combination of the past values y_{n-i} and the white noise v_n and is obtained by putting $\ell = 0$,

$$y_n = \sum_{i=1}^{m} a_i y_{n-i} + v_n. \tag{6.3}$$

On the other hand, the model obtained by putting $m = 0$,

$$y_n = v_n - \sum_{i=1}^{\ell} b_i v_{n-i}, \tag{6.4}$$

is called the *moving average model* (MA model) of order ℓ.

It should be noted that almost all analysis of stationary time series can be achieved by the use of AR models.

6.2 The Impulse Response Function

Using the *time shift operator* (or *lag operator*) B defined by $By_n \equiv y_{n-1}$, the ARMA model can be expressed as

$$\left(1 - \sum_{i=1}^{m} a_i B^i\right) y_n = \left(1 - \sum_{i=1}^{\ell} b_i B^i\right) v_n. \tag{6.5}$$

Here, let the AR operator and the MA operator be defined, respectively, by

$$a(B) \equiv \left(1 - \sum_{i=1}^{m} a_i B^i\right), \qquad b(B) \equiv \left(1 - \sum_{i=1}^{\ell} b_i B^i\right),$$

then the ARMA model can be concisely expressed as

$$a(B) y_n = b(B) v_n. \tag{6.6}$$

Dividing both sides of (6.6) by $a(B)$, the ARMA model can be expressed as $y_n = a(B)^{-1} b(B) v_n$. Therefore, if we define $g(B)$ as a formal infinite series

$$g(B) \equiv a(B)^{-1} b(B) = \sum_{i=0}^{\infty} g_i B^i, \tag{6.7}$$

the time series y_n that follows the ARMA model can be expressed by a moving average model with infinite order

$$y_n = g(B)v_n = \sum_{i=0}^{\infty} g_i v_{n-i}, \tag{6.8}$$

i.e., a linear combination of present and past realizations of white noise v_n.

The coefficients g_i; $i = 0, 1, \cdots$, correspond to the influence of the noise at time $n = 0$ to the time series at time i, and g_i is called the *impulse response function* of the ARMA model. Here, the impulse response g_i is obtained by the following recursive formula:

$$\begin{aligned} g_0 &= 1 \\ g_i &= \sum_{j=1}^{i} a_j g_{i-j} - b_i, \qquad i = 1, 2, \cdots, \end{aligned} \tag{6.9}$$

where $a_j = 0$ for $j > m$ and $b_j = 0$ for $j > \ell$.

Example Consider the following four models:

(a) The first order AR model: $y_n = 0.9y_{n-1} + v_n$

(b) The second order AR model: $y_n = 0.9\sqrt{3}y_{n-1} - 0.81y_{n-2} + v_n$

(c) The second order MA model: $y_n = v_n - 0.9\sqrt{2}v_{n-1} + 0.81v_{n-2}$

(d) The ARMA model with order (2,2):
$y_n = 0.9\sqrt{3}y_{n-1} - 0.81y_{n-2} + v_n - 0.9\sqrt{2}v_{n-1} + 0.81v_{n-2}$

The plots (a), (b), (c) and (d) of Figure 6.1 show the impulse response functions obtained from (6.9) for the four models. The impulse response function of the MA model is non-zero only for the initial ℓ points. On the other hand, if the model contains AR part, the impulse response function has non-zero values although it gradually decays.

6.3 The Autocovariance Function

Taking the expectation after multiplying by y_{n-k} on both sides of (6.1), yields

$$\mathrm{E}(y_n y_{n-k}) = \sum_{i=1}^{m} a_i \mathrm{E}(y_{n-i} y_{n-k}) + \mathrm{E}(v_n y_{n-k}) - \sum_{i=1}^{\ell} b_i \mathrm{E}(v_{n-i} y_{n-k}). \tag{6.10}$$

Here, from the expression of the ARMA model using the impulse response given in (6.7), the covariance between the time series y_m and the

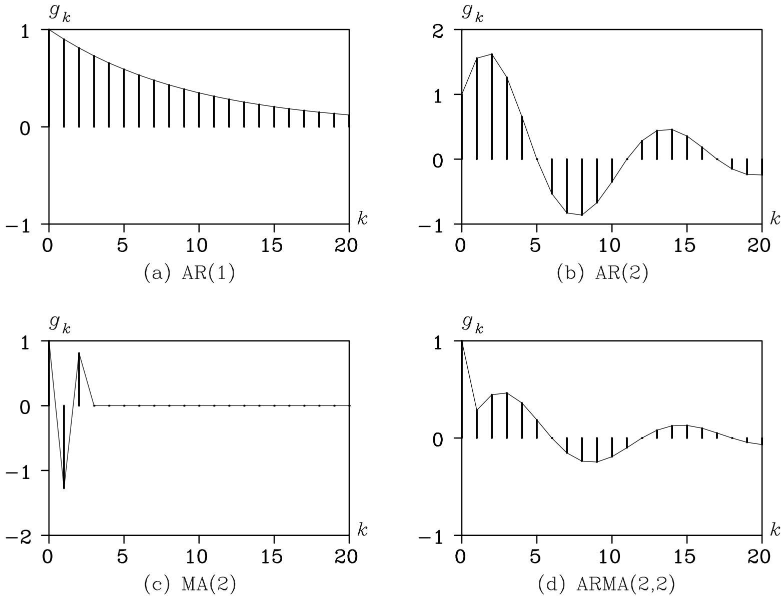

Figure 6.1: *Impulse response functions of four models.*

white noise v_n is given by

$$\mathrm{E}(v_n y_m) = \sum_{i=0}^{\infty} g_i \mathrm{E}(v_n v_{m-i}) = \begin{cases} 0 & n > m \\ \sigma^2 g_{m-n} & n \le m \end{cases}. \tag{6.11}$$

We obtain the following equation with respect to the autocovariance function $C_k \equiv \mathrm{E}(y_n y_{n-k})$:

$$\begin{aligned} C_0 &= \sum_{i=1}^{m} a_i C_i + \sigma^2 \left\{ 1 - \sum_{i=1}^{\ell} b_i g_i \right\} \qquad (6.12) \\ C_k &= \sum_{i=1}^{m} a_i C_{k-i} - \sigma^2 \sum_{i=1}^{\ell} b_i g_{i-k}, \qquad k = 1, 2, \cdots. \end{aligned}$$

Therefore, if the orders m and ℓ, the autoregressive and moving average coefficients a_i and b_i, and the innovation variance σ^2 of the ARMA model are given, we first compute the impulse response function $g_1, \cdots, g_\ell$ by (6.9) and then obtain the autocovariance function $C_0, C_1, \cdots$

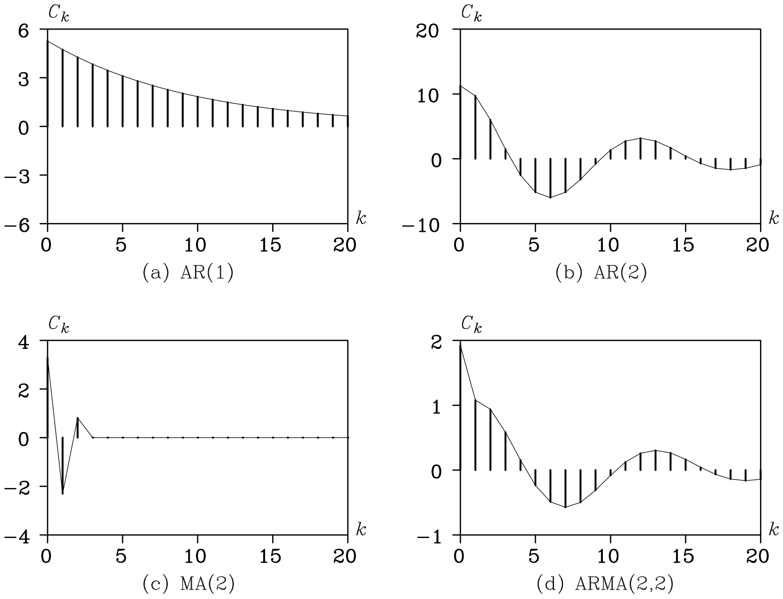

Figure 6.2: *Autocovariance functions of the four models.*

by solving (6.13). In particular, the following equation for the AR model obtained by putting $\ell = 0$ is called the *Yule-Walker equation*

$$\begin{aligned} C_0 &= \sum_{i=1}^{m} a_i C_i + \sigma^2 \\ C_k &= \sum_{i=1}^{m} a_i C_{k-i}. \end{aligned} \qquad (6.13)$$

Note that, since for univariate time series, the autocovariance function satisfies $C_{-k} = C_k$, the backward model satifies the same equation.

Example Figure 6.2 shows the autocovariance functions of the four models (a), (b), (c) and (d) shown in Figure 6.1. The autocovariance functions of (b) and (d) indicate a damped oscillation. On the other hand, for the MA model shown in (c), the autocovariance function becomes $C_k = 0$ for $k > 2$.

6.4 The Relation Between AR Coefficients and the PARCOR

As shown in Appendix B in this book, the following relation holds between the coefficients of the AR model with order $m-1$, a_i^{m-1}, and the coefficient a_i^m of the AR model with order m

$$a_i^m = a_i^{m-1} - a_m^m a_{m-i}^{m-1}, \qquad i = 1, \cdots, m-1. \tag{6.14}$$

The coefficient a_m^m is called the m-th PARCOR (partial autocorrelation coefficient). If the M PARCORs, $a_1^1, \cdots, a_M^M$, are given, repeated application of Eq. (6.14) yields the entire set of coefficients of the AR models with orders 2 through M. On the other hand, it can be seen from (6.14) that, if the coefficients $a_1^m, \cdots, a_m^m$ of the AR model of the highest order are given, by solving the equations

$$a_j^m = a_j^{m-1} - a_m^m \left(a_{m-j}^m + a_m^m a_j^{m-1} \right) \tag{6.15}$$

for $j = i$ and $m - i$, the coefficients of the AR model with order $m-1$ are obtained by

$$a_i^{m-1} = \frac{a_i^m + a_m^m a_{m-i}^m}{1 - (a_m^m)^2}. \tag{6.16}$$

The PARCORs $a_1^1, \cdots, a_m^m$ can be obtained by repeating the above computation. This argument reveals that estimation of the coefficients $a_1^m, \cdots, a_m^m$ of the AR model of order m is equivalent to estimation of the PARCORs up to the order m, $a_1^1, \cdots, a_m^m$.

Example Figure 6.3 shows the PARCORs of the four models (a), (b), (c) and (d). Contrary to the autocovariance function, we have $a_i^i = 0$ for $i > m$ for the AR model with order m, and they gradually decay in the cases of the MA model and the ARMA model.

6.5 The Power Spectrum of the ARMA Process

If an ARMA model of a time series is given, the power spectrum, as well as the autocovariance function, can be obtained. Actually, the *power spectrum* of the ARMA process (6.1) can be obtained from (6.8) as

$$\begin{aligned} p(f) &= \sum_{k=-\infty}^{\infty} C_k e^{-2\pi ikf} \qquad (6.17) \\ &= \sum_{k=-\infty}^{\infty} \mathrm{E}(y_n y_{n-k}) e^{-2\pi ikf} \end{aligned}$$

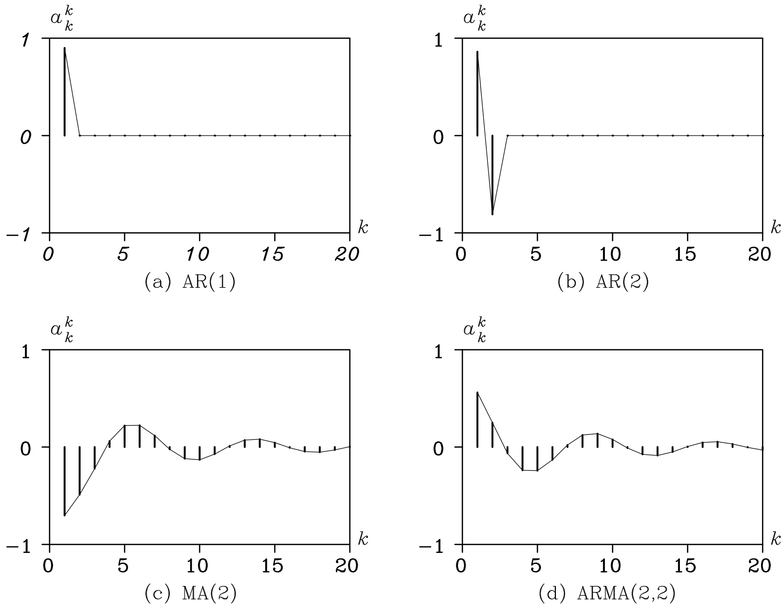

(a) AR(1)

(b) AR(2)

(c) MA(2)

(d) ARMA(2,2)

Figure 6.3: *PARCORs of the four models.*

$$
\begin{aligned}
&= \sum_{k=-\infty}^{\infty} \mathrm{E}\Big\{ \Big(\sum_{j=0}^{\infty} g_j v_{n-j} \Big) \Big(\sum_{p=0}^{\infty} g_p v_{n-k-p} \Big) \Big\} e^{-2\pi ikf} \\
&= \sum_{k=-\infty}^{\infty} \sum_{j=0}^{\infty} \sum_{p=0}^{\infty} g_j g_p \mathrm{E}\big(v_{n-j} v_{n-k-p}\big) e^{-2\pi ikf}.
\end{aligned}
$$

Here, using $g_p = 0$ for $p < 0$, from (6.2), the power spectrum is expressed as

$$
\begin{aligned}
p(f) &= \sigma^2 \sum_{k=-\infty}^{\infty} \sum_{j=0}^{\infty} g_j g_{j-k} e^{-2\pi ikf} \\
&= \sigma^2 \sum_{j=0}^{\infty} \sum_{k=-\infty}^{j} g_j e^{-2\pi ijf} g_{j-k} e^{-2\pi i(k-j)f} \\
&= \sigma^2 \sum_{j=0}^{\infty} \sum_{p=0}^{\infty} g_j e^{-2\pi ijf} g_p e^{2\pi ipf} \\
&= \sigma^2 \Big| \sum_{j=0}^{\infty} g_j e^{-2\pi ijf} \Big|^2, \qquad (6.18)
\end{aligned}
$$

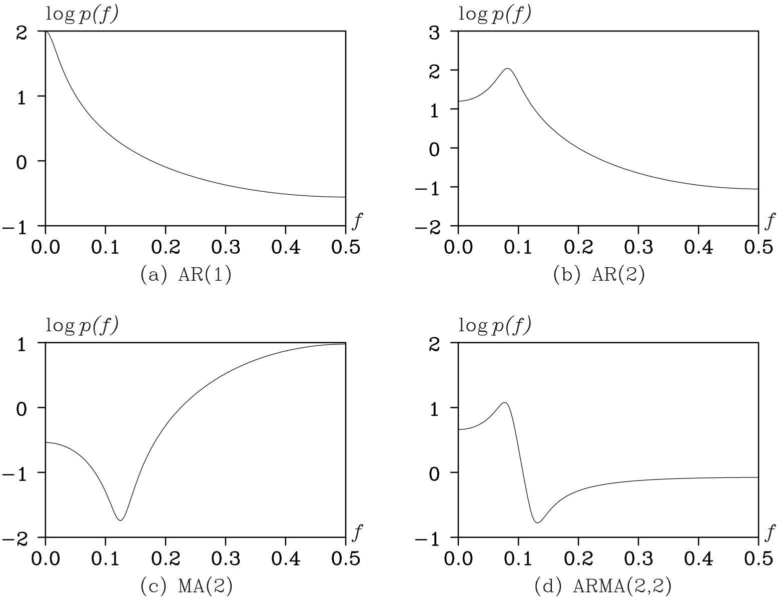

(a) AR(1)

(b) AR(2)

(c) MA(2)

(d) ARMA(2,2)

Figure 6.4: *Logarithm of the power spectra of the four models.*

where $\sum_{j=0}^{\infty} g_j e^{-2\pi ijf}$ is the Fourier transform of the impulse response function and is called the *frequency response function*. On the other hand, putting $B = e^{-2\pi if}$ in (6.7), it can be expressed as

$$\sum_{j=0}^{\infty} g_j e^{-2\pi ijf} = \left\{1 - \sum_{j=1}^{m} a_j e^{-2\pi ijf}\right\}^{-1} \left\{1 - \sum_{j=1}^{\ell} b_j e^{-2\pi ijf}\right\}. \qquad (6.19)$$

Therefore, substituting the above frequency response function into (6.18), the power spectrum of the ARMA model is given by

$$p(f) = \sigma^2 \frac{\left|1 - \sum_{j=1}^{\ell} b_j e^{-2\pi ijf}\right|^2}{\left|1 - \sum_{j=1}^{m} a_j e^{-2\pi ijf}\right|^2}. \qquad (6.20)$$

Example. Figure 6.4 shows the logarithm of the power spectra of the four models. The power spectrum of the AR model with order one

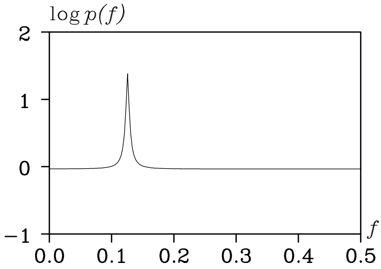

Figure 6.5: *Line-like spectrum of ARMA(2.2).*

does not have any peak or trough. A peak is seen in the plot (b) of the spectrum of the second order AR model and one trough is seen in the plot (c) of the second order MA model. On the other hand, the spectrum of the ARMA model of order (2.2) shown in the plot (d) has both one peak and one trough.

These examples indicate that there must be close relations between the AR and MA orders and the number of peaks and troughs in the spectra. The logarithm of the spectrum, $\log p(f)$ shown in Figure 6.4, is expressible as

$$\log p(f) = \log \sigma^2 - 2\log\left|1 - \sum_{j=1}^{m} a_j e^{-2\pi ijf}\right| + 2\log\left|1 - \sum_{j=1}^{\ell} b_j e^{-2\pi ijf}\right|. \tag{6.21}$$

Therefore, the peak and the trough of the spectrum appear at the local minimum of $|1-\sum_{j=1}^{m} a_j e^{-2\pi ijf}|$ and at the local minimum of $|1-\sum_{j=1}^{l} b_j e^{-2\pi ijf}|$, respectively. The number of peaks and troughs, respectively, correspond to the number of roots of the AR operator and the MA operator as will be explained in the next subsection. To express k peaks or k troughs, the AR order or the MA order must be higher than or equal to $2k$, respectively. Moreover, the locations and the heights of the peaks or the troughs are determined by the angles and the absolute values of the complex roots of the characteristic equation.

In particular, when the angles of the complex roots of the AR operator coincide with those of the MA operator, a line spectrum appears. For example, if the AR and MA coefficients of the ARMA (2.2) model are given by

$$\begin{aligned} m &= 2, \quad a_1 = 0.99\sqrt{2}, \quad a_2 = -0.99^2 \\ \ell &= 2, \quad b_1 = 0.95\sqrt{2}, \quad b_2 = -0.95^2, \end{aligned}$$

both characteristic equations have roots at $f = 0.125$ (= 45 degrees), and $\log p(f)$ has a line-like spectral peak as shown in Figure 6.5.

6.6 The Characteristic Equation

The characteristics of an ARMA model are determined by the roots of the following two polynomial equations:

$$a(B) = 1 - \sum_{j=1}^{m} a_j B^j = 0 \tag{6.22}$$

$$b(B) = 1 - \sum_{j=1}^{\ell} b_j B^j = 0. \tag{6.23}$$

Equations (6.22) and (6.23) are called the *characteristic equation* associated with the AR operator, and the MA operator, respectively. The roots of these equations are called the *characteristic roots*. If the roots of the characteristic equation $a(B) = 0$ of the AR operator all lie outside the unit circle, the influence of noise turbulence at a certain time decays as time progresses, and then the ARMA model becomes *stationary*.

On the other hand, if all roots of the characteristic equation $b(B) = 0$ of the MA operator lie outside the unit circle, the coefficient of h_i of $b(B)^{-1} = \sum_{i=0}^{\infty} h_i B^i$ converges and the ARMA model can be expressed by an AR model of infinite order as

$$y_n = -\sum_{i=1}^{\infty} h_i y_{n-i} + v_n. \tag{6.24}$$

In this case, the time series is called *invertible*.

As mentioned in the previous section, the positions of the roots of the two characteristic polynomials have a close relation to the shape of the spectrum. The peak of the spectrum (or trough) appears at $f = \theta/2\pi$, if the complex root of AR (or MA) operator is expressed in the form

$$z = \alpha + i\beta = re^{i\theta}. \tag{6.25}$$

Further, the closer the root r approaches to 1, the sharper the peak and trough of the spectrum become. Figure 6.6 shows the positions of the characteristic roots of the four models that have been used for the examples in this chapter. The symbols $*$ and $+$ denote the roots of the AR operator and the roots of the MA operator, respectively. For convenience in illustration, the position of $z^{-1} = r^{-1}e^{-i\theta}$ is displayed in Figure 6.6 instead of z.

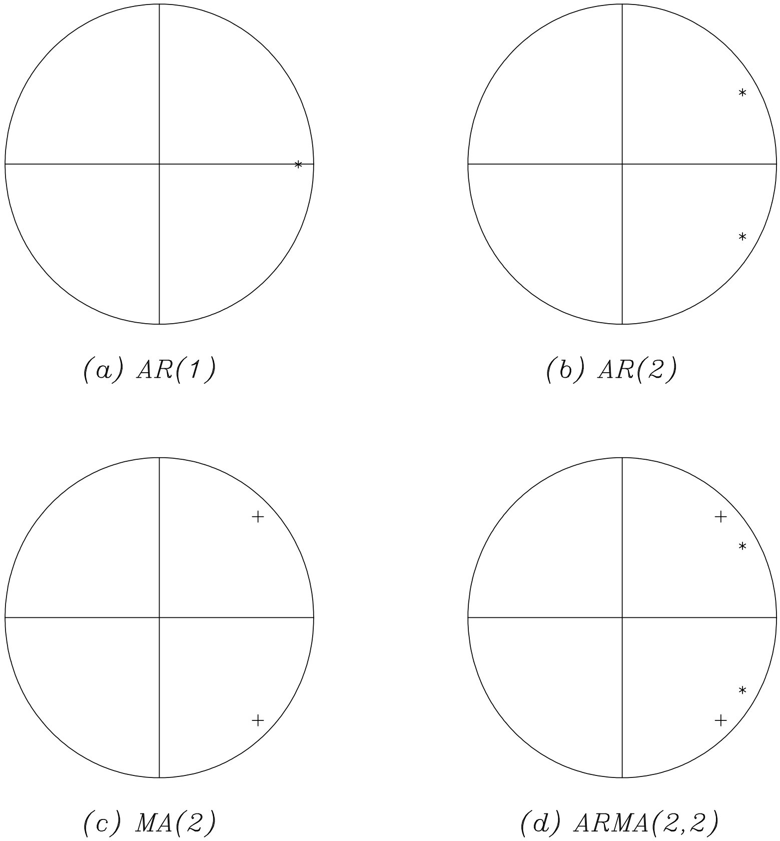

(a) AR(1)

(b) AR(2)

(c) MA(2)

(d) ARMA(2,2)

Figure 6.6 *Characteristic roots. (a) AR model of order 1, (b) AR model of order 2, (c) MA model with order 2 and (d) ARMA model with order (2,2).*

6.7 The Multivariate AR Model

For *multivariate time series*, $y_n = (y_n(1), \cdots, y_n(\ell))^T$, similar to the case of univariate time series, the model that expresses a present value of the time series as a linear combination of past values $y_{n-1}, \cdots, y_{n-M}$ and white noise is called a *multivariate autoregressive model* (MAR model)

$$y_n = \sum_{m=1}^{M} A_m y_{n-m} + v_n, \tag{6.26}$$

where A_m is the autoregressive coefficient matrix whose (i,j)-th element is given by $a_m(i,j)$, and v_n is an ℓ dimensional white noise that satisfies

$$\begin{aligned} \mathrm{E}(v_n) &= \begin{bmatrix} 0 \\ \vdots \\ 0 \end{bmatrix}, \qquad \mathrm{E}(v_n v_n^T) = \begin{bmatrix} \sigma_{11} & \cdots & \sigma_{1\ell} \\ \vdots & \ddots & \vdots \\ \sigma_{\ell 1} & \cdots & \sigma_{\ell\ell} \end{bmatrix} = W \\ \mathrm{E}(v_n v_m^T) &= \mathrm{O}, \qquad \text{for } n \neq m \\ \mathrm{E}(v_n y_m^T) &= \mathrm{O}, \qquad \text{for } n > m. \end{aligned} \tag{6.27}$$

Here, O denotes the $\ell \times \ell$ matrix with 0 elements, and W is an $\ell \times \ell$ symmetric matrix satisfying $\sigma_{ij} = \sigma_{ji}$. The cross-covariance function of $y_n(i)$ and $y_n(j)$ is defined by $C_k(i,j) = \mathrm{E}\{y_n(i)y_{n-k}(j)\}$. Then, the $\ell \times \ell$ matrix $C_k = \mathrm{E}(y_n y_{n-k}^T)$, the (i,j)-th component of which is $C_k(i,j)$, is called the *cross-covariance function*. Similar to the case of the univariate time series, for the multivariate AR model, C_k satisfies the Yule-Walker equation

$$C_0 = \sum_{j=1}^{M} A_j C_{-j} + W \tag{6.28}$$

$$C_k = \sum_{j=1}^{M} A_j C_{k-j} \qquad (k = 1, 2, \cdots). \tag{6.29}$$

As noted in Chapter 2, the cross-covariance function is not symmetric. Therefore, for multivariate time series, the Yule-Walker equations for the the backward AR model and the forward AR model are different.

The Fourier transform of the cross-covariance function $C_k(s,j)$ is called the *cross spectral density function*

$$\begin{aligned} p_{sj}(f) &= \sum_{k=-\infty}^{\infty} C_k(s,j) e^{-2\pi i k f} \\ &= \sum_{k=-\infty}^{\infty} C_k(s,j) \cos(2\pi k f) - i \sum_{k=-\infty}^{\infty} C_k(s,j) \sin(2\pi k f). \end{aligned} \tag{6.30}$$

Since the cross-covariance function is not an even function, the cross-spectrum given by (6.30) has an imaginary part and is a complex number. If the $\ell \times \ell$ matrix $P(f)$ is defined by

$$P(f) = \begin{bmatrix} p_{11}(f) & \cdots & p_{1\ell}(f) \\ \vdots & \ddots & \vdots \\ p_{\ell 1}(f) & \cdots & p_{\ell\ell}(f) \end{bmatrix}, \tag{6.31}$$

then the relations between the cross-spectrum matrix $P(f)$ and the cross-covariance matrix C_k are given by

$$\begin{aligned} P(f) &= \sum_{k=-\infty}^{\infty} C_k e^{-2\pi i k f} && (6.32) \\ C_k &= \int_{-\frac{1}{2}}^{\frac{1}{2}} P(f) e^{2\pi i k f} df. && (6.33) \end{aligned}$$

For time series that follow the multivariate AR model, the cross-spectrum can be obtained by (Whittle (1963))

$$P(f) = A(f)^{-1} W (A(f)^{-1})^*, \qquad (6.34)$$

where A^* denotes the complex conjugate of the matrix A, and $A(f)$ denotes the $\ell \times \ell$ matrix whose (j,k)-th component is defined by

$$A_{jk}(f) = \sum_{m=0}^{M} a_m(j,k) e^{-2\pi i m f}. \qquad (6.35)$$

Here, it is assumed that $a_0(j,j) = -1$ and $a_0(j,k) = 0$ for $j \neq k$. Given a frequency f, the cross spectrum is a complex number and can be expressed as

$$p_{jk}(f) = \alpha_{jk}(f) e^{i\phi_{jk}(f)}, \qquad (6.36)$$

where

$$\begin{aligned} \alpha_{jk}(f) &= \sqrt{(\Re\{p_{jk}(f)\})^2 + (\Im\{p_{jk}(f)\})^2} \\ \phi_{jk}(f) &= \arctan\left\{ \frac{\Im\{p_{jk}(f)\}}{\Re\{p_{jk}(f)\}} \right\}. \end{aligned}$$

$\Re$ and $\Im$ denote the real and imaginary parts of the complex number, respectively. Then, $\alpha_{jk}(f)$ is called the *amplitude spectrum* and $\phi_{jk}(f)$ is the *phase spectrum*. Moreover,

$$coh_{jk}(f) = \frac{\alpha_{jk}(f)^2}{p_{jj}(f) p_{kk}(f)} \qquad (6.37)$$

denotes the square of the correlation coefficient between frequency components of time series $y_n(j)$ and $y_n(k)$ at frequency f and is called the *coherency*.

For convenience, $A(f)^{-1}$ will be denoted as $B(f) = \big(b_{jk}(f)\big)$ in the following. If the components of the white noise v_n are mutually uncorrelated and the variance-covariance matrix becomes the diagonal matrix $W = \mathrm{diag}\{\sigma_1^2, \cdots, \sigma_\ell^2\}$, then the power spectrum of the i-th component of the time series can be expressed as

$$p_{ii}(f) = \sum_{j=1}^{\ell} b_{ij}(f)\sigma_j^2 b_{ij}(f)^* \equiv \sum_{j=1}^{\ell} |b_{ij}(f)|^2\sigma_j^2. \tag{6.38}$$

This indicates that the power of the fluctuation of the component i at frequency f can be decomposed into the effects of ℓ noises, i.e., $|b_{ij}(f)|^2\sigma_j^2$. Therefore, if we define $r_{ij}(f)$ by

$$r_{ij}(f) = \frac{|b_{ij}(f)|^2\sigma_j^2}{p_{ii}(f)}, \tag{6.39}$$

it represents the ratio of the effect of $v_n(j)$ in the fluctuation of $y_n(i)$ at frequency f.

The $r_{ij}(f)$ is called the *relative power contribution*, which is applicable to the analysis of a feedback system (Akaike (1968), Akaike and Nakagawa (1989)). However, for convenience in drawing figures, a *cumulative power contribution* is an effective tool, which is defined by

$$s_{ij}(f) = \sum_{k=1}^{j} r_{ik}(f) = \frac{\sum_{k=1}^{j} |b_{ik}(f)|^2\sigma_k^2}{p_{ii}(f)}. \tag{6.40}$$

Example Figure 6.7 shows the cross spectra obtained by using a three-variate AR model for the three-variate time series composed of the yaw rate, the pitch rate and the rudder angle shown in (a) and (h) of Figure 1.1 ($N = 500$ and $\triangle t = 2$ second) that were originally sampled every second. Three of nine plots on the diagonal in the figure show the logarithm of the power spectra of the yaw rate, the pitch rate and the rudder angle, respectively. As for the power spectra of the yaw rate, the maximum peak is seen in the vicinity of $f = 0.25$ (8 seconds cycle) and for the pitch rate and the rudder angle in the vicinity of $f = 0.125$ (16 seconds cycle). On the other hand, three plots above the diagonal show the absolute values of the amplitude spectra of the cross spectra, that is, the logarithm of the amplitude spectra and three plots below the diagonal show the phase spectra where some discontinuous jumps are seen. The reason for this is that the phase spectra are displayed within the range $[-\pi, \pi]$.

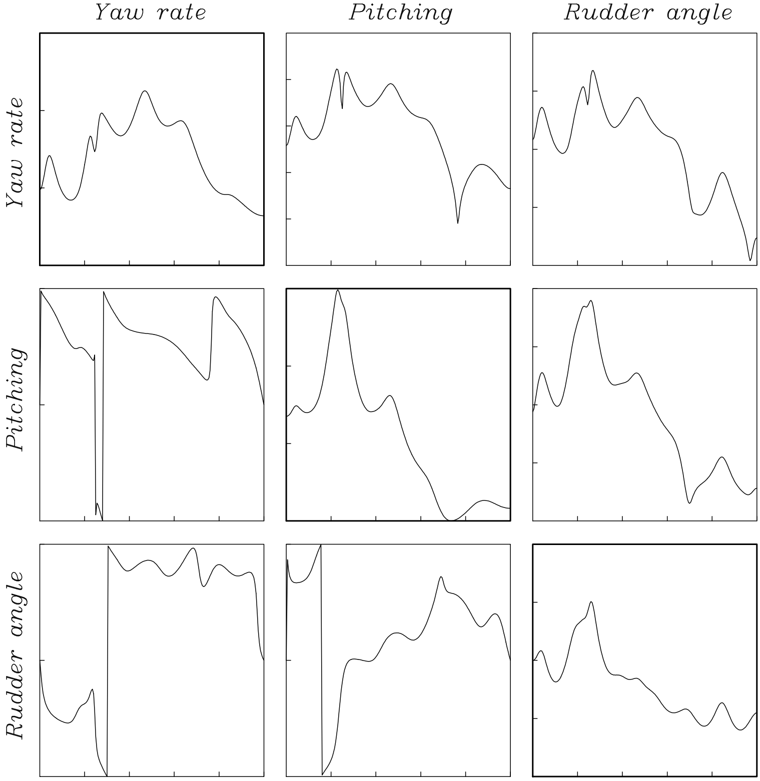

Figure 6.7 *Spectra (diagonal), amplitude spectra (above diagonal) and phase spectra (below diagonal) for the ship data.*

Figure 6.8 shows the power spectra and the coherencies. Three plots on the diagonal show the power spectra similarly to Figure 6.7. Three other plots above the diagonal show the coherencies. Yaw rate and pitching both have two significant peaks at the same frequencies. The peak of the rudder angle has slightly smaller frequency than those of yaw rate and pitching.

On the other hand, Figure 6.9 shows the power contributions. In Figure 6.9, the two plots on top, respectively, show the absolute and the relative power contributions of the yaw rate. Here, the plots in the left column show the absolute cumulative power contribution and the plots in the right column show the cumulative relative power contribution. All plots in both columns of Figure 6.9 show the contribution of the yaw rate,

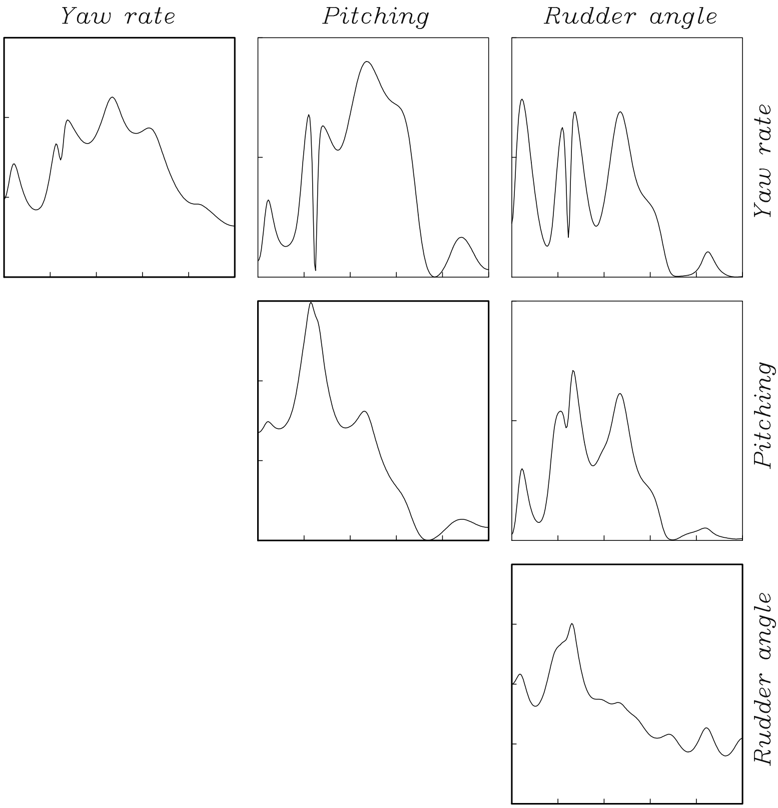

Figure 6.8: *Power spectra (3 in diagonal) and coherencies.*

the pitch rate and the rudder angle from the bottom to the top in each plot, respectively. The influence of the rudder angle is clearly visible for $f < 0.13$. However, the influence of the rudder angle is barely noticeable in the vicinity of $f = 0.14$ and 0.23, where the dominant power of the yaw rate is found. This is probably explained by noting that this data set has been observed under the control of a conventional PID autopilot system that is designed to suppress the power of variation in the frequency area $f < 0.13$.

Two plots in the second row show the power contribution of the pitching. The contribution of the rudder angle is almost 50 percent in the vicinity of $f = 0.1$, where the power spectrum is strong. This is thought to be a side effect of the steering to suppress the variation of the yaw

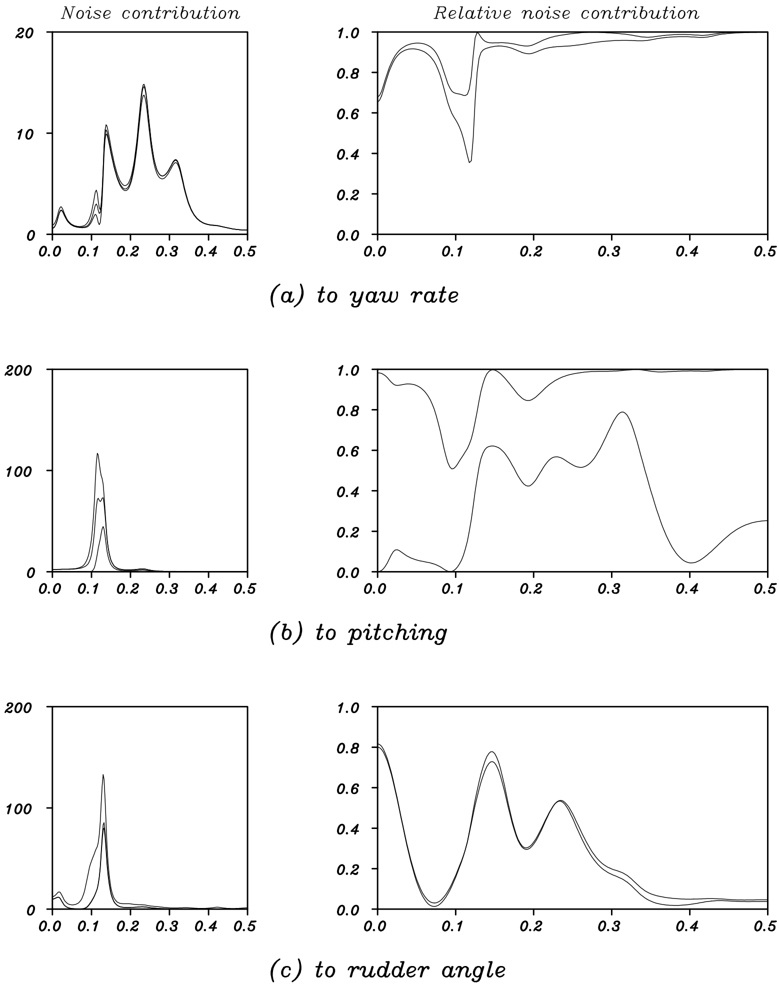

(a) to yaw rate

(b) to pitching

(c) to rudder angle

Figure 6.9: *Power contributions.*

rate. On the other hand, actual power is very small for $f > 0.14$ though a strong influence of the yaw rate is seen.

Two figures in the third row show the power contribution to the rudder angle. It can be seen that the influence of the yaw rate is extremely strong in the vicinity of $f = 0.12$, where the main power is located.

Moreover, it can also be seen that, in the range of $f < 0.08$, the contribution of the yaw rate becomes greater as the frequency decreases.

Problems

1.(1) Show the stationarity condition for AR(1).

(2) Show the stationarity condition for AR(2).

2. For an AR(1), $y_n = ay_{n-1} + v_n, \quad v_n \sim N(0, \sigma^2)$:

(1) Obtain the one-step-ahead prediction error variance.

(2) Obtain the two-step-ahead prediction error variance.

(3) Obtain the k-step-ahead prediction error variance.

3. Assuming that the time series follows the models shown below and that v_n follows a white noise with mean 0 and variance σ^2, obtain the autocovariance function C_k.

(1) AR model of order 1: $y_n = -0.9y_{n-1} + v_n$

(2) AR model of order 2: $y_n = 1.2y_{n-1} - 0.6y_{n-2} + v_n$

(3) MA model of order 1: $y_n = v_n - bv_{n-1}$

(4) ARMA model of order (1,1): $y_n = ay_{n-1} + v_n - bv_{n-1}$

4. Assume that a time series follows an AR model of order 1, $y_n = ay_{n-1} + v_n$, $v_n \sim N(0, 1)$.

(1) When the noise term v_n is not a white noise but follows an autoregressive process of order 1, $v_n = bv_{n-1} + w_n$, show that y_n follows an AR model of order 2.

(2) Obtain the autocovariance function C_k, $k = 0, 1, 2, 3$ of the contaminated series x_n, defined by $x_n = y_n + w_n, w_n \sim N(0, 0.1)$.

5.(1) Using the result of Problem 3 for Chapter 3 and the definition of the power spectrum, show that the power spectrum of MA model with order 1 can be expressed as $p(f) = |1 - be^{-2\pi i f}|^2$, where the right-hand side can be expressed as $1 + b^2 - 2b\cos(2\pi f)$.

(2) Using the fact that if $\sigma^2 = 1$, the spectrum of an AR model of order 1, $y_n = ay_{n-1} + v_n$, can be expressed as $p(f) = (1 - 2a\cos(2\pi f) + a^2)^{-1}$, and show that the maximum and the minimum of the spectrum occurs at $f = 0$ or $f = 0.5$. Also, consider where the spectrum $p(f)$ attains its maximum.

6. For an AR model of order 2, $y_n = a_1y_{n-1} + a_2y_{n-2} + v_n$, $v_n \sim N(0, \sigma^2)$:

(1) Show the formula to obtain the autocovariance function $C_0, C_1, \dots$.

(2) Show the expression to obtain the power spectrum $p(f)$, $0 \le f \le 1/2$.

(3) Obtain C_0, C_1, C_2 when $a_1 = 0.8$, $a_2 = -0.6$ and $\sigma^2 = 1$.

(4) For the same case, obtain the expression for the power spectrum $p(f)$. Investigate for which frequency f, $p(f)$ attains its maximum.

7. Assume that a time series y_n follows an MA model of order 1; $y_n = v_n - bv_{n-1}$, $v_n \sim N(0,1)$.

(1) Obtain the autocovariance function C_k, $\quad k = 0,1,2,3$.

(2) Express the time series by an AR model.

8.(1) Obtain the variance of the k-step-ahead prediction error $\varepsilon_{n+k|n}$ for an MA model of order 1; $y_n = v_n - bv_{n-1}$, $v_n \sim N(0,1)$.

(2) Express an AR model of order 1, $y_n = ay_{n-1} + v_n$, using an MA model of infinite order and obtain the variance of the k-step-ahead prediction error variance.

(3) Using the formal expansion of the random walk model $y_n = y_{n-1} + v_n$, obtain the MA model of infinite order. Using that expression, obtain the k-step-ahead prediction error variance of the random walk model.

Chapter 7

Estimation of an AR Model

Among the stationary time series models discussed in the preceding chapter, very efficient estimation methods can be derived for AR models. This chapter presents methods for estimating the parameters of the AR model by the Yule-Walker method, the least squares method and the PARCOR method. A method of determining the order of the AR model using the AIC is also shown. In addition, the Yule-Walker method and the least squares method for parameter estimation of the multivariate AR model are shown.

7.1 Fitting an AR Model

Assuming that a time series $y_1, \cdots, y_N$ is given, we consider the problem of fitting an *autoregressive model* (AR model)

$$y_n = \sum_{i=1}^{m} a_i y_{n-i} + v_n, \tag{7.1}$$

where m denotes the *order* of the autoregression, a_i is the *autoregressive coefficient* and v_n is white noise that follows a normal distribution with mean 0 and variance σ^2 (Akaike (1969), Box and Jenkins (1970), Akaike and Nakagawa (1989), Brockwell and Davis (1991)). σ^2 is sometimes called the *innovation variance*.

To identify an AR model, it is necessary to determine the order m and estimate the autoregressive coefficients $a_1, \cdots, a_m$ and the variance σ^2 based on the data. In the following, these parameters will be denoted by $\theta = (a_1, \cdots, a_m, \sigma^2)^T$.

Under the assumption that the order m is given, consider the estimation of the parameter θ by the maximum likelihood method. The joint distribution of time series $y = (y_1, \cdots, y_N)^T$, following the AR model, becomes a multivariate normal distribution. When the model (7.1) is given, the mean vector of the autoregressive process y is 0 and the variance-covariance matrix is given by

$$\Sigma = \begin{bmatrix} C_0 & C_1 & \cdots & C_{N-1} \\ C_1 & C_0 & \cdots & C_{N-2} \\ \vdots & \vdots & \ddots & \vdots \\ C_{N-1} & C_{N-2} & \cdots & C_0 \end{bmatrix}, \tag{7.2}$$

where the autocovariance function C_k is defined by (6.12). Therefore, the likelihood of the AR model is obtained by

$$\begin{aligned} L(\theta) &= p(y_1, \cdots, y_N | \theta) \\ &= (2\pi)^{-\frac{N}{2}} |\Sigma|^{-\frac{1}{2}} \exp\left\{ -\frac{1}{2} y^T \Sigma^{-1} y \right\}. \end{aligned} \tag{7.3}$$

However, when the number N of data is large, the computation of the likelihood by this method becomes difficult because it involves the inversion and computation of the determinant of the $N \times N$ matrix Σ. To obtain the maximum likelihood estimate of θ that maximizes (7.3), it is necessary to apply a numerical optimization method, since the likelihood is a complicated function of the parameter θ. In general, however, the likelihood of a time series model can be efficiently calculated by expressing it as a product of conditional distributions

$$\begin{aligned} L(\theta) &= p(y_1, \cdots, y_N | \theta) \\ &= p(y_1, \cdots, y_{N-1} | \theta) p(y_N | y_1, \cdots, y_{N-1}, \theta) \\ &\ \ \vdots \\ &= \prod_{n=1}^{N} p(y_n | y_1, \cdots, y_{n-1}, \theta). \end{aligned} \tag{7.4}$$

Using a Kalman filter, each term in the right hand side of (7.4) can be efficiently and exactly evaluated, which makes it possible to compute the exact likelihood of the ARMA model and other time series models. Such a method will be treated in Chapter 9. When the *maximum likelihood estimate* $\hat{\theta}$ of the AR model has been obtained, the AIC for the model is defined by

$$\begin{aligned} \text{AIC} &= -2\,(\text{maximum log-likelihood}) + 2\,(\text{number of parameters}) \\ &= -2 \log L(\hat{\theta}) + 2(m+1). \end{aligned} \tag{7.5}$$

To select the AR order m by the minimum AIC method, we calculate the AICs of the AR models with orders up to M, that is, $\text{AIC}_0, \cdots, \text{AIC}_M$, and select the order that results in the minimum AIC value (Akaike (1973, 1974), Sakamoto et al. (1986), Konishi and Kitagawa (2008)).

7.2 Yule-Walker Method and Levinson's Algorithm

As shown in Chapter 6, the autocovariance function of the AR model (7.1) of order m satisfies the *Yule-Walker equation* (Akaike (1969), Box and Jenkins (1970))

$$\begin{aligned} C_0 &= \sum_{i=1}^{m} a_i C_i + \sigma^2 & (7.6)\\ C_j &= \sum_{i=1}^{m} a_i C_{j-i}. & (7.7) \end{aligned}$$

On the other hand, once the time series has been obtained, by computing the sample autocovariance functions $\hat{C}_k$ and substituting them into (7.7), we obtain a system of linear equations for the unknown autoregressive coefficients $a_1, \cdots, a_m$,

$$\begin{bmatrix} \hat{C}_0 & \hat{C}_1 & \cdots & \hat{C}_{m-1} \\ \hat{C}_1 & \hat{C}_0 & \cdots & \hat{C}_{m-2} \\ \vdots & \vdots & \ddots & \vdots \\ \hat{C}_{m-1} & \hat{C}_{m-2} & \cdots & \hat{C}_0 \end{bmatrix} \begin{bmatrix} a_1 \\ a_2 \\ \vdots \\ a_m \end{bmatrix} = \begin{bmatrix} \hat{C}_1 \\ \hat{C}_2 \\ \vdots \\ \hat{C}_m \end{bmatrix}. \tag{7.8}$$

By solving this equation, the estimates $\hat{a}_i$ of the AR coefficients are obtained. Then, from (7.6), an estimate of the variance σ^2 is obtained by

$$\hat{\sigma}^2 = \hat{C}_0 - \sum_{i=1}^{m} \hat{a}_i \hat{C}_i. \tag{7.9}$$

The estimates $\hat{a}_1, \cdots, \hat{a}_m$, and $\hat{\sigma}^2$ obtained by this method are called the *Yule-Walker estimates*. Since the variance of the prediction errors of the AR model with coefficients a_i is given by

$$\begin{aligned} \mathrm{E}\left(v_n^2\right) &= \mathrm{E}\left(y_n - \sum_{i=1}^{m} a_i y_{n-i}\right)^2 \\ &= C_0 - 2\sum_{i=1}^{m} a_i C_i + \sum_{i=1}^{m}\sum_{j=1}^{m} a_i a_j C_{i-j}, & (7.10) \end{aligned}$$

we obtain equation (7.7) from

$$\frac{\partial \mathrm{E}(v_n^2)}{\partial a_i} = -2C_i + 2\sum_{j=1}^{m} a_j C_{i-j} = 0. \tag{7.11}$$

Therefore, we can consider that the Yule-Walker estimates obtained by solving (7.8) after substituting $\hat{C}_i$ for C_i in (7.11) approximately minimize the variance of prediction errors. To obtain the Yule-Walker estimates for an AR model of order m, it is necessary to solve a system of linear equations with m unknowns. In addition, to select the order of the AR model by the minimum AIC method, we need to evaluate the AIC values of the models with orders up to M, the maximum order. Namely, we have to estimate the coefficients by solving systems of linear equations with one unknown, ... , M unknowns.

However, with *Levinson's algorithm*, these solutions can be obtained quite efficiently. Hereinafter, the AR coefficients and the innovation variance of the AR model of order m are denoted as a_j^m and σ_m^2, respectively. Then Levinson's algorithm is defined as follows:

1. Set $\hat{\sigma}_0^2 = \hat{C}_0$ and $\mathrm{AIC}_0 = N(\log 2\pi\hat{\sigma}_0^2 + 1) + 2$
2. For $m = 1, \cdots, M$, repeat the following steps
   (a) $\hat{a}_m^m = \left(\hat{C}_m - \sum_{j=1}^{m-1} \hat{a}_j^{m-1} \hat{C}_{m-j} \right) \left(\hat{\sigma}_{m-1}^2 \right)^{-1}$,
   (b) $\hat{a}_i^m = \hat{a}_i^{m-1} - \hat{a}_m^m \hat{a}_{m-i}^{m-1}$ for $i = 1, \ldots, m-1$,
   (c) $\hat{\sigma}_m^2 = \hat{\sigma}_{m-1}^2 \{1 - (\hat{a}_m^m)^2\}$,
   (d) $\mathrm{AIC}_m = N(\log 2\pi\hat{\sigma}_m^2 + 1) + 2(m+1)$.

In Levinson's algorithm, the PARCOR $\hat{a}_m^m$ introduced in Chapter 6 plays an important role. This algorithm will be explained in detail later in Appendix B.

7.3 Estimation of an AR Model by the Least Squares Method

In this section, the least squares method explained in Chapter 5 will be applied to the estimation of the AR model. Putting $\theta = (a_1, \cdots, a_m, \sigma^2)^T$, from (7.4), the log-likelihood of the AR model becomes

$$\ell(\theta) = \sum_{n=1}^{N} \log p(y_n | y_1, \cdots, y_{n-1}). \tag{7.12}$$

Here, for the AR model of order m, since the distribution of y_n is specified by the values of $y_{n-1}, \cdots, y_{n-m}$ for $n > m$, each term in (7.12) is given by

$$p(y_n | y_1, \cdots, y_{n-1}) \quad = \quad p(y_n | y_{n-m}, \cdots, y_{n-1})$$

$$
\begin{aligned}
&= -\frac{1}{\sqrt{2\pi\sigma^2}}\exp\left\{-\frac{1}{2\sigma^2}\left(y_n-\sum_{i=1}^m a_i y_{n-i}\right)^2\right\} \\
\log p(y_n|y_1,\cdots,y_{n-1}) &= -\frac{1}{2}\log 2\pi\sigma^2 - \frac{1}{2\sigma^2}\left(y_n-\sum_{i=1}^m a_i y_{n-i}\right)^2.
\end{aligned}
\tag{7.13}
$$

Therefore, by ignoring the initial M $(M \geq m)$ terms of (7.12), the log-likelihood of the AR model is obtained as

$$
\ell(\theta) = -\frac{N-M}{2}\log 2\pi\sigma^2 - \frac{1}{2\sigma^2}\sum_{n=M+1}^{N}\left(y_n-\sum_{i=1}^m a_i y_{n-i}\right)^2 \tag{7.14}
$$

(Kitagawa and Akaike (1978), Sakamoto et al. (1986), Kitagawa and Gersch (1996)).

Similar to the case of the regression model, for arbitrarily given autoregressive coefficients $a_1,\cdots,a_m$, the maximum likelihood estimate of the variance σ^2 maximizing (7.14) satisfies

$$
\frac{\partial \ell(\theta)}{\partial \sigma^2} = -\frac{N-M}{2\sigma^2} + \frac{1}{2(\sigma^2)^2}\sum_{n=M+1}^{N}\left(y_n-\sum_{i=1}^m a_i y_{n-i}\right)^2 = 0, \tag{7.15}
$$

and is obtained as

$$
\hat{\sigma}^2 = \frac{1}{N-M}\sum_{n=M+1}^{N}\left(y_n-\sum_{i=1}^m a_i y_{n-i}\right)^2. \tag{7.16}
$$

Substituting this into (7.14), the log-likelihood becomes a function of the autoregressive coefficients $a_1,\cdots,a_m$

$$
\ell(a_1,\cdots,a_m) = -\frac{N-M}{2}\log 2\pi\hat{\sigma}^2 - \frac{N-M}{2}. \tag{7.17}
$$

Here, since the logarithm is a monotone increasing function, maximization of the approximate log-likelihood (7.17) can be achieved by minimizing the variance $\hat{\sigma}^2$. This means that the approximate maximum likelihood estimates of the AR model can be obtained by the least squares method. To obtain the least squares estimates of the AR models with orders up to M by the Householder transformation discussed in Chapter 5, define the matrix Z and the vector y by

$$
Z = \begin{bmatrix} y_M & y_{M-1} & \cdots & y_1 \\ y_{M+1} & y_M & \cdots & y_2 \\ \vdots & \vdots & \ddots & \vdots \\ y_{N-1} & y_{N-2} & \cdots & y_{N-M} \end{bmatrix}, \qquad y = \begin{bmatrix} y_{M+1} \\ y_{M+2} \\ \vdots \\ y_N \end{bmatrix}. \tag{7.18}
$$

For actual computation, construct the $(N-M)\times(M+1)$ matrix

$$X=[Z\,|\,y]=\begin{bmatrix} y_M & \cdots & y_1 & y_{M+1} \\ y_{M+1} & \cdots & y_2 & y_{M+2} \\ \vdots & \ddots & \vdots & \vdots \\ y_{N-1} & \cdots & y_{N-M} & y_N \end{bmatrix}, \qquad (7.19)$$

and transform it to an upper triangular matrix

$$HX=\begin{bmatrix} S \\ \mathrm{O} \end{bmatrix}=\begin{bmatrix} s_{11} & \cdots & s_{1M} & s_{1,M+1} \\ & \ddots & \vdots & \vdots \\ & & s_{MM} & s_{M,M+1} \\ & & & s_{M+1,M+1} \\ & \mathrm{O} & & \end{bmatrix}, \qquad (7.20)$$

by Householder transformation.

Then, for $0\le j\le M$, the innovation variance and the AIC of the AR model of order j are obtained by

$$\begin{aligned} \hat{\sigma}_j^2 &= \frac{1}{N-M}\sum_{i=j+1}^{M+1} s_{i,M+1}^2 \\ \mathrm{AIC}_j &= (N-M)(\log 2\pi\hat{\sigma}_j^2+1)+2(j+1). \end{aligned} \qquad (7.21)$$

Moreover, the least squares estimates of the autoregressive coefficients that are the solutions of the linear equations

$$\begin{bmatrix} s_{11} & \cdots & s_{1j} \\ & \ddots & \vdots \\ & & s_{jj} \end{bmatrix}\begin{bmatrix} a_1 \\ \vdots \\ a_j \end{bmatrix}=\begin{bmatrix} s_{1,M+1} \\ \vdots \\ s_{j,M+1} \end{bmatrix}, \qquad (7.22)$$

can be easily obtained by backward substitution as follows:

$$\begin{aligned} \hat{a}_j &= \frac{s_{j,M+1}}{s_{jj}} \\ \hat{a}_i &= \frac{s_{i,M+1}-s_{i,i+1}\hat{a}_{i+1}-\cdots-s_{i,j}\hat{a}_j}{s_{ii}}, \qquad i=j-1,\cdots,1. \end{aligned}$$

7.4 Estimation of an AR Model by the PARCOR Method

Assuming that the autocovariance functions $C_0, C_1, \cdots$ are given, Levinson's algorithm of Section 7.2 can be executed by using the following relation between the coefficients of the AR model of order $m-1$ and the coefficients of the AR model of order m:

$$a_j^m = a_j^{m-1} - a_m^m a_{m-j}^{m-1}. \tag{7.23}$$

Therefore, if we can estimate the PARCOR a_m^m, the other coefficients can be automatically determined by using the above relation. In Levinson's algorithm, we used the following formula for the estimation of a_m^m that is obtained by substituting the sample autocovariance functions $\hat{C}_0, \cdots, \hat{C}_m$ into (B.8) in the Appendix B:

$$\begin{aligned} \hat{a}_m^m &= \left\{ \hat{C}_0 - \sum_{j=1}^{m-1} \hat{a}_j^{m-1} \hat{C}_j \right\}^{-1} \left\{ \hat{C}_m - \sum_{j=1}^{m-1} \hat{a}_j^{m-1} \hat{C}_{m-j} \right\} \\ &= \left(\hat{\sigma}_{m-1}^2 \right)^{-1} \left\{ \hat{C}_m - \sum_{j=1}^{m-1} \hat{a}_j^{m-1} \hat{C}_{m-j} \right\}. \end{aligned} \tag{7.24}$$

In this section, we present another method of estimating PARCOR a_m^m directly from the time series $y_1, \cdots, y_N$ without using the sample autocovariance functions. First of all, let w_n^{m-1} denote the prediction error of the backward AR model with order $m-1$:

$$y_n = \sum_{j=1}^{m-1} a_j^{m-1} y_{n+j} + w_n^{m-1}. \tag{7.25}$$

In the case of univariate time series, since the autocovariance function is an even function, the AR coefficients of the forward model coincide with those of the backward model. Using this property, from Appendix (B.2), we have the expression

$$\begin{aligned} C_m - \sum_{j=1}^{m-1} a_j^{m-1} C_{m-j} &= \mathrm{E}\left\{ \left(y_n - \sum_{j=1}^{m-1} a_j^{m-1} y_{n-j} \right) y_{n-m} \right\} \\ &= \mathrm{E}\left(v_n^{m-1} y_{n-m} \right) \\ &= \mathrm{E}\left(v_n^{m-1} w_{n-m}^{m-1} \right). \end{aligned} \tag{7.26}$$

Therefore, the left-hand side of Equation (7.26) can be approximated by

$$\frac{1}{N-m} \sum_{n=m+1}^{N} v_n^{m-1} w_{n-m}^{m-1}. \tag{7.27}$$

On the other hand, from (B.4), we have

$$\begin{aligned} C_0 - \sum_{j=1}^{m-1} a_j^{m-1} C_j &= \mathrm{E}\Big\{ \Big(y_{n-m} - \sum_{j=1}^{m-1} a_j^{m-1} y_{n-m+j} \Big) y_{n-m} \Big\} \\ &= \mathrm{E}\big(w_{n-m}^{m-1} y_{n-m} \big) \\ &= \mathrm{E}\big(w_{n-m}^{m-1} \big)^2 . \end{aligned} \tag{7.28}$$

Using the equality $\mathrm{E}\big(w_{n-m}^{m-1}\big)^2 = \mathrm{E}\big(v_n^{m-1}\big)^2$, various estimates of (7.26) can be obtained corresponding to (7.28) as follows,

$$\frac{1}{N-m} \sum_{n=m+1}^{N} \big(w_{n-m}^{m-1} \big)^2 \tag{7.29}$$

$$\frac{1}{N-m} \Big\{ \sum_{n=m+1}^{N} \big(w_{n-m}^{m-1} \big)^2 \sum_{n=m+1}^{N} \big(v_n^{m-1} \big)^2 \Big\}^{\frac{1}{2}} \tag{7.30}$$

$$\frac{1}{2(N-m)} \Big\{ \sum_{n=m+1}^{N} \big(w_{n-m}^{m-1} \big)^2 + \sum_{n=m+1}^{N} \big(v_n^{m-1} \big)^2 \Big\}. \tag{7.31}$$

Based on these estimates, we obtain the following three estimators of PARCOR

$$\hat{a}_m^m = \sum_{n=m+1}^{N} v_n^{m-1} w_{n-m}^{m-1} \Big\{ \sum_{n=m+1}^{N} \big(w_{n-m}^{m-1} \big)^2 \Big\}^{-1} \tag{7.32}$$

$$\hat{a}_m^m = \sum_{n=m+1}^{N} v_n^{m-1} w_{n-m}^{m-1} \Big\{ \sum_{n=m+1}^{N} \big(w_{n-m}^{m-1} \big)^2 \sum_{n=m+1}^{N} \big(v_n^{m-1} \big)^2 \Big\}^{-\frac{1}{2}} \tag{7.33}$$

$$\hat{a}_m^m = 2 \sum_{n=m+1}^{N} v_n^{m-1} w_{n-m}^{m-1} \Big\{ \sum_{n=m+1}^{N} \big(w_{n-m}^{m-1} \big)^2 + \sum_{n=m+1}^{N} \big(v_n^{m-1} \big)^2 \Big\}^{-1} . \tag{7.34}$$

In addition to these estimators, we can define another estimator that could be obtained by replacing $\big(w_{n-m}^{m-1}\big)^2$ with $\big(v_n^{m-1}\big)^2$ in (7.32). The estimate of PARCOR obtained by (7.32) is a regression coefficient when the prediction error v_n^{m-1} of the forward model is regressed on the prediction error w_{n-m}^{m-1} of the backward model. Moreover, the estimate of (7.33) corresponds to the definition of PARCOR, since it is the correlation coefficient of v_n^{m-1} and w_{n-m}^{m-1}. The estimate of (7.34) minimizes the mean of the variances of the forward prediction errors and the backward prediction errors, and consequently Burg's algorithm based on the maximum entropy method (MEM) is obtained (Burg (1967)). The procedures to estimate the AR model from the time series $y_1, \cdots, y_N$ using the PARCOR method are described below. Here, for simplicity, the mean value of the time series y_n is assumed to be 0.

1. Set $v_n^0 = w_n^0 = y_n$, for $n = 1, \cdots, N$. In addition, for the AR model of order 0, compute $\hat{\sigma}_0^2 = N^{-1}\sum_{n=1}^N y_n^2$, and $\text{AIC}_0 = N(\log 2\pi\hat{\sigma}_0^2 + 1) + 2$.
2. For $m = 1, \cdots, M$, repeat the following steps (a)–(f).
   (a) Estimate the PARCOR $\hat{a}_m^m$ by any of the formulae (7.32), (7.33) or (7.34).
   (b) Obtain the AR coefficients $\hat{a}_1^m, \cdots, \hat{a}_{m-1}^m$ by (7.23).
   (c) For $n = m+1, \cdots, N$, obtain the forward prediction error as $v_n^m = v_n^{m-1} - \hat{a}_m^m w_{n-m}^{m-1}$.
   (d) For $n = m+1, \cdots, N$, obtain the backward prediction error as $w_{n-m}^m = w_{n-m}^{m-1} - \hat{a}_m^m v_n^{m-1}$.
   (e) Estimate the innovation variance of the AR model of order m by $\hat{\sigma}_m^2 = \hat{\sigma}_{m-1}^2 \left\{1 - (\hat{a}_m^m)^2\right\}$.
   (f) Obtain AIC by $\text{AIC}_m = N(\log 2\pi\hat{\sigma}_m^2 + 1) + 2(m+1)$.

7.5 Large Sample Distribution of the Estimates

On the assumption that the time series is generated by an AR model of order m, for large sample size n, the distribution of the estimates of the AR parameters is approximately given by

$$\hat{a}_j \sim N\left(a_j, n^{-1}\sigma^2\Sigma\right), \tag{7.35}$$

where Σ is the Toepliz matrix (7.2) generated from the autocovariance function and σ^2 is the innovation variance (Brockwell and Davis (1991), Shumway and Stoffer (2000).

On the other hand, if the time series follows AR model of order m, and if j is larger than m, the estimated PARCOR a_j^j, i.e., the j-th autoregressive coefficient of the AR model of order j ($j > m$), are approximately distributed independently with varaince $1/n$ (Quenouille (1948), Box and Jenkins (1970), Shumway and Stoffer (2000)), i.e.,

$$Var\left\{\hat{a}_j^j\right\} \simeq \frac{1}{n} \quad \text{for } j > m. \tag{7.36}$$

This property can be used to check the adequacy of the estimated order

Table 7.1 *Innovation variances and AIC values of the AR models of various orders fitted to the sunspot number data.*

m	σ_m^2	AIC$_m$	m	σ_m^2	AIC$_m$	m	σ_m^2	AIC$_m$
0	0.22900	317.05	7	0.06694	46.95	14	0.05766	26.45
1	0.09204	108.49	8	0.06573	44.73	15	0.05716	26.47
2	0.07058	49.17	9	0.05984	25.02	16	0.05701	27.84
3	0.06959	47.90	10	0.05829	20.96	17	0.05701	29.84
4	0.06868	46.85	11	0.05793	21.52	18	0.05669	30.53
5	0.06815	47.08	12	0.05780	23.02	19	0.05661	32.21
6	0.06805	48.72	13	0.05766	24.47	20	0.05615	32.32

of the model. The relation between AIC and the estimated PARCOR is considered in Problem 1 of this Chapter.

Example (AR modeling for sunspot number data) Table 7.1 summarizes the results of fitting AR models of orders up to 20 by the Yule-Walker method to the logarithm of the sunspot number data shown in Figure 1.1(b). Figure 7.1(a) shows the estimated PARCORs for orders $1,\ldots,20$. From Figure 7.1(b) that shows the change in AIC values as m varies, it can be seen that AIC is minimized at $m = 10$, and for larger m it gradually increases.

Since the sample size of the sunspot number data is $n = 231$, from (7.36), the large sample standard error of the estimated PARCOR is $(231)^{-1/2} \simeq 0.066$. It can be seen that the PARCORs for m = 11,...,16 are very small compared with this standarad error that supports the order selected by AIC.

On the other hand, plot (c) shows the spectrum obtained by the AR model of order $m = 10$ that minimizes the AIC. A strong peak is seen in the vicinity of the frequency $f = 0.1$, corresponding to a cycle of approximately 10 years.

Example (AR modeling and power spectra estimated through AR models) Figure 7.2 (a)–(f) shows the changes of AIC, when AR models with orders 1 to 20 are fitted to the time series shown in Figure 1.1 (a)–(f) by the Yule-Walker method. Figure 7.3 shows the power spectra of the time series obtained by the method presented in Chapter 6 using the AIC best AR model among the orders up to 20.

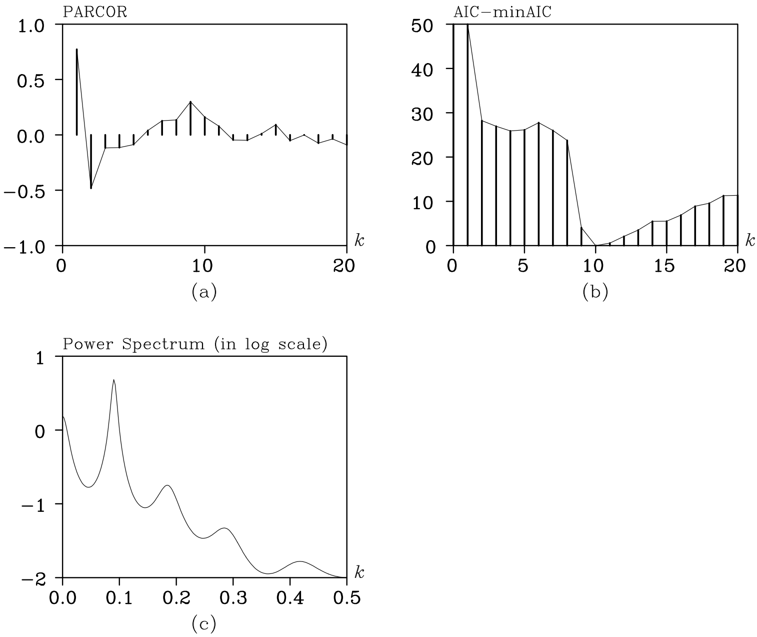

Figure 7.1 *Changes of PARCOR and AIC and estimated spectrum by the AIC best AR model for the sunspot number data.*

7.6 Estimation of a Multivariate AR Model by the Yule-Walker Method

In this section, estimation methods for multivariate AR models are shown. Hereinafter k denotes the number of variables (or dimensions) of a multivariate time series. The parameters of the multivariate AR model of order m

$$y_n = \sum_{i=1}^{m} A_i^m y_{n-i} + v_n, \qquad v_n \sim N(0, V_m), \tag{7.37}$$

are the variance-covariance matrix V_m of the innovation v_n and the AR coefficient matrices $A_1^m, \cdots, A_m^m$ (Akaike and Nakagawa (1989)).

When a multivariate AR model is given, the cross-covariance function is obtained from (6.28) and (6.29). On the other hand, using these equations, the estimates of the parameters of the multivariate AR model can be obtained through the sample cross-covariance function. For actual computation, similarly to the univariate AR model, they can be deter-

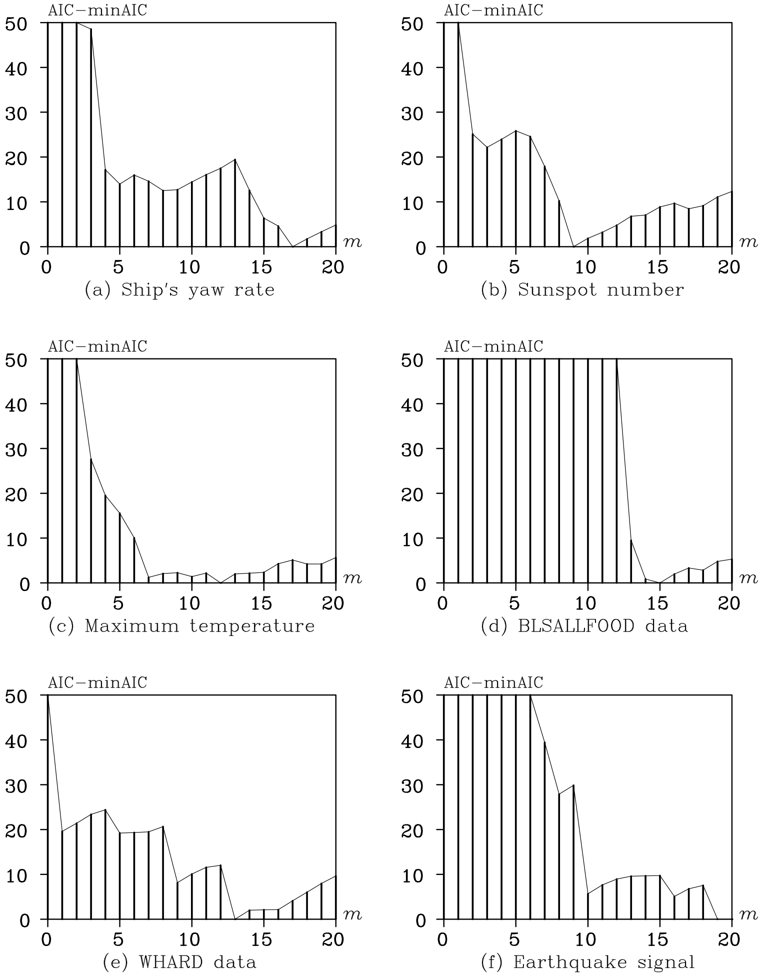

(a) Ship's yaw rate

(b) Sunspot number

(c) Maximum temperature

(d) BLSALLFOOD data

(e) WHARD data

(f) Earthquake signal

Figure 7.2: *Change in AIC values, as the order varies.*

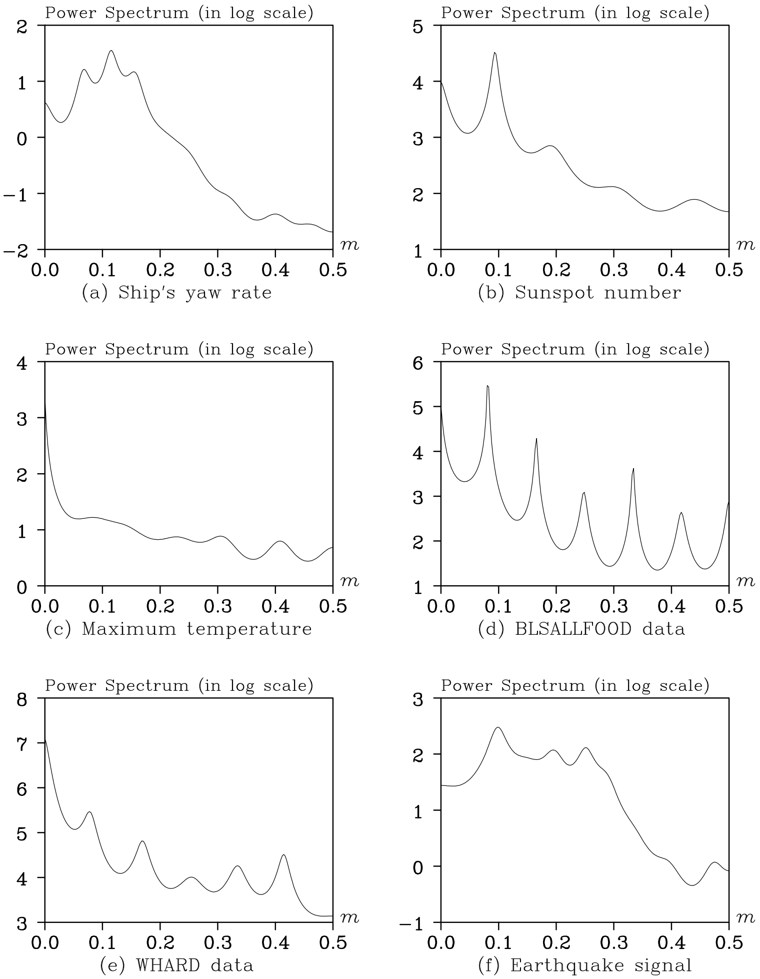

(a) Ship's yaw rate

(b) Sunspot number

(c) Maximum temperature

(d) BLSALLFOOD data

(e) WHARD data

(f) Earthquake signal

Figure 7.3: *Estimated spectra by AR models with minimum AIC orders.*

mined efficiently by the following algorithms. However, for a multivariate time series, the backward model is different from the forward model. In the case of a univariate time series, the forward AR model coincides with the backward AR model, because the autocovariance function is an even function. But this property is not satisfied by multivariate time series. Therefore, in order to derive an efficient algorithm similar to Levinson's algorithm, in addition to (7.37), we have to consider the backward multivariate AR model

$$y_n = \sum_{i=1}^{m} B_i^m y_{n+i} + u_n, \qquad u_n \sim N(0, U_m), \tag{7.38}$$

and we need to estimate the variance-covariance matrix U_m and the coefficients B_i^m, as well as A_i^m and V_m, simultaneously (Whittle (1963)).

1. Set $\hat{V}_0 = \hat{U}_0 = C_0$ and compute the AIC of the AR model of order 0 as
   $\mathrm{AIC}_0 = N(k \log 2\pi + \log|\hat{V}_0| + k) + k(k+1)$.
2. For $m = 1, \cdots, M$, repeat the following steps (a)–(e).
   (a) $W_m = C_m - \sum_{i=1}^{m-1} A_i^{m-1} C_{m-i}$.
   (b) Obtain the PARCOR matrices of the forward and backward AR models by $A_m^m = W_m U_{m-1}^{-1}$ and $B_m^m = W_m^T V_{m-1}^{-1}$.
   (c) Compute the AR coefficients of the forward and backward AR models by $A_i^m = A_i^{m-1} - A_m^m B_{m-i}^{m-1}$ and $B_i^m = B_i^{m-1} - B_m^m A_{m-i}^{m-1}$ for $i = 1, \ldots, m-1$.
   (d) Compute the innovation variance-covariance matrices by $V_m = C_0 - \sum_{i=1}^{m} A_i^m C_i^T$ and $U_m = C_0 - \sum_{i=1}^{m} B_i^m C_i$.
   (e) Compute the AIC value of the AR model of order m by $\mathrm{AIC}_m = N(k \log 2\pi + \log|\hat{V}_m| + k) + k(k+1) + 2k^2 m$.

By the above-mentioned algorithm, we compute $\mathrm{AIC}_0, \cdots, \mathrm{AIC}_M$, and select the m that results in the minimum AIC value as the best order of the multivariate AR model. In this method, it is assumed that the autoregressive coefficients $a_m(i,j)$ have common orders for all i and j.

Example Table 7.2 shows the results of fitting three-variate AR models of orders up to 20 by the Yule-Walker method for the ship's data shown in Figure 1.1. The AIC is minimized at $m = 10$, and increases gradually afterward. The power spectra, the cross spectra, the coherency, and the noise contribution, etc., that are shown in Chapter 6 are obtained from the multivariate AR model of order m =10, which attains the minimum AIC value.

Table 7.2: *AICs of multivariate AR models fitted to ship's data.*

m	AIC$_m$	m	AIC$_m$	m	AIC$_m$
0	7091.71	7	5105.83	14	5100.98
1	6238.80	8	5096.35	15	5113.05
2	5275.36	9	5087.91	16	5116.52
3	5173.02	10	5083.79	17	5129.42
4	5135.20	11	5093.79	18	5136.06
5	5136.63	12	5091.42	19	5143.56
6	5121.02	13	5097.98	20	5157.37

7.7 Estimation of a Multivariate AR Model by the Least Squares Method

To obtain the least squares estimates of the parameters of a multivariate AR model by the Householder method, we first transform the model (7.37) to the following expression with instantaneous response:

$$y_n = B_0 y_n + \sum_{i=1}^{m} B_i y_{n-i} + w_n, \qquad w_n \sim N(0,W). \tag{7.39}$$

(Takanami and Kitagawa (1991), Kitagawa and Gersch (1996)). Here, B_0 is a lower triangular matrix whose components on and above the diagonal are zero, thus

$$B_0 = \begin{bmatrix} 0 & 0 & \cdots & 0 \\ b_0(2,1) & 0 & \cdots & 0 \\ \vdots & \ddots & \ddots & \vdots \\ b_0(k,1) & \cdots & b_0(k,k-1) & 0 \end{bmatrix}. \tag{7.40}$$

The variance-covariance matrix W is assumed to be a diagonal matrix

$$W = \begin{bmatrix} \sigma_1^2 & 0 & \cdots & 0 \\ 0 & \sigma_2^2 & \ddots & \vdots \\ \vdots & \ddots & \ddots & 0 \\ 0 & \cdots & 0 & \sigma_k^2 \end{bmatrix}. \tag{7.41}$$

Since the model (7.39) can be expressed as

$$y_n = (I-B_0)^{-1} \sum_{i=1}^{m} B_i y_{n-i} + (I-B_0)^{-1} w_n, \tag{7.42}$$

by putting

$$\begin{aligned} A_i &= (I-B_0)^{-1}B_i \\ V &= (I-B_0)^{-1}W(I-B_0)^{-T}, \end{aligned} \tag{7.43}$$

there is a one-to-one correspondence between the multivariate AR model (7.38) and the multivariate model with instantaneous response given in (7.39). Therefore, if the coefficient matrices $B_0, B_1, \cdots, B_m$ and the variances $\sigma_1^2, \cdots, \sigma_k^2$ of the model (7.39) are estimated, the multivariate AR model will also be obtained by (7.43).

The advantage of this method is that we do not need to estimate all of the coefficients simultaneously, since the variance-covariance matrix W is a diagonal matrix. Namely, if we denote the coefficient matrix B_i as

$$B_i = \begin{bmatrix} b_i(1,1) & \cdots & b_i(1,k) \\ \vdots & \ddots & \vdots \\ b_i(k,1) & \cdots & b_i(k,k) \end{bmatrix}, \tag{7.44}$$

the coefficients of the k models, that is, $\{b_i(p,q),\ i = 1,\cdots,m,\ q = 1,\cdots,k,\ \sigma_p^2\}$ for $p = 1,\cdots,k$ can be estimated independently.

This method is far more computationally efficient than the method that estimates all of the coefficients at once. To realize the above estimation by the Householder method, firstly we construct an $(N-m)\times(km+k)$ matrix

$$X = \begin{bmatrix} y_m^T & \cdots & y_1^T & y_{m+1}^T \\ y_{m+1}^T & \cdots & y_2^T & y_{m+2}^T \\ \vdots & \ddots & \vdots & \vdots \\ y_{N-1}^T & \cdots & y_{N-m}^T & y_N^T \end{bmatrix}, \tag{7.45}$$

and transform it to an upper triangular matrix by the Householder transformation,

$$S = \begin{bmatrix} s_{11} & \cdots & s_{1,km+k} \\ & \ddots & \vdots \\ & & s_{km+k,km+k} \\ & \mathrm{O} & \end{bmatrix}. \tag{7.46}$$

It should be noted here that the $(km+1)\times(km+1)$ upper-left submatrix has all the necessary information to estimate the following model for the first component:

$$y_n(1) = \sum_{i=1}^{j} b_i(1,1)y_{n-i}(1) + \cdots + \sum_{i=1}^{j} b_i(1,k)y_{n-i}(k) + w_n. \tag{7.47}$$

That is, for $j \le m$, the residual variance and the AIC of the j-th order model are obtained by

$$\begin{aligned}\hat{\sigma}_j^2(1) &= \frac{1}{N-m}\sum_{i=kj+1}^{km+1} s_{i,km+1}^2, \\ \mathrm{AIC}_j(1) &= (N-m)(\log 2\pi\hat{\sigma}_j^2(1)+1)+2(kj+1). \qquad (7.48)\end{aligned}$$

The regression coefficients $c=(c_{11},\cdots,c_{1k},\cdots,c_{j1},\cdots,c_{jk})=(b_1(1,1),\cdots,b_1(1,k),\cdots,b_j(1,1),\cdots,b_j(1,k))^T$ are obtained as the solutions of the linear equations

$$\begin{bmatrix} s_{11} & \cdots & s_{1,kj} \\ & \ddots & \vdots \\ \mathrm{O} & & s_{kj,kj} \end{bmatrix}\begin{bmatrix} c_{11} \\ \vdots \\ c_{kj}\end{bmatrix} = \begin{bmatrix} s_{1,km+1} \\ \vdots \\ s_{kj,km+1}\end{bmatrix}. \qquad (7.49)$$

The solutions are easily obtained by the following backward substitution:

$$\begin{aligned}\hat{c}_{kj} &= s_{kj,km+1}/s_{kj,kj}, \\ \hat{c}_{\ell i} &= (s_{\ell i,km+1}-s_{\ell i,\ell i+1}\hat{c}_{\ell i+1}-\cdots-s_{\ell i,kj}\hat{c}_{kj})/s_{\ell i,\ell i} \\ & \qquad\qquad \text{for } i=1,\cdots,k \text{ and } j=1,\cdots,k. \qquad (7.50)\end{aligned}$$

Secondly, to estimate the model for the second component of the time series, transform the matrix (7.46) to the following form

$$S=\begin{bmatrix} s_{11} & \cdots & s_{1,km} & s_{1,km+1} & s_{1,km+2} & \cdots & s_{1,km+k} \\ s_{21} & \cdots & s_{2,km} & & s_{2,km+2} & \cdots & s_{2,km+k} \\ & \ddots & \vdots & & \vdots & & \vdots \\ & & s_{km+1,km} & & s_{km+1,km+2} & \cdots & s_{km+1,km+k} \\ & & & & s_{km+2,km+2} & \cdots & s_{km+2,km+k} \\ & & & & & \ddots & \vdots \\ & & & & & & s_{km+k,km+k} \\ & & \mathrm{O} & & & & \end{bmatrix}, \qquad (7.51)$$

by an appropriate Householder transformation. Then the upper-left $(km+2)\times(km+2)$ sub-matrix of this matrix contains all the information necessary for the estimation of the model for the second component.

For $j \le m$, the innovation variance and the AIC of the j-th order model for the second component are obtained by

$$\begin{aligned}\hat{\sigma}_j^2(2) &= \frac{1}{N-m}\sum_{i=kj+2}^{km+2} s_{i,km+2}^2 \\ \mathrm{AIC}_j(2) &= (N-m)(\log 2\pi\hat{\sigma}_j^2(2)+1)+2(kj+2). \qquad (7.52)\end{aligned}$$

To obtain the regression coefficients, we define the $(kj+1)$-dimensional vector c by $c = (b_1(2,1), \cdots, b_1(2,k), \cdots, b_j(2,1), \cdots, b_j(2,k), b_0(2,1))^T$ and then solve the following system of linear equations:

$$\begin{bmatrix} s_{11} & \cdots & s_{1,kj} & s_{1,km+1} \\ s_{21} & \cdots & s_{2,kj} & \\ & \ddots & \vdots & \\ & & s_{kj+1,kj} & \end{bmatrix} \begin{bmatrix} c_1 \\ c_2 \\ \vdots \\ c_{kj+1} \end{bmatrix} = \begin{bmatrix} s_{1,km+2} \\ s_{2,km+2} \\ \vdots \\ s_{kj+1,km+2} \end{bmatrix}. \tag{7.53}$$

Repeating this procedure up to the k-th component of the time series, we obtain the matrix

$$S = \begin{bmatrix} s_{11} & \cdots & s_{1,km} & s_{1,km+1} & \cdots & s_{1,km+k-1} & s_{1,km+k} \\ \vdots & & \vdots & & \ddots & \vdots & \vdots \\ s_{k-1,1} & \cdots & s_{k-1,km} & & & s_{k-1,km+k-1} & s_{k-1,km+k} \\ s_{k1} & \cdots & s_{k,km} & & & & s_{k,km+k} \\ & \ddots & \vdots & & & & \vdots \\ & & s_{km+k-1,km} & & & & s_{km+k-1,km+k} \\ & & & & & & s_{km+k,km+k} \\ & & & \mathrm{O} & & & \end{bmatrix} \tag{7.54}$$

by an appropriate Householder transformation.

For $j \le m$, the innovation variance and the AIC of the j-th order model are obtained by

$$\begin{aligned} \hat{\sigma}_j^2(k) &= \frac{1}{N-m} \sum_{i=kj+k}^{km+k} s_{i,km+k}^2 \\ \mathrm{AIC}_j(k) &= (N-m)(\log 2\pi\hat{\sigma}_j^2(k) + 1) + 2(kj+k). \end{aligned} \tag{7.55}$$

The regression coefficients of this model can be obtained by solving the system of linear equations

$$\begin{bmatrix} s_{11} & \cdots & s_{1,kj} & s_{1,km+1} & \cdots & s_{1,q-1} \\ \vdots & & \vdots & & \ddots & \vdots \\ s_{k-1,1} & \cdots & s_{k-1,kj} & & & s_{k-1,q-1} \\ s_{k1} & \cdots & s_{k,kj} & & & \\ & \ddots & \vdots & & & \\ & & s_{r,kj} & & & \end{bmatrix} \begin{bmatrix} c_1 \\ \vdots \\ c_{k-1} \\ c_k \\ \vdots \\ c_r \end{bmatrix} = \begin{bmatrix} s_{1,q} \\ \vdots \\ s_{k-1,q} \\ s_{k,q} \\ \vdots \\ s_{r,q} \end{bmatrix}, \tag{7.56}$$

where the vector c is defined by $c = (b_1(k,1),\cdots,b_1(k,k),\cdots,b_j(k,1),\cdots,$ $b_j(k,k),b_0(k,1),\cdots,b_0(k,k-1))^T$. Here, $q = km+k$ and $r = kj+k-1$.

This least square method has a significant advantage in that we can select a different order for each variable to enable more flexible modeling than the Yule-Walker method. In addition, it is also possible to specify a time-lag for a variable with respect to other variables or to specify a particular coefficient to be zero. A computer program for estimating such a sophisticated model can be found in Akaike et al. (1979).

Problems

1. Consider an AR model of order m: $y_n = a_1^m y_{n-1} + \cdots + a_m^m y_{n-m} + v_n$, $v_n \sim N(0,\sigma_m^2)$.
   (1) Using the relation $\sigma_m^2 = (1-(a_m^m)^2)\sigma_{m-1}^2$, show a criterion to judge whether AR(m) is better than AR$(m-1)$.
   (2) The PARCOR coefficients (a_j^j of AR(j)) are estimated by using 100 observations and are given by $a_1^1 = 0.9$, $a_2^2 = -0.6$, $a_3^3 = 0.3$, $a_4^4 = -0.1$, $a_5^5 = 0.15$. Assuming that $C_0 = 1$, compute σ_m^2, for $m = 1,\ldots,5$.
   (3) Assuming the situation of (2), compute AIC$_m$ for $m = 1,\cdots,5$ and determine the best order.
2. State the differences in the properties of the Yule-Walker method, the least squares method and the PARCOR method.
3. Show a method, based on AR models, of judging whether two time series x_n and y_n are independent.

Chapter 8

The Locally Stationary AR Model

Records of real-world phenomena can mostly be categorized as nonstationary time series. The simplest approach to modeling nonstationary time series is, firstly, to partition the time interval into several subintervals of appropriate size, on the assumption that the time series are stationary on each subinterval. Secondly, by fitting an AR model to each subinterval, we can obtain a series of models that approximate nonstationary time series. In this chapter, two modeling methods are shown for analysis of nonstationary time series, namely, a model for roughly deciding on the number of subintervals and the locations of their endpoints and a model for precisely estimating a change point. A more sophisticated time-varying coefficient AR model will be considered in Chapter 13.

8.1 Locally Stationary AR Model

It is assumed that the given time series $y_1, \cdots, y_N$ is nonstationary as a whole, but that we can consider it to be stationary on each subinterval of an appropriately constructed partition. Such a time series that satisfies piecewise stationarity is called a *locally stationary time series* (Ozaki and Tong (1975), Kitagawa and Akaike (1978), Kitagawa and Gersch (1996)). To be specific, k and N_i are assumed to denote the number of subintervals, and the number of observations in the i-th subinterval $(N_1 + \cdots + N_k = N)$, respectively. Actually, k and N_i are unknown in practical modeling. Therefore, in the analysis of locally stationary time series, it is necessary to estimate the number of subintervals, k, the locations of the dividing points and appropriate models for subintervals.

A *locally stationary AR model* is a nonstationary time series model, which has the property that, on each appropriately constructed subinterval, it is stationary and can be modeled by an AR model on each of these subintervals. More precisely, consider the i-th subinterval, $[n_{i0}, n_{i1}]$

where

$$n_{i0} = \sum_{j=1}^{i-1} N_j + 1, \qquad n_{i1} = \sum_{j=1}^{i} N_j.$$

For a locally stationary AR model, the time series y_n follows an AR model

$$y_n = \sum_{i=1}^{m_j} a_{ji} y_{n-i} + v_{nj}, \tag{8.1}$$

on the j-th subinterval, where v_{nj} is assumed to be white noise that satisfies $\mathrm{E}(v_{nj}) = 0$, $\mathrm{E}(v_{nj}^2) = \sigma_j^2$ and $\mathrm{E}(v_{nj} y_{n-m}) = 0$ for $m = 1, 2, \cdots$. The likelihood of the locally stationary AR model is given by

$$L = p(y_1, \cdots, y_N) = \prod_{j=1}^{k} \prod_{n=n_{j0}}^{n_{j1}} p(y_n | y_1, \cdots, y_{n-1}). \tag{8.2}$$

Therefore, similar to the case of the least square method of the AR model for stationary time series, ignoring the distributions of the first m_1 data points to replace N_1 by $N_1 - m_1$ and n_{10} with $m_1 + 1$, the likelihood of this model can be approximated by

$$\prod_{j=1}^{k} \left(\frac{1}{2\pi\sigma_j^2} \right)^{\frac{N_j}{2}} \exp\left\{ -\frac{1}{2\sigma_j^2} \sum_{n=n_{j0}}^{n_{j1}} \left(y_n - \sum_{i=1}^{m_j} a_{ji} y_{n-i} \right)^2 \right\}. \tag{8.3}$$

Here, if we consider this likelihood as a function of the number of subintervals: k, the length of the j-th interval: N_j, the autoregressive order: m_j, the autoregressive coefficients: $a_j = (a_{j1}, \cdots, a_{jm_j})^T$ and the variance of the white noise: σ_j^2, then the log-likelihood function can be expressed as

$$\begin{aligned} &\ell\ (k, N_j, m_j, a_j, \sigma_j^2; j = 1, \cdots, k) \\ &= -\frac{1}{2} \sum_{j=1}^{k} \left\{ N_j \log 2\pi\sigma_j^2 + \frac{1}{\sigma_j^2} \sum_{n=n_{j0}}^{n_{j1}} \left(y_n - \sum_{i=1}^{m_j} a_{ji} y_{n-i} \right)^2 \right\}. \end{aligned} \tag{8.4}$$

For arbitrarily given autoregressive coefficients a_j, by equating the first derivative of the log-likelihood with respect to σ_j^2 to 0, we obtain the maximum likelihood estimate of the variance σ_j^2 as

$$\hat{\sigma}_j^2 = \frac{1}{N_j} \sum_{n=n_{j0}}^{n_{j1}} \left(y_n - \sum_{i=1}^{m_j} a_{ji} y_{n-i} \right)^2. \tag{8.5}$$

From the above, substituting this into (8.4), the log-likelihood becomes

$$\begin{aligned}\ell\,(k,N_j,m_j,a_j,\hat{\sigma}_j^2;j=1,\cdots,k) \\ &= -\frac{1}{2}\sum_{j=1}^{k}\left(N_j\log\left(2\pi\hat{\sigma}_j^2\right)+N_j\right) \\ &= -\frac{N-m_1}{2}(\log 2\pi+1)-\frac{1}{2}\sum_{j=1}^{k}N_j\log\hat{\sigma}_j^2. \qquad (8.6)\end{aligned}$$

Therefore, the maximum likelihood estimate of $a_{j1},\cdots,a_{jm_j}$ is obtained by minimizing σ_j^2 using the least squares method that was described in Chapter 5. Since the AR model on the j-th interval has m_j AR coefficients and its variance as parameters, the AIC value for the locally stationary AR model is given by

$$\text{AIC} = (N-m_1)(\log 2\pi+1)+\sum_{j=1}^{k}N_j\log\hat{\sigma}_j^2+2\sum_{j=1}^{k}(m_j+1). \qquad (8.7)$$

The number of subintervals k, the length of the j-th subinterval N_j and the order of the AR model for the j-th interval m_j are obtained by finding the combinations that achieve the minimum AIC value among possible candidates.

8.2 Automatic Partitioning of the Time Interval into an Arbitrary Number of Subintervals

As shown in the previous section, the best locally stationary AR model can, in principle, be obtained by the least squares method and AIC. However, practically speaking, it would require an enormous amount of computation to find the model that minimizes the AIC by fitting locally stationary AR models for all possible combinations of numbers of subintervals, k, and data lengths, $N_1,\cdots,N_k$. In terms of practice, the following procedure was developed to determine the dividing points of the locally stationary AR model (Ozaki and Tong (1975)). Accordingly, only the points $n_i = iL$ are considered as candidates for dividing points, while the minimum unit L of division has been set beforehand. Then, the dividing points of the locally stationary AR model can automatically be decided by the following procedure.

1. Determine the basic span L and the highest order m of the AR model that is fitted to the subinterval of the length L. Here L is set to an

appropriate length so that an AR model of order m can be fitted on an interval of length L.

2. Fit AR models of orders up to m to the time series $y_1, \cdots, y_L$, and compute $\mathrm{AIC}_0(0), \cdots, \mathrm{AIC}_0(m)$ to find $\mathrm{AIC}_0 = \min_j \mathrm{AIC}_0(j)$. Further, set $k = 1$, $n_{10} = m+1$, $n_{11} = L$ and $N_1 = L - m$.

3. Fit AR models with orders up to m to the time series $y_{n_{k1}+1}, \cdots, y_{n_{k1}+L}$ and compute $\mathrm{AIC}_1(0)$, $\cdots$, $\mathrm{AIC}_1(m)$ to set $\mathrm{AIC}_1 = \min_j \mathrm{AIC}_1(j)$. AIC_1 is the AIC of a new model that was obtained under the assumption that the model changed at time $n_{k1}+1$. The AIC of the locally stationary AR model that divides the interval $[n_{k0},\, n_{k1}+L]$ into two subintervals, $[n_{ko},\, n_{k1}]$ and $[n_{k1}+1,\, n_{k1}+L]$, is given by

$$\mathrm{AIC}_D = \mathrm{AIC}_0 + \mathrm{AIC}_1.$$

   This model is called a *divided model*.

4. Considering $y_{n_{k0}}, \cdots, y_{n_{k1}+L}$ to be a stationary interval, fit AR models of orders up to m to compute $\mathrm{AIC}_P(0), \cdots, \mathrm{AIC}_P(m)$, and then put $\mathrm{AIC}_P = \min_j \mathrm{AIC}_P(j)$. On the assumption that the time series on the entire interval $[n_{k0}, n_{k1}+L]$ is stationary, the model is called a *pooled model*.

5. To judge the homogeneity of the two subintervals, compare the AIC_D value of the model of step 3 above and the AIC_P value of the model of step 4 above.

   (a) If $\mathrm{AIC}_D < \mathrm{AIC}_P$, it is judged that a divided model is better. In this case, $n_{k1}+1$ becomes the initial point of the current subinterval; we put $k \equiv k+1$, $n_{k0} \equiv n_{k-1,1}+1$, $n_{k1} = n_{k-1,1}+L$, $N_k = L$ and $\mathrm{AIC}_0 = \mathrm{AIC}_D$.

   (b) If $\mathrm{AIC}_D \geq \mathrm{AIC}_P$, a pooled model is adopted. In this case, the new subinterval $[n_{k1}+1, n_{k1}+L]$ is merged with the former subinterval, and $[n_{k0}, n_{k1}+L]$ becomes the new current subinterval. Therefore, we put $n_{k1} \equiv n_{k1}+L$, $N_k = N_k + L$, and $\mathrm{AIC}_0 = \mathrm{AIC}_P$.

6. If we have at least L remaining additional data points, we have to go back to step (3). Otherwise, the number of subintervals is k and $[1, n_{11}]$, $[n_{20}, n_{21}], \cdots, [n_{k0}, N]$ are the stationary subintervals.

In our approach, we fit two types of AR models whenever an additional time series of length L remains to be modeled. The process can be efficiently carried out by the method of data augmentation shown in Section 5.4 (Kitagawa and Akaike (1978)). In step 2, we firstly construct an $(L-m)\times(m+1)$ matrix from the initial time series; $y_1,\cdots,y_L$,

$$X_0 = \begin{bmatrix} y_m & \cdots & y_1 & y_{m+1} \\ \vdots & \ddots & \vdots & \vdots \\ y_{L-1} & \cdots & y_{L-m} & y_L \end{bmatrix}, \tag{8.8}$$

and then reduce it to upper triangular form by an appropriate Householder transformation H_0,

$$H_0X_0 = \begin{bmatrix} S \\ \mathrm{O} \end{bmatrix} = \begin{bmatrix} s_{11} & \cdots & s_{1m} & s_{1,m+1} \\ & \ddots & \vdots & \vdots \\ & & s_{mm} & s_{m,m+1} \\ & & & s_{m+1,m+1} \\ & \mathrm{O} & & \end{bmatrix}. \tag{8.9}$$

Then, the AIC of the AR model of order j fitted to $y_1,\cdots,y_L$ is obtained by

$$\hat{\sigma}_0^2(j) = \frac{1}{L-m}\sum_{i=j+1}^{m+1} s_{i,m+1}^2 \tag{8.10}$$

$$\mathrm{AIC}_0(j) = (L-m)\log\hat{\sigma}_0^2(j) + 2(j+1). \tag{8.11}$$

Here, and hereinafter in this chapter, we omit the term $(L-m)(\log 2\pi + 1)$ from AIC, since this term is a constant term, irrelevant for model selection. To execute step 3, we construct an $L\times(m+1)$ matrix from $y_{n_{k1}+1},\cdots,y_{n_{k1}+L}$

$$X_1 = \begin{bmatrix} y_{n_{k1}} & \cdots & y_{n_{k1}-m+1} & y_{n_{k1}+1} \\ \vdots & \ddots & \vdots & \vdots \\ y_{n_{k1}+L-1} & \cdots & y_{n_{k1}+L-m} & y_{n_{k1}+L} \end{bmatrix}, \tag{8.12}$$

and reduce it to an upper triangular matrix by a Householder transformation H_1,

$$H_1X_1 = \begin{bmatrix} R \\ \mathrm{O} \end{bmatrix} = \begin{bmatrix} r_{11} & \cdots & r_{1m} & r_{1,m+1} \\ & \ddots & \vdots & \vdots \\ & & r_{mm} & r_{m,m+1} \\ & & & r_{m+1,m+1} \\ & \mathrm{O} & & \end{bmatrix}. \tag{8.13}$$

Here, similar to step 2, the AIC of the AR model of order j fitted to the new time series of length L is obtained by

$$\begin{aligned} \hat{\sigma}_1^2(j) &= \frac{1}{L}\sum_{i=j+1}^{m+1} r_{i,m+1}^2 && (8.14)\\ \mathrm{AIC}_1(j) &= L\log\hat{\sigma}_1^2(j)+2(j+1). && (8.15) \end{aligned}$$

Then,

$$\mathrm{AIC}_D \equiv \min_j \mathrm{AIC}_0(j) + \min_j \mathrm{AIC}_1(j) \qquad (8.16)$$

becomes the AIC value for the locally stationary AR model. It is assumed that there was structural change at time $n_{k1}+1$.

Next, in order to fit an AR model to the pooled data $y_{n_{k0}},\cdots,y_{n_{k1}+L}$ in step 4, we construct the following $2(m+1)\times(m+1)$ matrix by augmenting the upper triangular matrix S obtained from the data $y_{n_{k0}},\cdots,y_{n_{k1}}$ with the upper triangular matrix R obtained in step 3,

$$X_2 = \begin{bmatrix} S \\ R \end{bmatrix} = \begin{bmatrix} s_{11} & \cdots & s_{1m} & s_{1,m+1} \\ & \ddots & \vdots & \vdots \\ & & s_{mm} & s_{m,m+1} \\ \mathrm{O} & & & s_{m+1,m+1} \\ r_{11} & \cdots & r_{1m} & r_{1,m+1} \\ & \ddots & \vdots & \vdots \\ & & r_{mm} & r_{m,m+1} \\ \mathrm{O} & & & r_{m+1,m+1} \end{bmatrix}, \qquad (8.17)$$

and reduce it to upper triangular form by a Householder transformation:

$$H_2X_2 = \begin{bmatrix} T \\ \mathrm{O} \end{bmatrix} = \begin{bmatrix} t_{11} & \cdots & t_{1m} & t_{1,m+1} \\ & \ddots & \vdots & \vdots \\ & & t_{mm} & t_{m,m+1} \\ & & & t_{m+1,m+1} \\ & & \mathrm{O} & \end{bmatrix}. \qquad (8.18)$$

Then the AIC value for the AR model of order j is obtained by

$$\begin{aligned} \hat{\sigma}_P^2(j) &= \frac{1}{N_k+L}\sum_{i=j+1}^{m+1} t_{i,m+1}^2, && (8.19)\\ \mathrm{AIC}_P(j) &= (N_k+L)\log\hat{\sigma}_P^2(j)+2(j+1). && (8.20) \end{aligned}$$

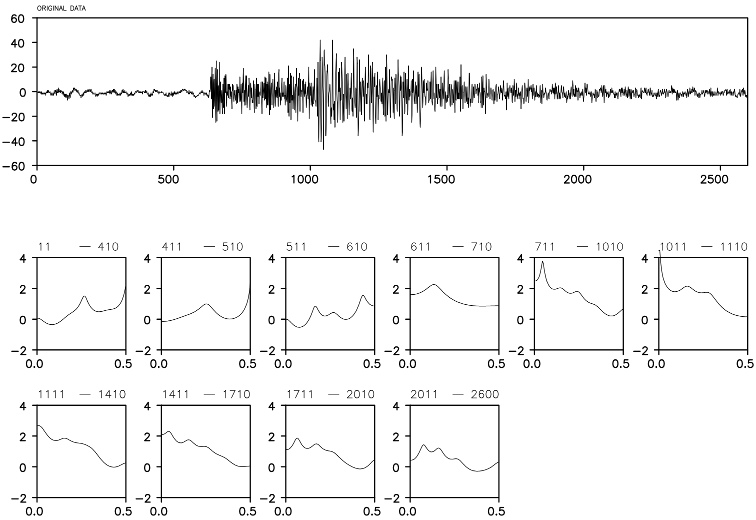

Figure 8.1 *The east-west component record of seismic wave and estimated spectra obtained by a locally stationary AR model.*

Therefore, by finding the minimum (over j) of $\mathrm{AIC}_P(j)$, thus,

$$\mathrm{AIC}_P \equiv \min_j \mathrm{AIC}_P(j), \tag{8.21}$$

we obtain the AIC value for the AR model, which was obtained under the assumption that the structural change did not occur at time $n_{k1}+1$.

In step 5, replace the matrix S with the matrix T if $\mathrm{AIC}_D < \mathrm{AIC}_P$ or with the matrix R if $\mathrm{AIC}_D \geq \mathrm{AIC}_P$. Then go back to step 3.

Example (Locally stationary modeling of seismic data) Figure 8.1 shows the results of fitting a locally stationary AR model to the east-west component of a seismogram $(N = 2600)$ with $L = 100$ and $m = 10$ (Takanami and Kitagawa (1991)). The record involves microtremors as the noise and two types of seismic wave; the P-wave and the S-wave. The power spectra shown in the figures are obtained from AR models estimated on the decided stationary subintervals. Structural changes have been detected at nine points, n =410, 510, 610, 710, 1010, 1110, 1410, 1710 and 2010. The change around $n = 600$ corresponds to a change in the spectrum and the variance caused by the arrival of the P-wave. The section $n = 600 - 1000$ corresponds to the P-wave. Whereas the spectrum during $n = 600 - 700$ contains a single strong periodic component, various periodic components with different periods are intermingled during the latter half of the P-wave, $n = 700 - 1000$. The S-wave appears after $n = 1000$. We can see not only a decrease in power due to the reduction of the amplitude but also that the main peak shifts from the low frequency range to the high frequency range. After $n = 2000$, no significant change in the spectrum could be detected.

8.3 Precise Estimation of a Change Point

In the previous sections, we have presented a method of automatically dividing the time interval of a nonstationary time series into several subintervals in which the time series could be regarded as stationary. Here, we consider a method of detecting the precise time of a structural change by assuming that a structural change of the time series y_n occurred within the time interval $[n_0, n_1]$. A multivariate extension of this method is shown in Takanami and Kitagawa (1991).

Assuming that the structural change occurred at time n; $n_0 \le n \le n_1$, a different AR model is fitted to each subinterval $[1, n-1]$ and $[n, N]$, respectively. Then the sum of the two AIC values of the AR models fitted to these time series yields the AIC value of a locally stationary AR model with a structural change at time n. To obtain a precise estimate of the time of structural change based on the locally stationary AR models, we could compute the AICs for all n such that $n_0 \le n \le n_1$ to find the minimum value. With this method, because we have to estimate AR models for all n, a huge amount of computation is required. However, we can derive a computationally very efficient procedure for obtaining the AIC values for all the locally stationary AR models by using the method of data augmentation shown in Section 5.4.

According to this procedure, from the time series $y_1, \cdots, y_{n_0}$, we first construct an $(n_0 - m) \times (m+1)$ matrix

$$X_0 = \begin{bmatrix} y_m & \cdots & y_1 & y_{m+1} \\ \vdots & \ddots & \vdots & \vdots \\ y_{n_0-1} & \cdots & y_{n_0-m} & y_{n_0} \end{bmatrix}, \tag{8.22}$$

and reduce it to upper triangular form by a Householder transformation:

$$H_0 X_0 = \begin{bmatrix} S \\ \mathrm{O} \end{bmatrix} = \begin{bmatrix} s_{11} & \cdots & s_{1m} & s_{1,m+1} \\ & \ddots & \vdots & \vdots \\ & & s_{mm} & s_{m,m+1} \\ & & & s_{m+1,m+1} \\ & & \mathrm{O} & \end{bmatrix}. \tag{8.23}$$

Then, the AIC value for the AR model of order j fitted to the time series $y_1, \cdots, y_{n_0}$ is obtained by

$$\begin{aligned} \hat{\sigma}_0^2(j) &= \frac{1}{n_0 - m} \sum_{i=j+1}^{m+1} s_{i,m+1}^2, & (8.24) \\ \mathrm{AIC}_0(j) &= (n_0 - m) \log \hat{\sigma}_0^2(j) + 2(j+1). & (8.25) \end{aligned}$$

Therefore, on the assumption that a structural change occurred at time $n_0 + 1$, the AIC value for the best AR model on the first part of the interval is given by

$$\mathrm{AIC}_0^1 \equiv \min_j \mathrm{AIC}_0(j). \quad (8.26)$$

To obtain the AIC value for the AR model fitted to the augmented data $y_1, \cdots, y_{n_0+p}$, where p is the number of additional data points $(p \geq 1)$, we construct an $(m+p+1) \times (m+1)$ matrix X_1 by augmenting the upper triangular matrix obtained in the previous step with the new data

$$X_1 = \begin{bmatrix} s_{11} & \cdots & s_{1m} & s_{1,m+1} \\ & \ddots & \vdots & \vdots \\ & & s_{mm} & s_{m,m+1} \\ & & & s_{m+1,m+1} \\ y_{n_0} & \cdots & y_{n_0-m+1} & y_{n_0+1} \\ \vdots & & \vdots & \vdots \\ y_{n_0+p-1} & \cdots & y_{n_0-m+p} & y_{n_0+p} \end{bmatrix}, \quad (8.27)$$

and reduce it to upper triangular form by an appropriately defined Householder transformation H_1:

$$H_1 X_1 = \begin{bmatrix} R \\ \mathrm{O} \end{bmatrix} = \begin{bmatrix} r_{11} & \cdots & r_{1m} & r_{1,m+1} \\ & \ddots & \vdots & \vdots \\ & & r_{mm} & r_{m,m+1} \\ & & & r_{m+1,m+1} \\ & \mathrm{O} & & \end{bmatrix}. \quad (8.28)$$

The AIC value for the AR model of order j fitted to the augmented data $y_1, \cdots, y_{n_0+p}$ is obtained by

$$\begin{aligned} \hat{\sigma}_1^2(j) &= \frac{1}{n_0 - m + p} \sum_{i=j+1}^{m+1} r_{i,m+1}^2, \\ \mathrm{AIC}_1(j) &= (n_0 - m + p) \log \hat{\sigma}_1^2(j) + 2(j+1). & (8.29) \end{aligned}$$

Therefore, under the assumption that the structural change occurred at time $n_0 + p + 1$, the AIC value for the best AR model for the first-half interval is obtained by

$$\mathrm{AIC}_1^1 \equiv \min_j \mathrm{AIC}_1(j). \tag{8.30}$$

Repeating this procedure, the AIC values for the AR models fitted to the time series $\{y_1, \cdots, y_{n_0}\}$, $\{y_1, \cdots, y_{n_0+p}\}, \cdots, \{y_1, \cdots, y_{n_1}\}$; i.e., AIC_0^1, $\mathrm{AIC}_1^1, \cdots, \mathrm{AIC}_\ell^1$ can be obtained.

The AIC values for the AR models after the structural change can similarly be obtained. With respect to the AICs of the latter-half AR models, we first fit AR models to the data $y_{n_1+1}, \cdots, y_N$ and then augment with p observations successively; i.e., we fit AR models to $\{y_{n_1+1}, \cdots, y_N\}, \{y_{n_1-p+1}, \cdots, y_N\}, \{y_{n_1-2p+1}, \cdots, y_N\}, \cdots, \{y_{n_0+1}, \cdots, y_N\}$ and compute the AIC values for the models, AIC_ℓ^2, $\mathrm{AIC}_{\ell-1}^2, \cdots, \mathrm{AIC}_0^2$.

Then,

$$\mathrm{AIC}_j = \mathrm{AIC}_j^1 + \mathrm{AIC}_j^2 \tag{8.31}$$

yields the AIC value for the locally stationary AR model on the assumption that the structural change occurred at time $n_0 + jp + 1$. Therefore, we can estimate the time point of structural change by finding the j for which the minimum of $\mathrm{AIC}_0, \cdots, \mathrm{AIC}_\ell$ is attained.

Example (Estimation of the arrival times of P-wave and S-wave) Figure 8.2 shows the results of precisely examining the change points around $n = 600$ and $n = 1000$, where the substantial changes are seen in Figure 8.1. Plot (b) shows the enlarged part of $n = 400 - 800$ where the first half might be considered as the microtremors and the latter half might be the P-wave. In plot (a), the value of AIC obtained by (8.31) is shown and the minimum value 3364 attained at $n = 630$. Accordingly, it can be inferred that the P-wave arrived at a time corresponding to $n = 630$.

Plot (d) shows the enlarged part of $n = 800 - 1200$ and the first and the latter half of the plot are the P-wave and the S-wave, respectively. From the value of AIC shown in plot (c), we can infer that the S-wave arrived at a time corresponding to $n = 1026$. In plot (a), the AIC has a clear minimum and the estimate of the arrival time is very accurate, whereas plot (c) shows a gradual change in the AIC and the detection of the arrival time of S-wave is correspondingly rather more difficult than that of the P-wave.

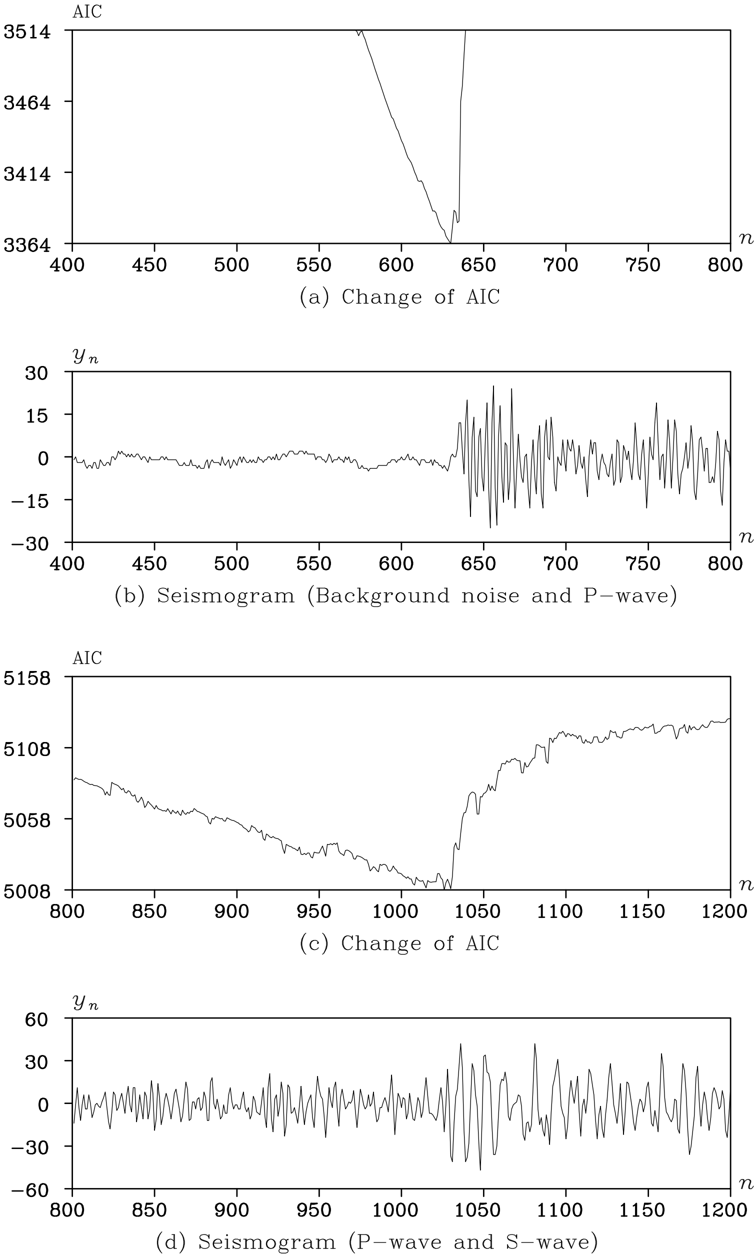

(a) Change of AIC

(b) Seismogram (Background noise and P−wave)

(c) Change of AIC

(d) Seismogram (P−wave and S−wave)

Figure 8.2: *Estimation of the arrival times of the P-wave and the S-wave.*

Problems

1. In locally stationary AR modeling, what kind of model should we use if the mean of the time series changes over time. State the expression of the AIC for that model.
2. Corresponding to the time series shown in Figure 1.2, consider a locally stationary AR model for the situation where only the variance of the time series changes over time.
3. Referring to the polynomial regression model introduced in Chapter 11, obtain the AIC of the model in which the polynomial changes over time.
4. In Problem 2, consider models that reflect the continuity or the smoothness of the trend.
5. Assuming that the Householder transformations for (8.22) and (8.27) need $\frac{1}{2}n_0m^2$ and $\frac{1}{2}(p+1)m^2$ computations, compare the amount of computation required for an ordinary AR model and the locally stationary AR model presented in Section 8.3.

Chapter 9

Analysis of Time Series with a State-Space Model

Various models used in time series analysis can be treated entirely within the state-space model framework. Many problems of time series analysis can be formulated in terms of the state estimation of a state-space model. This chapter presents algorithms for the Kalman filter and a smoothing algorithm for efficient state estimation. In addition, applications to the increasing horizon prediction, interpolation and parameter estimation of a time series are dealt with.

9.1 The State-Space Model

It is assumed that y_n is an ℓ-variate time series. The following model for the time series is called a *state-space model*.

$$
\begin{aligned}
x_n &= F_n x_{n-1} + G_n v_n, && \text{(system model)} \qquad (9.1)\\
y_n &= H_n x_n + w_n, && \text{(observation model)}, \qquad (9.2)
\end{aligned}
$$

where x_n is a k-dimensional unobservable vector, referred to as the *state* (Anderson and Moore (1979)). v_n is a system noise or a state noise, that is, an m-dimensional white noise with mean vector zero and variance-covariance matrix Q_n. On the other hand, w_n is called observation noise; it is assumed to be an ℓ-dimensional Gaussian white noise with mean vector zero and the variance-covariance matrix R_n. F_n, G_n and H_n are $k \times k$, $k \times m$ and $\ell \times k$ matrices, respectively. Many linear models used in time series analysis are expressible in terms of state-space models.

With respect to the concept of the state-space model, it has the following two interpretations. First, if we consider the observation model of (9.2) as a regression model that expresses a mechanism for obtaining the time series y_n, then the state x_n corresponds to the regression coefficients. In this case, the system model (9.1) expresses the time-change of the regression coefficients.

On the other hand, on the assumption that x_n is considered as the unknown signal, the system model expresses the generation mechanism of the signal, and the observation model expresses the structure of the actually observed signal, which was obtained by constructing a transformed signal, contaminated by an additive noise.

Example (State-space representation of an AR model) Here, we shall consider an AR model for the time series y_n

$$y_n = \sum_{i=1}^{m} a_i y_{n-i} + v_n, \tag{9.3}$$

where a_i is the AR coefficient and v_n is a Gaussian white noise with mean zero and variance σ^2.

Then, if the state vector is defined as $x_n = (y_n, y_{n-1}, \cdots, y_{n-m+1})^T$, it can easily be verified that there is a relation between the two states, x_n and x_{n-1}:

$$x_n = Fx_{n-1} + Gv_n. \tag{9.4}$$

Here, F and G are the $m \times m$ matrix and the m dimensional vector defined by

$$F = \begin{bmatrix} a_1 & a_2 & \cdots & a_m \\ 1 & & & \\ & \ddots & & \\ & & 1 & 0 \end{bmatrix}, \qquad G = \begin{bmatrix} 1 \\ 0 \\ \vdots \\ 0 \end{bmatrix}, \tag{9.5}$$

respectively.

On the other hand, since the first component of the state x_n is the observation y_n, by putting $H = [\,1\ 0\ \cdots\ 0\,]$, we obtain the observation model

$$y_n = Hx_n. \tag{9.6}$$

Furthermore, assigning $Q = \sigma^2$ and $R = 0$ to the variances of the system noise and the observation noise, respectively, a state-space model representation of the AR model can be obtained. Thus, the AR model is a special form of the state-space model, in that the state vector x_n is completely determined by the observations until time n, and then the observation noise becomes zero.

It should be noted here that representation in terms of the state-space model is not unique. For example, given the state-space models (9.1) and (9.2), for any non-singular matrix T, by defining a new state z_n, the matrix F_n' and the vectors G_n' and H_n' by

$$z_n = Tx_n, \qquad F_n' = TF_nT^{-1}, \qquad G_n' = TG_n, \qquad H_n' = H_nT^{-1}, \tag{9.7}$$

we obtain a state-space model equivalent to the models (9.1) and (9.2):

$$\begin{aligned} z_n &= F_n' z_{n-1} + G_n' v_n \\ y_n &= H_n' z_n + w_n. \end{aligned}$$

Next, we define the state as

$$x_n = (y_n, \tilde{y}_{n+1|n-1}, \cdots, \tilde{y}_{n+m-1|n-1})^T,$$

where $\tilde{y}_{n+i|n-1} = \sum_{j=i+1}^m a_j y_{n+i-j}$ expresses the part of the one-step-ahead predictor $y_{n+i|n-i+1} = \sum_{j=1}^m a_j y_{n+i-j}$ of y_{n+i}, that can be determined by the observations up to time $n-1$. Here, we define F, G and H by

$$F = \begin{bmatrix} a_1 & 1 & & \\ a_2 & & \ddots & \\ \vdots & & & 1 \\ a_m & & & 0 \end{bmatrix}, \quad G = \begin{bmatrix} 1 \\ 0 \\ \vdots \\ 0 \end{bmatrix}, \quad H = [1\ 0 \cdots 0], \quad (9.8)$$

and, consequently, we obtain another expression of the AR model.

In general, many of the models treated in this book, such as the ARMA model, the trend component model and the seasonal component model, can be expressed in the form

$$\begin{aligned} F_i &= \begin{bmatrix} a_{1i} & 1 & & \\ a_{2i} & & \ddots & \\ \vdots & & & 1 \\ a_{mi} & & & 0 \end{bmatrix}, \quad G_i = \begin{bmatrix} 1 \\ b_{1i} \\ \vdots \\ b_{m-1,i} \end{bmatrix}, \quad (9.9) \\ H_i &= [c_{1i} c_{2i} \cdots c_{m,i}]. \end{aligned}$$

In actual time series analysis, a synthetic model that consists of p components may be used. If the dimensions of the p states are $m_1, \cdots, m_p$, respectively, with $m = m_1 + \cdots + m_p$, then by defining an $m \times m$ matrix, an $m \times p$ matrix and an m vector

$$F = \begin{bmatrix} F_1 & & \\ & \ddots & \\ & & F_p \end{bmatrix}, \quad G = \begin{bmatrix} G_1 & & \\ & \ddots & \\ & & G_p \end{bmatrix}, \quad H = [H_1 \cdots H_p], \quad (9.10)$$

a state-space model of the time series is obtained. In this book, this state-space model is used as the standard form.

9.2 State Estimation via the Kalman Filter

A particularly important problem in state-space modeling is to estimate the state x_n based on the observations of the time series y_n. The reason is that tasks such as prediction, interpolation and likelihood computation for the time series can be systematically analyzed by using the state estimation.

In this section, we shall consider the problem of estimating the state x_n at time n based on the set of observations $Y_j = \{y_1, \cdots, y_j\}$. In particular, for $j < n$, the state estimation problem is equivalent to estimation of the future state based on the present and past observations and is called *prediction*. For $j = n$, the problem is to estimate the current state, which is called a *filter*. On the other hand, for $j > n$, the problem is to estimate a past state x_j based on the observations until the present time and this is called *smoothing*.

A general approach to these state estimation problems is to obtain the conditional distribution $p(x_n|Y_j)$ of the state x_n. Then, as the state-space model defined by (9.1) and (9.2) is a linear model, and moreover the noises v_n and w_n, and the initial state x_0 follow normal distributions, all these conditional distributions become normal distributions. Therefore, to solve the problem of state estimation of the state-space model, it is sufficient to obtain the mean vectors and the variance-covariance matrices of the conditional distributions. In general, in order to obtain the conditional joint distribution of states $x_1, \cdots, x_n$ given the observations $y_1, \cdots, y_n$, a huge amount of computation is necessary.

However, for the state-space model, a very computationally efficient procedure for obtaining the joint conditional distribution of the state has been developed by means of a recursive computational algorithm. This algorithm is known as the *Kalman filter* (Kalman (1960), Anderson and Moore (1976)). In the following, the conditional expectation and the variance-covariance matrix of the state x_n are denoted by

$$\begin{aligned} x_{n|j} &\equiv \mathrm{E}\left(x_n|Y_j\right) \\ V_{n|j} &\equiv \mathrm{E}\left[\,(x_n - x_{n|j})(x_n - x_{n|j})^T\,\right]. \end{aligned} \tag{9.11}$$

It is noted that only the conditional distributions with $j = n-1$ (one-step-ahead prediction) and $j = n$ (filter) are treated in the Kalman filter algorithm. As shown in Figure 9.1, the Kalman filter could be realized by repeating the one-step-ahead prediction and the filter with the following algorithm. The derivation of the Kalman filter is shown in Appendix C.

$$\begin{tikzcd}
x_{1|0} \arrow[r] \arrow[d, Rightarrow] & x_{2|0} \arrow[r] & x_{3|0} \arrow[r] & x_{4|0} \arrow[r] & x_{5|0} \arrow[r] & {} \\
x_{1|1} \arrow[r, Rightarrow] & x_{2|1} \arrow[r] \arrow[d, Rightarrow] & x_{3|1} \arrow[r] & x_{4|1} \arrow[r] & x_{5|1} \arrow[r] & {} \\
x_{1|2} & x_{2|2} \arrow[l] \arrow[r, Rightarrow] & x_{3|2} \arrow[r] \arrow[d, Rightarrow] & x_{4|2} \arrow[r] & x_{5|2} \arrow[r] & {} \\
x_{1|3} & x_{2|3} \arrow[l] & x_{3|3} \arrow[l] \arrow[r, Rightarrow] & x_{4|3} \arrow[r] \arrow[d, Rightarrow] & x_{5|3} \arrow[r] & {} \\
x_{1|4} & x_{2|4} \arrow[l] & x_{3|4} \arrow[l] & x_{4|4} \arrow[l] \arrow[r, Rightarrow] & x_{5|4} \arrow[r] \arrow[d, Rightarrow] & {} \\
 & & & & {} &
\end{tikzcd}$$

Figure 9.1 *Recursive computation by the Kalman filter and smoothing algorithm. $\Rightarrow$: prediction, $\Downarrow$: filter, $\leftarrow$: smoothing, $\rightarrow$: increasing horizon prediction.*

[One-step-ahead prediction]

$$\begin{aligned} x_{n|n-1} &= F_n x_{n-1|n-1} \\ V_{n|n-1} &= F_n V_{n-1|n-1} F_n^T + G_n Q_n G_n^T. \end{aligned} \tag{9.12}$$

[Filter]

$$\begin{aligned} K_n &= V_{n|n-1} H_n^T (H_n V_{n*n-1} H_n^T + R_n)^{-1} \\ x_{n|n} &= x_{n|n-1} + K_n (y_n - H_n x_{n|n-1}) \\ V_{n|n} &= (I - K_n H_n) V_{n|n-1}. \end{aligned} \tag{9.13}$$

In the algorithm for one-step-ahead prediction, the predictor (or mean) vector $x_{n|n-1}$ of x_n is obtained simply by multiplying the transition matrix F_n by the filter of x_{n-1}, $x_{n-1|n-1}$. Moreover, the variance-covariance matrix $V_{n|n-1}$ consists of two terms; the first term expresses the influence of the transformation by F_n, and the second shows the influence of the system noise v_n. In the filter algorithm, the Kalman gain K_n is initially obtained. The prediction error of y_n and its variance-covariance matrices are obtained as $y_n - H_n x_{n|n-1}$ and $H_n V_{n|n-1} H_n^T + R_n$, respectively. Here, the mean vector of the filter of x_n can be obtained as the sum of the prediction vector $x_{n|n-1}$ and the prediction error multiplied by the Kalman gain. Then, since $x_{n|n}$ can be re-expressed as

$$x_{n|n} = K_n y_n + (I - K_n H_n) x_{n|n-1},$$

it can be seen that $x_{n|n}$ is a weighted sum of the new observation y_n and the predictor, $x_{n|n-1}$.

Next, $V_{n|n}$ can be written as

$$V_{n|n} = V_{n|n-1} - K_n H_n V_{n|n-1}.$$

Here, the second term of the right-hand side shows the improvement in accuracy of the state estimation of x_n, resulting from the information added by the new observation y_n.

9.3 Smoothing Algorithms

The problem of smoothing is to estimate the state vector x_n based on the time series $Y_m = y_1, \cdots, y_m$ for $m > n$. There are three types of smoothing algorithm. If $m = N$, the smoothing algorithm estimates the state based on the entire set of observations and is called *fixed-interval smoothing*. If $n = m - k$, it always estimates the state k steps before, and is called *fixed-lag smoothing*. If n is set to a fixed time point, e.g., $n = 1$, it estimates a specific point, such as the initial state, and is called *fixed-point smoothing*. Compared with the filtering algorithm that uses the observations up to time n for estimation of the state x_n, fixed-interval smoothing yields a more accurate estimate of the state x_n, by using all available data.

Fixed-interval smoothing

$$\begin{aligned} A_n &= V_{n|n} F_{n+1}^T V_{n+1|n}^{-1} \\ x_{n|N} &= x_{n|n} + A_n (x_{n+1|N} - x_{n+1|n}) \\ V_{n|N} &= V_{n|n} + A_n (V_{n+1|N} - V_{n+1|n}) A_n^T. \end{aligned} \tag{9.14}$$

As shown in this algorithm, the fixed-interval smoothing estimates, $x_{n|N}$ and $V_{n|N}$, can be derived from results obtained by the Kalman filter, i.e., $x_{n|n-1}$, $x_{n|n}$, $V_{n|n-1}$ and $V_{n|n}$. Therefore, to perform fixed-interval smoothing, we initially obtain $x_{n|n-1}, x_{n|n}, V_{n|n-1}, V_{n|n}$, $n = 1, \cdots, N$ by the Kalman filter and compute $x_{N-1|N}$, $V_{n-1|N}$ through $x_{1|N}$, $V_{1|N}$ backward in time (see Figure 9.1). It should be noted that the initial values $x_{N|N}$ and $V_{N|N}$ necessary to perform the fixed-interval smoothing algorithm can be obtained by the Kalman filter.

9.4 Increasing Horizon Prediction of the State

It will be shown that by repeating one-step-ahead prediction by means of the Kalman filter, we can perform increasing horizon prediction, that is, to obtain $x_{n+k|n}$ and $V_{n+k|n}$ for $k = 1, 2, \cdots$. Let us consider the problem of estimating the increasing horizon prediction, i.e., estimating the state

x_{n+j} for $j > 1$ based on the time series $Y_n = y_1, \cdots, y_n$. Firstly, the mean vector $x_{n+1|n}$ and the variance-covariance matrix $V_{n+1|n}$ of the one-step-ahead predictor of x_{n+1} are obtained by the Kalman filter. Here, since the future observation y_{n+1} is unavailable, it is assumed that $Y_{n+1} = Y_n$. In this case, we have that $x_{n+1|n+1} = x_{n+1|n}$ and $V_{n+1|n+1} = V_{n+1|n}$. Therefore, from the one-step-ahead prediction algorithm of the Kalman filter for the period $n+1$, we have

$$\begin{aligned} x_{n+2|n} &= F_{n+2}x_{n+1|n} \\ V_{n+2|n} &= F_{n+2}V_{n+1|n}F_{n+2}^T + G_{n+2}Q_{n+2}G_{n+2}^T. \end{aligned} \tag{9.15}$$

This means that two-step-ahead prediction can be realized by repeating the prediction step of the Kalman filter twice without the filtering step. In general, j-step-ahead prediction based on Y_n can be performed using the relation that $Y_n = Y_{n+1} = \cdots = Y_{n+j}$, by repeating the prediction step j times. Summarizing the above, the algorithm for the increasing horizon prediction $x_{n+1}, \cdots, x_{n+j}$ based on the observation Y_n can be given as follows:

The increasing horizon prediction

For $i = 1, \cdots, j$, repeat

$$\begin{aligned} x_{n+i|n} &= F_{n+i}x_{n+i-1|n} \\ V_{n+i|n} &= F_{n+i}V_{n+i-1|n}F_{n+i}^T + G_{n+i}Q_{n+i}G_{n+i}^T. \end{aligned} \tag{9.16}$$

9.5 Prediction of Time Series

Future values of time series can be immediately predicted by using the predicted state x_n obtained as shown above. When Y_n is given, from the relation between the state x_n and the time series y_n, which is expressed by the observation model (9.2), the mean and the variance-covariance matrix of y_{n+j} are denoted by $y_{n+j|n} \equiv \mathrm{E}(y_{n+j}|Y_n)$ and $d_{n+j|n} \equiv \mathrm{Cov}(y_{n+j}|Y_n)$, respectively. Then, we can obtain the mean and the variance-covariance matrix of the j-step-ahead predictor of the time series y_{n+j} by

$$\begin{aligned} y_{n+j|n} &= \mathrm{E}\left(H_{n+j}x_{n+j} + w_{n+j}|Y_n\right) \\ &= H_{n+j}x_{n+j|n} \qquad (9.17) \\ d_{n+j|n} &= \mathrm{Cov}(H_{n+j}x_{n+j} + w_{n+j}|Y_n) \\ &= H_{n+j}\mathrm{Cov}(x_{n+j}|Y_n)H_{n+j}^T + H_{n+j}\mathrm{Cov}(x_{n+j}, w_{n+j}|Y_n) \\ &\quad + \mathrm{Cov}(w_{n+j}, x_{n+j}|Y_n)H_{n+j}^T + \mathrm{Cov}(w_{n+j}|Y_n) \\ &= H_{n+j}V_{n+j|n}H_{n+j}^T + R_{n+j}. \qquad (9.18) \end{aligned}$$

As indicated previously, the predictive distribution of y_{n+j} based on the observation Y_n of the time series becomes a normal distribution with mean $y_{n+j|n}$ and variance-covariance matrix $d_{n+j|n}$. These are easily obtained by (9.17) and (9.18). That is, the mean of the predictor of y_{n+j} is given by $y_{n+j|n}$ and the standard error is given by $(d_{n+j|n})^{1/2}$. It should be noted that the one-step-ahead predictor $y_{n|n-1}$ and $d_{n|n-1}$ of the time series y_n have already been obtained and were applied in the algorithm for the Kalman filter (9.13).

Example (Increasing horizon prediction of BLSALLFOOD data) Figure 9.2 shows the results of the increasing horizon prediction of the BLSALLFOOD data, $N = 156$. In this prediction, the AR model was fitted to the initial 120 observations and the estimated AR model was used for increasing horizon prediction of the succeeding 36 observations, $y_{121},\cdots,y_{156}$. In the estimation of the AR model, we firstly obtain a time series with mean zero, y_n^* by deleting the sample mean, $\bar{y}$ of the time series,

$$y_n^* = y_n - \bar{y},$$

and then the parameters of the AR model are obtained by applying the Yule-Walker method to the time series $y_1^*,\cdots,y_N^*$.

The increasing horizon prediction of the time series $y_{n+j|n}^*$ is obtained by applying the Kalman filter to the state-space representation of the AR model; the increasing horizon prediction value of the time series y_{n+j} is then obtained by

$$y_{n+j|n} = y_{n+j|n}^* + \bar{y}.$$

Figure 9.2 shows the mean $y_{120+j|120}$, $j = 1,\cdots,36$, and its ± 1 standard error interval $y_{120+j|120} \pm \sqrt{d_{120+j|120}}$ of the predictive distribution obtained by this method. The actual time series is indicated by a solid curve for $n \leq 120$ and by the symbol $\circ$ for $n > 120$.

Plots (a), (b), (c) and (d) show the results of the increasing horizon prediction obtained by AR models of orders $m = 1, 5, 10$ and 15, respectively. In the case of the first order AR model shown in plot (a), the increasing horizon prediction value rapidly attenuates exponentially, which indicates that the information on the periodic behavior of this data is not effectively used for the prediction. In the case of $m = 5$ shown in plot (b), the predictor reasonably reproduced the cyclic behavior for the first year, but after one year passed, the predicted value rapidly decayed. The predictors for the AR model with $m = 10$ reproduce the actual behavior of the time series relatively well. Finally, the predictors for the AR model with $m = 15$ accurately reproduce the details of the wave form of

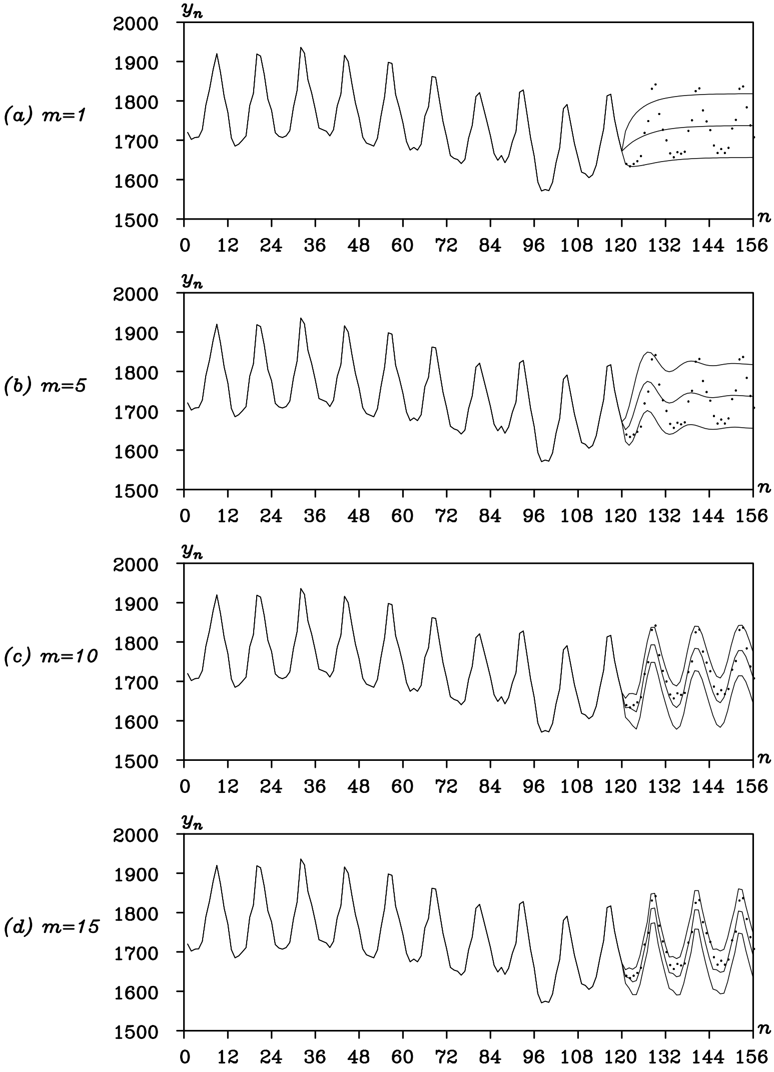

Figure 9.2 *Increasing horizon predictive distributions (bold line: mean, thin line: ± (standard deviation) and ○: observed value). Orders of the AR models are 1, 5, 10 and 15, respectively.*

the actual time series. In contrast to the one-step-ahead prediction, the increasing horizon prediction may lead to significant differences among the results from AR models of different assumed orders. These results indicate that prediction by a model of improper order may yield such an inappropriate prediction that appropriate model selection is extremely important for the increasing horizon prediction.

9.6 Likelihood Computation and Parameter Estimation for a Time Series Model

Assume that the state-space representation for a time series model specified by a parameter θ is given. When the time series $y_1, \cdots, y_N$ of length N is given, the N dimensional joint density function of $y_1, \cdots, y_N$ specified by this time series model is denoted by $f_N(y_1, \cdots, y_N|\theta)$. Then, the likelihood of this model is defined by

$$L(\theta) = f_N(y_1, \cdots, y_N|\theta). \tag{9.19}$$

By repeatedly applying the relation

$$f_n(y_1, \cdots, y_n|\theta) = f_{n-1}(y_1, \cdots, y_{n-1}|\theta) g_n(y_n|y_1, \cdots, y_{n-1}, \theta),$$

for $n = N, N-1, \cdots, 2$, the likelihood of the time series model can be expressed as a product of conditional density functions:

$$L(\theta) = \prod_{n=1}^{N} g_n(y_n|y_1, \cdots, y_{n-1}, \theta) = \prod_{n=1}^{N} g_n(y_n|Y_{n-1}, \theta). \tag{9.20}$$

For simplicity of notation here, we let $Y_0 = \emptyset$ (empty set) and then $f_1(y_1|\theta) \equiv g_1(y_1|Y_0, \theta)$. By taking the logarithm of $L(\theta)$, the *log-likelihood* of the model is obtained as

$$\ell(\theta) = \log L(\theta) = \sum_{n=1}^{N} \log g_n(y_n|Y_{n-1}, \theta). \tag{9.21}$$

As shown in (9.17) and (9.18), since $g_n(y_n|Y_{n-1}, \theta)$ is the conditional distribution of y_n given the observation Y_{n-1} and it is, in fact, a normal distribution with mean $y_{n|n-1}$ and variance-covariance matrix $d_{n|n-1}$, it can be expressed as (Kitagawa and Gersch (1996))

$$g_n(y_n|Y_{n-1}, \theta) = \left(\frac{1}{\sqrt{2\pi}}\right)^{\ell} |d_{n|n-1}|^{-\frac{1}{2}} \times \exp\left\{-\frac{1}{2}(y_n - y_{n|n-1})^T d_{n|n-1}^{-1} (y_n - y_{n|n-1})\right\}. \tag{9.22}$$

Therefore, by substituting this density function into (9.21), the log-likelihood of this state-space model is obtained as

$$\begin{aligned}\ell(\theta) \quad = \quad & -\frac{1}{2}\left\{ \ell N \log 2\pi + \sum_{n=1}^{N} \log |d_{n|n-1}| \right. \\ & \left. + \sum_{n=1}^{N} (y_n - y_{n|n-1})^T d_{n|n-1}^{-1} (y_n - y_{n|n-1}) \right\}. \qquad (9.23)\end{aligned}$$

Stationary time series models such as the AR models, the ARMA models and many other nonstationary time series models such as trend and seasonal adjustment models can be expressed in the form of linear Gaussian state-space models. Accordingly, for such time series models, a unified algorithm for computing the log-likelihood can be obtained by using the Kalman filter and (9.23). The maximum likelihood estimates of the parameters of the time series model can be obtained by maximizing this log-likelihood by a numerical optimization method, which will be described later in Appendix C. Examples of parameter estimation for state-space models are described in Chapter 10 to Chapter 15.

In this way, the parameters contained in the state-space model can be estimated by numerical maximization of the log-likelihood of (9.23), but this generally requires considerable computation. Therefore, if the maximum likelihood estimate or a good approximation can be obtained analytically, this method should be used for efficient estimation. For instance, on the assumption that there is no missing observation in estimating an AR model, we should use the Yule-Walker method, the least squares method or the PARCOR method, which have been shown in Chapter 7, rather than the above method. Furthermore, whenever an exact maximum likelihood estimate is necessary, we should use these approximations as an initial estimate of the numerical optimization.

When maximization of the log-likelihood is necessary but there is not such an approximation method available, we may reduce the dimension of the parameter vector to be estimated by numerical optimization. In the state-space models (9.1) and (9.2), it is assumed that the dimension of the time series is $\ell = 1$ and the variance of w_n is constant with $R_n = \sigma^2$. Then, if $\tilde{V}_{n|n}$, $\tilde{V}_{n|n-1}$, $\tilde{Q}_n$, and $\tilde{R}$ are defined by

$$\begin{aligned} V_{n|n-1} &= \sigma^2 \tilde{V}_{n|n-1}, & V_{n|n} &= \sigma^2 \tilde{V}_{n|n}, \\ Q_n &= \sigma^2 \tilde{Q}_n, & \tilde{R} &= 1, \qquad (9.24)\end{aligned}$$

then it follows that the Kalman filters (9.12) and (9.13) yield identical results, even if those parameters are used.

In one-step-ahead prediction, it is obvious that we can obtain identical results, even if we replace $V_{n-1|n-1}$ and $V_{n|n-1}$ by $\tilde{V}_{n-1|n-1}$ and $\tilde{V}_{n|n-1}$, respectively. In the filtering step, we have

$$\begin{aligned} K_n &= V_{n|n-1}H_n^T(H_nV_{n|n-1}H_n^T+R_n)^{-1} \\ &= \sigma^2\tilde{V}_{n|n-1}H_n^T\sigma^{-2}(H_n\tilde{V}_{n|n-1}H_n^T+1)^{-1} \\ &= \tilde{V}_{n|n-1}H_n^T(H_n\tilde{V}_{n|n-1}H_n^T+\tilde{R})^{-1} \\ &= \tilde{K}_n. \end{aligned} \tag{9.25}$$

Assuming that $\tilde{R}=1$, the obtained Kalman gain $\tilde{K}_n$ is identical to K_n. Therefore, in the filtering step, we may use $\tilde{V}_{n|n}$ and $\tilde{V}_{n|n-1}$ instead of $V_{n|n}$ and $V_{n|n-1}$. Furthermore, it can be seen that the vectors $x_{n|n-1}$ and $x_{n|n}$ of the state do not change under these modifications. In summary, if R_n is time-invariant and $R=\sigma^2$ is an unknown parameter, we may apply the Kalman filter by setting $R=1$. Since we then have $d_{n|n-1}=\sigma^2\tilde{d}_{n|n-1}$ from (9.18), this yields

$$\ell(\theta)=-\frac{1}{2}\left\{N\log 2\pi\sigma^2+\sum_{n=1}^{N}\log\tilde{d}_{n|n-1}+\frac{1}{\sigma^2}\sum_{n=1}^{N}\frac{(y_n-y_{n|n-1})^2}{\tilde{d}_{n|n-1}}\right\}. \tag{9.26}$$

From the likelihood equation

$$\frac{\partial\ell}{\partial\sigma^2}=-\frac{1}{2}\left\{\frac{N}{\sigma^2}-\frac{1}{(\sigma^2)^2}\sum_{n=1}^{N}\frac{(y_n-y_{n|n-1})^2}{\tilde{d}_{n|n-1}}\right\}=0, \tag{9.27}$$

the maximum likelihood estimate of σ^2 is obtained by

$$\hat{\sigma}^2=\frac{1}{N}\sum_{n=1}^{N}\frac{(y_n-y_{n|n-1})^2}{\tilde{d}_{n|n-1}}. \tag{9.28}$$

Furthermore, denoting the parameters in θ except for the variance σ^2 by θ^*, by substituting (9.28) for (9.26), we have

$$\ell(\theta^*)=-\frac{1}{2}\left\{N\log 2\pi\hat{\sigma}^2+\sum_{n=1}^{N}\log\tilde{d}_{n|n-1}+N\right\}. \tag{9.29}$$

By this method, it is possible to reduce the dimension of the parameter vector by one. Summarizing the above, the procedure used here is as follows:

1. Apply the Kalman filter by putting $R = 1$.
2. Obtain an estimate of the variance $\hat{\sigma}^2$ by (9.28).
3. Obtain the log-likelihood $\ell(\theta^*)$ by (9.29).
4. Repeating the above steps (1)–(3), obtain the maximum likelihood estimate $\hat{\theta}^*$ by maximizing the log-likelihood $\ell(\theta^*)$ by means of numerical optimization.

9.7 Interpolation of Missing Observations

In observing time series, a part of the time series might not be able to be obtained because of unexpected factors, such as the breakdown of the observational devices, physical constraints of the observed objects or the observation systems. In such cases, the actual unobserved data are called *missing observations*, or missing values. Even when only a few percent of the observations are missing, the length of continuously observed data that can be used for the analysis might become very short. In such a situation, sometimes we may fill the missing observations with zeros, the mean value of the time series or by linear interpolation. As can be seen in the numerical examples following, such ad hoc interpolation for missing observations may cause a large bias in the analysis, since it is equivalent to arbitrarily assuming a particular model.

In this section, we shall explain a method of computing the likelihood of the time series model and interpolating the missing observations using the state-space model and the Kalman filter (Jones (1980), Kohn and Ansley (1986), Kitagawa and Gersch (1996)). Applying the state-space model of time series, it is possible to compute an exact likelihood even when there are missing observations in the data. Thus, we can obtain maximum likelihood estimates of unknown parameters.

Let $I(n)$ be the set of time instances at which the time series was actually observed. If there are no missing observations, it is obvious that $I(n) = \{1, \cdots, n\}$. Then, for the observations $Y_n \equiv \{y_i | \, i \in I(n)\}$, the log-likelihood of the time series is given by

$$\begin{aligned} \ell(\theta) &= \log p(Y_N|\theta) \\ &= \sum_{n \in I(N)} \log p(y_n|Y_{n-1}, \theta). \end{aligned} \tag{9.30}$$

Since $Y_n \equiv Y_{n-1}$ holds when the observation y_n is missing, as in the case of increasing horizon prediction, the Kalman filter algorithm can be performed by just skipping the filtering step. Namely, the predictive distribution $p(x_n|Y_{n-1})$ of the state, or equivalently, the mean $x_{n|n-1}$ and the variance-covariance matrix $V_{n|n-1}$, can be obtained by repeating the prediction step for all n and the filtering step for n such that $n \in I(N)$. Therefore, after computing $y_{n|n-1}$ and $d_{n|n-1}$ by equations (9.17) and (9.18), similarly to the preceding section, the log-likelihood of the time series model is defined as

$$\begin{aligned} \ell(\theta) &= -\frac{1}{2} \sum_{n \in I(N)} \Big\{ \ell \log 2\pi + \log |d_{n|n-1}| \\ &\quad + (y_n - y_{n|n-1})^T d_{n|n-1}^{-1} (y_n - y_{n|n-1}) \Big\}. \end{aligned} \qquad (9.31)$$

If a time series model is already given, the model can be used for *interpolation of missing observations*. Similar to the likelihood computation, firstly, we obtain the predictive distributions $\{x_{n|n-1}, V_{n|n-1}\}$ and the filter distributions $\{x_{n|n}, V_{n|n}\}$ using the Kalman filter and skipping the filtering steps. Then, we can obtain the smoothed estimates of the missing observations by applying the fixed-interval smoothing algorithm (9.14). The variance-covariance matrix of the estimate is obtained by $d_{n|N} = H_n V_{n|N} H_n^T + R_n$. Consequently, an estimate of the missing observation y_n is obtained as $y_{n|N} = H_n x_{n|N}$.

Thus, the results of interpolation by optimal models are significantly different from conventional interpolations, which are generated by replacing missing observations with the mean or by straight-line interpolation. As can be seen from this example, interpolation of the missing observations by a particular algorithm corresponds to assuming a particular time series model, different from the true model generating the data. Therefore, if we perform interpolation without carefully selecting the model, it may cause significant bad effects in the subsequent analysis.

Example (Interpolation of missing observations in BLSALLFOOD data) Figure 9.3 shows the results of a numerical interpolation experiment for the BLSALLFOOD data. Within 156 observations of data, in total 50 observations are assumed to be missing: $y_{41}, \cdots, y_{70}$ and $y_{101}, \cdots, y_{120}$. They are interpolated by AR models of orders 0, 1, 5, 10 and 15, respectively. It should be noted that order 15 is the AIC best order. AR coefficients are obtained by maximizing the log-likelihood defined by (9.31). Interpolation by the AR model of order 0 is equivalent to replacing the missing observations with the mean of the whole time series. Since the interpolations with the first or the 5th order AR model cannot capture the wave pattern of the time series well, interpolation with these models cannot reproduce the actual observations shown by the symbol ∘. On the other hand, by using the AR model of order 10, the cyclic behavior of the data is reproduced well. Furthermore, it can be seen from plot (e) that the AIC best model of order 15 can reproduce the details of the data remarkably well.

Problems

1. Show that, using the transformation (9.7), we can obtain a state-space model, which is equivalent to the one given in (9.1) and (9.2).

2. Assume that the state-space model $x_n = x_{n-1} + v_n$, $y_n = x_n + w_n$ for the 1-dimensional state x_n is given, where $v_n \sim N(0, \tau^2)$, $w_n \sim N(0,1)$ and $x_0 \sim N(0, 10^2)$.

   (1) Show the Kalman filter algorithm for this model.

   (2) Show the relation between $V_{n+1|n}$ and $V_{n|n-1}$.

   (3) If $V_{n|n-1} \rightarrow V$ as $n \rightarrow \infty$, show that V satisfies the equation $V^2 - \tau^2 V - \tau^2 = 0$.

   (4) Consider the Kalman filter algorithm as $n \rightarrow \infty$ (stationary Kalman filter).

3. Let the solution of the equation $V^2 - \tau^2 V - \tau^2 = 0$ be denoted by V. Obtain the variance of the one-step-ahead predictor, filter and smoother in the steady state. For $\tau^2 = 1, 0.1, 0.01, 0.001$, evaluate these variances.

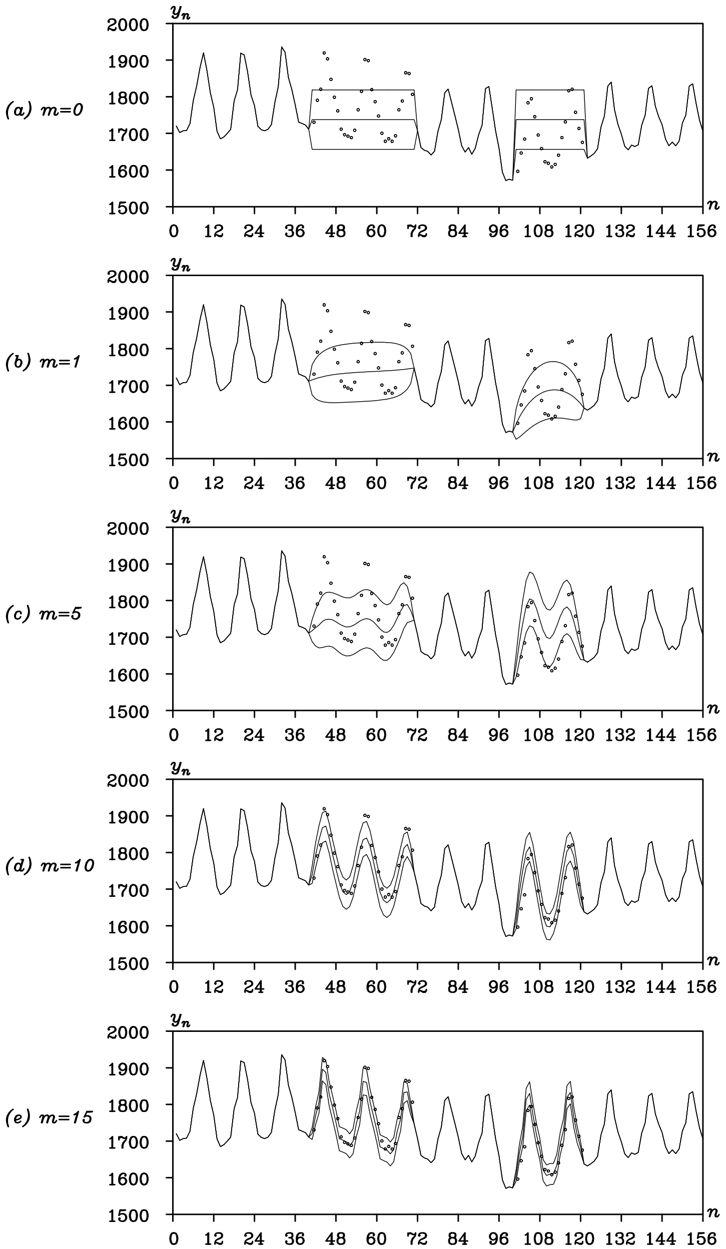

Figure 9.3 *Interpolation of missing values (bold line: mean, thin line: ± (standard deviation) and ○: observed value). Orders of the AR models are 0, 1, 5, 10 and 15.*

Chapter 10

Estimation of the ARMA Model

In this chapter, a method for efficiently computing the log-likelihood of the ARMA model is explained based on the state-space representation and the Kalman filter technique. Applying the numerical optimization method shown in Chapter 4, it is possible to maximize the log-likelihood. By this procedure, the maximum likelihood estimates of the parameters of the ARMA model can be obtained.

10.1 State-Space Representation of the ARMA Model

Assume that a stationary ARMA model (autoregressive moving average model) of order (m,ℓ) (Box and Jenkins (1970), Brockwell and Davis (1981))

$$y_n = \sum_{j=1}^{m} a_j y_{n-j} + v_n - \sum_{j=1}^{\ell} b_j v_{n-j} \tag{10.1}$$

is given. Here, v_n is a Gaussian white noise with mean zero and variance σ^2 and $\tilde{y}_{n+i|n-1}$ is defined as

$$\tilde{y}_{n+i|n-1} = \sum_{j=i+1}^{m} a_j y_{n+i-j} - \sum_{j=i}^{\ell} b_j v_{n+i-j}, \tag{10.2}$$

where $\tilde{y}_{n+i|n-1}$ is a part of y_{n+i} that can be directly expressed by the observations until time $n-1$, y_{n-1}, y_{n-2}, $\cdots$, and the noise inputs until time n, v_n, v_{n-1}, $\cdots$. Then, the following relations hold:

$$\begin{aligned} y_n &= a_1 y_{n-1} + \tilde{y}_{n|n-2} + v_n. \\ \tilde{y}_{n+i|n-1} &= a_{i+1} y_{n-1} + \tilde{y}_{n+i|n-2} - b_i v_n. \\ \tilde{y}_{n+k-1|n-1} &= a_k y_{n-1} - b_{k-1} v_n. \end{aligned} \tag{10.3}$$

Therefore, setting $k = \max(m, \ell+1)$ and defining the k-dimensional state vector x_n as

$$x_n = (y_n, \tilde{y}_{n+1|n-1}, \cdots, \tilde{y}_{n+k-1|n-1})^T, \tag{10.4}$$

the ARMA model can be expressed in the form of a state-space model:

$$\begin{aligned} x_n &= Fx_{n-1} + Gv_n \\ y_n &= Hx_n. \end{aligned} \tag{10.5}$$

Here the $k \times k$ matrix F and the k-dimensional vectors G and H are defined as

$$\begin{aligned} F &= \begin{bmatrix} a_1 & 1 & & \\ a_2 & & \ddots & \\ \vdots & & & 1 \\ a_k & & & \end{bmatrix}, \quad G = \begin{bmatrix} 1 \\ -b_1 \\ \vdots \\ -b_{k-1} \end{bmatrix} \\ H &= [\ 1 \quad 0 \quad \cdots \quad 0\ ], \end{aligned} \tag{10.6}$$

respectively, where $a_i = 0$ for $i > m$ and $b_i = 0$ for $i > \ell$.

In summary, an ARMA model can be expressed by a state-space model where the coefficient matrices F, G and H are time-invariant and the observation noise is zero.

10.2 Initial State of an ARMA Model

In order to apply the Kalman filter to the state-space representation of the ARMA model, it is necessary to specify the mean $x_{0|0}$ and the variance-covariance matrix $V_{0|0}$ of the initial state. Since $x_{0|0}$ and $V_{0|0}$ express the distribution of the filter without any observations of the time series y_n, they can be evaluated by computing the mean and the variance-covariance matrix of x_0 in the stationary state. Firstly, since $\mathrm{E}(v_n) = 0$, it is obvious that $\mathrm{E}(y_n) = 0$ and $\mathrm{E}(\tilde{y}_{n+i|n-1}) = 0$. Since the expected value of x_n becomes 0, the initial state vector is defined as $x_{0|0} = (0, \cdots, 0)^T$. Next, if the (i, j)-th element of the variance-covariance matrix $V_{0|0}$ is denoted by V_{ij}, it can be obtained as

$$\begin{aligned} V_{11} &= \mathrm{E}(y_0 y_0) = C_0 \\ V_{1i} &= V_{i1} = \mathrm{E}\left(y_0 \tilde{y}_{i-1|-1}\right) \\ &= \mathrm{E}\left\{ y_0 \left(\sum_{j=i}^{m} a_j y_{i-1-j} - \sum_{j=i-1}^{\ell} b_j v_{i-1-j} \right) \right\} \\ &= \sum_{j=i}^{m} a_j C_{j+1-i} - \sum_{j=i-1}^{\ell} b_j g_{j+1-i} \sigma^2 \\ V_{ij} &= \mathrm{E}\left(\tilde{y}_{i-1|-1} \tilde{y}_{j-1|-1}\right) \end{aligned}$$

$$\begin{aligned}
&= \sum_{p=i}^{m}\sum_{q=j}^{m} a_p a_q \mathrm{E}\left(y_{i-1-p} y_{j-1-q}\right) - \sum_{p=i}^{m}\sum_{q=j-1}^{\ell} a_p b_q \mathrm{E}\left(y_{i-1-p} v_{j-1-q}\right) \\
&- \sum_{p=i-1}^{\ell}\sum_{q=j}^{m} b_p a_q \mathrm{E}\left(v_{i-1-p} y_{j-1-q}\right) + \sum_{p=i-1}^{\ell}\sum_{q=j-1}^{\ell} b_p b_q \mathrm{E}\left(v_{i-1-p} v_{j-1-q}\right) \\
&= \sum_{p=i}^{m}\sum_{q=j}^{m} a_p a_q C_{q-j-p+i} - \sum_{p=i}^{m}\sum_{q=j-1}^{\ell} a_p b_q g_{q-j-p+i}\sigma^2 \\
&- \sum_{p=i-1}^{\ell}\sum_{q=j}^{m} b_p a_q g_{p-i-q+j}\sigma^2 + \sum_{p=i-1}^{\ell} b_p b_{p+j-i}\sigma^2. \qquad (10.7)
\end{aligned}$$

Here, we note that C_i and g_i are the autocovariance function and the impulse response function, respectively, of the ARMA model, which we can obtain by the method shown in Chapter 6.

10.3 Maximum Likelihood Estimate of an ARMA Model

Using the above results for the state-space representation of the ARMA model, we can compute the log-likelihood for the ARMA model specified by the parameter $\theta = (\sigma^2, a_1, \cdots, a_m, b_1, \cdots, b_\ell)^T$. Firstly, the initial state $x_{0|0}$ and its variance-covariance matrix $V_{0|0}$ are provided by the method specified in the preceding section. Next, the one-step-ahead prediction of the state $x_{n|n-1}$ and its variance-covariance matrix $V_{n|n-1}$ can be computed by the Kalman filter for $n = 1, \cdots, N$. Then, using (9.23), the log-likelihood of the ARMA model can be obtained as

$$\ell(\theta) = -\frac{N}{2}\log 2\pi - \frac{1}{2}\sum_{n=1}^{N} \log d_{n|n-1} - \frac{1}{2}\sum_{n=1}^{N} \frac{(y_n - y_{n|n-1})^2}{d_{n|n-1}}, \quad (10.8)$$

where $d_{n|n-1} = HV_{n|n-1}H^T$ and $y_{n|n-1} = Hx_{n|n-1}$ (Jones (1980), Brockwell and Davis (1981)).

The maximum likelihood estimate of the parameter vector θ can be obtained by maximizing the log-likelihood $\ell(\theta)$ using a numerical optimization method. It is noted that the variance σ^2 can easily be obtained without applying a numerical optimization method by the following procedure, which is similar to the method shown in Section 9.6.

1. Apply the Kalman filter after setting $\sigma^2 = 1$ and obtain $d_{n|n-1}$ and $y_{n|n-1}$ for $n = 1, \cdots, N$.
2. Obtain the maximum likelihood estimate of σ^2 by $\hat{\sigma}^2 = N^{-1}\sum_{n=1}^{N}(y_n - y_{n|n-1})^2/d_{n|n-1}$.

3. Obtain the log-likelihood function for the AR coefficients $a_1,\cdots,a_m$, and the MA coefficients $b_1,\cdots,b_\ell$ by $\ell'(a_1,\cdots,a_m,b_1,\cdots,b_\ell) \equiv \ell(\hat{\sigma}^2,a_1,\cdots,a_m,b_1,\cdots,b_\ell)$.

The maximum likelihood estimate of $\theta' = (a_1,\cdots,a_m,b_1,\cdots,b_\ell)^T$ can be obtained by applying a numerical optimization method to the log-likelihood function obtained by the above-mentioned procedure. In actual computation, however, to satisfy the stationarity and invertibility conditions, we often apply the following transformations of the parameters.

For the condition of stationarity for the AR coefficients $a_1,\cdots,a_m$, PARCORs $c_1,\cdots,c_m$ should satisfy $-1 < c_i < 1$ for all $i = 1,\cdots,m$. It can be seen that this condition is guaranteed, if the transformed coefficients α_i defined by

$$\alpha_i = \log\left(\frac{1+c_i}{1-c_i}\right), \tag{10.9}$$

satisfy $-\infty < \alpha_i < \infty$ for all $i = 1,\cdots,m$.

Conversely, for arbitrary $(\alpha_1,\cdots,\alpha_m)^T \in \mathrm{R}^m$, if c_i is defined by

$$c_i = \frac{e^{\alpha_i}-1}{e^{\alpha_i}+1}, \tag{10.10}$$

then it always satisfies $|c_i| < 1$ and the corresponding AR coefficients satisfy the stationarity condition.

On the other hand, to guarantee the invertibility condition for any $(\beta_1,\cdots,\beta_\ell)^T \in \mathrm{R}^\ell$, let d_i be defined as

$$d_i = \frac{e^{\beta_i}-1}{e^{\beta_i}+1}, \tag{10.11}$$

and formally obtain the corresponding MA coefficients $b_1,\cdots,b_\ell$ by considering $d_1,\cdots,d_\ell$ to be the PARCORs.

Then, for arbitrary $\theta'' = (\alpha_1,\cdots,\alpha_m,\beta_1,\cdots,\beta_\ell)^T \in \mathrm{R}^{m+\ell}$, the corresponding ARMA model will always satisfy the stationarity and invertibility conditions.

10.4 Initial Estimates of Parameters

The initial values of the AR and MA coefficients are necessary for numerical optimization procedures to obtain the maximum likelihood estimates of the parameters of the ARMA model. For AR models obtained by setting $\ell = 0$, the initial estimates of the AR coefficients can be rather

Table 10.1: *AIC values for ARMA models with various orders.*

		ℓ					
		0	1	2	3	4	5
	0		141.1	73.3	58.5	377.0	54.1
	1	105.3	64.6	138.9	55.7	62.4	58.0
	2	43.0	39.2	41.0	228.7	23.7	25.0
m	3	41.3	41.1	92.5	14.8	25.4	21.1
	4	40.5	41.9	27.0	16.7	14.0	22.9
	5	40.9	42.8	18.6	14.3	13.9	16.8

Table 10.2: *Log-likelihood values for ARMA models with various order.*

		ℓ					
		0	1	2	3	4	5
	0		−68.6	−33.7	−25.2	−**183.5**	−21.0
	1	−50.7	−29.3	−**65.4**	−22.9	−22.2	−22.0
	2	−18.5	−15.6	−15.5	−**108.4**	−4.8	−4.5
m	3	−16.6	−15.5	−**40.2**	−0.4	−**4.7**	−1.5
	4	−15.2	−15.0	−6.5	−0.4	2.0	−**1.5**
	5	−14.5	−14.5	−1.3	1.9	3.1	**2.6**

easily obtained by fitting AR models by the Yule-Walker or least squares method. However, for $\ell > 0$, we should carefully select initial values, since the log-likelihood may have several local maxima, which accordingly yield different estimates, depending on the choice of initial values. Therefore, it should be noted that we cannot always obtain the best estimates using the default initial values, which are automatically set by the time series analysis software.

Example (Sunspot number data) Table 10.1 shows the AIC values when ARMA models are fitted to the logarithm of the sunspot number data within the range $0 \leq m$, $\ell \leq 5$. From Table 10.1, it can be seen that the best model is the ARMA model with $m = 5$ and $\ell = 4$. On the other hand, Table 10.2 summarizes the values of the log-likelihoods of the fitted ARMA models $\ell(i, j)$, $0 \leq i, j \leq 5$. From Table 10.2, the log-likelihood values for the ARMA models denoted in boldface, such as $\ell(1,2)$, $\ell(3,2)$ and $\ell(2,3)$, etc., are apparently too small compared with

Table 10.3: *Estimation of ARMA models with modified initial values.*

order	log-likelihood	AIC
(0,4)	−22.5	55.0
(1,2)	−23.8	55.5
(2,3)	−12.2	36.4
(3,2)	−15.4	42.8
(3,4)	−0.4	16.3
(4,5)	2.0	16.0
(5,5)	3.7	14.5

the values for other surrounding models. Note that the maximum log-likelihood of the ARMA (i,j) should be larger than or equal to those of AR $(i-1,j)$ and AR $(i,j-1)$, i.e., $\ell(i,j) \geq \ell(i-1,j)$ and $\ell(i,j) \geq \ell(i,j-1)$. Therefore, this means that the log-likelihood for these models did not converge to the global maximum from the default initial values of the parameters.

By assuming that $a_3 = 0$ in the ARMA (3,2) model, we can obtain the ARMA (2,2) model. Therefore, it is expected that the maximum log-likelihood value for the ARMA (3,2) model is larger than that of the ARMA (2,2) model. Accordingly, the AIC values for the ARMA (i,j) model in Table 10.1 do not increase by more than 2 compared with those of the ARMA $(i,j-1)$ and ARMA $(i-1,j)$ models.

Therefore, if the log-likelihood value for the ARMA(i,j) violates either $\ell(i,j) \geq \ell(i-1,j)$ or $\ell(i,j) \geq \ell(i,j-1)$, then it indicates that we could not obtain the global maximum of the log-likelihood function in estimating the parameters of ARMA(i,j). Such log-likelihood values are highlighted in boldface in Table 10.2.

In these cases, a better model can be always obtained by using the coefficients of a model with a larger log-likelihood among the left and above models in Table 10.2 as the initial values for numerical optimization. Table 10.3 shows the log-likelihoods and the AICs of the models obtained by using these modified initial values. It can be seen that those initial values certainly satisfy the conditions that $\ell(i,j) \geq \ell(i-1,j)$ and $\ell(i,j) \geq \ell(i,j-1)$ for all i and j.

In the maximum likelihood estimation of the parameters of the ARMA models, it is certain to increase the AR and MA orders gradually by using the estimators of the lower order models. However, it should be also noted that even if the above-mentioned conditions are satisfied, it is not guaranteed that the estimated parameters actually converge to the global maxima. We often see that since the ARMA model is very flexible and versatile, if we fit an ARMA model with large AR and MA orders, it has a tendency to adjust itself to a small peak or trough of the periodogram. Thus the log-likelihood has many local maxima. To avoid using those inappropriate models in estimating ARMA models, it is recommended that the power spectrum of the estimated ARMA model be drawn, to ensure that the estimated model converges to the global maximum.

Problems

1. Using the expression of equation (9.5), obtain the initial variance-covariance matrix for the maximum likelihood estimates of the AR model of order *m*.
2. Describe what we should check to apply the transformation (10.9) to parameter estimation for the ARMA model.

Chapter 11

Estimation of Trends

In economic time series, we frequently face long-lasting increasing or decreasing trends. In this chapter, we initially consider a polynomial regression model to analyze time series with such tendencies. Secondly, we shall introduce a trend model to estimate a complicated trend that we cannot express in terms of a simple parametric model such as a polynomial or trigonometric regression model. The trend component model treated in this chapter, representing stochastic changes of parameters, forms a framework for modeling various types of nonstationary time series that will be introduced in succeeding chapters.

11.1 The Polynomial Trend Model

The WHARD data in Figure 1.1(e) show a tendency to increase over the entire time domain. Such a long-term tendency often seen in economic time series such as the one depicted in Figure 1.1(e) is called *trend*. Needless to say, estimating the trend of such a time series is a very natural way of capturing the tendency of the time series and predicting its future behavior. However, even in the case of analyzing short-term behavior of a time series with a trend, we often analyze the time series after removing the trend, because it is not appropriate to directly apply a stationary time series model such as the AR model to the original series. In this section, we shall explain the *polynomial regression model* as a simple tool to estimate the trend of a time series.

For the polynomial regression model, the time series y_n is expressed as the sum of the trend t_n and a residual w_n

$$y_n = t_n + w_n, \tag{11.1}$$

where w_n follows a Gaussian distribution with mean 0 and variance σ^2. It is assumed that the trend component can be expressed as a polynomial

$$t_n \quad = \quad a_0 + a_1 x_n + \cdots + a_m x_n^m. \tag{11.2}$$

Since the above polynomial regression model is a special case of the regression model, we can easily estimate the model by the method shown in Chapter 5. That is, to fit a polynomial trend model, it suffices to define the j-th explanatory variable as $x_{nj} = x_n^{j-1}$, and construct the matrix X as

$$X = \begin{bmatrix} 1 & x_1 & \cdots & x_1^m & y_1 \\ \vdots & \vdots & & \vdots & \vdots \\ 1 & x_N & \cdots & x_N^m & y_N \end{bmatrix} \tag{11.3}$$

Then, by reducing the matrix X to upper triangular form by an appropriate Householder transformation U,

$$UX = \begin{bmatrix} S \\ \mathrm{O} \end{bmatrix} = \begin{bmatrix} s_{11} & \cdots & s_{1,m+2} \\ & \ddots & \vdots \\ & & s_{m+2,m+2} \\ & \mathrm{O} & \end{bmatrix}, \tag{11.4}$$

the residual variance of the polynomial regression model of order j is obtained as

$$\hat{\sigma}_j^2 = \frac{1}{N} \sum_{i=j+2}^{m+2} s_{i,m+2}^2. \tag{11.5}$$

Since the j-th order model has $j+2$ parameters, i.e., $j+1$ regression coefficients and the variance, the AIC is obtained as

$$\mathrm{AIC}_j = N \log 2\pi\hat{\sigma}_j^2 + N + 2(j+2). \tag{11.6}$$

The AIC best order is then obtained by finding the minimum of the AIC$_j$. Given the AIC best order j, the maximum likelihood estimates $\hat{a}_0, \cdots, \hat{a}_j$ of the regression coefficients are obtained by solving the system of linear equations

$$\begin{bmatrix} s_{11} & \cdots & s_{1,j+1} \\ & \ddots & \vdots \\ & & s_{j+1,j+1} \end{bmatrix} \begin{bmatrix} a_0 \\ \vdots \\ a_j \end{bmatrix} = \begin{bmatrix} s_{1,m+2} \\ \vdots \\ s_{j+1,m+2} \end{bmatrix}. \tag{11.7}$$

Here, since the matrix S is in upper triangular form, this system of linear equations can be easily solved by backward substitution.

Example (Maximum temperature data) Table 11.1 summarizes the residual variance $\hat{\sigma}_j^2$ and the AIC$_j$ values of the polynomial regression models fitted to the maximum temperature data shown in Figure 1.1(c).

Table 11.1 *Maximum temperature data: The residual variances and AIC values of the polynomial regression models.*

j	$\hat{\sigma}_j^2$	AIC$_j$	j	$\hat{\sigma}_j^2$	AIC$_j$
0	60.09	1996.55	4	10.18	1141.74
1	58.89	1988.81	5	9.64	1117.51
2	33.61	1718.14	6	8.97	1084.22
3	23.74	1551.26	7	8.96	1085.90

Table 11.2 *(Log) WHARD data: The residual variances and AIC values of the polynomial regression models.*

j	$\hat{\sigma}_j^2$	AIC$_j$	j	$\hat{\sigma}_j^2$	AIC$_j$
0	0.02752	−550.91	8	0.00115	−1027.44
1	0.00163	−986.60	9	0.00112	−1029.21
2	0.00150	−998.22	10	0.00107	−1033.60
3	0.00149	−996.98	11	0.00107	−1031.65
4	0.00147	−997.43	12	0.00106	−1031.51
5	0.00142	−1000.63	13	0.00106	−1029.62
6	0.00123	−1021.24	14	0.00105	−1029.76
7	0.00122	−1019.98	15	0.00102	−1032.34

As shown in Table 11.1, the AIC was minimized at order 6, although the residual variance $\hat{\sigma}_j^2$ decreases monotonically.

Similarly, Table 11.2 shows the results for the logarithm of the WHARD data. In this example, although the residual variance decreases as the order increases, the AIC was minimized at order 10.

Plots (a) and (b) of Figure 11.1 show the original time series and the trends estimated using the AIC best polynomial regression models. In plot (a) of the maximum temperature data, a gradual and smooth change of temperature is reasonably captured by the estimated trend. Also in the case of the logarithm of the WHARD data, plot (b) shows a generally smoothly changing trend. In this case, however, we see that the estimated trend changes too rapidly at the start of the series. Moreover, the abrupt drop in sales in 1974 and 1975, which corresponds to n around 95 in plot (b), is not clearly detected. We shall consider a method to solve these problems later in Section 11.3.

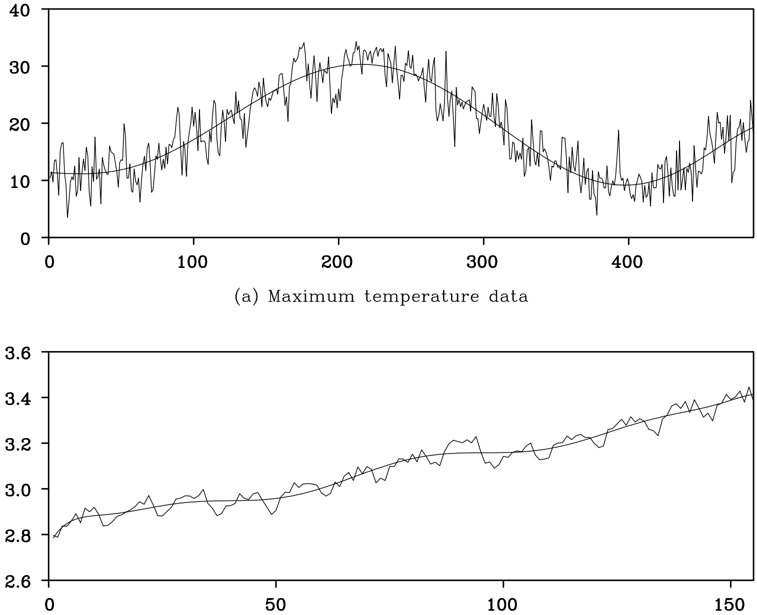

(a) Maximum temperature data

(b) WHARD data

Figure 11.1 *Trends of maximum temperature data and WHARD data estimated by the polynomial regression model.*

11.2 Trend Component Model–Model for Probabilistic Structural Changes

The polynomial trend model treated in the previous section can be expressed as

$$y_n \sim N(t_n, \sigma^2). \tag{11.8}$$

For this model, it is assumed that the time series is distributed as a normal distribution with mean value given by the polynomial t_n and constant variance σ^2.

This type of parametric model can yield a good estimate of the trend, when the actual trend is a polynomial or can be closely approximated by a polynomial. However, in other cases, a parametric model may not reasonably capture the characteristics of the trend or it may become too sensitive to random noise.

Consider a polynomial of the first order, i.e., a straight line, given by

$$t_n = an + b. \tag{11.9}$$

Here, if we define the time shift operator Δ by $\Delta t_n \equiv t_n - t_{n-1}$, then we have

$$\Delta t_n = a, \qquad \Delta^2 t_n = 0. \tag{11.10}$$

This means that the first order polynomial is the solution of the initial value problem for the second order difference equation

$$\Delta^2 t_n = 0, \qquad \Delta t_0 = a, \qquad t_0 = b. \tag{11.11}$$

In general, a polynomial of order $k-1$ can be considered a solution of the difference equation of order k,

$$\Delta^k t_n = 0. \tag{11.12}$$

In order to make the polynomial more flexible, we assume that $\Delta^k t_n \approx 0$ instead of using the exact difference equation (11.12). This can be achieved by introducing a stochastic difference equation of order k,

$$\Delta^k t_n = v_n, \tag{11.13}$$

where v_n is assumed to be a white noise that follows a normal distribution with mean 0 and variance $\tau^2, N(0, \tau^2)$. In the following, we call the model (11.13) a *trend component model* (Kitagawa and Gersch (1984, 1996). Because the solution of the difference equation $\Delta^k t_n = 0$ is a polynomial of order $k-1$, the trend component model of order k can be considered as an extension of a polynomial of order $k-1$. When the variance τ^2 of the noise is small, the realization of a trend component model locally becomes a smooth function that resembles the polynomial. However, a remarkable difference from the polynomial is that the trend component model can express a very flexible function globally.

Example (Random walk model) For $k = 1$, this model becomes a *random walk model* which can be defined by

$$t_n = t_{n-1} + v_n, \qquad v_n \sim N(0, \tau^2). \tag{11.14}$$

This model expresses that the trend is locally constant and can be expressed as $t_n \approx t_{n-1}$.

For $k = 2$, the trend component model becomes

$$t_n = 2t_{n-1} - t_{n-2} + v_n \tag{11.15}$$

for which it is assumed that the trend is locally a linear function and satisfies $t_n - 2t_{n-1} + t_{n-2} \approx 0$. In general, the k-th order difference operator of the trend component model (11.13) is given by

$$\Delta^k = (1-B)^k = \sum_{i=0}^{k} {}_k\mathrm{C}_i (-B)^i. \tag{11.16}$$

Therefore, using the binomial coefficient $c_i = (-1)^{i+1}{}_k\mathrm{C}_i$, the trend component model of order k can be expressed as

$$t_n = \sum_{i=1}^{k} c_i t_{n-i} + v_n. \tag{11.17}$$

Note that $c_1 = 1$ for $k = 1$ and $c_1 = 2$ and $c_2 = -1$ for $k = 2$. Although these models are not stationary, they can formally be considered as AR models of order k, by defining the state vector x_n and F, G and H as

$$x_n = \begin{bmatrix} t_n \\ t_{n-1} \\ \vdots \\ t_{n-k+1} \end{bmatrix}, \quad F = \begin{bmatrix} c_1 & c_2 & \cdots & c_k \\ 1 & & & \\ & \ddots & & \\ & & 1 & \end{bmatrix}, \quad G = \begin{bmatrix} 1 \\ 0 \\ \vdots \\ 0 \end{bmatrix},$$
$$H = [\, 1 \quad 0 \quad \cdots \quad 0 \,], \tag{11.18}$$

thus leading to a state-space representation of the trend model,

$$\begin{aligned} x_n &= Fx_{n-1} + Gv_n \\ t_n &= Hx_n. \end{aligned} \tag{11.19}$$

Example (State-space representation of trend models) For $k = 1$, the state-space model is obtained by putting

$$x_n = t_n, \qquad F = G = H = 1. \tag{11.20}$$

For $k = 2$, the state-space models of the trend models are obtained by

$$x_n = \begin{bmatrix} t_n \\ t_{n-1} \end{bmatrix}, \quad F = \begin{bmatrix} 2 & -1 \\ 1 & 0 \end{bmatrix}, \quad G = \begin{bmatrix} 1 \\ 0 \end{bmatrix}, \quad H = [\,1 \ 0\,] \tag{11.21}$$

or

$$x_n = \begin{bmatrix} t_n \\ -t_{n-1} \end{bmatrix}, \quad F = \begin{bmatrix} 2 & 1 \\ -1 & 0 \end{bmatrix}, \quad G = \begin{bmatrix} 1 \\ 0 \end{bmatrix}, \quad H = [\,1 \ 0\,]. \tag{11.22}$$

Note that the model (11.22) yields the canonical representation of the trend model treated in Chapter 9. Moreover, for $k = 2$, the state vector may alternatively be defined as $x_n = (t_n, \delta t_n)^T$

$$F = \begin{bmatrix} 1 & 1 \\ 0 & 1 \end{bmatrix}, \quad G = \begin{bmatrix} 1 \\ 1 \end{bmatrix}, \quad H = [\,1\ 0\,]. \tag{11.23}$$

Since $\delta t_n \equiv \Delta t_n$ holds for this model, we can easily confirm that it is equivalent to the model (11.21). The advantage of using this representation is that it can easily be generalized (Harvey (1989)); we can extend the trend component model by setting

$$v_n = \begin{bmatrix} v_{n1} \\ v_{n2} \end{bmatrix}, \quad F = \begin{bmatrix} 1 & 1 \\ 0 & 1 \end{bmatrix}, \quad G = \begin{bmatrix} 1 & 1 \\ 0 & 1 \end{bmatrix}, \quad H = [\,1\ 0\,]. \tag{11.24}$$

Here, the trend component satisfies

$$\begin{aligned} \delta t_n &= \delta t_{n-1} + v_{n2} \\ t_n &= t_{n-1} + \delta t_{n-1} + v_{n1} + v_{n2} \\ &= t_{n-1} + \delta t_n + v_{n1}. \end{aligned} \tag{11.25}$$

In contrast to the ordinary trend model with one-dimensional system noise, in this case, we have $\Delta t_n = \delta t_n + v_{n1}$. This extended trend model has the characteristic of allowing both level and slope to have independent noises, thus expressing a more flexible trend component.

11.3 Trend Model

A trend in a time series expresses a rough tendency of the phenomenon. In other words, an actually observed time series represents a superposition of a trend and various variations around it. Here, we consider the simplest case where the time series is expressed as

$$y_n = t_n + w_n, \tag{11.26}$$

where w_n is a white noise. This is the simplest model that expresses a generating mechanism for observations; it can be considered as a special form of the observation model given in Chapter 9.

To estimate the trend component t_n from the time series y_n, we consider the following *trend model* that consists of the trend component model and the above observation model,

$$\Delta^k t_n = v_n \tag{11.27}$$

$$y_n = t_n + w_n. \tag{11.28}$$

Here, v_n is similar to (11.13), a Gaussian white noise with mean 0 and variance τ^2, and w_n is a Gaussian white noise with mean 0 and variance σ^2.

The observation model in equation (11.28), $y_n = t_n + w_n$, is assumed to express the condition that the time series y_n is obtained by adding an independent noise to the trend. On the other hand, the trend component model (11.27) expresses the change in the trend. Actual time series are usually not as simple as this; they often require more sophisticated modeling and this will be treated in the next chapter. Based on the state-space representation of the trend component model, the state-space representation of the trend model is as follows:

$$\begin{aligned} x_n &= Fx_{n-1} + Gv_n \\ y_n &= Hx_n + w_n, \end{aligned} \tag{11.29}$$

where the state vector x_n is an appropriately defined k-dimensional vector, and F, G and H are the $k \times k$ matrix, the k-dimensional column vector and the k-dimensional row vector determined by (11.27) and (11.28), respectively. This model differs from the trend component model (11.18) only in that it contains an additional observation noise. As an example, for $k = 2$, the matrices and vectors above are defined by

$$\begin{aligned} x_n &= \begin{bmatrix} t_n \\ t_{n-1} \end{bmatrix}, \quad F = \begin{bmatrix} 2 & -1 \\ 1 & 0 \end{bmatrix}, \quad G = \begin{bmatrix} 1 \\ 0 \end{bmatrix} \\ H &= \begin{bmatrix} 1 & 0 \end{bmatrix}. \end{aligned} \tag{11.30}$$

Once the order k of the trend model and the variances τ^2 and σ^2 have been specified, the smoothed estimates $x_{1|N}, \cdots, x_{N|N}$ are obtained by the Kalman filter and the fixed-interval smoothing algorithm presented in Chapter 9. Since the first component of the state vector is t_n, the first component of $x_{n|N}$, namely, $Hx_{n|N}$, is the smoothed estimate of the trend $t_{n|N}$.

Example (Trend of maximum temperature data) Figure 11.2 shows various estimates of the trend of the maximum temperature data obtained by changing the variance of the system noise τ^2 for the first order trend model, $k = 1$. The variance of the observation noise σ^2 is estimated by the maximum likelihood method. Plot (a) shows the case of $\tau^2 = 0.223 \times 10^{-2}$. The estimated trend reasonablly captures the annual cycles of the temperature data. In plot (b) where the model is $k = 1$ and

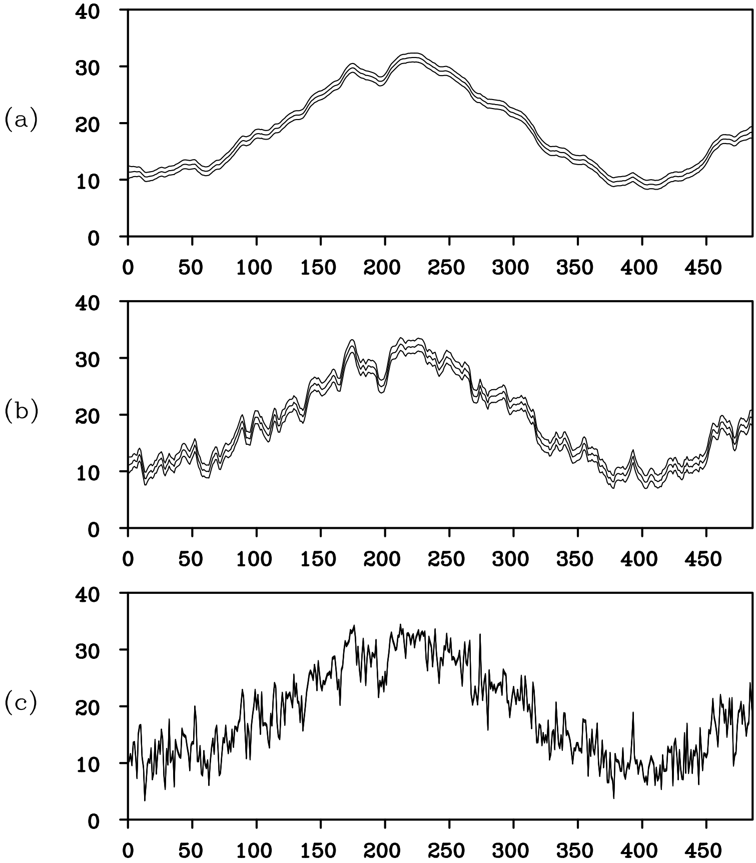

Figure 11.2 *Trend of the temperature data obtained by the first order trend models.*

$\tau^2 = 0.223$, the estimated trend reveals more detailed changes in temperature. Plot (c) shows the case of $k = 1$ and $\tau^2 = 0.223 \times 10^2$. The estimated trend just follows the observed time series.

On the other hand, Figure 11.3 shows the estimated trends obtained by the models with $k = 2$. The estimated trend in (a) obtained by $\tau^2 = 0.321 \times 10^{-5}$ is too smooth and the estimated trend in (c) obtained by $\tau^2 = 0.0321$ becomes an undulating curve. But in plot (b), it is evident that the estimate obtained by $\tau^2 = 0.321 \times 10^{-3}$ yields a reasonable trend. Comparing Figures 11.2 (a) and (b) with Figure 11.3 (b), we

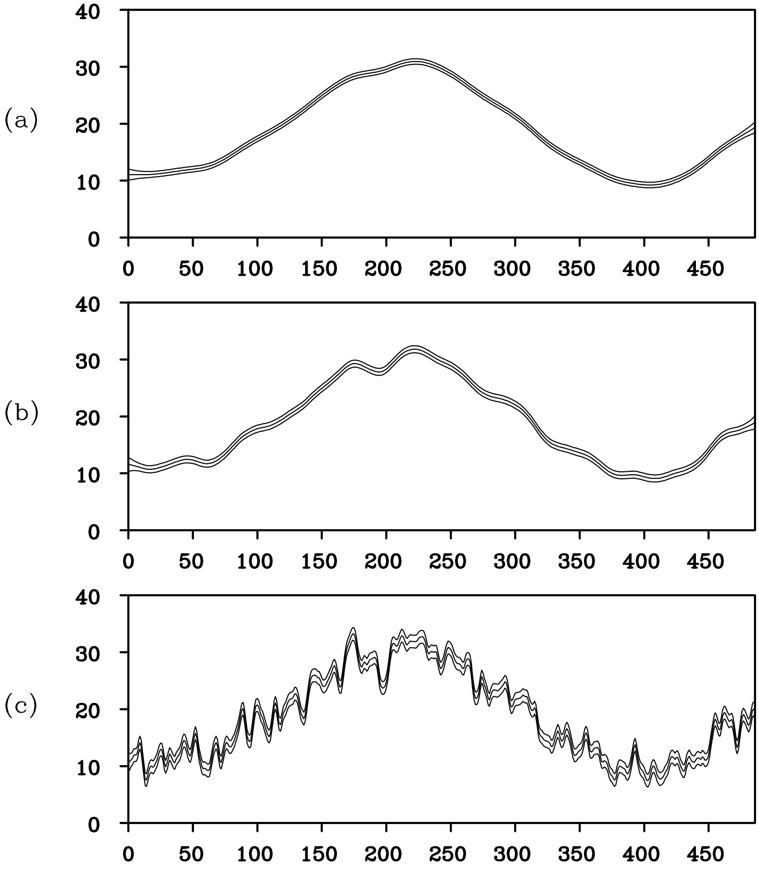

Figure 11.3 *Trend of temperature data obtained by the second order trend models.*

can see that the second order trend model yields a considerably smoother trend. As shown in the above examples, the trend model contains the order k and the variances τ^2 and σ^2 as parameters, which yield a variety of trend estimates. To obtain a good estimate of the trend, it is necessary to select appropriate parameters.

The estimates of the variances τ^2 and σ^2 are obtained by the maximum likelihood method. Using the method shown in Subsection 9.6, however, if the ratio $\lambda = \tau^2/\sigma^2$ is specified, the estimate of σ^2 is automatically obtained. Therefore, the estimate of the trend is controlled by the variance ratio of the system noise and the observation noise. Here λ is called a *trade-off parameter*. The order of the trend model k can be determined by the information criterion AIC. Often for analysis, $k = 2$ is used. However, for situations where the trend is variable, $k = 1$ may be used instead.

Table 11.3: *AIC values for trend models.*

$k = 1$		$k = 2$	
τ^2	AIC	τ^2	AIC
0.223×10^{-2}	2690	0.321×10^{-5}	2556
0.223	2448	0.321×10^{-3}	2506
0.223×10^{2}	2528	0.0321	2562

Table 11.3 summarizes the values of τ^2 and AIC for the models used for Figure 11.2. AIC is minimized at $\tau^2 = 0.223$ for $k = 1$ and at $\tau^2 = 0.321 \times 10^{-3}$ for $k = 2$. Incidentally, these estimates are obtained by the maximum likelihood method. Comparison of the AIC values for $k = 1$ and $k = 2$ reveals that the AIC for $k = 1$ is significantly smaller. It should be noted that according to the AIC, the wiggly trend obtained using $k = 1$ is preferable to the nicely smooth trend obtained with $k = 2$. This is probably because the noise w_n is assumed to be a white noise; thus, the trend model is inappropriate for the maximum temperature data.

Figure 11.4 shows the observations, the estimated trend and the residuals when the time series is decomposed by the model, $k = 2$ and $\tau^2 = 0.321 \times 10^{-3}$. Obviously, the residuals reveal strong correlation and does not seem to be a white noise sequence.

As shown in the next chapter, we can obtain a smoother trend that fits the data better using a seasonal adjustment model by decomposing the time series into three components; trend, AR component and observation noise. Using a seasonal adjustment model, we can obtain a smoother trend that better fits the data.

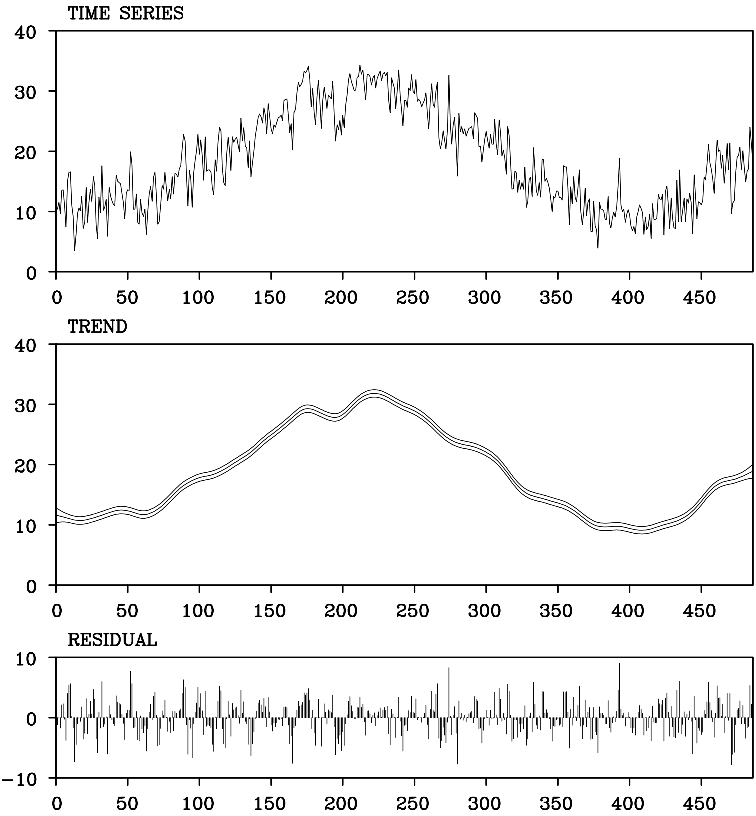

Figure 11.4 *Temperature data and the trend and residuals obtained by the trend model with* $k = 2$ *and* $\tau^2 = 0.321 \times 10^{-3}$.

Problems

1. According to the random walk hypothesis for stock prices, a stock price y_n follows a random walk model $y_n = y_{n-1} + v_n$, $v_n \sim N(0, \sigma^2)$.

   (1) Assume that $y_n = 17{,}000$ and $\sigma^2 = 40{,}000$ on a certain day. Obtain the k-days ahead prediction of the stock price and its prediction error variance for $k = 1, \ldots, 5$.

   (2) Obtain the probability that the stock price exceeds 17,000 Yen after 4 days have passed.

   (3) Do actual stock prices satisfy the random walk hypothesis? If not, consider a modification of the model.

(4) Estimate the trend of actual stock price data (Nikkei 225 Japanese stock price data and software for estimating the trend is given at the web site http://www.ism.ac.jp/˜sato.)

2. Give an example of a parametric trend model other than the polynomial trend model.

Chapter 12

The Seasonal Adjustment Model

The seasonal adjustment model is treated in this chapter as an example of extensions of the trend model. Many economic time series repeatedly show similar patterns in the vicinity of the same season of every year. In judging a tendency or prediction of such time series, we should carefully take into account these characteristics to avoid misleading results. A seasonal adjustment method is developed for analyzing time series that repeat similar patterns of variation at constant intervals (Shiskin (1976), Akaike (1980ab), Cleveland et al. (1982), Kitagawa and Gersch (1984)). Seasonal adjustment models decompose a time series y_n into three components of trend t_n, seasonal component s_n and white noise w_n to represent it as $y_n = t_n + s_n + w_n$.

12.1 Seasonal Component Model

In time series, a patterned variation s_n that appears repeatedly every year is called a *seasonal component*. In the following, p denotes the period length of the seasonal component. Here, we put $p = 12$ for monthly data and $p = 4$ for quarterly data, respectively. Then, the seasonal component s_n approximately satisfies

$$s_n = s_{n-p}. \qquad (12.1)$$

Using the lag operator B, since s_{n-p} is denoted as $B^p s_n$, the seasonal component approximately satisfies

$$(1 - B^p)s_n = 0. \qquad (12.2)$$

Similar to the stochastic trend component model introduced in Chapter 11, a model for the seasonal component that gradually changes with time, is given by (Kitagawa and Gersch (1984, 1996))

$$(1 - B^p)^\ell s_n = v_{n2}, \qquad v_{n2} \sim N(0, \tau_2^2). \qquad (12.3)$$

In particular, setting $\ell = 1$, we can obtain a random walk model for the seasonal component by

$$s_n = s_{n-p} + v_{n2}. \tag{12.4}$$

In this model, it is assumed that s_{pn+i}, $n = 1, 2, \ldots$ is a random walk for any $i = 1, \ldots, p$.

Therefore, assuming that the time series consists of the trend component t_n, the seasonal component s_n and the observation noise w_n, we can obtain a basic model for seasonal adjustment as

$$y_n = t_n + s_n + w_n, \tag{12.5}$$

with the trend component model (11.15) in the previous chapter and the above seasonal component model (12.3).

However, the apparently most natural model (12.4) for seasonal adjustment may not work well in practice, because the trend component model and the seasonal component model both contain the common factor $(1-B)^q$, $(q \geq 1)$. This can be seen by comparing the back-shift operator expression of the trend model (11.18) to the seasonal component model (12.3) with the decomposition

$$(1-B^p)^\ell = (1-B)^\ell (1+B+\cdots+B^{p-1})^\ell.$$

Here, assume that e_n is an arbitrary solution of the difference equation

$$(1-B)^q e_n = 0. \tag{12.6}$$

For $q = 1$, e_n is an arbitrary constant. If we define new components t'_n and s'_n as

$$\begin{aligned} t'_n &= t_n + e_n \\ s'_n &= s_n - e_n, \end{aligned}$$

then they satisfy (11.15), (12.3) and

$$y_n = t'_n + s'_n + w_n. \tag{12.7}$$

Therefore, we have infinitely many ways to decompose the time series yielding the same noise inputs v_{n1}, v_{n2} and w_n. Moreover, since the likelihood of the model corresponding to those decompositions is determined only by v_{n1}, v_{n2} and w_n, it is impossible to discriminate between the goodness of the decompositions by the likelihood. Once we use component models with common factors, we lose uniqueness of the decomposition.

A simple method to guarantee uniqueness of decomposition is to ensure that none of the component models share any common factors. Since $1-B^p = (1-B)(1+B+\cdots+B^{p-1})$ and the sufficient condition for $(1-B^p)^\ell = 0$ is

$$(1+B+\cdots+B^{p-1})^\ell = 0, \tag{12.8}$$

$S_n \approx S_{n-p}$ is attained, if

$$\sum_{i=0}^{p-1} B^i s_n \approx 0 \tag{12.9}$$

is satisfied. Therefore, as a stochastic model of a seasonal component that gradually changes with time, we may use the following model:

$$\left(\sum_{i=0}^{p-1} B^i\right)^\ell s_n = v_{n2}, \qquad v_{n2} \sim N\big(0, \tau_2^2\big). \tag{12.10}$$

In this book, the above model is called a *seasonal component model* with period p and order ℓ. In actual analysis, except for situations where the seasonal component shows a significant trend in its changes, the first order model

$$\sum_{i=0}^{p-1} s_{n-i} = v_{n2}, \qquad v_{n2} \sim N\big(0, \tau_2^2\big) \tag{12.11}$$

is usually used.

To obtain a state-space representation of the seasonal component model, initially we expand the operator in (12.9) as follows:

$$\left(\sum_{i=0}^{p-1} B^i\right)^\ell = 1 - \sum_{i=1}^{\ell(p-1)} d_i B^i. \tag{12.12}$$

The coefficient d_i is given by $d_i = -1, i = 1,\ldots,p-1$ for $\ell = 1$ and $d_i = -i-1, i \le p-1$, and $d_i = i+1-2p, p \le i \le 2(p-1)$ for $\ell = 2$. Since the seasonal component model given in (12.12) is formally a special case of an autoregressive model, the state-space representation of the seasonal component model can be given as

$$x_n = \begin{bmatrix} s_n \\ s_{n-1} \\ \vdots \\ s_{n-\ell(p-1)+1} \end{bmatrix}, \; F = \begin{bmatrix} d_1 & d_2 & \cdots & d_{\ell(p-1)} \\ 1 & & & \\ & \ddots & & \\ & & 1 & \end{bmatrix}, \; G = \begin{bmatrix} 1 \\ 0 \\ \vdots \\ 0 \end{bmatrix}$$

$$H = [\,1,\ 0, \ldots, 0\,]. \tag{12.13}$$

12.2 Standard Seasonal Adjustment Model

For standard seasonal adjustment, the time series y_n is decomposed into the following three components

$$y_n = t_n + s_n + w_n, \tag{12.14}$$

where t_n, s_n and w_n are the trend component, the seasonal component and the observation noise, respectively. Combining the basic model (12.12) with the trend component model and the seasonal component model, we obtain the following standard seasonal adjustment models,

$$\begin{array}{lll}
y_n = t_n + s_n + w_n & \text{(observation model)} & (12.15) \\
\triangle^k t_n = v_{n1} & \text{(trend component model)} & (12.16) \\
\left(\sum_{i=0}^{p-1} B^i \right)^{\ell} s_n = v_{n2} & \text{(seasonal component model)} & (12.17)
\end{array}$$

where $w_n \sim N(0,\sigma^2)$, $v_{n1} \sim N(0,\tau_1^2)$ and $v_{n2} \sim N(0,\tau_2^2)$.

The above model is called the standard *seasonal adjustment model.* For a seasonal adjustment model with trend order k, period p and seasonal order $\ell = 1$, let the $(k+p-1)$ dimensional state vector be defined by $x_n = (t_n,\cdots,t_{n-k+1},s_n,s_{n-1},\cdots,s_{n-p+2})^T$, and define a 2-dimensional noise vector as $v_n = (v_{n1},v_{n2})^T$, and the matrices F, G and H by

$$F = \begin{bmatrix} F_1 & \mathrm{O} \\ \mathrm{O} & F_2 \end{bmatrix}, \quad G = \begin{bmatrix} G_1 & \mathrm{O} \\ \mathrm{O} & G_2 \end{bmatrix}, \quad H = [H_1 \ \ H_2], \tag{12.18}$$

then the state-space representation of the seasonal adjustment model is obtained as

$$\begin{aligned} x_n &= F x_{n-1} + G v_n \\ y_n &= H x_n + w_n. \end{aligned} \tag{12.19}$$

Here, F_1, G_1 and H_1 are the matrices and vectors used for the state-space representation of the trend component model, and similarly, F_2, G_2 and H_2 are the matrices and vectors used for the representation of the seasonal component model. For instance, if $k = 2$, $\ell = 1$ and $p = 4$, then F, G and H are defined by

$$F = \begin{bmatrix} 2 & -1 & & & \\ 1 & 0 & & & \\ & & -1 & -1 & -1 \\ & & 1 & & \\ & & & 1 & \end{bmatrix}, \quad G = \begin{bmatrix} 1 & 0 \\ 0 & 0 \\ 0 & 1 \\ 0 & 0 \\ 0 & 0 \end{bmatrix}$$

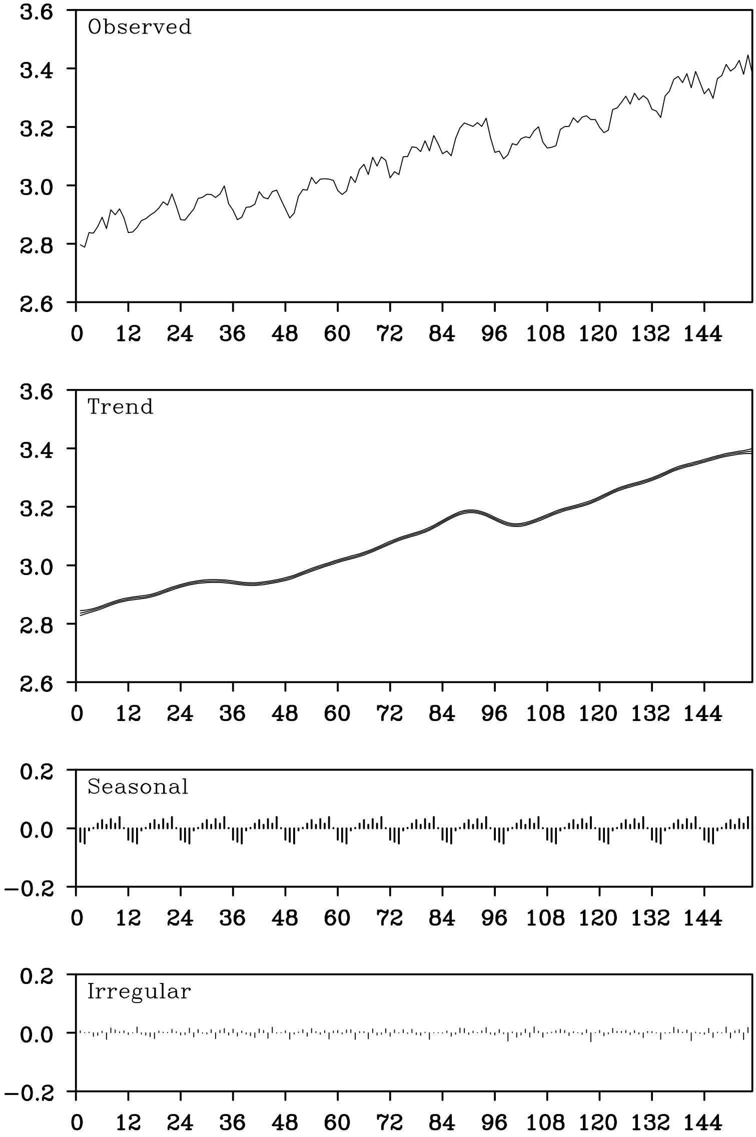

Figure 12.1 *Seasonal adjustment of WHARD data by a standard seasonal adjustment model.*

$$H = [\ 1\ \ 0\ \ 1\ \ 0\ \ 0\ ]. \tag{12.20}$$

Example (Seasonal adjustment of WHARD data) Figure 12.1 shows the estimates of the trend, the seasonal and the noise components of the logarithm of WHARD data using the standard seasonal adjustment model. The maximum likelihood estimates of the parameters are $\hat{\tau}_1^2 = 0.0248$, $\hat{\tau}_2^2 = 0.11 \times 10^{-7}$, $\hat{\sigma}^2 = 0.156 \times 10^{-3}$, and AIC $= -728.50$. Plot (b) in Figure 12.1 shows the estimated trend component $t_{n|N}$ and ±1 standard error interval. A very smooth upward trend is evident, except for the years 1974 and 1975 where a rapid decrease in the trend is detected, and the estimated seasonal component is very stable over the whole interval.

Using the seasonal adjustment model, we can predict time series with seasonal variation. Figure 12.2 shows the increasing horizon prediction over two years, i.e., 24 observations using the initial 132 observations by the method shown in Chapter 9. In the figure, the mean of the predictive distribution $y_{132+j|132}$ and the ±1 standard error interval, i.e., $\pm\sqrt{d_{132+j|132}}$ for $j = 1, \ldots, 24$ are plotted. The actual observations are denoted by the symbol ∘. In this case, very good increasing horizon prediction can be attained, because the estimated trend and seasonal components are steady. However, it should be noted that ±1 standard error interval is very wide.

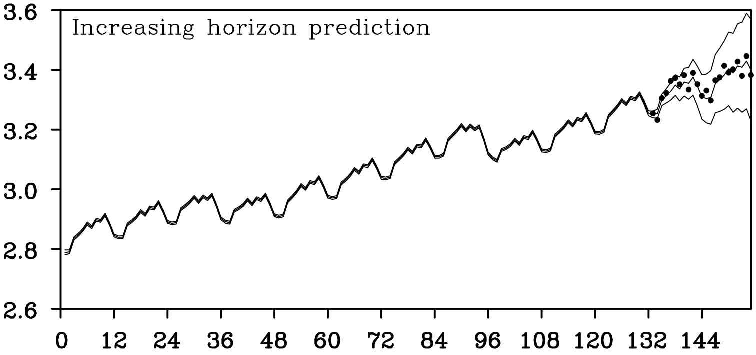

Figure 12.2: *Increasing horizon prediction using a seasonal adjustment model.*

12.3 Decomposition Including a Stationary AR Component

In this section, we consider an extension of the standard seasonal adjustment method (Kitagawa and Gersch (1984)). In the standard seasonal adjustment method, the time series is decomposed into three components, i.e., the trend component, the seasonal component and the observation noise. These components are assumed to follow the models given in (12.15) and (12.16), and the observation noise is assumed to be a white noise. Therefore, if a significant deviation from that assumption is present, then the decomposition obtained by the standard seasonal adjustment method might become inappropriate. Figure 12.3 shows the decomposition of the BLSALLFOOD data of Figure 1.1(d) that was obtained by the seasonal adjustment method for the model with $k = 2$, $\ell = 1$ and $p = 12$. In this case, different from the case shown in the previous section, the estimated trend shows a wiggle, particularly in the latter part of the data.

Let us consider the problems when the above-mentioned wiggly trend is obtained. Similarly to the Figure 12.2, Figure 12.4 shows the increasing horizon prediction for the latter two years (24 observations) of the BLSALLFOOD data based on the former 132 observations. In this case, apparently the predicted mean $y_{132+j|132}$ provides a reasonable prediction of the actual time series y_{132+j}. However, it is evident that prediction by this model is not reliable, because an explosive increase in the size of the confidence interval is observed.

Figure 12.5 shows the overlay of 13 increasing horizon predictions that are obtained by assuming the starting point to be $n = 126,\ldots,138$, respectively. The increasing horizon predictions starting at and before $n = 130$ have significant downward bias. On the other hand, the increasing horizon predictions starting at and after $n = 135$ have significant upward bias. This is the reason that the explosive increase in the width of the confidence interval of the increasing horizon predictions has occurred as the lead time has increased. The stochastic trend component model in the seasonal adjustment model can flexibly express a complex trend component. But in the increasing horizon prediction with this model, the predicted mean $t_{n+j|n}$ can simply be obtained by using the difference equation

$$\Delta^k t_{n+j|n} = 0. \tag{12.21}$$

Therefore, whether the predicted values may go up or down is decided by the starting point of the trend. From these results, we see that if the estimated trend is wiggly, it is not appropriate to use the standard

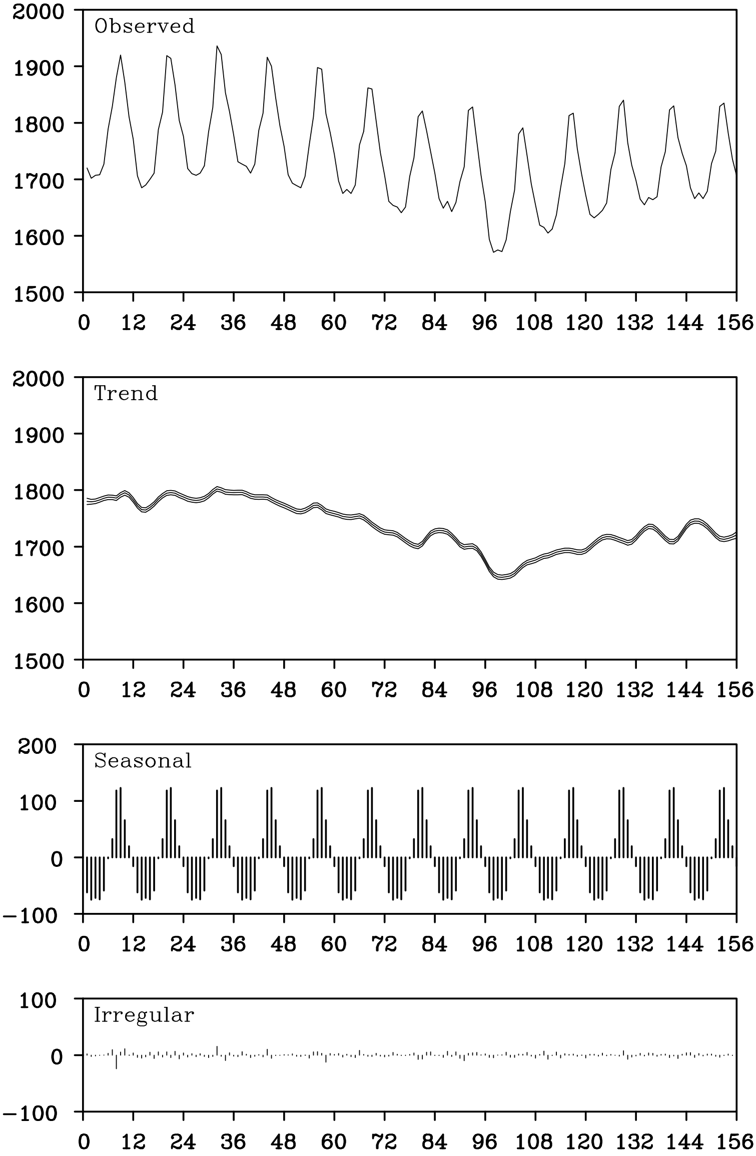

Figure 12.3 *Seasonal adjustment of BLSALLFOOD data by the standard seasonal adjustment model.*

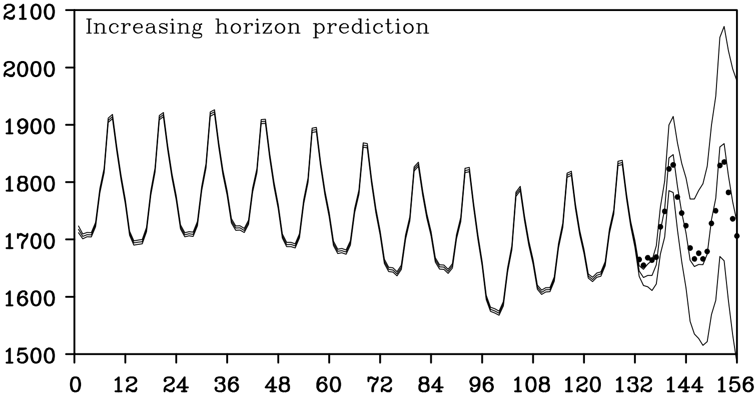

Figure 12.4 *Increasing horizon prediction of BLSALLFOOD data (prediction starting point: $n = 132$).*

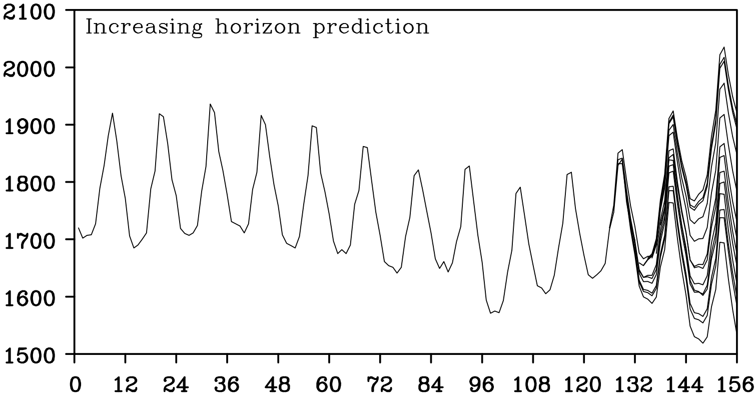

Figure 12.5 *Increasing horizon prediction of BLSALLFOOD data with floating starting points (prediction starting point: n =126, . . . , 138).*

seasonal adjustment model for increasing horizon prediction.

In predicting one year or two years ahead, it is possible to obtain a better prediction with a smoother curve by using a smaller value than the maximum likelihood estimate for the system noise variance of the trend component, τ_1^2. However, this method suffers from the following problems; it is difficult to reasonably determine τ_1^2 and, moreover, prediction with a small lead time such as one-step-ahead prediction becomes significantly worse than that obtained by the maximum likelihood model.

To achieve good prediction for both short and long lead times, we consider an extension of the standard seasonal adjustment model by including a new component p_n as

$$y_n = t_n + s_n + p_n + w_n. \tag{12.22}$$

Here, p_n is a *stationary AR component model* that is assumed to follow an AR model

$$p_n = \sum_{i=1}^{m_3} a_i p_{n-i} + v_{n3}, \tag{12.23}$$

where v_{n3} is assumed to be a Gaussian white noise with mean 0 and variance τ_3^2. This model expresses a short-term variation, for instance, the cycle of an economic time series, not a long-term tendency like the trend component. In the model (12.22), the trend component obtained by the standard seasonal adjustment model is further decomposed into the smoother trend component t_n and the short-term variation p_n. As shown in Chapter 9, the state-space representation of the AR model (12.22) is obtained by defining the state vector $x_n = (p_n, p_{n-1}, \ldots, p_{n-m_3+1})^T$ and

$$F_3 = \begin{bmatrix} a_1 & a_2 & \cdots & a_{m_3} \\ 1 & & & \\ & \ddots & & \\ & & 1 & \end{bmatrix}, \quad G_3 = \begin{bmatrix} 1 \\ 0 \\ \vdots \\ 0 \end{bmatrix}, \tag{12.24}$$

$$H_3 = [\ 1 \quad 0 \quad \cdots \quad 0\ ], \qquad Q_3 = \tau_3^2.$$

Therefore, using the state-space representation for the composite model shown in Chapter 9, the state-space model for the decomposition of (12.22) is obtained by defining

$$F = \begin{bmatrix} F_1 & & \\ & F_2 & \\ & & F_3 \end{bmatrix}, \quad G = \begin{bmatrix} G_1 & 0 & 0 \\ 0 & G_2 & 0 \\ 0 & 0 & G_3 \end{bmatrix},$$

$$H = [\ H_1 \quad H_2 \quad H_3\ ], \quad Q = \begin{bmatrix} \tau_1^2 & 0 & 0 \\ 0 & \tau_2^2 & 0 \\ 0 & 0 & \tau_3^2 \end{bmatrix}. \tag{12.25}$$

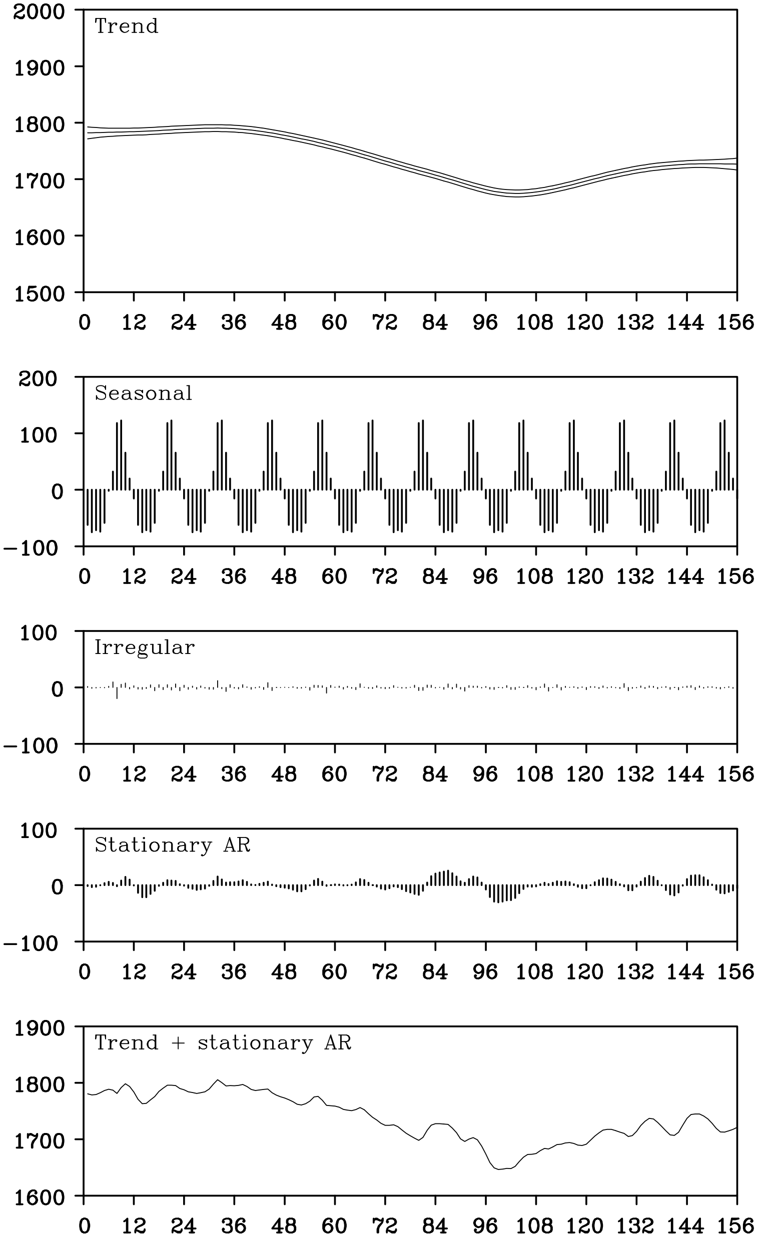

Figure 12.6 *Seasonal adjustment of BLSALLFOOD data by the model, including stationary AR components.*

Example (Seasonal adjustment with stationary AR component) Figure 12.6 shows the decomposition of BLSALLFOOD data into trend, seasonal, stationary AR and observation noise components by this model. The estimated trend expresses a very smooth curve similar to Figure 12.1. On the other hand, a short-term variation is detected as the stationary AR component and the (trend component) + (stationary AR component) resemble the trend component of Figure 12.3. The AIC value for this model is 1336.54, which is significantly smaller than that of the standard seasonal adjustment model, 1369.30.

Figure 12.7 shows the increasing horizon prediction with this model starting from $n = 132$. It can be seen that a good prediction was achieved with both short and long lead times.

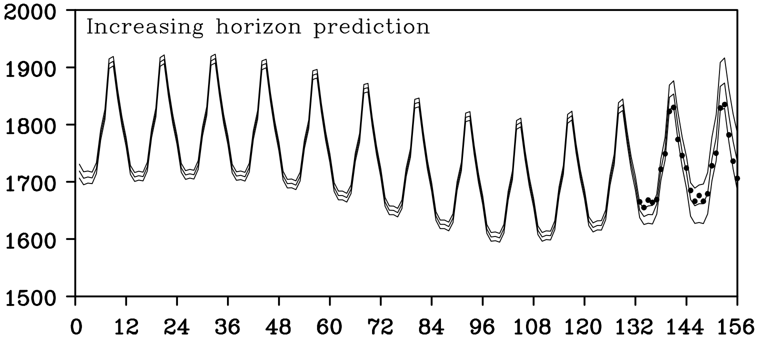

Figure 12.7 *Increasing horizon prediction of the BLSALLFOOD data by the model, including stationary AR components.*

12.4 Decomposition Including a Trading-Day Effect

Monthly economic time series, such as the amount of sales at a department store, may strongly depend on the number of the days of the week in each month, because there are marked differences in sales depending on the days of the week. For example, a department store may have more customers on Saturdays and Sundays or may regularly close on a specific day of a week. A similar phenomenon can often be seen in environmental data, for example, the daily amounts of NO_x and CO_2 recorded.

A *trading-day adjustment* has been developed to remove such trading-day effects that depend on the number of the days of the week (Cleveland and Devlin (1980), Hillmer (1982)). To develop a model-based method for trading-day adjustment, we have to develop a proper model for the trading-day effect component (Akaike and Ishiguro (1983), Kitagawa and Gersch (1984, 1996)). Hereinafter, the numbers from Sunday to Saturday in the n-th data, y_n, are denoted as $d^*_{n1},\cdots,d^*_{n7}$. Note that each d^*_{ni} takes a value 4 or 5 for monthly data. Then the effect of the trading-day is expressed as

$$td_n = \sum_{i=1}^{7} \beta_{ni} d^*_{ni}. \tag{12.26}$$

The coefficient β_{ni} expresses the effect of the number of the i-th day of the week on the value of y_n. Here, to guarantee uniqueness of the decomposition of the time series, we impose the restriction on it that the sum of all coefficients amounts to 0, that is,

$$\beta_{n1} + \cdots + \beta_{n7} = 0. \tag{12.27}$$

Since the last coefficient is defined by $\beta_{n7} = -(\beta_{n1} + \cdots + \beta_{n6})$, the trading-day effect can be expressed by using $\beta_{n1},\ldots,\beta_{n6}$ as

$$\begin{aligned} td_n &= \sum_{i=1}^{6} \beta_{ni}(d^*_{ni} - d^*_{n7}) \\ &\equiv \sum_{i=1}^{6} \beta_{ni} d_{ni}, \end{aligned} \tag{12.28}$$

where $d_{ni} \equiv d^*_{ni} - d^*_{n7}$ is the difference in the number of the i-th day of the week and the number of Saturdays in the n-th month corresponding to y_n.

On the assumption that these coefficients gradually change, following the first order trend model

$$\Delta\beta_{ni} = v^{(i)}_{n4}, \qquad v^{(i)}_{n4} \sim N(0,\tau_4^2), \qquad\qquad i = 1,\ldots,6, \tag{12.29}$$

the state-space representation of the trading-day effect model is obtained by

$$\begin{aligned} &F_{n4} = G_{n4} = I_6, \qquad H_{n4} = [d_{n1},\ldots,d_{n6}] \\ &x_{n4} = \begin{bmatrix} \beta_{n1} \\ \vdots \\ \beta_{n6} \end{bmatrix}, \quad Q = \begin{bmatrix} \tau_4^2 & & \\ & \ddots & \\ & & \tau_4^2 \end{bmatrix}. \end{aligned} \tag{12.30}$$

In this representation, H_{n4} becomes a time-dependent vector. For simplicity, the variance-covariance matrix Q is assumed to be a diagonal matrix with equal diagonal elements. In actual analysis, however, we often assume that the coefficients are time-invariant, i.e.,

$$\beta_{ni} \equiv \beta_i, \tag{12.31}$$

where we may put either $\tau_4^2 = 0$ or $G = 0$ for the state-space representation of this model.

The state-space model for the decomposition of the time series

$$y_n = t_n + s_n + p_n + td_n + w_n \tag{12.32}$$

can be obtained by using

$$x_n = \begin{bmatrix} x_{n1} \\ x_{n2} \\ x_{n3} \\ x_{n4} \end{bmatrix}, F = \begin{bmatrix} F_1 & & & \\ & F_2 & & \\ & & F_3 & \\ & & & F_4 \end{bmatrix}, G = \begin{bmatrix} G_1 & 0 & 0 \\ 0 & G_2 & 0 \\ 0 & 0 & G_3 \\ 0 & 0 & 0 \end{bmatrix},$$

$$H = [\ H_1 \quad H_2 \quad H_3 \quad H_{n4}\ ], \quad Q = \begin{bmatrix} \tau_1^2 & 0 & 0 \\ 0 & \tau_2^2 & 0 \\ 0 & 0 & \tau_3^2 \end{bmatrix}. \tag{12.33}$$

Example (Seasonal adjustment with trading-day effect) Figure 12.8 shows the results of the logarithm of the WHARD data, the decomposition into the trend, the seasonal, the trading-day effect and the noise components by the seasonal adjustment model with trading-day effect. The estimated trend and seasonal components are similar to the decomposition by the standard seasonal adjustment model shown in Figure 12.1. Although the extracted trading-day effect component is apparently minuscule, it can be seen that the plot of seasonal component plus trading-day effect component reproduces the details of the observed time series. The AIC value for this model is -778.18, which is significantly smaller than that for the standard seasonal adjustment model, -728.50. Once the time-invariant coefficients of trading-day effects β_i are estimated, this can contribute to a significant increase in the accuracy of prediction, because $d_{n1}, \cdots, d_{n6}$ are known, even for the future.

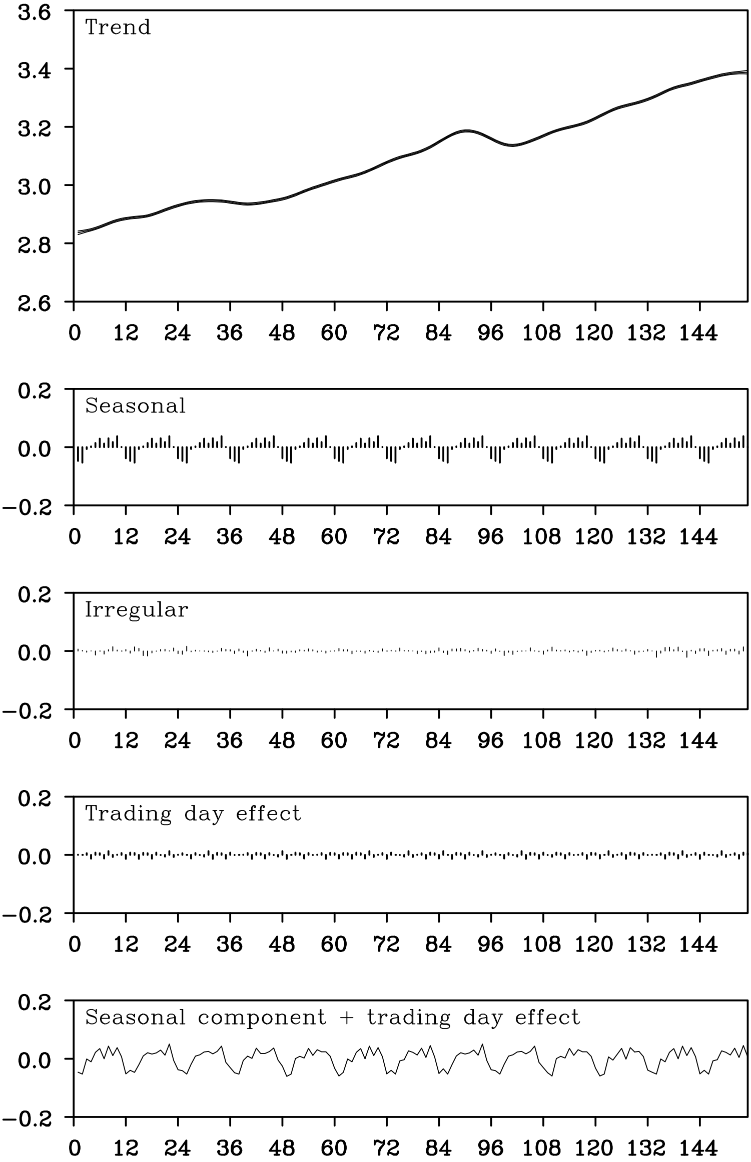

Figure 12.8: *Trading-day adjustment for WHARD data.*

Problems

1. Describe what we should check when decomposing a time series using a seasonal adjustment model with a stationary AR component.
2. Consider a different seasonal component model from that given in 12.1.
3. In trading day adjustments, consider a model that takes into account the following components:
   (1) The effects of the weekend (Saturday and Sunday) and weekdays are different.
   (2) There are three different effects, i.e., Saturday, Sunday and the weekdays.
4. Consider any other possible effects related to seasonal adjustments that are not considered in this book.
5. Try seasonal adjustment of an actual time series. You may use the WebDecomp software at website http://www.ism.ac.jp/˜sato.

Chapter 13

Time-Varying Coefficient AR Model

There are two types of nonstationary time series, one with a drifting mean value and another which has a structure that varies around the mean value over time. In the latter type of nonstationary time series, the variance, the autocovariance function, and the power spectrum of the time series change over time.

In this chapter, two methods are presented for the analysis of such nonstationary time series. One is an estimation method for time-varying variance and the other is a method for modeling the time-varying coefficient AR model. Estimation of the time-varying variance is equivalent to the estimation of the stochastic volatility in financial time series analysis. Early treatment of AR model with time-varying coefficients are reported in Whittle (1965), Subba Rao (1970) and Bohlin (1976). A state-space modeling for the time-varying AR model was introduced in Kitagawa (1983) and Kitagawa and Gersch (1985,1996). Extension of the state-space modeling to multivariate time series was shown in Jiang and Kitagawa (1993).

13.1 Time-Varying Variance Model

The time series y_n, $n = 1,\dots,N$ is assumed to be a Gaussian white noise with mean 0 and time-varying variance σ_n^2. Assuming that $\sigma_{2m-1}^2 = \sigma_{2m}^2$, if we define a transformed series $s_1,\dots,s_{N/2}$ by

$$s_m = y_{2m-1}^2 + y_{2m}^2, \tag{13.1}$$

s_m is distributed as a χ^2-distribution with 2 degrees of freedom, i.e., an exponential distribution. Therefore, the probability density function of s_m is given by

$$f(s) = \frac{1}{2\sigma^2} e^{-s/2\sigma^2}. \tag{13.2}$$

The probability density function of the random variable z_m defined by the transformation

$$z_m = \log\left(\frac{s_m}{2}\right), \tag{13.3}$$

may be expressed as

$$g(z) = \frac{1}{\sigma^2}\exp\left\{z - \frac{e^z}{\sigma^2}\right\} = \exp\left\{(z - \log\sigma^2) - e^{(z-\log\sigma^2)}\right\}. \tag{13.4}$$

This means that the transformed series z_m can be written as

$$z_m = \log\sigma^2 + w_m, \tag{13.5}$$

where w_m follows a double exponential distribution with probability density function

$$h(w) = \exp\{w - e^w\}. \tag{13.6}$$

Therefore, an independent time series with time-varying variance is expressed by the state-space model for the trend of the logarithm of the variance,

$$\begin{aligned} \Delta^k t_m &= v_m \\ z_m &= t_m + w_m, \end{aligned} \tag{13.7}$$

and the logarithm of the variance of the original time series y_n is estimated by obtaining the trend of the transformed series z_m.

It should be noted that the distribution of the noise w_m is not Gaussian. However, since the mean and the variance of the double exponential distribution are given by $-\zeta = 0.57722$ (Euler constant) and $\pi^2/6$, respectively, we can approximate it with a Gaussian distribution as follows:

$$w_m \sim N\left(-\zeta, \frac{\pi^2}{6}\right). \tag{13.8}$$

(Wahba (1980) used this property in smoothing the log periodogram with a cross-validated smoothing spline.) We can estimate the trend t_m with the Kalman filter. Then $t_{m|M} + \gamma$ with $M = N/2$ yields a smoothed estimate of $\log\sigma_m^2$. In Chapter 14, an exact method of estimating the logarithm of the variance will be given, by using the exact probability distribution (13.6) and a non-Gaussian filter and a smoother.

So far, the transformed series defined as the mean of two consecutive squared time series shown in equation (13.1) has been used in estimating

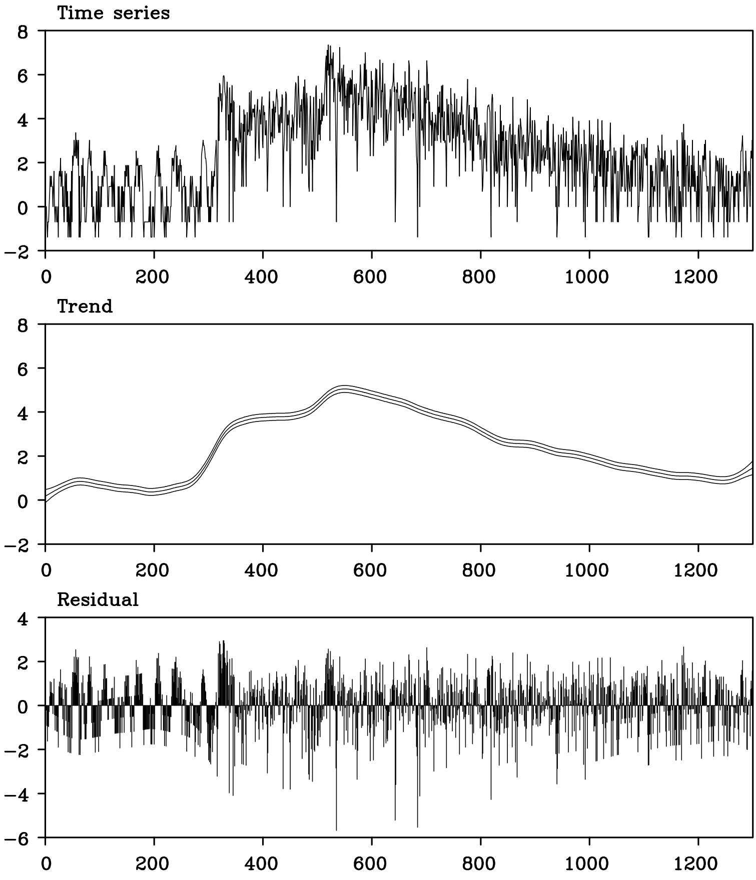

Figure 13.1 *Estimation of time-varying variance and standardized time series. From top to bottom: transformed data, estimated time-varying log-variance and the normalized time series.*

the variance of the time series. This is just to make the noise distribution $g(z)$ closer to a Gaussian distribution, and it is not essential in estimating the variance of the time series. In fact, if we use a non-Gaussian filter for trend estimation, we may use the transformed series $s_n = y_n^2$, $n = 1,\ldots,N$, and with this transformation, it is not necessary to assume that $\sigma_{2m-1}^2 = \sigma_{2m}^2$.

Example (Time-varying variance of a seismic data) Figure 13.1 depicts the transformed time series s_m obtained using the equation (13.3) for the seismic data shown in Figure 1.1, which are estimates of the logarithm of the variance, $\log \hat{\sigma}_m^2$, and the normalized time series $\tilde{y}_n = y_n/\hat{\sigma}_{n/2}$. The parameters of the trend model used for the estimation are the order of the trend k, with a value of 2 and the system noise variance $\hat{\tau}^2$, with a value of 0.66×10^{-5}. By this method, we can obtain a time series with a variance roughly equal to 1, although the actual seismic data are not a white noise.

13.2 Time-Varying Coefficient AR Model

The characteristics of stationary time series can be expressed by an autocovariance function or a power spectrum. Therefore, for nonstationary time series with a time-varying stochastic structure, it is natural to consider that its autocovariance function and power spectrum change over time. For a stationary time series, its autocovariance function and power spectrum are characterized by selecting the orders and coefficients of an AR model or ARMA model. Therefore, for a nonstationary time series with a time-varying stochastic structure, it is natural to consider that these coefficients and the order of the model change with time.

In this section, an autoregressive model with time-varying coefficients for the nonstationary time series y_n is modeled as

$$y_n = \sum_{j=1}^{m} a_{nj} y_{n-j} + w_n, \tag{13.9}$$

where w_n is a Gaussian white noise with mean 0 and variance σ^2 (Kozin and Nakajima (1980), Kitagawa (1983)).

This model is called the *time-varying coefficients AR model* of order m and a_{nj} is called the *time-varying AR coefficient* with time lag j at time n. Given the time series $y_1, \dots, y_N$, this time-varying coefficients AR model contains at least mN unknown coefficients. The difficulty with this type of model is, therefore, that we cannot obtain meaningful estimates by applying the maximum likelihood method or the least squares method to the model (13.9).

To circumvent this difficulty, we apply a stochastic trend component model to represent time-varying parameters of the AR model, similar to the treatment of the trend model and the seasonal adjustment model. For a trend component model, the trend component t_n was assumed to be an unknown parameter of the model; we then introduced a model for time-change of the parameter. Since the AR coefficient a_{nj} changes over time

n, a constraint model

$$\Delta^k a_{nj} = v_{nj}, \qquad j = 1, \ldots, m \tag{13.10}$$

is used where Δ is the difference operator with respect to the time n, defined as $\Delta a_{nj} = a_{nj} - a_{n-1,j}$ (Kitagawa (1983), Kitagawa and Gersch (1985, 1996)).

In (13.10), k is assumed to be 1 or 2. The vector $v_n = (v_{n1}, \ldots, v_{nm})^T$ is an m-dimensional Gaussian white noise with mean vector 0 and variance-covariance matrix Q. Since v_{ni} and v_{nj} are usually assumed to be independent for $i \neq j$, Q becomes a diagonal matrix with diagonal elements $\tau_{11}^2, \ldots, \tau_{mm}^2$; thus, it can be expressed as $Q = \text{diag}\{\tau_{11}^2, \ldots, \tau_{mm}^2\}$. It is assumed further in this section that $\tau_{11}^2 = \cdots = \tau_{mm}^2 = \tau^2$. The rationale for the above assumption will be discussed later in Section 13.4.

Next, to estimate the AR coefficients of the time-varying AR model (13.9) associated with the component model (13.10), we develop a corresponding state-space representation. For $k = 1$ and $k = 2$, the state vectors are defined by $x_{nj} = a_{nj}$ and $x_{nj} = (a_{nj}, a_{n-1,j})^T$, respectively. Then the time-varying coefficient AR model in equation (13.10) can be expressed as

$$x_{nj} = F^{(k)} x_{n-1,j} + G^{(k)} v_{nj}, \tag{13.11}$$

where $F^{(1)}$, $F^{(2)}$, $G^{(1)}$ and $G^{(2)}$ are defined as

$$\begin{aligned} F^{(1)} &= G^{(1)} = 1 \\ F^{(2)} &= \begin{bmatrix} 2 & -1 \\ 1 & 0 \end{bmatrix}, \quad G^{(2)} = \begin{bmatrix} 1 \\ 0 \end{bmatrix}. \end{aligned} \tag{13.12}$$

Here, assuming the j-th term of equation (13.9) to be the j-th component of this model, it can be expressed as

$$a_{nj} y_{n-j} = H_n^{(kj)} x_{nj}, \tag{13.13}$$

where $H_n^{(1j)} = y_{n-j}$ and $H_n^{(2j)} = (y_{n-j}, 0)$. Then the j-th component of the time-varying coefficient AR model is given by a state-space model with $F^{(k)}$, $G^{(k)}$ and $H_n^{(kj)}$ as follows:

$$\begin{aligned} x_{nj} &= F^{(k)} x_{n-1,j} + G^{(k)} v_{nj} \\ a_{nj} y_{n-j} &= H_n^{(kj)} x_{nj}. \end{aligned} \tag{13.14}$$

Moreover, noting that $H^{(1)} = 1$ and $H^{(2)} = (1, 0)$, $H_n^{(kj)}$ is given by

$$H_n^{(kj)} = y_{n-j} H^{(k)}. \tag{13.15}$$

Using the above component model, a state-space representation of the time-varying coefficients AR model is obtained as

$$\begin{aligned} x_n &= Fx_{n-1} + Gv_n \\ y_n &= H_n x_n + w_n, \end{aligned} \tag{13.16}$$

where, the $km \times km$ matrix F, the $km \times m$ matrix G and the km-dimensional vectors H_n and x_n are defined by

$$\begin{aligned} F &= \begin{bmatrix} F^{(k)} & & \\ & \ddots & \\ & & F^{(k)} \end{bmatrix} = I_m \otimes F^{(k)} \\ G &= \begin{bmatrix} G^{(k)} & & \\ & \ddots & \\ & & G^{(k)} \end{bmatrix} = I_m \otimes G^{(k)} \\ H_n &= [H_n^{(k1)}, \ldots, H_n^{(km)}] = (y_{n-1}, \ldots, y_{n-m}) \otimes H^{(k)} \\ x_n &= \begin{cases} (a_{n1}, \ldots, a_{nm})^T, & \text{for } k=1 \\ (a_{n1}, a_{n-1,1}, \ldots, a_{nm}, a_{n-1,m})^T, & \text{for } k=2 \end{cases} \\ Q &= \begin{bmatrix} \tau^2 & & \\ & \ddots & \\ & & \tau^2 \end{bmatrix}, \qquad R = \sigma^2. \end{aligned} \tag{13.17}$$

Here, I_m is the $m \times m$ unit matrix and $\otimes$ denotes the Kronecker product of the matrices A and B, i.e., for the $k \times \ell$ matrix A and the $m \times n$ matrix B, $A \otimes B$ is the $km \times \ell n$ matrix whose (i, j) component is given by $a_{p+1,r+1}b_{q+1,s+1}$ for $i-1 = pm+q$, $j-1 = r\ell+s$. Hence, the time-varying coefficients AR model (13.9) and the component model for the time-varying coefficients are expressible in the form of a state-space model.

For instance, for $m = 2$ and $k = 2$, the state-space model is defined as

$$\begin{bmatrix} a_{n1} \\ a_{n-1,1} \\ a_{n2} \\ a_{n-1,2} \end{bmatrix} = \begin{bmatrix} 2 & -1 & 0 & 0 \\ 1 & 0 & 0 & 0 \\ 0 & 0 & 2 & -1 \\ 0 & 0 & 1 & 0 \end{bmatrix} \begin{bmatrix} a_{n-1,1} \\ a_{n-2,1} \\ a_{n-1,2} \\ a_{n-2,2} \end{bmatrix} + \begin{bmatrix} 1 & 0 \\ 0 & 0 \\ 0 & 1 \\ 0 & 0 \end{bmatrix} \begin{bmatrix} v_{n1} \\ v_{n2} \end{bmatrix}$$

$$y_n = (y_{n-1}, 0, y_{n-2}, 0) \begin{bmatrix} a_{n1} \\ a_{n-1,1} \\ a_{n2} \\ a_{n-1,2} \end{bmatrix} + w_n \tag{13.18}$$

$$\begin{bmatrix} v_{n,1} \\ v_{n,2} \end{bmatrix} \sim N\left(\begin{bmatrix} 0 \\ 0 \end{bmatrix}, \begin{bmatrix} \tau^2 & 0 \\ 0 & \tau^2 \end{bmatrix} \right), \qquad w_n \sim N(0, \sigma^2).$$

The above state-space model contains several unknown parameters. For these parameters, since the log-likelihood function can be computed by the method presented in Chapter 9, the variance σ^2 of the observation noise w_n and the variance τ^2 of the system noise v_n can be estimated by the maximum likelihood method. The AR order m and the order k of the smoothness can be determined by minimizing the information criterion AIC. Given the orders m and k and the estimated variances $\hat{\sigma}^2$ and $\hat{\tau}^2$, the smoothed estimate of the state vector $x_{n|N}$ is obtained by the fixed interval smoothing algorithm. Then, the $((j-1)k+1)^{th}$ element of the estimated state gives the smoothed estimate of the unknown time-varying AR coefficient $\hat{a}_{n,j|N}$.

Storage of size $mk \times mk \times N$ is necessary to obtain the smoothed estimates of these time-varying AR coefficients simultaneously. If either the AR order m or the series length N is large, the necessary memory size may exceed the memory of the computer and may make the computation impossible. Making an assumption that the AR coefficients change only once every r time-steps for some integer $r > 1$ may be the simplest method of mitigating such memory problems of the computing facilities. For example, if $r = 20$, the necessary memory size is obviously reduced by a factor of 20. If the AR coefficients change slowly and gradually, such an approximation has only a slight effect on the estimation of coefficients. To execute the Kalman filter and smoother for $r > 1$, we repeat the filtering step r times at each step of the one-step-ahead prediction.

Example (Time-varying coefficient AR models for seismic data) Table 13.1 summarizes the AIC's of time-varying coefficient AR models fitted to the normalized seismic data shown in Figure 13.1, with various orders obtained by putting $r = 20$.

Since the observation noise variance σ^2 is assumed to be a constant in the TVCAR modeling, if the variance of the time series significantly changes as can be observed in Figure 1.1(f), it is better to fit the model to a transformed time series. For instance, Figure 13.1 shows that the variance of the time series is approximately homoscedastic. For this data, the AIC was minimized at $m = 8$ for $k = 1$ and $m = 4$ for $k = 2$.

Table 13.1 *AIC's of time-varying coefficients AR models fitted to normalized seismic data.*

m	$k=1$	$k=2$	m	$k=1$	$k=2$
1	6492.5	6520.4	6	4831.9	4873.8
2	5527.7	5643.2	7	4821.6	4878.7
3	5070.0	5134.5	8	4805.1	4866.9
4	4820.0	4853.9	9	4813.4	4884.9
5	4846.0	4886.0	10	4827.1	4911.9

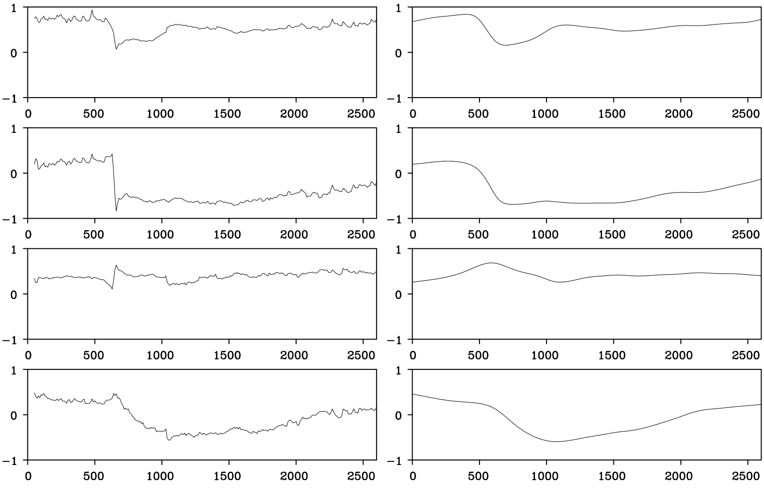

(a) k=1

(b) k=2

Figure 13.2 *Estimated time-varying PARCOR for the normalized seismic data. Only the first four PARCOR's are shown. Left plots: k* = 1*, right plots: k* = 2*. Horizontal axis: time point, vertical axis: value of PARCOR.*

Figure 13.2 shows the time-varying coefficients in the case of the TVCAR models with the AIC best fit orders m for $k=1$ and $k=2$. Note that the figure depicts the time-varying PARCORs b_{ni} for $i=1,2,3,4$, instead of the AR coefficients. The plots on the left-hand side are for the case of $k=1$ and on the right-hand side are for the case of $k=2$. From the figure, we see that the estimated coefficients vary with time corresponding to the arrivals of the P-wave and the S-wave at $n=630$ and $n=1026$, respectively, which were estimated by using the locally stationary AR model. In Figure 13.2, the estimates using $k=2$ are very smooth. However, as is apparent in the figure, the estimates with $k = 2$ do not appropriately correspond to the abrupt changes of the time series that correspond to the arrival of the P-wave and the S-wave. Compared with this, the estimates obtained from the TVCAR model with $k = 1$ are variable. According to the AIC criterion, the TVCAR model with $k = 1$ is considered to be a better model than that with $k = 2$. In Section 13.5, we shall consider a method for obtaining smooth estimates that has the capacity to adapt to abrupt structural changes.

13.3 Estimation of the Time-Varying Spectrum

For a stationary AR model, the power spectrum is given by

$$p(f) = \frac{\sigma^2}{\left|1 - \sum_{j=1}^{m} a_j e^{-2\pi ijf}\right|^2}, \qquad -\frac{1}{2} \le f \le \frac{1}{2}. \tag{13.19}$$

Therefore, in the case that the AR coefficients at time n are given by a_{nj} for the time-varying coefficient AR model (13.9), the instantaneous spectrum at time n can be defined by

$$p_n(f) = \frac{\sigma^2}{\left|1 - \sum_{j=1}^{m} a_{nj} e^{-2\pi ijf}\right|^2}, \qquad -\frac{1}{2} \le f \le \frac{1}{2}. \tag{13.20}$$

Using the time-varying AR coefficients a_{nj} introduced in the previous section, we can estimate the time-varying power spectrum as a function of time, which is called the *time-varying spectrum*.

Example (Time-varying spectrum of a seismic data) Figure 13.3 illustrates the time-varying spectrum obtained from the equation (13.20). The left plot shows the case for $k = 1$, and the right plot shows the case for $k = 2$. In the plots of Figure 13.3, the horizontal and the vertical axes indicate the frequency and the logarithm of the spectra, respectively, and the slanted axis indicates time. From the figures, it can be seen that the power of the spectrum around $f = 0.25$ increases with the arrival of the P-wave. Subsequently, the power around $f = 0.1$ increases with the arrival of the S-wave. After that, the peaks of the spectra gradually shift to the right, and the spectrum eventually converges to that of the original background motions.

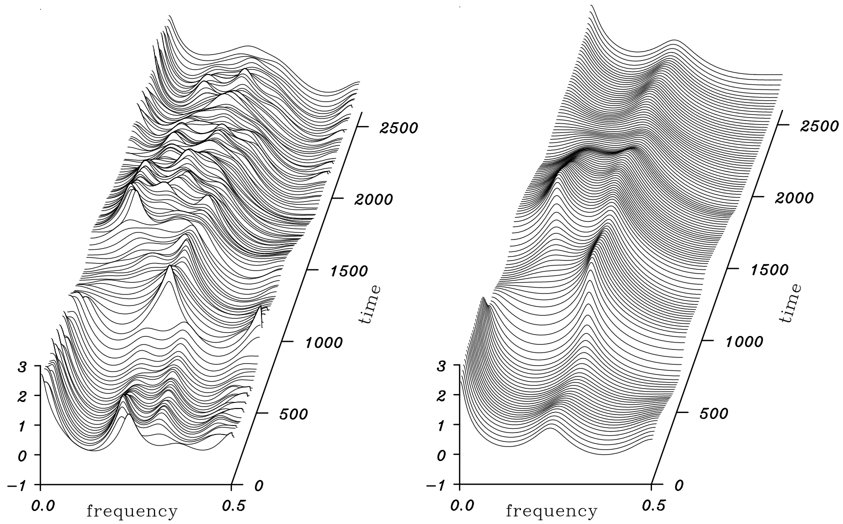

(a) k=1 (b) k=2

Figure 13.3: *Time-varying spectra of a seismic data.*

13.4 The Assumption on System Noise for the Time-Varying Coefficient AR Model

As stated in Section 13.2, the time-varying AR coefficients can be estimated by approximating the time-change of AR coefficients using the trend component models and then the TVCAR model can be expressed in a state-space form. In the state-space model (13.17), the variance-covariance matrix for the system noise is assumed to be a diagonal form given by $Q = \mathrm{diag}\left\{\tau^2, \cdots, \tau^2\right\}$. This seems to be a very strong assumption; however, in this section, it will be shown that it arises naturally, by considering the smoothness of the frequency response function of the AR operator.

Firstly, we consider the Fourier transform of the AR coefficients of the TVCAR model,

$$A(f,n) = 1 - \sum_{j=1}^{m} a_{nj} e^{-2\pi i j f}, \qquad -\frac{1}{2} \le f \le \frac{1}{2}. \tag{13.21}$$

This is the frequency response function of the AR model considered as a whitening filter. Then the time-varying spectrum of (13.20) can be expressed as

$$p_n(f) = \frac{\sigma^2}{|A(f,n)|^2}. \tag{13.22}$$

Since the characteristics of the power spectrum are determined by the frequency response function $A(f,n)$, we can obtain good estimates of the time-varying spectrum by controlling the smoothness of $A(f,n)$. By considering the smoothness of $A(f,n)$ with respect to n, we can obtain the following models for the change over time of the AR coefficients. Considering the k-th difference of the $A(f,n)$ to evaluate the smoothness of the change over time of the AR coefficients, we obtain

$$\Delta^k A(f,n) = \sum_{j=1}^{m} \Delta^k a_{nj} e^{-2\pi ijf}. \tag{13.23}$$

Then, taking the integral of the square of $\Delta^k A(f,n)$, we obtain

$$\int_{-\frac{1}{2}}^{\frac{1}{2}} |\Delta^k A(f,n)|^2 df = \sum_{j=1}^{m} (\Delta^k a_{jn})^2. \tag{13.24}$$

Therefore, it is possible to curtail the change over time of the power spectrum, by reducing the sum of the squares of the k-th differences of the AR coefficients. Since the squares of the k-th differences of the AR coefficients add up with the same weights to each term in equation (13.24), this is equivalent to making the natural assumption that in equation (13.10),

$$\tau_{11}^2 = \cdots = \tau_{mm}^2 = \tau^2, \tag{13.25}$$

and that

$$\Delta_n^k a_{jn} = v_{nj}, \qquad v_{nj} \sim N(0,\tau^2), \qquad j = 1,\cdots,m. \tag{13.26}$$

13.5 Abrupt Changes of Coefficients

For the seismic data shown in Figure 13.1, it can be seen that the behavior of the wave form changes abruptly as a new signal arrives at a certain time. In this case, the estimated time-varying coefficients often become too variable or too smooth to capture the change of the characteristics as seen in Figure 13.2.

In such a case, by applying the locally stationary AR model shown in Chapter 8, we can obtain estimates of the change points. By using the estimates of arrival times of a new signal, we may obtain better estimates of the time-varying AR coefficients. Abrupt changes are assumed to be detected at times $n = n_1, \ldots, n_p$. Corresponding to these points, the noise term v_{nj} of (13.10) takes a large negative or positive value. This indicates that it is necessary to increase the variance τ^2 at the time points $n = n_1, \ldots, n_p$.

Precisely, when τ^2 is increased in this way, the absolute value of the k-th time-difference of a_{nj} also becomes larger. Thus, for $k = 1$, the coefficient a_{nj} shows a stepwise behavior and produces a discontinuous point. On the other hand, for $k = 2$, the slope of a_{nj} changes abruptly and yields a bending point. To yield a jump for a model with $k \geq 2$, it is necessary to add noise to each component of the state vector. Therefore, we can realize the jump either by initializing the state and the variance-covariance matrix $x_{n|n-1}$ and $V_{n|n-1}$ or by adding a large positive value to all diagonal elements of $V_{n|n-1}$ for $n = n_1, \ldots, n_p$. This method is applicable to trend estimation as well as for the time-varying coefficient modeling.

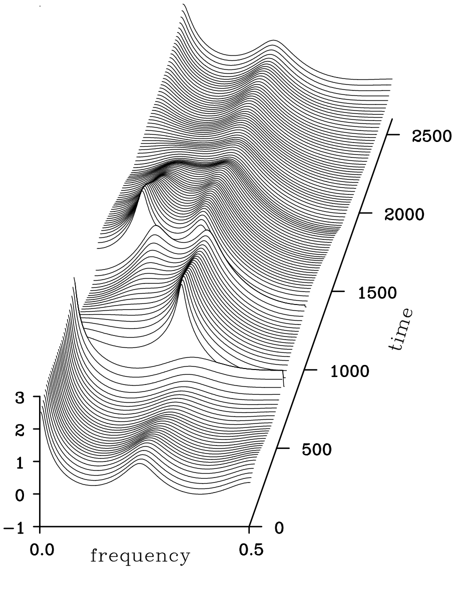

Figure 13.4 *Time-varying spectrum estimated by assuming discontinuities in the parameters.*

Example (Time-varying spectrum with abrupt structural changes) Figure 13.4 shows the time-varying AR coefficients and the time-varying spectrum estimated by the model with $k = 2$ and $m = 4$ and by assuming that sudden jumps occur at $n = 630$ and at $n = 1026$, that correspond to the arrivals of the P-wave and the S-wave, respectively. The estimated coefficients jump twice at those two points but change very smoothly elsewhere.

Moreover, from Figure 13.4, we can observe two characteristics of the series, firstly, that the dominant frequencies gradually shift to the right after the S-wave arrives, and secondly, that the direct current $(f = 0)$ component increases towards its value in the spectrum of the background microtremors.

Problems

1. Give an example of a heteroscedastic (variance changing over time) time series other than earthquake data.
2. Consider a method of estimating a regression model whose coefficients change over time.

Chapter 14

Non-Gaussian State-Space Model

In this chapter, we extend the state-space model to cases where the system noise and/or the observation noise are non-Gaussian. This non-Gaussian model is applicable when there are sudden changes in the parameters caused by structural changes of the system or by outliers in the time series. For the general non-Gaussian models we consider here, it may often be the case that we do not obtain good estimates of the state by using Kalman filtering and the smoothing algorithms. Even in such cases, however, we can derive a similar exact sequential formula to realize filtering and smoothing algorithms using numerical integration.

14.1 Necessity of Non-Gaussian Models

As shown in the previous chapters, various types of time series models can be expressed in terms of the linear-Gaussian state-space model

$$\begin{aligned} x_n &= Fx_{n-1} + Gv_n \\ y_n &= Hx_n + w_n, \end{aligned} \tag{14.1}$$

where y_n is the time series, x_n is the unknown state vector, and v_n and w_n are Gaussian white noises.

The state-space model is a very useful tool for time series modeling, since it is a natural representation of a time series model and provides us with very efficient computational methods, such as Kalman filtering and smoothing algorithms. Although many important time series models are expressible as linear-Gaussian state-space models, there are some other situations where extensions of the model are necessary, such as the case of a nonstationary time series with time-varying stochastic structure that sometimes contains both smooth and abrupt changes. Although a linear-Gaussian state-space model can reasonably express gradual structural changes of nonstationary time series, it is necessary to build a complex model to properly address abrupt changes. To remove the influence of outliers in the data, development of an automatic detection method for the outliers and a robust estimation procedure is necessary (West (1981), Meinhold and Singpurwalla (1989) and Carlin et al. (1992)). In addition, nonlinear systems and discrete processes cannot be adequately modeled by standard linear Gaussian state-space models.

Let us consider possible solutions to these problems. In state-space modeling, changes in the stochastic structure are often reflected by changes in the state. Assuming a heavy-tailed distribution such as the Cauchy distribution for the system noise v_n, both smooth changes that occur with high probability and abrupt changes that occur with low probability can be expressed by a single noise distribution.

Similarly, it is reasonable to deal with outliers in time series by using a heavy-tailed distribution for the observation noise w_n. On the other hand, if the system contains nonlinearity or if the observations are discrete values, the distribution of the state vector inevitably becomes non-Gaussian.

Therefore, as a key to the solution of problems that occur with standard state-space modeling, a treatment of non-Gaussian state distributions is essential. In the following sections, the recursive filter and smoothing algorithms for the estimation of the unknown states of non-Gaussian state-space models and their applications are presented.

14.2 Non-Gaussian State-Space Models and State Estimation

Consider the following state-space model

$$
\begin{aligned}
x_n &= Fx_{n-1} + Gv_n \qquad &\text{(system model)} \qquad &(14.2)\\
y_n &= Hx_n + w_n \qquad &\text{(observation model)} \qquad &(14.3)
\end{aligned}
$$

where the system noise v_n and the observation noise w_n are white noises that follow the density functions $q(v)$ and $r(w)$, respectively. In contrast to the state-space models presented in the previous chapters, these distributions are not necessarily Gaussian.

In this case, the distribution of the state vector x_n generally becomes non-Gaussian. Consequently, the state-space model of equations (14.2) and (14.3) is called a *non-Gaussian state-space model*. Clearly, this non-Gaussian state-space model is an extension of the standard state-space model.

As in Chapter 9, the information from the time series obtained by time j is denoted as $Y_j \equiv \{y_1, \dots, y_j\}$. Similarly, the set of realizations of the state x_n up to time j is denoted as $X_j \equiv \{x_1, \dots, x_j\}$. Further, the initial state vector x_0 is assumed to be distributed according to the probability density function $p(x_0|Y_0)$. Here, the state estimation problem is to obtain the conditional distribution of the state vector x_n, given the information Y_m. There are three versions of the state estimation problem, depending on the relation between n and m. Specifically, for $n > m$, $n = m$ and $n < m$, it is called the prediction problem, the filtering problem and the smoothing problem, respectively.

For the linear-Gaussian state-space model, the Kalman filter provides a recursive algorithm for obtaining the conditional mean and the conditional variance-covariance matrix of the state vector. On the other hand, with the general non-Gaussian state-space model, it is necessary to obtain the conditional densities for state estimation.

However, for the state-space models defined by (14.2) and (14.3), by using the relations $p(x_n|x_{n-1}, Y_{n-1}) = p(x_n|x_{n-1})$ and $p(y_n|x_n, Y_{n-1}) = p(y_n|x_n)$, we can derive recursive formulas for obtaining the one-step-ahead predictive distribution $p(x_n|Y_{n-1})$ and the filtering distribution $p(x_n|Y_n)$ as follows (Kitagawa (1987)). Note that the following algorithm can be applied to general nonlinear state-space model (Kitagawa (1991), Kitagawa and Gersch (1996)).

[One-step-ahead prediction]

$$\begin{aligned} p(x_n|Y_{n-1}) &= \int_{-\infty}^{\infty} p(x_n, x_{n-1}|Y_{n-1}) dx_{n-1} \\ &= \int_{-\infty}^{\infty} p(x_n|x_{n-1}, Y_{n-1}) p(x_{n-1}|Y_{n-1}) dx_{n-1} \\ &= \int_{-\infty}^{\infty} p(x_n|x_{n-1}) p(x_{n-1}|Y_{n-1}) dx_{n-1}, \end{aligned} \tag{14.4}$$

[Filtering]

$$\begin{aligned} p(x_n|Y_n) &= p(x_n|y_n, Y_{n-1}) \\ &= \frac{p(y_n|x_n, Y_{n-1}) p(x_n|Y_{n-1})}{p(y_n|Y_{n-1})} \\ &= \frac{p(y_n|x_n) p(x_n|Y_{n-1})}{p(y_n|Y_{n-1})}, \end{aligned} \tag{14.5}$$

where $p(y_n|Y_{n-1})$ is obtained as $\int p(y_n|x_n)p(x_n|Y_{n-1})dx_n$. The one-step-ahead prediction formula (14.4) is an extension of the one-step-ahead prediction of the Kalman filter. Here, $p(x_n|x_{n-1})$ is the density function of the state x_n when the previous state x_{n-1} is given, which is determined by the system model (14.2). Therefore, if the filter $p(x_{n-1}|Y_{n-1})$ of x_{n-1} is given, the one-step-ahead predictor $p(x_n|Y_{n-1})$ can be evaluated. On the other hand, the filter formula (14.5) is an extension of the filtering step of the Kalman filter. $p(y_n|x_n)$ is the conditional distribution of the observation y_n, when the state x_n is given. It is determined by the observation model of (14.3). Therefore, if the predictive distribution $p(x_n|Y_{n-1})$ of x_n is given, then the filter density $p(x_n|Y_n)$ is computable.

Next, we consider the smoothing problem. Using the equation $p(x_n|x_{n+1},Y_N) = p(x_n|x_{n+1},Y_n)$ that holds for the state-space models of (14.2) and (14.3), we obtain

$$\begin{aligned} p(x_n,x_{n+1}|Y_N) &= p(x_{n+1}|Y_N)p(x_n|x_{n+1},Y_N) \\ &= p(x_{n+1}|Y_N)p(x_n|x_{n+1},Y_n) \\ &= p(x_{n+1}|Y_N)\frac{p(x_n|Y_n)p(x_{n+1}|x_n,Y_n)}{p(x_{n+1}|Y_n)} \\ &= p(x_{n+1}|Y_N)\frac{p(x_n|Y_n)p(x_{n+1}|x_n)}{p(x_{n+1}|Y_n)}. \qquad (14.6) \end{aligned}$$

Integration of both sides of (14.6) yields the following sequential formula for the smoothing problem:

[Smoothing formula]

$$\begin{aligned} p(x_n|Y_N) &= \int_{-\infty}^{\infty} p(x_n,x_{n+1}|Y_N)dx_{n+1} \\ &= p(x_n|Y_n)\int_{-\infty}^{\infty} \frac{p(x_{n+1}|Y_N)p(x_{n+1}|x_n)}{p(x_{n+1}|Y_n)}dx_{n+1}. \qquad (14.7) \end{aligned}$$

In the right-hand side of the formula (14.7), $p(x_{n+1}|x_n)$ is determined by the system model (14.2). On the other hand, $p(x_n|Y_n)$ and $p(x_{n+1}|Y_n)$ are obtained by equations (14.4) and (14.5), respectively. Thus, the smoothing formula (14.7) indicates that if $p(x_{n+1}|Y_N)$ is given, we can compute $p(x_n|Y_N)$.

Since $p(x_N|Y_N)$ can be obtained by filtering (14.5), by repeating the smoothing formula (14.7) for $n = N-1,\ldots,1$ in a similar way as for the fixed interval smoothing presented in Chapter 9, we can obtain the smoothing distributions $p(x_{N-1}|Y_N),\ldots,p(x_1|Y_N)$, successively.

14.3 Numerical Computation of the State Estimation Formula

As shown in the previous section, we can derive recursive estimation formulas for the non-Gaussian state-space model that are natural extensions of the Kalman filter. Adopting this comprehensive algorithm, we can extensively treat various types of time series models. However, in the practical application of the algorithm, difficulties often arise in calculating the formulas of the filter and smoother.

For a linear Gaussian state-space model, all the conditional distributions $p(x_n|Y_{n-1})$, $p(x_n|Y_n)$ and $p(x_n|Y_N)$ become normal distributions. Therefore, in that case, only the mean vectors and the variance-covariance matrices need to be evaluated, and correspondingly (14.4), (14.5) and (14.7) become equivalent to the ordinary Kalman filter and the smoothing algorithms. However, since the conditional distribution $p(x_n|Y_j)$ of the state generally becomes a non-Gaussian distribution, it cannot be specified using only the mean vector and the variance-covariance matrix. Various algorithms have been presented, for instance, the extended Kalman filter (Anderson and Moore (1979)) and the second order filter, to approximate the non-Gaussian distribution by a single Gaussian distribution with properly determined mean vector and variance-covariance matrix. In general, however, they do not perform well.

This section deals with the method of realizing the non-Gaussian filter and the non-Gaussian smoothing algorithm by numerically approximating the non-Gaussian distributions (Kitagawa (1987)). In this approach, a non-Gaussian state density function is approximated numerically using functions such as a step function, a piecewise linear function or a spline. Then, the formulas (14.4)–(14.7) can be evaluated by numerical computation. Since this approach requires a huge amount of computation, it used to be considered an impractical method. Nowadays, with the development of high-speed computers, those numerical methods have become practical, at least for the low-dimensional systems. In this section, we approximate the density functions that appeared in (14.4), (14.5) and (14.7) by simple step functions (Kitagawa and Gersch (1996)).

To be specific, the density function $f(t)$ to be approximated is defined on a line: $-\infty < t < \infty$. To approximate this density function by a step function, the domain of the density function is firstly restricted to a finite interval $[t_0, t_d]$, which is then divided into d sub-intervals $t_0 < t_1 < \cdots < t_d$. Here, t_0 and t_d are assumed to be sufficiently small and large numbers, respectively, and for simplicity, the width of the sub-intervals is assumed to be identical. Then the i-th point is given by $t_i = t_0 + i\Delta t$ with $\Delta t = (t_d - t_0)/d$. In the actual programming of the ends of the sub-intervals, however, t_0 and t_i change, adapting to changes in the location of the density function. For simplicity, however, ends of the sub-intervals are assumed to be fixed in the following.

In a step-function approximation, the function $f(t)$ is approximated

Table 14.1: *Approximation of density functions.*

density function	approximation	denotation
$p(x_n\|Y_{n-1})$	$\{d;t_0,\cdots,t_d;p_1,\cdots,p_d\}$	$\tilde{p}(t)$
$p(x_n\|Y_n)$	$\{d;t_0,\cdots,t_d;f_1,\cdots,f_d\}$	$\tilde{f}(t)$
$p(x_n\|Y_N)$	$\{d;t_0,\cdots,t_d;s_1,\cdots,s_d\}$	$\tilde{s}(t)$
$q(v)$	$\{2d+1;t_{-d},\cdots,t_d;q_{-d},\cdots,q_d\}$	$\tilde{q}(v)$

by f_i on the sub-interval $[t_{i-1},t_i]$. If the function $f(t)$ is actually a step-function, it is given by $f_i = f(t_i)$. But in general, it may be defined by

$$f_i = \Delta t \int_{t_{i-1}}^{t_i} f(t)dt. \tag{14.8}$$

Using those values, the step-function approximation of the function $f(t)$ is specified by $\{d;t_0,\ldots,t_d;f_1,\ldots,f_d\}$. In the following, the approximated function is denoted by $\tilde{f}(t)$. For the numerical implementation of the non-Gaussian filter and the smoothing formula, it is necessary to approximate the density functions $p(x_n|Y_{n-1})$, $p(x_n|Y_n)$, $p(x_n|Y_N)$ and the system noise density $q(v)$ as shown in Table 14.1. Here, it is clear that we should use the observation noise density $r(v)$ directly, without discretizing it. Alternative approaches for numerical integrations are Gauss-Hermite polynomial integration (Schnatter (1992)), a random replacement of knots spline function approximation (Tanizaki (1993)) and Monte Carlo integration (Carlin et al. (1992), Frühwirth-Schnatter (1994), Carter and Kohn (1993)).

In the following, we show a procedure for numerical evaluation of the simplest one-dimensional trend model:

$$\begin{aligned} x_n &= x_{n-1} + v_n, \\ y_n &= x_n + w_n. \end{aligned} \tag{14.9}$$

[One-step-ahead prediction]

For $i = 1,\ldots,d$, compute

$$\begin{aligned} p_i = \tilde{p}(t_i) &= \int_{t_0}^{t_d} \tilde{q}(t_i - s)\tilde{f}(s)ds \\ &= \sum_{j=1}^{d} \int_{t_{j-1}}^{t_j} \tilde{q}(t_i - s)\tilde{f}(s)ds \end{aligned}$$

$$= \quad \Delta t \sum_{j=1}^{d} q_{i-j} f_j. \tag{14.10}$$

[Filtering]

For $i = 1, \ldots, d$, compute

$$f_i = \tilde{f}(t_i) = \frac{r(y_n - t_i)\tilde{p}(t_i)}{C} = \frac{r(y_n - t_i)p_i}{C}, \tag{14.11}$$

where the normalizing constant C is obtained by

$$\begin{aligned} C = \int_{t_0}^{t_d} r(y_n - t)\tilde{p}(t)dt \quad &= \quad \sum_{j=1}^{d} \int_{t_{j-1}}^{t_j} r(y_n - t)\tilde{p}(t)dt \\ &= \quad \Delta t \sum_{j=1}^{d} r(y_n - t_j)p_j. \end{aligned} \tag{14.12}$$

[Smoothing]

For $i = 1, \ldots, d$, compute

$$\begin{aligned} s_i \,=\, \tilde{s}(t_i) \quad &= \quad \tilde{f}(t_i) \int_{t_0}^{t_d} \frac{\tilde{q}(t_i - u)\tilde{s}(u)}{\tilde{p}(u)} du \\ &= \quad \tilde{f}(t_i) \sum_{j=1}^{d} \int_{t_{j-1}}^{t_j} \frac{\tilde{q}(t_i - u)\tilde{s}(u)}{\tilde{p}(u)} du \\ &= \quad \Delta t \cdot f(t_i) \sum_{j=1}^{d} \frac{q_{i-j} s_j}{p_j}. \end{aligned} \tag{14.13}$$

It should be noted that, in practical computation, even after the prediction step (14.10) and the smoothing (14.13), the density functions should be normalized so that the value of the integral over the whole interval becomes 1. This can be achieved, for example, by modifying f_i to $f_i/I(f)$, where $I(f)$ is defined by

$$I(f) = \int_{t_0}^{t_d} f(t)dt = \Delta t \left(f_1 + \cdots + f_d\right). \tag{14.14}$$

14.4 Non-Gaussian Trend Model

In the trend model considered in Chapter 11, in cases where the distribution of the system noise v_n or the observation noise w_n is non-Gaussian,

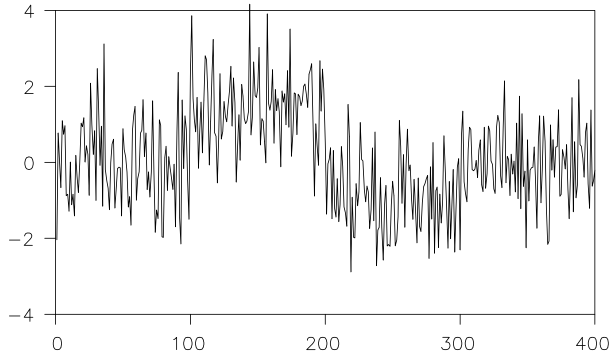

Figure 14.1: *Data generated by the model of (14.15).*

we obtain a *non-Gaussian trend model.* In this section, numerical examples are given in order to explain the features of the non-Gaussian model.

Example (Non-Gaussian trend estimation) Figure 14.1 shows the data generated by the following models:

$$y_n \sim N(\mu_n, 1), \qquad \mu_n = \begin{cases} 0, & 1 \le n \le 100 \\ 1, & 101 \le n \le 200 \\ -1, & 201 \le n \le 300 \\ 0, & 301 \le n \le 400 \end{cases}. \tag{14.15}$$

In the plot, it can be seen that the mean value function, μ_n, abruptly changes three times. For estimation of a changing mean value function with the structural changes shown in Figure 14.1, we consider the following first order trend model:

$$\begin{aligned} t_n &= t_{n-1} + v_n \\ y_n &= t_n + w_n, \end{aligned} \tag{14.16}$$

where the observation noise w_n is assumed to be Gaussian and the system noise v_n follows the type IV Pearson family of distributions:

$$q(v_n) = \frac{c}{(\tau^2 + v_n^2)^b}, \qquad \frac{1}{2} < b < \infty. \tag{14.17}$$

Here, b and τ^2 denote the shape parameter and the dispersion parameter,

Table 14.2 *Non-Gaussian model with Pearson family of distributions with various values of shape parameter b.*

b	τ^2	σ^2	log-likelihood	AIC
0.60	0.211×10^{-9}	1.042	−597.19	1198.38
0.75	0.299×10^{-7}	1.043	−597.39	1198.78
1.00	0.353×10^{-4}	1.045	−597.99	1198.98
1.50	0.303×10^{-2}	1.045	−599.13	1202.26
3.00	0.406×10^{-1}	1.046	−600.40	1204.80
∞	0.140×10^{-1}	1.048	−600.69	1205.38

respectively, and c is a normalizing constant, which makes the value of the integral of $q(v)$ over the whole interval equal to 1 and is given by $c = \tau^{2b-1}\Gamma(b)/\Gamma(\frac{1}{2})\Gamma(b-\frac{1}{2})$ (Johnson and Kotz (1970)). The Pearson family of distributions can express various symmetric probability density functions with heavier-tailed distributions than the normal distributions. Here, the Pearson family of distributions yields the Cauchy distribution for $b = 1$, the t distribution with k degrees of freedom for $b = (k+1)/2$ and the normal distribution as $b \to \infty$.

Table 14.2 summarizes the values of the maximum likelihoods and the AICs of the Pearson family of distributions with $b = 3/k$, $(k = 0,\dots,5)$. Here, it is shown that the AIC is minimized at $b = 0.60$, and the AIC of the normal distribution model $(b = \infty)$ is the maximum.

The plot on the left-hand side of Figure 14.2 depicts the change over time of the smoothed distribution of the trend $p(t_n|Y_N)$, obtained from the Gaussian model (for $b = \infty$), and the corresponding plot obtained from the non-Gaussian model with $b = 1.0$ is shown on the right-hand side. The left plot (a) shows that the distribution of the trend estimated by the Gaussian model gradually shifts left or right with the progress of time n. On the other hand, for the case of the non-Gaussian model shown in the right plot (b), the estimated density is seen to be very stable with abrupt changes at only three time points.

In Figure 14.3, the plot on the left-hand side shows the mean and the $\pm 1,2,3$ standard deviation intervals of the estimated distribution at each time point for the Gaussian model. On the other hand, the plot on the right-hand side shows the $0.13, 2.27, 15.87, 50.0, 84.13, 97.73$ and 99.87 percentile points of the estimated trend distribution that correspond to the mean and $\pm 1,2,3$ intervals of the Gaussian distribution. Comparing plot (a) with (b) of Figure 14.3, it can be seen that the non-Gaussian model yields a smoother estimate than the Gaussian model and clearly detects jumps in the trend.

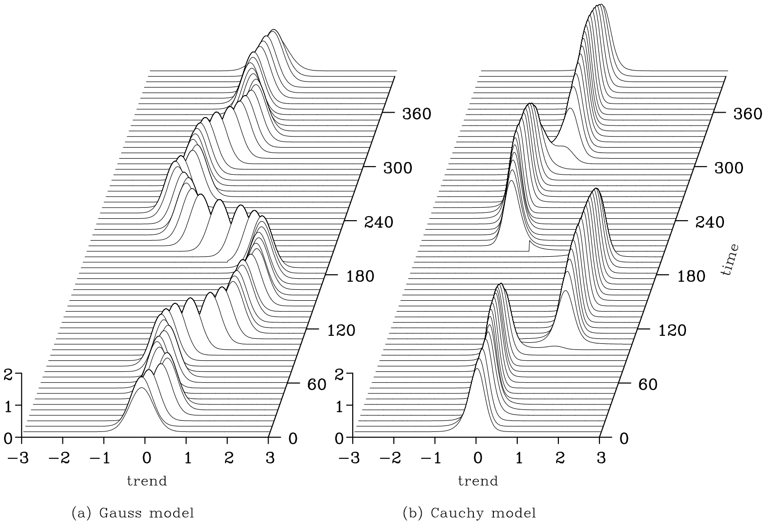

(a) Gauss model

(b) Cauchy model

Figure 14.2 *Changes over time of the smoothed distribution of the trend. Left: Gaussian model, right: non-Gaussian model.*

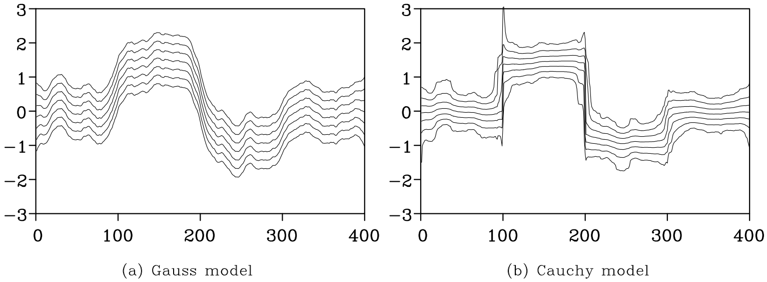

(a) Gauss model

(b) Cauchy model

Figure 14.3 *Estimation of trend by Gaussian (left plot) and non-Gaussian (right plot) models.*

14.5 Non-Symmetric Distribution–A Time-Varying Variance Model

The distribution of data observed from the real world sometimes reveals non-symmetry. This might be due to certain characteristics or nonlinearity of the data generating mechanism. If we apply the least squares method to such a data set, we may obtain a biased estimate of the trend. Thus, if the distribution of the observations is known, we may obtain a better estimates by using a non-Gaussian distribution $r(w)$ for filtering and smoothing. In this section, for the estimation of the time-varying variance, we reconsider the model treated in Section 13.1;

$$\begin{aligned} t_m &= t_{m-1} + v_m, \\ y_m &= t_m + w_m. \end{aligned} \tag{14.18}$$

Example In Chapter 13, the double exponential distribution for the observation noise w_n is approximated by a Gaussian distribution $N(-\zeta, \pi^2/6)$. Here, we shall compare the distribution obtained by the Gaussian approximation with the exact distribution obtained by numerical computation. Figure 14.4 shows the transformed seismic data that are derived from the original data of Figure 1.1(f). The plotted data set was obtained by sampling every two points after filtering by $\tilde{y}_n = y_n - 0.5y_{n-1}$ and transformed by the method discussed in Section 13.1. In this chapter, since it is assumed that the time series is a white noise, this transformation was applied in order to weaken the strong autocorrelation that can be observed in the first part of the data.

Fitting the Gaussian model with $\sigma^2 = \pi^2/6$ to the data, we obtain the maximum likelihood estimate $\hat{\tau}^2 = 0.04909$ and AIC $= 2165.10$. Figure 14.5 shows the wiggly trend estimated by this model. This is due to the outliers in Figure 14.4, creating a large deviation that strongly affects the estimated trend.

On the other hand, the maximum likelihood estimates of the non-Gaussian model with a Cauchy distribution for the system noise and a double exponential distribution for the observation noise

$$\begin{aligned} q(x) &= \frac{1}{\pi}\frac{\tau}{\tau^2 + x^2} \\ r(x) &= \exp\{x - e^x\} \end{aligned} \tag{14.19}$$

are $\hat{\tau}^2 = 0.000260$ and AIC $= 2056.97$, respectively.

From the big differences between the AIC values of the two models, it is evident that the non-Gaussian model is much better than the

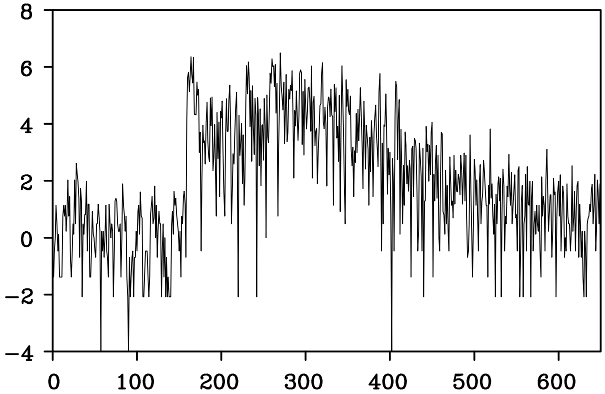

Figure 14.4: *Transformed seismic data.*

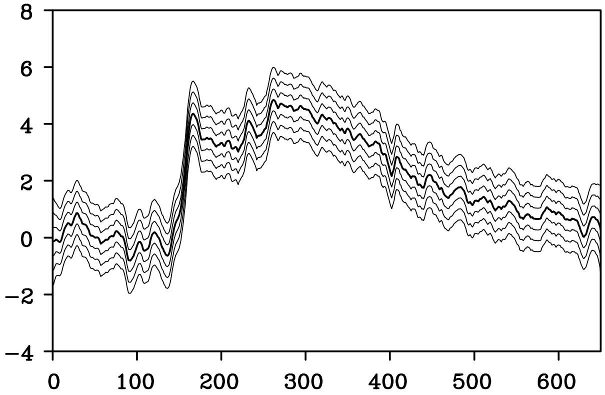

Figure 14.5: *Estimated trend (log-variance) by Gaussian model.*

Gaussian model. Actually, as shown in Figure 14.6, the trend obtained with the non-Gaussian model is smoother by far than the one obtained by the Gaussian model and clearly detected sudden increases in the variance due to the arrivals of the P-wave and the S-wave. Moreover, the plot of this model depicts that the observations with a large deviation downward influence only the curve of 0.13 percent points but not that of the 50 percent points. In summary, by non-Gaussian smoothing with an appropriate model, we can obtain an estimate of the trend which is

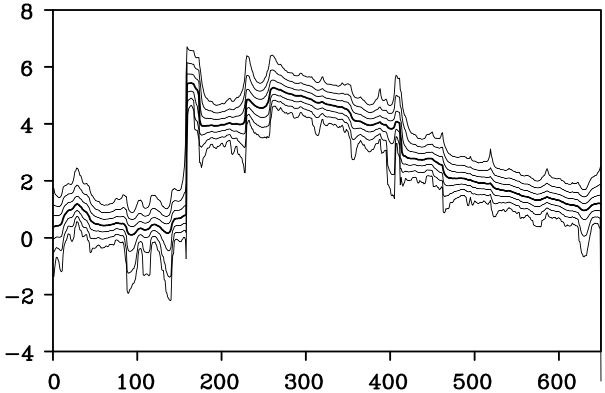

Figure 14.6: *Estimated trend (log-variance) by a non-Gaussian model.*

able to automatically detect a jump of the parameter but is not unduly influenced by a non-symmetric distribution. This estimation method of a time-varying variance can be used for the estimation of the stochastic volatility of a financial time series.

Example (Stock price index data) Figure 14.7 (a) shows the series obtained by applying the method shown in Section 13.1 to the difference of the logarithm of Nikkei 225 stock price index data. On the other hand, Figure 14.7(b) shows the posterior distribution of the estimate of log σ_n^2 obtained as the trend of this series estimated by the non-Gaussian model of (14.18). In addition, an estimate of the volatility is obtained from the exponent of $1/2$ of the central curve (the 50 percent curve) in plot (b), i.e., by

$$\exp\left(\log \hat{\sigma}_n^2/2\right) = \sqrt{\hat{\sigma}_n^2} = \hat{\sigma}_n.$$

This method of estimating time-varying variance can be immediately applied to the smoothing of the periodogram. Since the periodogram follows the χ^2 distribution with 2 degrees of freedom, the series obtained by taking the logarithm of the periodogram thus follows distributions, which are approximately equivalent to (14.19). Therefore, the method treated in this chapter can be applied to smoothing of the logarithm of the periodogram as well. Moreover, using a non-Gaussian model, it is

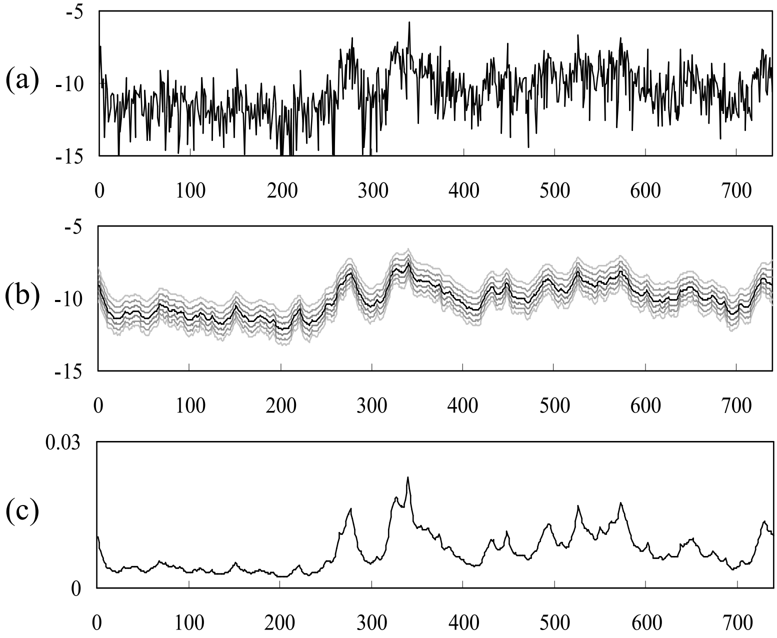

Figure 14.7 *(a) Transformed Nikkei 225 stock price index data, (b) posterior distribution of* $\log\sigma_n^2$*, (c) estimates of volatility.*

possible to estimate the time-varying variance from the transformed data

$$z_n = \log y_n^2. \tag{14.20}$$

In this case, for the density function of the observation noise, we use the density function obtained as the logarithm of the χ^2 distribution with 1 degree of freedom, i.e.,

$$r(w) = \frac{1}{\sqrt{2\pi}} \exp\left\{ \frac{w - e^w}{2} \right\}. \tag{14.21}$$

Here the time-varying variance can be estimated without making the assumption that $\log\sigma_{2m-1}^2 = \log\sigma_{2m}^2$. Figure 14.8 shows the estimate of $\log\sigma_n^2$ obtained by applying this method to the logarithm of the differences of the Nikkei 225 stock price index data.

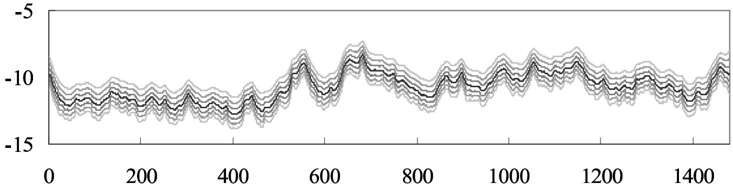

Figure 14.8 *The smoothed distribution obtained by the model of (14.21) for the Nikkei 225 stock price index data.*

14.6 Applications of the Non-Gaussian State-Space Model

In this section, several applications of non-Gaussian state-space model are presented. Certain typical cases for the non-Gaussian state-space model are dealt with in detail in this section.

14.6.1 Processing of the outliers by a mixture of Gaussian distributions

Here, we consider outliers to follow a distribution different from the usual noise distribution of observations. To process the outliers using a time series, assuming that the outliers appear with probability $\alpha \ll 1$, we may use a mixture of Gaussian distributions for the observation noise w_n,

$$r(w) = (1-\alpha)\varphi(w;\mu,\sigma^2) + \alpha\varphi(w;\xi,\delta^2). \tag{14.22}$$

The Gaussian-sum filter and smoother for this Gaussian-mixture noise model is given in Alspach and Sorenson (1972) and Kitagawa (1989, 1994). Here $\varphi(x;\mu,\sigma^2)$ denotes the density function of the normal distribution with mean μ and variance σ^2. The first and second terms on the right-hand side express the distribution of the normal observations, and the distribution of the outliers, respectively. In particular, by putting $\xi = \mu = 0$ and $\delta^2 \gg \sigma^2$, the observation noise of the outliers is assumed to have zero mean but possess a large variance. The Cauchy distribution may be considered as an approximation of the above-mentioned mixture distribution. Therefore, the outliers can be treated for example using the Cauchy distribution or the Pearson family of distributions, which can be used to generate a density function of the observation noise. On the other hand, if outliers always appear on the positive side of the time series, as shown in Figure 1.1(h) of the groundwater data, we can estimate the trend ignoring the outliers by setting $\xi \gg \mu$ and $\delta^2 = \sigma^2$.

14.6.2 A nonstationary discrete process

Non-Gaussian models can also be applied to the smoothing of discrete processes, for instance, nonstationary binomial distributions and Poisson distributions. Consider the time series $m_1, \ldots, m_N$ that takes integer values. Assume that the probability of taking value m_n at time n is given by the Poisson distribution

$$P(m_n|p_n) = \frac{e^{-p_n} {p_n}^{m_n}}{m_n!}. \tag{14.23}$$

Here, p_n denotes the expected frequency of the occurrences of a certain event at a unit time. The mean of the Poisson distribution is not a constant and gradually changes with time. Such a model is called a *nonstationary Poisson process model*. As a model for the change over time of the Poisson mean, p_n, we may use the trend component model $p_n = p_{n-1} + v_n$. Here, since p_n is required to be positive, $0 < p_n < \infty$, we define a new variable $\theta_n = \log p_n$ and assume a trend component model. Therefore, the model for smoothing the nonstationary Poisson process becomes

$$\begin{aligned} \theta_n &= \theta_{n-1} + v_n, & (14.24) \\ P(m_n|\theta_n) &= \frac{e^{-p_n} {p_n}^{m_n}}{m_n!}, & (14.25) \end{aligned}$$

where p_n is defined by $p_n = e^{\theta_n}$. The first and second models correspond to the system model and the observation model and yield conditional distributions of θ_n and m_n, respectively. Therefore, the non-Gaussian filtering method presented in this chapter can be applied to the discrete process, and we can estimate the time-varying Poisson mean value from the data.

Similarly, the non-Gaussian state-space model can be applied to the smoothing of an inhomogeneous binary process. Assume that the probability of a certain event occurring m_n times in the ℓ_n observations at time n is given by the binomial distribution

$$P(m_n|p_n, \ell_n) = \begin{pmatrix} \ell_n \\ m_n \end{pmatrix} {p_n}^{m_n} (1 - p_n)^{\ell_n - m_n}. \tag{14.26}$$

Here, p_n is called the binomial probability and expresses the expected number of occurrences of a certain event. In this case, if p_n varies with time, this model is called the *inhomogeneous binary process model.* p_n can be estimated by the following model:

$$\begin{aligned} \theta_n &= \theta_{n-1} + v_n, \\ P(m_n|\theta_n, \ell_n) &= \begin{pmatrix} \ell_n \\ m_n \end{pmatrix} p_n^{m_n}(1-p_n)^{\ell_n - m_n}, \end{aligned} \tag{14.27}$$

where $p_n = e^{\theta_n}/(1+e^{\theta_n})$.

14.6.3 A direct method of estimating the time-varying variance

In Section 14.5, the time-varying variance was estimated by smoothing the logarithm of the square of the original time series. However, it is also possible to estimate the time-varying variance directly using the following model:

$$\begin{aligned} t_n &= t_{n-1} + v_n, \\ y_n &\sim N(0, e^{t_n}). \end{aligned} \tag{14.28}$$

Since the variance always takes a positive value in this model, the state t_n can be taken as the logarithm of the variance. Here, $\exp(t_n)$ becomes an estimate of the variance at time n. From the estimation of the time-varying variance of the Nikkei 225 stock price index data, we can obtain equivalent results to Figure 4.8. Here the obtained log-likelihood values for each model are different. This is because the transformed data are quite different in each case. As shown in Chapter 4.6, we can confirm that these two models have exactly the same AIC values by compensating for the effect of data transformation by evaluating the Jacobian of the transformation.

Problems

1. Discuss the advantages of using the Cauchy distribution or the two-sided exponential (Laplace) distribution in time series modeling.
2. Verify that when y_n follows a normal distribution with mean 0 and variance 1, the distribution of $v_n = \log y_n^2$ is given by (14.21).
3. Consider a model for which the trend follows a Gaussian distribution with probability α and is constant with probability $1-\alpha$.

Chapter 15

The Sequential Monte Carlo Filter

In this chapter, we consider a sequential Monte Carlo filter and smoother, which is also called a particle filter or bootstrap filter. Distinct in character from other numerical approximation methods, the sequential Monte Carlo filter has been developed as a practical method for filtering and smoothing high-dimensional nonlinear non-Gaussian state-space models. In the sequential Monte Carlo filter, an arbitrary non-Gaussian distribution is approximated by many particles that can be considered to be independent realizations of the distribution. Then, a recursive filtering and smoothing are realized by two simple manipulations of particles, namely, the time-evolution of each particle and re-sampling, in other words, sampling with replacement (Gordon et al. (1993), Kitagawa (1996), Doucet et al. (2001)).

15.1 The Nonlinear Non-Gaussian State-Space Model and Approximations of Distributions

In this section, we consider the following nonlinear non-Gaussian state-space model

$$x_n = F(x_{n-1}, v_n) \tag{15.1}$$

$$y_n = H(x_n, w_n), \tag{15.2}$$

where y_n is a time series, x_n is the k-dimensional state vector, and the models of (15.1) and (15.2) are called the system model and the observation model, respectively (Kitagawa and Gersch (1996)).

These models are generalizations of the state-space models that have been treated in the previous chapters. The system noise v_n and the observation noise w_n are assumed to be ℓ dimensional and one-dimensional white noises that follow the density functions $q(v)$ and $r(w)$, respectively. The initial state vector x_0 is assumed to follow the density function $p_0(x)$. In general, the functions F and H are assumed to be nonlinear functions. For the function $y = H(x,w)$, assuming that x and y are given, w is

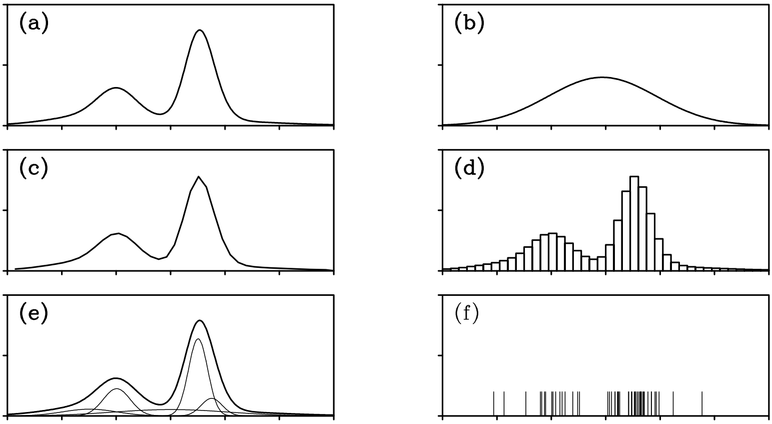

Figure 15.1 *Various approximation methods for a non-Gaussian distribution: (a) assumed true distribution, (b) normal approximation, (c) piecewise linear function approximation, (d) step function approximation, (e) Gaussian mixture approximation and (f) particle realizations.*

uniquely determined as $w = G(y,x)$, where G is a differentiable function with respect to y (Kitagawa (1996)).

As examples of nonlinear functions $H(x,w)$ that satisfy the above-mentioned requirements, we may consider $H(x,w) = H_1(x) + w$ and $H(x,w) = e^x w$, and in these cases $G(y,x)$ are given by $G(y,x) = y - H_1(x)$ and $G(y,x) = e^{-x}y$, respectively. For simplicity, y_n and w_n are assumed to be one-dimensional models here. However, we can consider the natural extensions of these models to the multi-dimensional versions.

In this chapter, we consider the problem of state estimation for the nonlinear non-Gaussian state-space model. As stated in the previous chapter, the set of observations obtained by time t is denoted as $Y_t \equiv \{y_1,\dots,y_t\}$, and we consider a method of obtaining the distributions based on particle approximations of the predictive distribution $p(x_n|Y_{n-1})$, the filter distribution $p(x_n|Y_n)$ and the smoothing distribution $p(x_n|Y_N)$.

Figure 15.1 shows the effects of different methods of approximating a non-Gaussian distribution. Plot (a) depicts the assumed true distribution that has two peaks. Plot (b) shows the approximation by a single Gaussian distribution, which corresponds to the model approximation by linear-Gaussian state-space models and the extended Kalman filter.

From plot (b), it is obvious that if the true distribution has two or more peaks or the distribution is highly skewed, a good approximation cannot be obtained. Plots (c) and (d) show the approximation by a piecewise linear function with 40 nodes, and by a step function with 40 nodes, respectively. In the previous chapter, these approximations were applied to the non-Gaussian filter and the smoother. In practical use, however, we usually set the number of nodes to several hundred or more. Consequently, very precise approximations to any types of distributions can be obtained by these methods.

Plot (e) shows the Gaussian mixture approximations with five Gaussian components. The faint curves depict the contributions of Gaussian components and the bold curve depicts the Gaussian-mixture approximation obtained by summing up these Gaussian components. The Gaussian-sum filter and the smoother can be easily obtained by this approximation.

In this chapter, distinct from the approximations discussed above, the true distribution can be represented by using many particles in the sequential Monte Carlo method. Each particle is considered as a realization generated from the true distribution. Plot (f) shows 100 realizations generated from the assumed true distribution shown in plot (a). In plot (f), many short vertical lines above the horizontal axis are seen, which express the location of the particles. Comparing plot (a) with plot (f), the peaks of the density function in plot (a) correspond to the concentrated particles in plot (f).

Figure 15.2 compares the empirical distribution functions obtained from the realizations and the true cumulative distribution functions. Plots (a)–(c) depict the cases of $m = 10$, $m = 100$ and $m = 1000$, respectively. The true distribution function and the empirical distribution function are illustrated with the bold curve and the fainter curve, respectively. For $m = 10$, the appearance of the empirical distribution function differs from the true distribution function; however, as the number of particles increases to $m = 100$ and $m = 1000$, we can obtain closer approximations.

With the sequential Monte Carlo filter, the predictive distribution, the filter distribution and the smoothing distribution are approximated by m particles as shown in Table 15.1. The number of particles m is usually set between 1000 and 100,000, the actual number chosen depending on the complexity of the distribution and the required accuracy. This process is equivalent to approximating a true cumulative distribution function by an empirical distribution function defined using m particles.

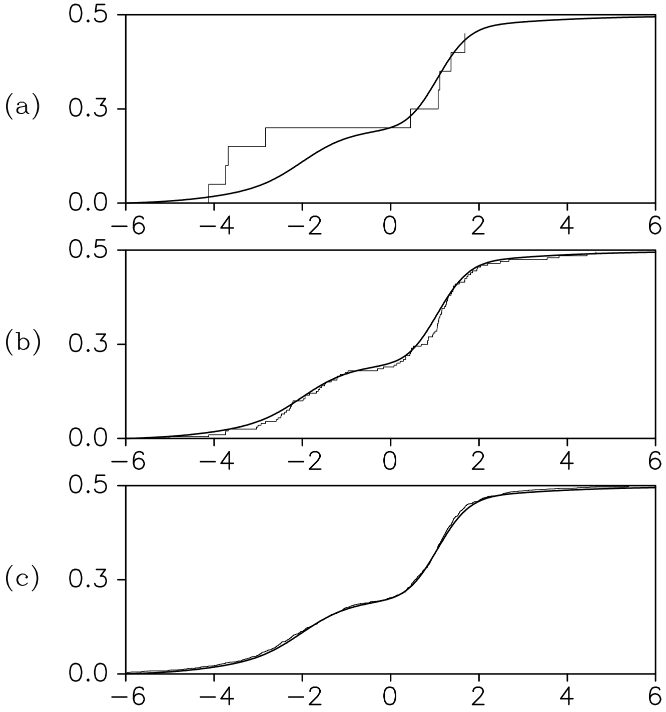

Figure 15.2 *Comparison between the empirical distribution functions and the true cumulative distribution functions for various numbers of particles: (a)* $m = 10$, *(b)* $m = 100$ *and (c)* $m = 1000$.

Table 15.1 *Approximations of distributions used in the sequential Monte Carlo filter and the smoother.*

Distributions	Density functions	Approximations by particles
Predictive distribution	$p(x_n \vert Y_{n-1})$	$\{p_n^{(1)},\dots,p_n^{(m)}\}$
Filter distribution	$p(x_n \vert Y_n)$	$\{f_n^{(1)},\dots,f_n^{(m)}\}$
Smoothing distribution	$p(x_n \vert Y_N)$	$\{s_{n\vert N}^{(1)},\dots,s_{n\vert N}^{(m)}\}$
Distribution of system noise	$p(v_n)$	$\{v_n^{(1)},\dots,v_n^{(m)}\}$

15.2 Monte Carlo Filter

The Monte Carlo filter algorithm that is presented in this section is particularly useful to recursively generate the particles by approximating the one-step-ahead predictive distribution and the filter distribution.

In Monte Carlo filtering, the particles $\{p_n^{(1)},\dots,p_n^{(m)}\}$ that follow the predictive distribution, are generated from the particles $\{f_n^{(1)},\dots,f_{n-1}^{(m)}\}$ used for the approximation of the filter distribution of the previous state. Then, the realizations $\{f_n^{(1)},\dots,f_n^{(m)}\}$ of the filter can be generated by re-sampling the realizations $\{p_n^{(1)},\dots,p_n^{(m)}\}$ of the predictive distribution (Gordon et al. (1993), Kitagawa (1996)).

15.2.1 One-step-ahead prediction

For the one-step-ahead predictive step, we assume that m particles $\{f_{n-1}^{(1)},\dots,f_{n-1}^{(m)}\}$ can be considered as the realizations generated from the filter distribution $p(x_{n-1}|Y_{n-1})$ of the previous step x_{n-1}, and the particles $v_n^{(1)},\dots,v_n^{(m)}$ can be considered as independent realizations of the system noise v_n.

That is, for $j=1,\dots,m$, it is the case that

$$f_{n-1}^{(j)} \sim p(x_{n-1}|Y_{n-1}), \quad v_n^{(j)} \sim q(v). \tag{15.3}$$

Then, the particle $p_n^{(j)}$ is defined by

$$p_n^{(j)} = F(f_{n-1}^{(j)}, v_n^{(j)}), \tag{15.4}$$

where $p_n^{(j)}$ is assumed to be a particle generated from the one-step-ahead predictive distribution of the state x_n. (See Appendix D.)

15.2.2 Filtering

In the next step of filtering, we compute $\alpha_n^{(j)}$, the Bayes factor (or likelihood) of the particle $p_n^{(j)}$ with respect to the observation y_n. That is, for $j=1,\dots,m$,

$$\alpha_n^{(j)} = p(y_n|p_n^{(j)}) = r(G(y_n, p_n^{(j)}))\left|\frac{\partial G}{\partial y_n}\right|, \tag{15.5}$$

where G is the inverse function of H in the observation model, and r is the probability density function of the observation noise w. Here,

$\alpha_n^{(j)}$ can be considered as a weighting factor representing the importance of the particle $p_n^{(j)}$. Then, we obtain m particles $f_n^{(1)},\ldots,f_n^{(m)}$, by re-sampling $p_n^{(1)},\ldots,p_n^{(m)}$ with probabilities proportional to the "likelihoods" $\alpha_n^{(1)},\ldots,\alpha_n^{(m)}$. Namely, a new particle $f_n^{(j)}$ is obtained according to

$$f_n^{(j)} = \begin{cases} p_n^{(1)} & \text{probability } \alpha_n^{(1)}/(\alpha_n^{(1)}+\cdots+\alpha_n^{(m)}) \\ \vdots & \vdots \\ p_n^{(m)} & \text{probability } \alpha_n^{(m)}/(\alpha_n^{(1)}+\cdots+\alpha_n^{(m)}). \end{cases} \tag{15.6}$$

Then, $\{f_n^{(1)},\ldots,f_n^{(m)}\}$ can be considered as the realizations generated from the filter distribution $p(x_n|Y_n)$. (See Appendix D.)

15.2.3 *Algorithm for the Monte Carlo filter*

In summary, the following algorithm for the Monte Carlo filter is obtained:

```
1. Generate k-dimensional random numbers $f_0^{(j)} \sim p_0(x)$ for $j = 1,\ldots,m$.
2. Repeat the following steps for $n = 1,\ldots,N$.
   (i) For $j = 1,\ldots,m$,
      • Generate ℓ-dimensional random numbers $v_n^{(j)} \sim q(v)$.
      • Obtain the new particle $p_n^{(j)} = F(f_{n-1}^{(j)}, v_n^{(j)})$.
      • Evaluate the Bayes factor $\alpha_n^{(j)} = r(G(y_n, p_n^{(j)})) \left|\frac{\partial G}{\partial y_n}\right|$.
   (ii) Generate $\{f_n^{(1)},\ldots,f_n^{(m)}\}$ by repeated re-sampling (sampling
        with replacement) m times from $\{p_n^{(1)},\ldots,p_n^{(m)}\}$ with prob-
        abilities proportional to $\{\alpha_n^{(1)},\ldots,\alpha_n^{(m)}\}$.
```

15.2.4 *Likelihood of a model*

The state-space models defined by (15.1) and (15.2) usually contain some unknown parameters θ, such as the variance of the noise and the coefficients of the nonlinear functions F and H. When the observations $y_1,\ldots,y_N$ are given from (9.21), the log-likelihood of the model specified by the parameter θ is given by

$$\ell(\theta) \quad = \quad \sum_{n=1}^{N} \log p(y_n|Y_{n-1}), \tag{15.7}$$

where $p(y_1|Y_0)$ is taken as $p_0(y_1)$. Here, using the Monte Carlo approximation of the predictive distribution,

$$\begin{aligned} p(y_n|Y_{n-1}) &= \int p(y_n|x_n)p(x_n|Y_{n-1})dx_n \\ &\cong \frac{1}{m}\sum_{j=1}^{m} p(y_n|p_n^{(j)}) = \frac{1}{m}\sum_{j=1}^{m} \alpha_n^{(j)}, \end{aligned} \tag{15.8}$$

the log-likelihood can be approximated by

$$\ell(\theta) = \sum_{n=1}^{N} \log p(y_n|Y_{n-1}) \cong \sum_{n=1}^{N} \log\left(\sum_{j=1}^{m} \alpha_n^{(j)}\right) - N\log m. \tag{15.9}$$

The maximum likelihood estimate $\hat{\theta}$ of the parameter θ is obtained by numerically maximizing the above log-likelihood function. However, it should be noted that the log-likelihood, which was obtained by the Monte Carlo filter contains an inherent error due to the Monte Carlo approximation, which consequently makes maximum likelihood estimation difficult. To solve this problem, a self-organizing state-space model is proposed, in which the unknown parameter θ is included in the state vector (Kitagawa (1998)). Accordingly, we can estimate the state and the parameter simultaneously.

15.2.5 Re-sampling method

Here we consider the *re-sampling method*, which is indispensable to the filtering step. The basic algorithm of the re-sampling method based on random sampling is as follows (Kitagawa (1996)):

For $j = 1, ..., m$, repeat the following steps (a)–(c).

(a) Generate uniform random number $u_n^{(j)} \in U[0,1]$.

(b) Search for i that satisfies $C^{-1}\sum_{\ell=1}^{i-1} \alpha_n^{(\ell)} < u_n^{(j)} \le C^{-1}\sum_{\ell=1}^{i} \alpha_n^{(\ell)}$,
where $C = \sum_{\ell=1}^{m} \alpha_n^{(\ell)}$.

(c) Obtain a particle that approximates the filter by setting $f_n^{(j)} = p_n^{(i)}$.

It should be noted here that, the objective of resampling is to re-express the distribution function determined by the particles

$\left\{p_n^{(1)}, \ldots, p_n^{(m)}\right\}$ with weights $\left\{\alpha_n^{(1)}, \ldots, \alpha_n^{(m)}\right\}$ by representing the empirical distribution function defined by re-sampled particles with equal weights. Accordingly, it is not essential to perform exact random sampling.

Considering the above, we can develop various modifications of the re-sampling method with regard to sorting and random number generation. One considerable modification involves *stratified sampling*, that is, dividing the interval [0, 1) into m sub-intervals and then obtaining one particle $u_n^{(j)}$ from each sub-interval. In this case, the step (a) is replaced by one of the following two steps:

(a-S) Generate a uniform random number $u_n^{(j)} \sim U\left((j-1)/m, j/m\right]$,

(a-D) For fixed $\alpha \in (0,1]$, set $u_n^{(j)} = (j-\alpha)/m$.

α may be an arbitrarily fixed real number $0 \leq \alpha < 1$, e.g., $1/2$, or a uniform random number. To perform the stratified sampling rigorously, it is necessary to take the above-mentioned steps based on the sorted particles after sorting $p_n^{(1)}, \ldots, p_n^{(m)}$ and $\alpha_n^{(1)}, \ldots, \alpha_n^{(m)}$ according to the magnitude of $p_n^{(1)}, \ldots, p_n^{(m)}$. However, when the number of particles, m, is large, the sorting algorithm becomes the most time-consuming step in the Monte Carlo filtering algorithm.

Furthermore, since the objective of stratified sampling is to obtain exactly one particle from each group of particles with total weight $1/m$, it is not necessary to sort the stratified sample. From the results of the numerical experiment, it is evident that more accurate approximations were obtained by stratified re-sampling than with the original random sampling. Moreover, the numerical experiment suggests that between the two choices (a-S) and (a-D) of stratified re-sampling algorithms, (a-D) performs better.

15.2.6 Numerical examples

In order to exemplify how the one-step-ahead predictive distribution and the filter distribution are approximated by particles, we consider the result of one cycle of the Monte Carlo filter, i.e., $n = 1$. Assume that the following one-dimensional linear non-Gaussian state-space model is given:

$$\begin{aligned} x_n &= x_{n-1} + v_n, \\ y_n &= x_n + w_n, \end{aligned} \tag{15.10}$$

where v_n and w_n are white noises that follow the Cauchy distribution with probability density function $q(v) = \sqrt{0.1}\pi^{-1}(v^2 + 0.1)^{-1}$, and the standard normal distribution $N(0,1)$, respectively. The initial state distribution $p_0(x_0)$ is assumed to follow the standard normal distribution. However, it is evident that normality of the distribution is not essential for the Monte Carlo filtering method.

Under the above-mentioned assumptions, the one-step-ahead predictive distribution $p(x_1|Y_0)$ and the filter $p(x_1|Y_1)$ were obtained. Here, a small number of particles was used, that is, m was set to $m = 100$, in order to make features of the illustrations clearly visible. In actual computations, however, we use a large number of particles for approximation.

The curve in Figure 15.3(a) shows the assumed distribution of the initial state $p_0(x_0)$. The vertical lines show the locations of 100 realizations generated from $p_0(x_0)$, and the histogram, which was obtained from these particles, approximates the probability density function. The bold curve in plot (b) depicts the true distribution function of the initial state and the fainter curve shows the empirical distribution function obtained from the particles shown in plot (a). Similar to these plots, plots (c) and (d) depict the probability density function, the realizations and the cumulative distribution, together with its empirical counterpart of the system noise.

Plots (e) and (f) illustrate the predictive distribution, $p(x_1|Y_0)$. The curve in plot (e) shows the "true" probability function obtained by numerical integration of the two density functions of plots (a) and (c). Plot (f) shows the "true" cumulative distribution function obtained by integrating the density function in plot (e). On the other hand, the vertical lines in plot (e) indicate the location of the particles $p_1^{(j)}$ obtained by substituting a pair of particles shown in plots (a) and (c) into the equation (D.4). The histogram defined by the particles $p_1^{(1)},\dots,p_1^{(m)}$ approximates the true density function shown in plot (e). The empirical distribution function and the true distribution function are shown in plot (f).

The curve in plot (g) shows the filter density function obtained from the non-Gaussian filter using the equation (14.5), when the observation $y_1 = 2$ is given. With respect to plot (g), the particles are located in the same place as plot (e); however, the heights of the lines are proportional to the likelihood of the particle $\alpha_n^{(j)}$. Different from plot (f), the cumulative distribution function in plot (h) approximates the filter distribution, although the steps of plot (h) are located identically to those of plot (f). Plot (i) shows the locations of the particles, the histogram and the exact filter distribution after re-sampling. Further it can be seen that the density function and the cumulative distribution function in plots (i) and (j) are reasonable approximations to plots (g) and (h), respectively.

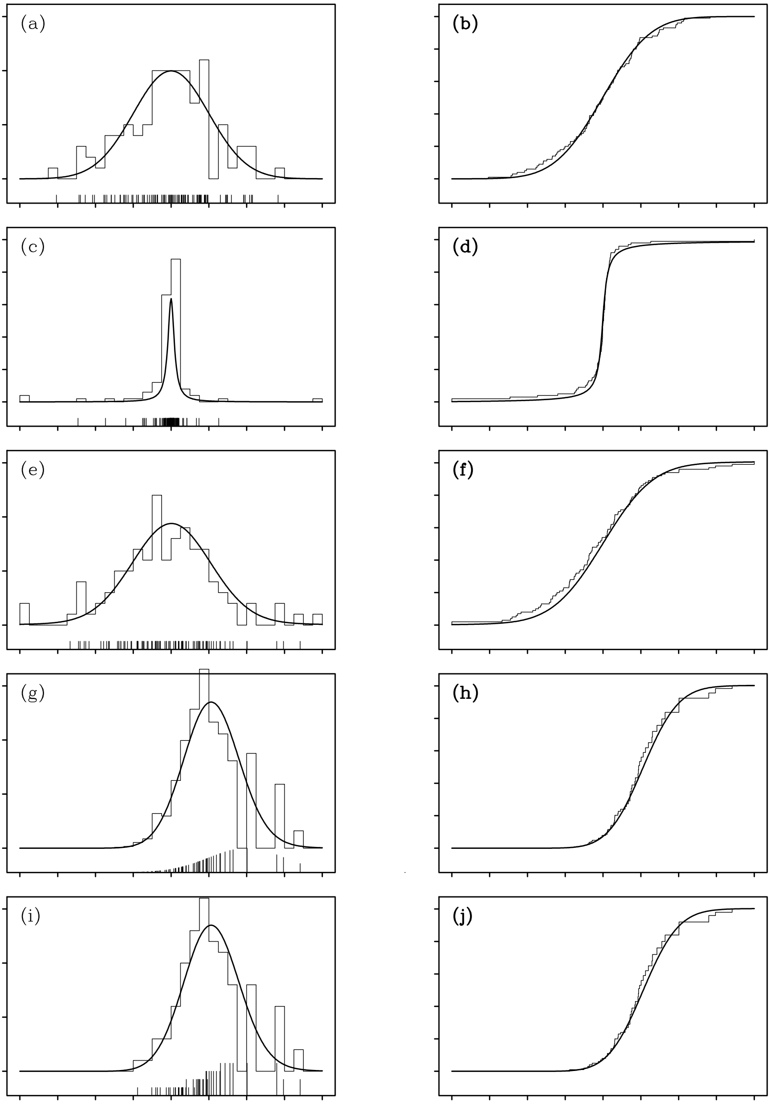

Figure 15.3 *One step of the Monte Carlo filter. The figures in the left-hand column illustrate the probability density functions, 100 realizations and the histogram, respectively, and the figures in the right-hand column depict the distribution functions and the empirical distribution functions obtained from the realizations, respectively. (a) and (b): the initial state distributions. (c) and (d): the system noise distribution. (e) and (f): the one-step-ahead predictive distributions. (g) and (h): the filter distributions. (i) and (j): the filter distributions after re-sampling.*

15.3 Monte Carlo Smoothing Method

The Monte Carlo filter method presented in the previous section, can be further extended to create a smoothing algorithm by preserving past particles. In the following, the vector of the particles $(s_{1|n}^{(j)},\ldots,s_{n|n}^{(j)})^T$ denotes the j-th realization from the n-dimensional joint distribution function $p(x_1,\ldots,x_n|Y_n)$.

To achieve the objective of smoothing, it is necessary only to modify Step 2(d) of the algorithm discussed in Section 15.2 as follows.

(d-S) For $i=1,\ldots,m$, by re-sampling the n-dimensional vector $(s_{1|n-1}^{(j)},\ldots,s_{n-1|n-1}^{(j)},p_n^{(j)})^T$, generate $(s_{1|n}^{(j)},\ldots,s_{n-1|n}^{(j)},s_{n|n}^{(j)})^T$.

In this modification, by re-sampling $\{(s_{1|n-1}^{j},\ldots,s_{n-1|n-1}^{(j)},p_n^{(j)})^T, j=1,\ldots,m\}$ with the same weights as used in step (2)(ii) of subsection 15.2.3, fixed-interval smoothing for a nonlinear non-Gaussian state-space model can be achieved (Kitagawa (1996)).

In actual computation, however, since a finite number of particles (m particles) is repeatedly re-sampled, the number of different particles gradually decreases and then the weights become concentrated on a small number of particles, thus causing the shape of the distribution to finally collapse. Consequently, in terms of the smoothing algorithm, a modification for Step (d-S) should be carried out as follows:

(d-L) For $j=1,\ldots,m$, generate $(s_{n-L|n}^{(j)},\ldots,s_{n-1|n}^{(j)},s_{n|n}^{(j)})$. Here, L is assumed to be a fixed integer, usually less than 30, and $f_n^{(j)} = s_{n|n}^{(j)}$ by re-sampling $(s_{n-L|n-1}^{(j)},\ldots,s_{n-1|n-1}^{(j)},p_n^{(j)})$.

Then, it is interesting that this modified algorithm turns out to correspond to the L-lag fixed-lag smoothing algorithm. If L is fixed too large, the fixed-lag smoother $p(x_n|Y_{n+L})$ precisely approximates the fixed-interval smoother $p(x_n|Y_N)$. On the other hand, the distribution determined by $x_{n|n+L}^{(1)},\ldots,x_{n|n+L}^{(m)}$ is rather remote from $p(x_n|Y_{n+L})$. Therefore, L should be taken not so large, i.e., $L=20$ or 30.

The following example shows the results of state estimation by the Monte Carlo filter for the artificially generated time series shown in Figure 14.1. The estimation is carried out by applying a first order trend model;

$$\begin{aligned} x_n &= x_{n-1}+v_n, \\ y_n &= x_n+w_n, \end{aligned} \qquad (15.11)$$

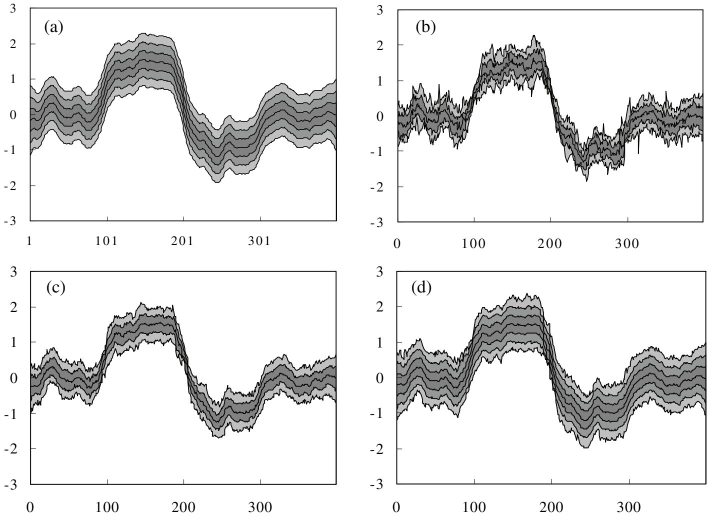

Figure 15.4 *The results of the Monte Carlo filter: (a) the exact filter distribution using a Kalman filter. (b) – (d) the fixed-lag* $(L = 20)$ *smoothed densities ((b)* $m = 100$*, (c)* $m = 1000$*, (d)* $m = 10,000$*) with a Monte Carlo filter.*

where w_n is a Gaussian white noise with mean 0 and variance σ^2. For the system noise, two models are considered, namely, a Gaussian distribution and a Cauchy distribution.

Figure 15.4 (a) depicts the exact filter distribution obtained by the Kalman filter when the system noise is Gaussian. The bold curve in the middle shows the mean of the distribution and the three gray areas illustrate $\pm 1\sigma$, $\pm 2\sigma$ and $\pm 3\sigma$ confidence intervals.

On the other hand, plots (b), (c) and (d) show the fixed-lag $(L = 20)$ smoothed densities obtained by using $m = 100, 1000$ and $10,000$ particles, respectively. The dark gray area shows the $\pm 1\sigma$ interval and the light gray area shows the $\pm 2\sigma$ intervals. In plot (d), the $\pm 3\sigma$ interval is also shown.

For $m = 100$ in plot (b), although general tendencies of the distributional change of plot (a) are captured, large variation is seen which indicates that the estimate is not particularly good. However, as the number of particles increases, more accurate approximations to the “true” distribution are obtained. In particular, for $m = 10,000$ shown in plot (d),

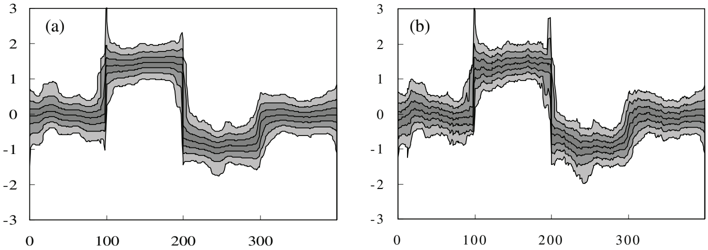

Figure 15.5 *Smoothing with Cauchy distribution model: (a) The exact distribution obtained from the non-Gaussian smoothing algorithm. (b) The results of Monte Carlo smoothing* $(m = 10,000)$.

a very good approximation of the curves are obtained except the $\pm 3\sigma$ interval of which curves are slightly variable.

Figure 15.5 shows the results when the system noise is assumed to be a Cauchy distribution. The figure on the left-hand side depicts the "exact" results obtained using the non-Gaussian smoothing algorithm, which was treated in Chapter 14. On the other hand, the figure on the right-hand side depicts the results obtained by Monte Carlo smoothing with $m = 10,000$ and $L = 20$. Although the curves are more variable in comparison with the figure on the left-hand side, the abrupt changes around $n = 100, 200$ and 300 are captured in a reasonable way. Moreover, the $\pm 3\sigma$ interval is also well approximated.

15.4 Nonlinear Smoothing

The Monte Carlo filtering and smoothing algorithms can also be used for filtering and smoothing for the nonlinear state-space model (Kitagawa (1991)). Figures 15.6 (a) and (b) depict examples of series x_n and y_n generated by the nonlinear state-space model

$$\begin{aligned} x_n &= \frac{1}{2}x_{n-1} + \frac{25x_{n-1}}{x_{n-1}^2+1} + 8\cos(1.2n) + v_n, \\ y_n &= \frac{x_n^2}{10} + w_n, \end{aligned} \tag{15.12}$$

where $v_n \sim N(0,1)$, $w_n \sim N(0,10)$, $v_0 \sim N(0,5)$. Here, we consider the problem of estimating the unknown state x_n based on 100 observations, y_n, $n = 1,\ldots,100$. Because of the nonlinearity and the sinusoidal input

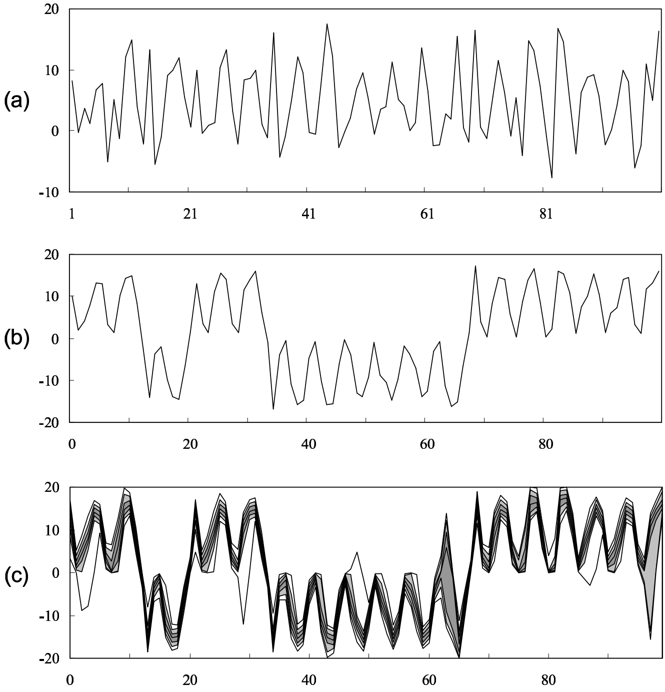

Figure 15.6 *Nonlinear smoothing: (a) Data y_n. (b) Unknown State x_n. (c) Smoothed distribution of x_n obtained by the Monte Carlo smoother.*

in the system model in equation (15.12), the state x_n occasionally shifts between the positive and negative regions. However, since in the observation model, the state x_n is squared, and x_n^2 contaminated with an observation noise w_n is observed, it is quite difficult to discriminate between positivity and negativity of the true state.

It is well known that the extended Kalman filter occasionally diverges for this model. Figure 15.6 (c) shows the smoothed posterior distribution $p(x_n|Y_N)$ obtained by the Monte Calro filter and smoother. It can be seen that a quite reasonable estimate of the state x_n is obtained with this method.

The key to the success of the nonlinear filtering and smoothing is that the Monte Carlo filter can reasonably express the non-Gaussian state densities. Figure 15.7 (a) and (b), respectively, show the marginal posterior state distributions $p(x_t|Y_{t+j})$, $j = -1, 0, 1, 2$, for $t = 30$ and 48.

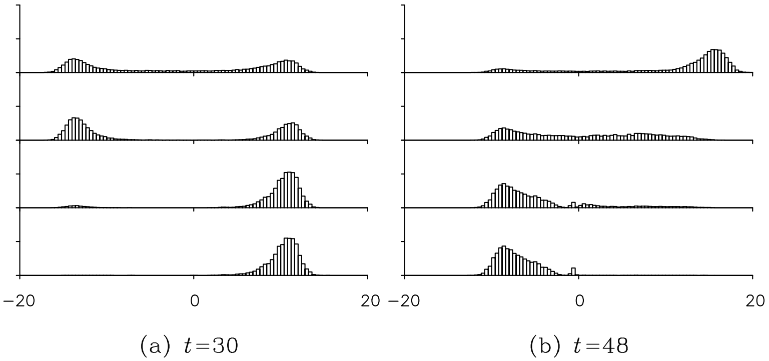

Figure 15.7 *Fixed-point smoothing for t* = 30 *(left) and t* = 48 *(right). From top to bottom, predictive distributions, filter distributions, 1-lag smoothers and 2-lag smoothers.*

For both $t = 30$ and 48, the predictive distribution $p(x_t|Y_{t-1})$ and the filter distribution $p(x_t|Y_t)$ are bimodal. However, in the 2-lag smoother for $t = 30$, $p(x_{30}|Y_{32})$, the left-half of the distribution disappeared and the distribution becomes unimodal. The same phenomenon can be seen for $t = 48$. In this case, the right peak is higher than the left one in the predictive distribution. However, in the smoother distributions, the peak in the right half domain disappears. In such a situation, the extended Kalman filter is very likely to yield an estimate with reverse sign.

Problems

1. Consider a model for the Nikkei 225 data shown in Figure 1.1(g) that takes into account changes in the trend and the volatility simultaneously.
2. In Monte Carlo filtering, how many particles should we use to increase the accuracy of the estimate 10-fold.
3. For the Monte Carlo filter, if we do not restrict every particle to have the same weight but allow some to have different weights, is it possible to develop a procedure without re-sampling?
4. Compare the amount of information required to be stored to carry out fixed-interval smoothing and fixed-lag smoothing.

Chapter 16

Simulation

In this chapter, we first explain methods for generating random numbers that follow various distributions. A unified method for simulating time series is obtained by using the state-space model. Namely, a realization of white noise can be obtain by generating random numbers that follow a specified distribution. In modeling, a time series model is generally considered an output of a system with a white noise input. Therefore, if a time series model is given, we can obtain realizations of the system by generating a time series that follows the model by using random numbers.

16.1 Generation of Uniform Random Numbers

A sequence of independently generated numbers that follows a certain distribution is called a sequence of random numbers or simply *random numbers*. In other words, the random numbers are realizations of white noises. A time series model represents a time series as a sequence of realizations of a system with white noise input. Therefore, we can generate a time series by properly specifying the time series model and the random numbers, and this method is called a *simulation* of a time series model. In actual computation for simulating a time series, we usually use pseudo-random numbers generated using an appropriate algorithm. Normal random numbers, i.e., random numbers that follow a normal distribution, are frequently necessary for simulating time series. Such a sequence of random numbers is obtained by generating *uniform random numbers*, and then transforming them to the specified distribution.

A well-known conventional method for generating uniform random numbers is the *linear congruence method*. With this method, a sequence of integers $I_1, I_2, \cdots$ is generated from

$$I_k \equiv aI_{k-1} + c \quad (\mathrm{mod}\ m), \tag{16.1}$$

starting from an initial integer I_0.

In particular, for $c = 0$, this method is called the *multiplicative congruence method*. The generated integer I_k takes a value in $[0, m)$. Therefore, I_k/m is distributed on $[0, 1)$.

However, we note here that since the period of the series generated by this method is at most m, it is not possible to generate a sequence of random numbers longer than m. The constants a, c and m have to be selected carefully, and examples of the combination of constants are

$$\begin{array}{lll} a = 1229 & c = 351750 & m = 1664501 \\ a = 1103515245 & c = 12345 & m = 2^{31} \end{array}$$

(Knuth (1997)). The latter combination were used in C language until 1990-th. It is known that if $m = 2^p$, $a = 5 \pmod{m}$ and c is an odd number, then the period of the sequence generated by this algorithm attains the possible maximum period of m, i.e., it contains all of the numbers between 0 and $m - 1$ once each.

By the lagged Fibonacci method, the sequence of integers I_n is generated by

$$I_{n+p} = I_{n+q} + I_n \pmod{m}, \tag{16.2}$$

where m is usually set to 2^k (k ia the bit length). Then the generated series has the period at largest $2^{k-1}(2^p - 1)$. In the current C language, $p = 31$, $q = 3$, $m = 2^{31}$ are used to attain the period of about 2^{60}.

In the generalize feedback shift register (GFSR) algorithm (Lewis and Payne (1973)), k-dimensional vector of binary sequence is generated by

$$I_{n+p} = I_{n+q} \oplus I_n, \tag{16.3}$$

where $p > q$ and $\oplus$ denotes the excusive OR operation. The integers p and q are determined so that the polynomial $X^p + X^q + 1$ is irreducible. Then, the period of the sequence becomes at largest $2^p - 1$. Some examples of p and q are $p = 521$, $q = 158$ (period $2^{521} - 1$), $p = 521$, $q = 32$ (period $2^{521} - 1$) and $p = 607$, $q = 273$ (period $2^{607} - 1$).

Twisted GFSR algorithm (Matsumoto and Kurita (1994)) generates a k-dimensional binary sequence by

$$I_{n+p} = I_{n+q} \oplus I_n A, \tag{16.4}$$

where A is a $k \times k$ regular matrix such as the companion matrix. In the frequently used TT800 algorithm, $p = 25$ and $q = 7$ are used. This sequnce has the period of $2^{pk} - 1$. Further, Matsumoto and Nishimura (1998) developed the Mersenne twister algorithm

$$I_{n+p} = I_{n+q} \oplus I_{n+1} B \oplus I_n A. \tag{16.5}$$

They showed that for $p = 624$, by taking A and B appropriately, the generated series has a period of length $2^{19937} - 1$ and are distributed uniformly on the 623 dimensional space.

Different from these families of pseudo-random numbers that are generated in software using certain algorithms, hardware for generating physical (hardware) random numbers has also been developed. Such hardware can be used when more precise random numbers are necessary in a simulation, because random numbers generated in this way are supposed to be free from any cycles or correlations.

16.2 Generation of Gaussian White Noise

A realization of Gaussian white noise is obtained by generating a sequence of random numbers that follows a normal distribution, namely, *normal random numbers*. The Box-Muller transform (Box and Muller (1958)) for generating normal random numbers is well known. This method applies the fact that, given two independent uniform random numbers U_1 and U_2 on [0,1],

$$\begin{aligned} X_1 &= \sqrt{-2\log U_1}\cos 2\pi U_2, \\ X_2 &= \sqrt{-2\log U_1}\sin 2\pi U_2 \end{aligned} \tag{16.6}$$

independently follow the standard normal distribution $N(0,1)$.

In practice, however, Marsaglia's algorithm that follows can avoid the explicit evaluation of sine and cosine functions and thus can generate normal random numbers more efficiently.

1. Generate the uniform random numbers U_1 and U_2.
2. Put $V_1 = 2U_1 - 1$ and $V_2 = 2U_2 - 1$.
3. Put $S^2 = V_1^2 + V_2^2$.
4. Return to Step (1), if $S^2 \geq 1$.
5. Put $X_1 = V_1\sqrt{\frac{-2\log S}{S}}$ and $X_2 = V_2\sqrt{\frac{-2\log S}{S}}$.

Figure 16.1 (a) shows 200 uniform random numbers generated by the multiplicative congruence method of (16.1) with the initial value $I_0 = 1990103011$. On the other hand, plot (b) shows normal random numbers (white noise) obtained with Marsaglia's algorithm using these uniform random numbers. Plot (c) depicts the histogram and the sample autocorrelation function computed from those random numbers, where the histogram looks somewhat different from the density of the normal

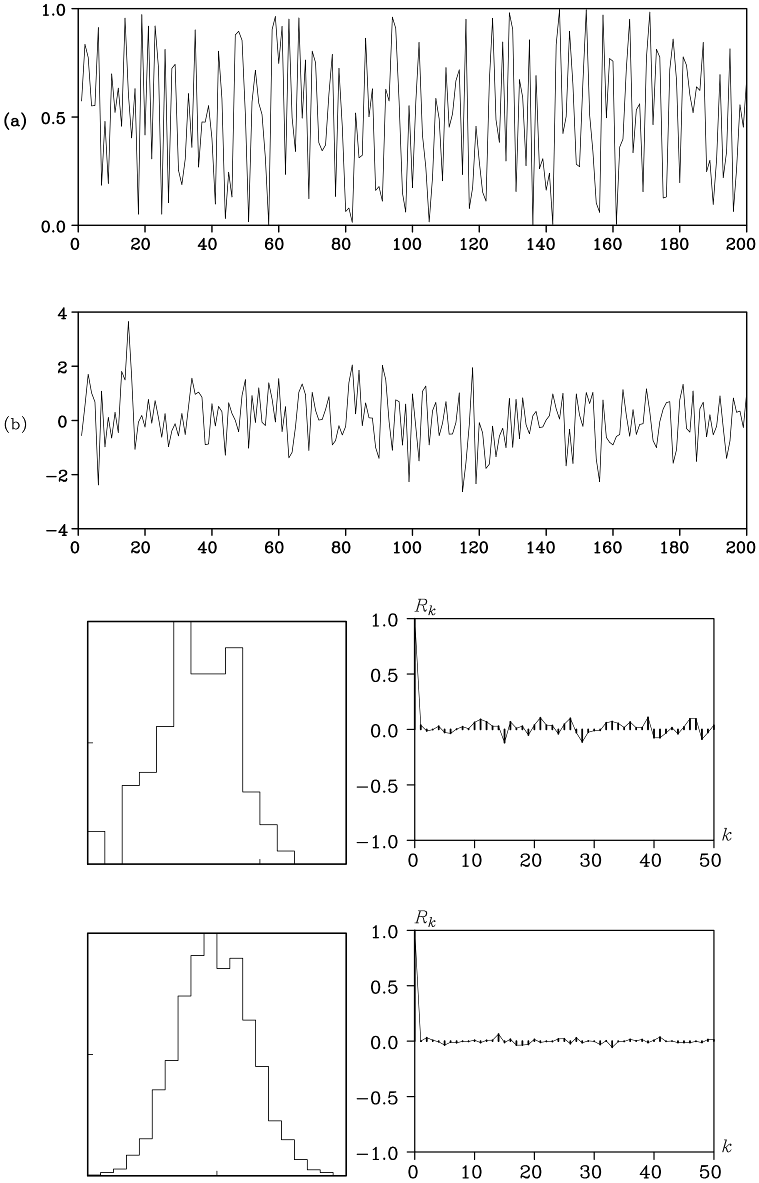

Figure 16.1 *Realizations, histograms and autocorrelation functions of uniform random numbers and white noise.*

distribution. Plot (d) shows the histogram and the sample autocorrelation function, respectively, when the number of realizations is increased to 2000. It can be seen that the histogram resembles the normal density and that the sample autocorrelation function approaches zero.

16.3 Simulation Using a State-Space Model

Using the realizations of white noise introduced in the previous subsection, we can generate a time series that follows a given time series model. This is called the *simulation* of the time series. Assume that the time series model is represented in the form of the state-space model :

$$\begin{aligned} x_n &= Fx_{n-1} + Gv_n, & (16.7)\\ y_n &= Hx_n + w_n. & (16.8)\end{aligned}$$

Based on this state-space model, if the initial state vector x_0, and N realizations of k-dimensional Gaussian white noise with mean 0 and variance-covariance matrix Q, $v_1,\dots,v_N$, are given, the realizations of the state vectors, $x_1,\dots,x_N$ can be easily obtained by repeatedly substituting them into the system model of (16.7). Further, if the realizations of ℓ-dimensional Gaussian white noise with mean 0 and the variance-covariance matrix R, $w_1,\dots,w_N$, are given, the time series $y_1,\dots,y_N$ can be generated by the observation model of (16.8).

A k-dimensional Gaussian white noise with mean 0 and variance-covariance matrix Q can be obtained from k one-dimensional Gaussian white noises generated by the method shown in the previous subsection. Define a k-dimensional vector $u_n = (u_n^{(1)},\cdots,u_n^{(k)})^T$, where $u_n^{(j)}$ is a one-dimensional Gaussian white noise, then u_n becomes a k-dimensional Gaussian white noise with mean vector 0 and unit variance-covariance matrix I_k. Here, we assume that a $k \times k$ lower triangular matrix L such that $Q = LL^T$ can be obtained by the *Cholesky decomposition* of the positive-definite symmetric matrix Q. Then, the k-dimensional vector v_n defined by

$$v_n = Lu_n \qquad (16.9)$$

satisfies

$$\mathrm{E}(v_n v_n^T) = \mathrm{E}(Lu_n u_n^T L^T) = L\mathrm{E}(u_n u_n^T)L^T = LI_kL^T = Q, \qquad (16.10)$$

showing that v_n becomes a normal white noise with mean vector 0 and the variance-covariance matrix Q.

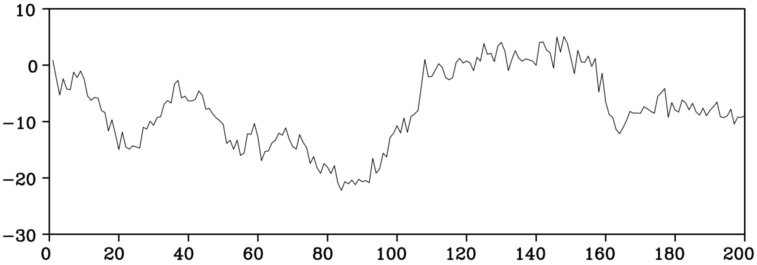

Figure 16.2: *Simulation of a random walk model.*

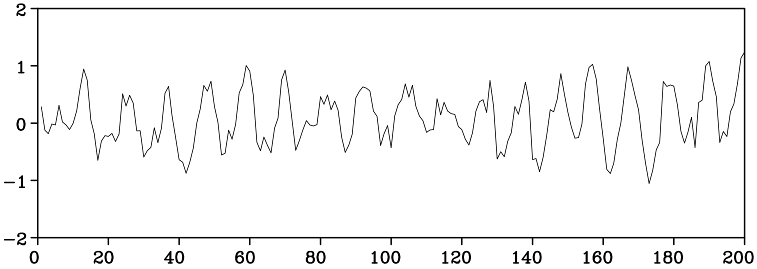

Figure 16.3: *Simulation of an AR model.*

Example (Simulation of a random walk model) Figure 16.2 shows the results of the simulation for the random walk model

$$
\begin{aligned}
x_n &= x_{n-1} + v_n, \\
y_n &= x_n + w_n, \qquad (16.11)
\end{aligned}
$$

where the system noise v_n follows the normal distribution $N(0, \pi^2/6)$ and the observation noise w_n is the standard Gaussian white noise that follows $N(0,1)$ and the initial state is $x_0 = 0$.

Example (Simulation of an AR model) Figure 16.3 shows the results of the simulation for the AR model with order 10 fitted to the logarithms of the sunspot number data. Since the state-space representation for the AR model does not have any observation noise, we set $R = 0$. Here, the initial state is set to $x_0 = (0, \dots, 0)^T$ and 400 time series are generated. To remove the effects of the 0 initial state, the first 200 observations are discarded and Figure 16.3 shows only the latter half of the data.

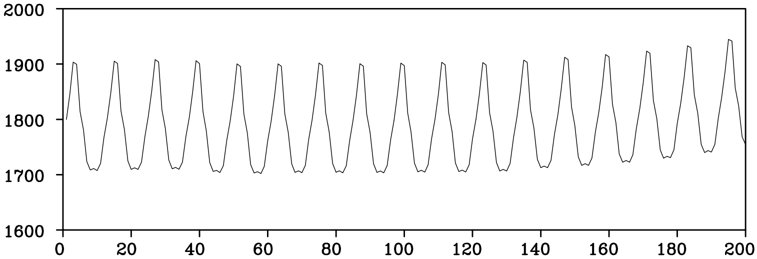

Figure 16.4: *Simulation of a seasonal adjustment model.*

Example (Simulation of a seasonal adjustment model) Figure 16.4 shows the results of a simulation for the seasonal adjustment model. The model is shown in Figure 12.6 with the stationary AR component ($m_1 = 2$, $m_2 = 1$, $m_3 = 2$ and $p = 12$). As the initial state vector x_0, the vector $x_{0|N}$ is used for the smoothed estimate of the initial vector, which is obtained from the actual seasonal data. Although the simulation of the seasonal adjustment model resembles the actual time series shown in Figure 1.1(d), it is evident that the trend component of Figure 16.4 is considerably different from that of Figure 1.1(d).

16.4 Simulation with the Non-Gaussian State-Space Model

The method of simulation for the state-space model presented in the previous section can be easily extended to the simulation of a non-Gaussian time series model. Consider a non-Gaussian state-space model,

$$x_n = Fx_{n-1} + Gv_n, \qquad (16.12)$$

$$y_n = Hx_n + w_n, \qquad (16.13)$$

where v_n and w_n are not necessarily Gaussian and are distributed according to the density functions $q(v)$ and $r(w)$, respectively.

For simplicity, it is assumed that the k components of v_n and the ℓ components of w_n are mutually independent. To simulate the above non-Gaussian state-space model, it is necessary to develop a method of generating realizations of white noise that follow an arbitrarily defined density function $p(x)$. For some specific distributions, such as the Cauchy distribution, the χ^2 distribution and the two-sided exponential (Laplace) distribution, they can be generated by a transformation of the uniform random numbers or the normal random numbers. In the following subsection, some examples are given.

16.4.1 χ^2 *distribution*

The χ^2 *distribution* with j degrees of freedom can be expressed as

$$\chi_j^2 = X_1^2 + \cdots + X_j^2, \tag{16.14}$$

where $X_1, \cdots, X_j$ are normal random variables. Therefore, to generate random numbers that follow the χ^2 distribution, we initially generate j normal random numbers and then obtain χ_j^2 using equation (16.14). In particular, *exponential random numbers* are obtained by putting $j = 2$. Further, by defining $Z = \log \chi_2^2$, we obtain the *double exponential random numbers*. Note that an exponential random number can be obtained from a uniform random number directly by setting

$$v = -\log u, \tag{16.15}$$

given the uniform random number u. Then, the double exponential random number is efficiently obtained by

$$v = \log(-\log u). \tag{16.16}$$

16.4.2 Cauchy distribution

The density function of the *Cauchy distribution* that was used for the non-Gaussian model in Chapter 14 is given by

$$p(x) = \frac{1}{\pi(x^2+1)}. \tag{16.17}$$

To generate Cauchy random numbers, we generate a uniform random number on $[0,1)$, and for $u \neq 0.5$, define v by

$$v = \tan \pi u. \tag{16.18}$$

16.4.3 Arbitrary distribution

In general, random numbers that follow an arbitrary density function $f(x)$ can be generated by using the inverse function of the distribution function. The distribution function is a monotone increasing function defined by

$$F(x) = \int_{-\infty}^{x} f(t)dt, \tag{16.19}$$

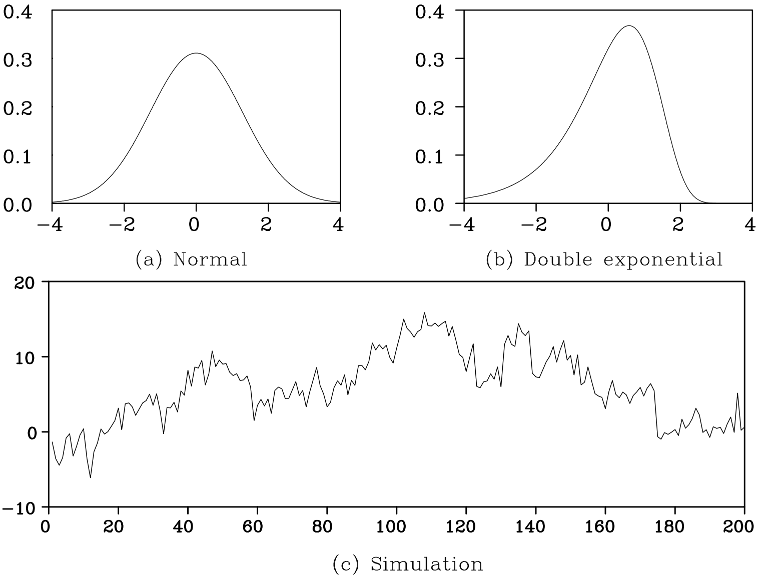

Figure 16.5: *Density functions of system noise and the results of the simulation.*

which satisfies $0 \leq F(x) \leq 1$, $F(-\infty) = 0$, and $F(\infty) = 1$. Here, if we obtain an inverse function $G(y) \equiv F^{-1}(y)$, $0 \leq y \leq 1$, that satisfies $F(G(y)) = y$, then G is a function from $(0,1)$ to $(-\infty,\infty)$. Therefore, if u is a uniform random number on $[0,1)$, $v = G(u)$ becomes a random number that follows the density function $f(v)$. Applying this method, we can generate random numbers that follow various distributions by using the density functions discussed in Chapter 4.

Example (Trend model with double-exponential noise) Figure 16.5 shows the results of the simulation, which were obtained by replacing the system noise of the random walk model in Figure 16.2 by $v_n = r_n + \zeta$, where r_n denotes a double exponential random number and $\zeta = 0.57722$ denotes the Euler constant.

For comparison, plots (a) and (b) show the density functions of the normal distribution used in Figure 16.2 and the double exponential distribution. Even though the two density functions have the same mean and the same variance, they have different shapes, and so different simulation results are obtained.

As shown in Figure 16.2, simulation with the density given in plot (a) yields symmetric movement around the trend. On the other hand, in

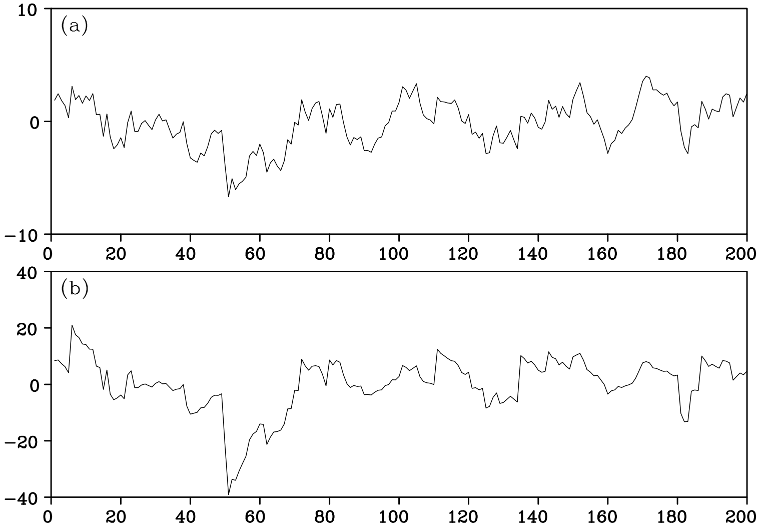

Figure 16.6 *Simulation of an AR model with different noise distributions: (a) normal distribution, (b) Cauchy distribution.*

plot (c) obtained by using the density in plot (b), the behavior around the trend shows asymmetric upward and downward tendencies. We can observe such typical asymmetric behavior of time series frequently in financial data.

Example (AR models with Gaussian and non-Gaussian noise) Figure 16.6 shows the simulation results for the AR model of first order:

$$y_n = 0.9y_{n-1} + v_n. \tag{16.20}$$

Here, in plots (a) and (b), v_n is assumed to be the standard normal distribution $N(0,1)$ and the Cauchy distribution $C(0,1)$, respectively. Even though the AR models are of the same order and have the same AR coefficients, the two time series in plots (a) and (b) appear quite different, because the distributions of the noise v_n are different. In particular, in plot (b), the time series occasionally shows big jumps, and the width of the fluctuation is, as a whole, more than twice as large as that of plot (a).

Problems

1. Assume that U and V are uniform random numbers defined on $[0,1]$. What distribution does $W = U + V$ follow?
2. In the simulation of an AR model $y_n = ay_{n-1} + v_n$, $v_n \sim N(0,1)$, we usually generate $m+n$ data elements and discard the initial m realizations. How large should m be?
3. Show a method of simulating future values based on observations up to the present time.

Appendix A

Algorithms for Nonlinear Optimization

In this appendix, we briefly discuss algorithms for nonlinear optimization. For simplicity, we consider the case where the objective function $f(x)$ is approximated by its Taylor series expansion up to the second order:

$$f(x) = f(x^*) + (x - x^*)^T g(x^*) + \frac{1}{2}(x - x^*)^T H(x - x^*), \tag{A.1}$$

where $x = (x_1, \ldots, x_m)^T$ and

$$g(x) = \begin{bmatrix} \frac{\partial f(x)}{\partial x_1} \\ \vdots \\ \frac{\partial f(x)}{\partial x_m} \end{bmatrix}, \quad H = \begin{bmatrix} \frac{\partial^2 f}{\partial x_1 \partial x_1} & \cdots & \frac{\partial^2 f}{\partial x_1 \partial x_m} \\ \vdots & \ddots & \vdots \\ \frac{\partial^2 f}{\partial x_m \partial x_1} & \cdots & \frac{\partial^2 f}{\partial x_m \partial x_m} \end{bmatrix}. \tag{A.2}$$

From (A.1), we have

$$g(x) = g(x^*) + H(x - x^*) \tag{A.3}$$

and if x^* is assumed to minimize the objective function $f(x)$, $g(x^*) = 0$ holds and we have

$$g(x) = H(x - x^*). \tag{A.4}$$

Therefore, if the current approximation is x, by computing H and $g(x)$, the solution x^* is obtained as

$$x^* = x - H^{-1} g(x). \tag{A.5}$$

In actual problems, the objective function $f(x)$ is rarely expressible as a quadratic form such as that of (A.1) and the solution x^* is not obtained by applying (A.5) only once. Moreover, because the matrix H is not usually constant but changes depending on x, it is necessary to repeat the recursion

$$x_k = x_{k-1} - H_{k-1}^{-1} g(x_{k-1}), \tag{A.6}$$

using an appropriately determined initial value x_0.

This procedure is called the *Newton-Raphson method*. However, since the likelihood function of the time series model is usually a very complex function of the parameters and it is sometimes difficult to obtain H_k analytically, the following algorithm, known as the *quasi-Newton method*, is used (Nocedal and Wright (2006)).

1. Put $k=1$ and choose an initial value x_0 and H_0^{-1} suitably. As a default value, we may put $H_0 = I$.
2. Calculate the gradient vector $g(x_{k-1})$.
3. Obtain the direction vector by $h_k = H_{k-1}^{-1} g(x_{k-1})$.
4. Put $x_k = x_{k-1} - \lambda_k h_k$ and find λ_k, which minimizes $f(x_k)$ by a linear search.
5. Obtain an estimate of H_k^{-1} using either the DFP formula or the BFGS formula that follow.

   [DFP formula] (Fletcher (1980))

   $$H_k^{-1} = H_{k-1}^{-1} + \frac{\Delta x_k \Delta x_k^T}{\Delta x_k^T \Delta g_k} - \frac{H_{k-1}^{-1} \Delta g_k \Delta g_k^T H_{k-1}^{-1}}{\Delta g_k^T H_{k-1}^{-1} \Delta g_k}, \tag{A.7}$$

   [BFGS formula] (Broyden (1970))

   $$H_k^{-1} = \left(I - \frac{\Delta g_k \Delta x_k^T}{\Delta g_k^T \Delta x_k} \right)^T H_{k-1}^{-1} \left(I - \frac{\Delta g_k \Delta x_k^T}{\Delta g_k^T \Delta x_k} \right) + \frac{\Delta x_k \Delta x_k^T}{\Delta x_k^T \Delta g_k}, \tag{A.8}$$

   where $\Delta x_k = x_k - x_{k-1}$ and $\Delta g_k = G(x_k) - g(x_{k-1})$.
6. If the convergence condition is not satisfied, go back to step 2 after setting $k = k+1$.

This quasi-Newton method has the following two advantages. Firstly, it is not necessary to compute the Hessian matrix H_k and its inverse H_k^{-1} directly. Secondly, it can usually find the minimum even when the objective function is far from being a quadratic function, since it automatically adjusts the step width λ_k by a linear search. BFGS formula has an advantage the it does not require precise linear search.

Appendix B

Derivation of Levinson's Algorithm

In this appendix, we derive the Levinson's algorithm (Levinson (1947)) for estimating the AR coefficients for univariate time series model effectively. Whittle (1963) showed an extension of an algorithm for multivariate time series. However, since for multi-variate time series, the coefficients of the backward AR model are different from those of the forward AR model, the algorithm needs to treat twice as many number of recursions as the univariate case.

Assume that the autocovariance function C_k, $k = 0, 1, \cdots$ is given and that the Yule-Walker estimates of the AR model of order $m-1$ have already been obtained. In the following, since we consider AR models with different orders, the AR coefficients, the prediction error and the prediction error variance of the AR model of order $m-1$ are denoted by $\hat{a}_1^{m-1}, \ldots, \hat{a}_{m-1}^{m-1}$, v_n^{m-1} and $\hat{\sigma}_{m-1}^2$, respectively. Next, we consider a method of efficiently obtaining Yule-Walker estimates $\hat{a}_1^m, \ldots, \hat{a}_m^m$ and $\hat{\sigma}_m^2$ for the parameters of the AR model of order m using the estimates for the AR model of order $m-1$.

Since the coefficients $\hat{a}_1^{m-1}, \ldots, \hat{a}_{m-1}^{m-1}$ satisfy the following Yule-Walker equation of order $m-1$, we have that

$$C_k = \sum_{j=1}^{m-1} \hat{a}_j^{m-1} C_{j-k}, \qquad k = 1, \ldots, m-1. \tag{B.1}$$

This means that v_n^{m-1} satisfies

$$\mathrm{E}\left\{v_n^{m-1} y_{n-k}\right\} = \mathrm{E}\left\{\left(y_n - \sum_{j=1}^{m-1} \hat{a}_j^{m-1} y_{n-j}\right) y_{n-k}\right\} = 0, \tag{B.2}$$

for $k = 1, \ldots, m-1$. Here, we consider a *backward AR model* of order $m-1$ that represents the present value of the time series y_n with future values $y_{n+1}, \ldots, y_{n+m-1}$,

$$y_n = \sum_{i=1}^{m-1} a_j y_{n+i} + w_n^{m-1}. \tag{B.3}$$

Then, since $C_{-k} = C_k$ holds for a univariate time series, this backward AR model also satisfies the same Yule-Walker equation (B.1). Therefore, the backward prediction error w_n^{m-1} satisfies

$$\mathrm{E}\left\{ w_{n-m}^{m-1} y_{n-k} \right\} = \mathrm{E}\left\{ \left(y_{n-m} - \sum_{j=1}^{m-1} \hat{a}_j^{m-1} y_{n-m+j} \right) y_{n-k} \right\} = 0, \quad \text{(B.4)}$$

for $k = 1, \ldots, m-1$. Here, we define the weighted sum of the forward prediction error v_n^{m-1} and the backward prediction error w_{n-m}^{m-1} by

$$\begin{aligned} z_n &\equiv v_n^{m-1} - \beta w_{n-m}^{m-1} \\ &\equiv y_n - \sum_{j=1}^{m-1} \hat{a}_j^{m-1} y_{n-j} - \beta \left(y_{n-m} - \sum_{j=1}^{m-1} \hat{a}_j^{m-1} y_{n-m+j} \right) \\ &= y_n - \sum_{j=1}^{m-1} \left(\hat{a}_j^{m-1} - \beta \hat{a}_{m-j}^{m-1} \right) y_{n-j} - \beta y_{n-m}. \end{aligned} \quad \text{(B.5)}$$

z_n is a linear combination of $y_n, y_{n-1}, \ldots, y_{n-m}$ and from (B.2) and (B.4), it follows that

$$\mathrm{E}\{z_n y_{n-k}\} = 0 \quad \text{(B.6)}$$

for $k = 1, \ldots, m-1$. Therefore, if the value of β is determined so that $\mathrm{E}(z_n y_{n-m}) = 0$ holds for $k = m$, the Yule-Walker equation of order m will be satisfied. For that purpose, from

$$\begin{aligned} &\mathrm{E}\left(z_n y_{n-m}\right) \\ &= \mathrm{E}\left\{ y_n - \sum_{j=1}^{m-1} \hat{a}_j^{m-1} y_{n-j} - \beta \left(y_{n-m} - \sum_{j=1}^{m-1} \hat{a}_j^{m-1} y_{n-m+j} \right) \right\} y_{n-m} \\ &= C_m - \sum_{j=1}^{m-1} \hat{a}_j^{m-1} C_{m-j} - \beta \left(C_0 - \sum_{j=1}^{m-1} \hat{a}_j^{m-1} C_j \right) = 0, \end{aligned} \quad \text{(B.7)}$$

β is determined as

$$\begin{aligned} \beta &= \left(C_0 - \sum_{j=1}^{m-1} \hat{a}_j^{m-1} C_j \right)^{-1} \left(C_m - \sum_{j=1}^{m-1} \hat{a}_j^{m-1} C_{m-j} \right) \\ &= \left(\sigma_{m-1}^2 \right)^{-1} \left(C_m - \sum_{j=1}^{m-1} \hat{a}_j^{m-1} C_{m-j} \right). \end{aligned} \quad \text{(B.8)}$$

Therefore, if we denote this β as $\hat{a}_m^m$ and define a_j^m by

$$\hat{a}_j^m \equiv \hat{a}_j^{m-1} - \hat{a}_m^m \hat{a}_{m-j}^{m-1}, \quad \text{(B.9)}$$

then from (B.5) – (B.7), we have

$$\mathrm{E}\left\{\left(y_n - \sum_{j=1}^{m} \hat{a}_j^m y_{n-j}\right) y_{n-k}\right\} = C_k - \sum_{j=1}^{m} \hat{a}_j^m C_{k-j} = 0 \tag{B.10}$$

for $k = 1, \ldots, m$.

In addition, the innovation variance of the AR model with order m can be expressed as

$$\begin{aligned}
\hat{\sigma}_m^2 &= C_0 - \sum_{j=1}^{m} \hat{a}_j^m C_j \\
&= C_0 - \sum_{j=1}^{m-1} \left(\hat{a}_j^{m-1} - \hat{a}_m^m \hat{a}_{m-j}^{m-1}\right) C_j - \hat{a}_m^m C_m \\
&= C_0 - \sum_{j=1}^{m-1} \hat{a}_j^{m-1} C_j - \hat{a}_m^m \left(C_m - \sum_{j=1}^{m-1} \hat{a}_{m-j}^{m-1} C_j\right) \\
&= \hat{\sigma}_{m-1}^2 - \hat{a}_m^m \left(C_m - \sum_{j=1}^{m-1} \hat{a}_{m-j}^{m-1} C_j\right). \qquad \text{(B.11)}
\end{aligned}$$

Using (B.8), it follows that $C_m - \sum_{j=1}^{m-1} \hat{a}_{m-j}^{m-1} C_j = \hat{a}_m^m \hat{\sigma}_{m-1}^2$ and then $\hat{\sigma}_m^2$ is obtained as follows:

$$\hat{\sigma}_m^2 = \hat{\sigma}_{m-1}^2 \left(1 - (\hat{a}_m^m)^2\right). \tag{B.12}$$

Appendix C

Derivation of the Kalman Filter and Smoother Algorithms

In this appendix, a brief derivation of the Kalman filter (Kalman (1960)) and the fixed interval smoothing algorithm (Bierman (1977)) are given.

C.1 Kalman Filter

[One-Step-Ahead Prediction]

From $x_n = F_n x_{n-1} + G_n v_n$, we obtain

$$\begin{aligned} x_{n|n-1} &= \mathrm{E}\,(x_n|Y_{n-1}) \\ &= \mathrm{E}\,(F_n x_{n-1} + G_n v_n|Y_{n-1}) \\ &= F_n \mathrm{E}\,(x_{n-1}|Y_{n-1}) \\ &= F_n x_{n-1|n-1}, \end{aligned} \tag{C.1}$$

$$\begin{aligned} V_{n|n-1} &= \mathrm{E}\,(x_n - x_{n|n-1})^2 \\ &= \mathrm{E}\,(F_n(x_{n-1} - x_{n-1|n-1}) + G_n v_n)^2 \\ &= F_n \mathrm{E}\,(x_{n-1} - x_{n-1|n-1})^2 F_n^T + G_n \mathrm{E}\,(v_n^2) G_n^T \\ &= F_n V_{n-1|n-1} F_n^T + G_n Q_n G_n^T, \end{aligned} \tag{C.2}$$

where for simplicity of notation, xx^T is abbreviated as x^2.

[Filter]

Denote the prediction error of y_n by ε_n; then from $y_n = H_n x_n + w_n$, it can be expressed as

$$\begin{aligned} \varepsilon_n &\equiv y_n - \mathrm{E}\,(y_n|Y_{n-1}) \\ &= H_n x_n + w_n - \mathrm{E}\,(H_n x_n + w_n|Y_{n-1}) \\ &= H_n x_n + w_n - H_n \mathrm{E}\,(x_n|Y_{n-1}) \\ &= H_n(x_n - x_{n|n-1}) + w_n. \end{aligned} \tag{C.3}$$

Therefore, we have

$$\begin{aligned} \mathrm{Var}(\varepsilon_n) &= H_n V_{n|n-1} H_n^T + R_n, &\text{(C.4)}\\ \mathrm{Cov}(x_n, \varepsilon_n) &= \mathrm{Cov}(x_n, H_n(x_n - x_{n|n-1}) + w_n) \\ &= \mathrm{Var}(x_n - x_{n|n-1}) H_n^T \\ &= V_{n|n-1} H_n^T. &\text{(C.5)}\end{aligned}$$

Using the facts that $Y_n = \{Y_{n-1}, y_n\} = Y_{n-1} \oplus \varepsilon_n$ and that in the case of the normal distribution, the conditional expectation of x_n given Y_n is expressible by orthogonal projection, it follows that

$$\begin{aligned} x_{n|n} = \mathrm{E}(x_n|Y_n) &= \mathrm{Proj}(x_n|Y_n) \\ &= \mathrm{Proj}(x_n|Y_{n-1}, \varepsilon_n) \\ &= \mathrm{Proj}(x_n|Y_{n-1}) + \mathrm{Proj}(x_n|\varepsilon_n). &\text{(C.6)}\end{aligned}$$

Because $\mathrm{Proj}(x_n|\varepsilon_n)$ is obtained by regressing x_n on ε_n, from (C.4) and (C.5),

$$\begin{aligned} \mathrm{Proj}(x_n|\varepsilon_n) &= \mathrm{Cov}(x_n, \varepsilon_n)\mathrm{Var}(\varepsilon_n)^{-1}\varepsilon_n \\ &= V_{n|n-1} H_n^T (H_n V_{n|n-1} H_n^T + R_n)^{-1} \varepsilon_n \\ &\equiv K_n \varepsilon_n. &\text{(C.7)}\end{aligned}$$

Therefore, we have

$$x_{n|n} = x_{n|n-1} + K_n \varepsilon_n. \tag{C.8}$$

In addition, from

$$\begin{aligned} V_{n|n-1} &= \mathrm{E}(x_n - x_{n|n-1})^2 \\ &= \mathrm{E}(x_n - x_{n|n} + K_n \varepsilon_n)^2 \\ &= V_{n|n} + K_n \mathrm{Var}(\varepsilon_n) K_n^T, &\text{(C.9)}\end{aligned}$$

we have

$$\begin{aligned} V_{n|n} &= V_{n|n-1} - K_n H_n V_{n|n-1} \\ &= (I - K_n H_n) V_{n|n-1}. &\text{(C.10)}\end{aligned}$$

C.2 Smoothing

$\delta_{n+1} \equiv x_{n+1} - x_{n+1|n}$ is assumed to be the prediction error of x_{n+1}. Define Z_n by

$$Z_n \equiv Y_n \oplus \delta_{n+1} \oplus \{v_{n+1}, \ldots, v_N, w_{n+1}, \ldots, w_N\}.$$

Then, we have the decomposition

$$\begin{aligned} z_n &\equiv \mathrm{Proj}(x_n|Z_n) \\ &= \mathrm{Proj}(x_n|Y_n) + \mathrm{Proj}(x_n|\delta_{n+1}) \\ &+ \mathrm{Proj}(x_n|v_{n+1},\ldots,v_N,w_{n+1},\ldots,w_N), \end{aligned} \tag{C.11}$$

and it follows that

$$\begin{aligned} &\mathrm{Proj}(x_n|Y_n) = x_{n|n} \\ &\mathrm{Proj}(x_n|\delta_{n+1}) = \mathrm{Cov}(x_n,\delta_{n+1})\mathrm{Var}(\delta_{n+1})^{-1}\delta_{n+1} \\ &\mathrm{Proj}(x_n|v_{n+1},\ldots,v_N,w_{n+1},\ldots,w_N) = 0. \end{aligned} \tag{C.12}$$

In addition, we have

$$\mathrm{Var}(\delta_{n+1}) = V_{n+1|n}, \tag{C.13}$$

$$\begin{aligned} \mathrm{Cov}(x_n,\delta_{n+1}) &= \mathrm{Cov}(x_n, F_{n+1}(x_n - x_{n|n}) + G_{n+1}v_{n+1}) \\ &= \mathrm{E}\,(x_n - x_{n|n})^2 F_{n+1}^T \\ &= V_{n|n}F_{n+1}^T. \end{aligned} \tag{C.14}$$

Therefore, by putting $A_n = V_{n|n}F_{n+1}^T V_{n+1|n}^{-1}$, we have

$$z_n = x_{n|n} + A_n(x_{n+1} - x_{n+1|n}). \tag{C.15}$$

Here, considering that Z_N generates Y_N, we obtain

$$\begin{aligned} x_{n|N} &= \mathrm{Proj}(x_n|Y_N) \\ &= \mathrm{Proj}(\mathrm{Proj}(x_n|Z_N)|Y_N) \\ &= \mathrm{Proj}(z_n|Y_N) \\ &= x_{n|n} + A_n(x_{n+1|N} - x_{n+1|n}). \end{aligned} \tag{C.16}$$

Further, using

$$x_n - x_{n|N} + A_n x_{n+1|N} = x_n - x_{n|n} + A_n x_{n+1|n}, \tag{C.17}$$

and $\mathrm{E}\left\{(x_n - x_{n|N})x_{n+1|N}^T\right\} = \mathrm{E}\left\{(x_n - x_{n|n})x_{n+1|n}^T\right\} = 0$, we obtain

$$V_{n|N} + A_n\mathrm{E}\left\{x_{n+1|N}x_{n+1|N}^T\right\}A_n^T = V_{n|n} + A_n\mathrm{E}\left\{x_{n+1|n}x_{n+1|n}^T\right\}A_n^T. \tag{C.18}$$

Here, using

$$
\begin{aligned}
\mathrm{E}\left\{(x_{n+1}-x_{n+1|N})x_{n+1|N}^T\right\} &= 0\\
\mathrm{E}\left\{(x_n-x_{n|n})x_{n+1|n}^T\right\} &= 0,
\end{aligned}
$$

we obtain

$$
\begin{aligned}
&\mathrm{E}\left\{x_{n+1|N}x_{n+1|N}^T\right\}\\
&\quad= \mathrm{E}\left\{(x_{n+1|N}-x_{n+1}+x_{n+1})(x_{n+1|N}-x_{n+1}+x_{n+1})^T\right\}\\
&\quad= V_{n+1|N}+\mathrm{E}\left\{x_{n+1}x_{n+1}^T\right\}+2\mathrm{E}\left\{(x_{n+1|N}-x_{n+1})x_{n+1}^T\right\}\\
&\quad= V_{n+1|N}+\mathrm{E}\left\{x_{n+1}x_{n+1}^T\right\}-2\mathrm{E}\left\{(x_{n+1|N}-x_{n+1})(x_{n+1|N}-x_{n+1})^T\right\}\\
&\quad= \mathrm{E}\left\{x_{n+1}x_{n+1}^T\right\}-V_{n+1|N}, \qquad \text{(C.19)}
\end{aligned}
$$

and

$$
\mathrm{E}\left\{x_{n+1|n}x_{n+1|n}^T\right\} = \mathrm{E}\left\{x_{n+1}x_{n+1}^T\right\}-V_{n+1|n}. \qquad \text{(C.20)}
$$

Substituting this into (C.18) yields

$$
V_{n|N} = V_{n|n}+A_n(V_{n+1|N}-V_{n+1|n})A_n^T. \qquad \text{(C.21)}
$$

Appendix D

Algorithm for the Monte Carlo Filter

This appendix presents a derivation of the Monte Carlo filter algorithm. The readers are referred to Kitagawa (1996) and Doucet et al. (2001) for details.

D.1 One-Step-Ahead Prediction

Assume that m particles $\{f_{n-1}^{(1)},\ldots,f_{n-1}^{(m)}\}$ that can be considered as m independent realizations from the conditional distribution $p(x_{n-1}|Y_{n-1})$ of the state x_{n-1}, and m particles $\{v_n^{(1)},\ldots,v_n^{(m)}\}$ from the system noise density $p(v)$ are given. Namely, assume that

$$f_{n-1}^{(i)} \sim p(x_{n-1}|Y_{n-1}), \quad v_n^{(i)} \sim q(v). \tag{D.1}$$

Then, it can be shown that the one-step-ahead predictive distribution of x_n is given by

$$\begin{aligned} &p(x_n|Y_{n-1}) \\ &\quad = \int\int p(x_n,x_{n-1},v_n|Y_{n-1})dx_{n-1}dv_n \qquad \text{(D.2)} \\ &\quad = \int\int p(x_n|x_{n-1},v_n,Y_{n-1})p(v_n|x_{n-1},Y_{n-1})p(x_{n-1}|Y_{n-1})dx_{n-1}dv_n. \end{aligned}$$

Since the system noise v_n is independent of past states and observations, the conditional distribution of the system noise satisfies $p(v_n|x_{n-1},Y_{n-1}) = p(v_n)$. On the other hand, since x_n depends only on x_{n-1} and v_n, $p(x_n|x_{n-1},v_n,Y_{n-1}) = p(x_n|x_{n-1},v_n) = \delta(x_n - F(x_{n-1},v_n))$, and we have

$$p(x_n|Y_{n-1}) = \int\int \delta(x_n - F(x_{n-1},v_n))p(v_n)p(x_{n-1}|Y_{n-1})dx_{n-1}dv_n. \tag{D.3}$$

Therefore, when realizations $\{v_n^{(j)}\}$ of $p(v_n)$ and $\{f_{n-1}^{(j)}\}$ of $p(x_{n-1}|Y_{n-1})$ are given, realizations $\{p_n^{(j)}\}$ of $p(x_n|Y_{n-1})$ are obtained by

$$p_n^{(j)} = F(f_{n-1}^{(j)},v_n^{(j)}). \tag{D.4}$$

D.2 Filter

When m independent realizations $p_n^{(1)},\ldots,p_n^{(m)}$ of the distribution $p(x_n|Y_{n-1})$ are given, it is equivalent to approximate the distribution $p(x_n|Y_{n-1})$ by the empirical distribution function

$$P_n(x) = \frac{1}{m}\sum_{i=1}^{m} I(x, p_n^{(i)}), \tag{D.5}$$

where $I(x,a) = 0$ for $x < a$ and $I(x,a) = 1$ otherwise. This means that the predictive distribution $p(x_n|Y_{n-1})$ is approximated by the probability function

$$\Pr(x_n = p_n^{(j)}|Y_{n-1}) = \frac{1}{m}, \qquad \text{for } j = 1,\ldots,m. \tag{D.6}$$

Then, given the observation y_n, the posterior distribution of x_n is obtained by

$$\begin{aligned} \Pr(x_n = p_n^{(j)}|Y_n) &= \Pr(x_n = p_n^{(j)}|Y_{n-1}, y_n) \\ &= \lim_{\Delta y \to 0} \frac{\Pr(x_n = p_n^{(j)}, y_n \le y \le y_n + \Delta y|Y_{n-1})}{\Pr(y_n \le y \le y_n + \Delta y|Y_{n-1})} \\ &= \frac{p(y_n|p_n^{(j)})\Pr(x_n = p_n^{(j)}|Y_{n-1})}{\sum_{i=1}^{m} p(y_n|p_n^{(i)})\Pr(x_n = p_n^{(i)}|Y_{n-1})} \\ &= \frac{\alpha_n^{(j)} \cdot \frac{1}{m}}{\sum_{i=1}^{m} \alpha_n^{(i)} \cdot \frac{1}{m}} = \frac{\alpha_n^{(j)}}{\sum_{i=1}^{m} \alpha_n^{(i)}}. \end{aligned} \tag{D.7}$$

The cumulative distribution function

$$\frac{1}{\sum_{i=1}^{m} \alpha_n^{(i)}} \sum_{i=1}^{m} \alpha_n^{(i)} I(x, p_n^{(i)}) \tag{D.8}$$

corresponding to this $\Pr(x_n = p_n^{(j)}|Y_n)$ has jumps with jump sizes proportional to $\alpha_n^{(1)},\ldots,\alpha_n^{(m)}$ given by the right-hand side of the equation (15.9) only at the m points $p_n^{(1)},\ldots,p_n^{(m)}$.

Although the approximation of the distribution of the filter was obtained using this expression (D.8), it is convenient to re-approximate it by m particles $f_n^{(1)},\ldots,f_n^{(m)}$ with equal weights to perform the computation of the prediction (D.1) in the next time step. This corresponds to representing the distribution of (D.8) by the empirical distribution function

$$\frac{1}{m}\sum_{i=1}^{m} I(x, f_n^{(i)}). \tag{D.9}$$

The m realizations $\{f_n^{(1)},\ldots,f_n^{(m)}\}$ can be obtained by re-sampling $\{p_n^{(1)},\ldots,p_n^{(m)}\}$ with probabilities

$$\Pr(f_n^{(j)} = p_n^{(i)}|Y_n) = \frac{\alpha_n^{(i)}}{\alpha_n^{(1)}+\cdots+\alpha_n^{(m)}}, \qquad j=1,\ldots,m. \tag{D.10}$$

D.3 Smoothing

For smoothing, assume that $\Pr(x_1 = s_{1|n-1}^{(j)},\ldots,x_{n-1} = s_{n-1|n-1}^{(j)}|Y_{n-1}) = 1/m$ and $v_n^{(j)} \sim q(v)$ and define $(p_{1|n-1}^{(j)},\ldots,p_{n|n-1}^{(j)})$ as follows:

$$p_{i|n-1}^{(j)} = \begin{cases} s_{i|n-1}^{(j)}, & \text{for } i=1,\ldots,n-1 \\ F(s_{n-1|n-1}^{(j)}, v_n^{(j)}), & \text{for } i=n. \end{cases} \tag{D.11}$$

Then, $(p_{1|n-1}^{(j)},\ldots,p_{n|n-1}^{(j)})$ can be considered as a realization from the joint distribution of $(x_1,\ldots,x_n)$ when the observation Y_{n-1} is given. Next, given the observation y_n, the distribution $\Pr(x_1 \le p_{1|n-1}^{(j)},\ldots,x_n \le p_{n|n-1}^{(j)}|Y_{n-1})$ can be updated as follows:

$$\begin{aligned}
&\Pr(x_1 = p_{1|n-1}^{(j)},\ldots,x_n = p_{n|n-1}^{(j)}|Y_n) \\
&= \Pr(x_1 = p_{1|n-1}^{(j)},\ldots,x_n = p_{n|n-1}^{(j)}|Y_{n-1},y_n) \\
&= \frac{p(y_n|x_1 = p_{1|n-1}^{(j)},\ldots,x_n = p_{n|n-1}^{(j)})}{p(y_n|Y_{n-1})} \\
&\quad \times \Pr(x_1 = p_{1|n-1}^{(j)},\ldots,x_n = p_{n|n-1}^{(j)}|Y_{n-1}) \\
&= \frac{p(y_n|p_{n|n-1}^{(j)})\Pr(x_1 = p_{1|n-1}^{(j)},\ldots,x_n = p_{n|n-1}^{(j)}|Y_{n-1})}{p(y_n|Y_{n-1})}.
\end{aligned} \tag{D.12}$$

Since $p_{n|n-1}^{(j)}$ is the same as the particle $p_n^{(j)}$ of the filter algorithm

(D.5), the smoothing distribution $p(x_1,\ldots,x_n|Y_n)$ can be obtained by re-sampling m n-dimensional vectors $(p_{1|n-1}^{(j)},\ldots,p_{n|n-1}^{(j)})^T$, $j=1,\ldots,m$ with the same weights as the filter.

Answers to the Problems

Chapter 1

1. It is important to select the sampling interval appropriately. If it is too wide, it is not possible to capture the features of the continuous time series. On the other hand, if it is too narrow, many parameters in the modeling may be used up on nonessentials, thus preventing effective representation of the time series. A rough rule of thumb is to set the sampling interval as $1/5$ to $1/10$ of the dominant period.

2. (An example.) Time series obtained by recording the sales amount of instant coffee at a store. Since values are non-negative, the distribution of the time series is asymmetric. Also this series may suddenly increase due to discounting or due to promotion activities.

3.(1) By solving (1.1) with respect to y, we obtain $y = e^z/(1+e^z)$.

(2) $z = \log\{(y-a)/(b-y)\}$, and the inverse transformation is given by $y = (a+be^z)/(1+e^z)$.

4. If the time series contains observation noise and is expressed as $y_n = a + bn + \varepsilon_n$, the difference of y_n becomes $\Delta y_n = b + \varepsilon_n - \varepsilon_{n-1}$. Therefore, although the trend component is removed, the noise components become more complex.

5. The corrected value of this year is affected by the change of the trend in the previous year. For example, if the slope of the trend increased in the middle of the previous year, the annual rate looks as if it decreased from the middle of this year.

6.(1) Assume that $y_n = T_n + w_n$, $T_n = a + bn$, and $w_n \sim N(0,\sigma^2)$ is a white noise, then

$$\begin{aligned}\hat{T}_n &= \frac{1}{3}(y_{n-1}+y_n+y_{n+1}) \\ &= \frac{1}{3}(T_{n-1}+T_n+T_{n+1}) + \frac{1}{3}(w_{n-1}+w_n+w_{n+1}).\end{aligned}$$

Here, the first term on the right-hand side is T_n. On the other hand, the mean of the second term is 0 and from $E(w_{n-1}+w_n+w_{n+1})^2 = 3\sigma^2$, the variance becomes $\sigma^2/3$.

(2) By setting the number of terms large, we can get smoother estimates. On the other hand, this makes it difficult to detect sudden structural changes and estimates may become sensitive to outlying observations. The moving median has the opposite properties.

Chapter 2

1. A Gaussian distribution is completely specified by its mean and variance. Therefore, if the mean and the variance are time-invariant, this also means that the distribution is time-invariant and becomes strongly stationary.

2. Consider a time series with a standard Cauchy distribution. Then obviously, it is strongly stationary. However, since the Cauchy distribution does not have a mean or variance, the series cannot be weakly stationary.

3. $C_k = E(y_n - \mu)(y_{n+k} - \mu) = E(y_{n+k} - \mu)(y_n - \mu) = E(y_n - \mu)(y_{n-k} - \mu) = C_{-k}$. The third equality holds only for a stationary time series y_n.

4. $C_0 = Ey_n^2 = Ev_n^2 - 2cEv_nv_{n-1} + c^2Ev_{n-1}^2 = 1 + c^2$, $C_1 = E(v_n - cv_{n-1})(v_{n-1} - cv_{n-2}) = -c$, $C_k = 0\ (k \geq 2)$.

5. For arbitrary $\alpha = (\alpha_1, \ldots, \alpha_k)$ with not all components zero,

$$\begin{aligned} \alpha C \alpha^T &= \sum_{i=1}^{k}\sum_{j=1}^{k} \alpha_i\alpha_j C_{i-j} = \sum_{i=1}^{k}\sum_{j=1}^{k} \alpha_i\alpha_j E(y_{n-i}y_{n-j}) \\ &= E\left(\sum_{i=1}^{k} \alpha_i y_{n-i}\right)^2 \geq 0 \end{aligned}$$

6.(1) By taking the expectation of both sides,

$$E[\hat{C}_k(i,j)] = \frac{1}{N}\sum_{n=k+1}^{N} C_k(i,j) = \frac{N-k}{N}C_k(i,j)$$

(2) Since the sample autocovariance function defined by (2.21) is positive semi-definite, it has the significant advantage that the estimated AR models always become stationary. If N is replaced by $N-k$, we can get an unbiased estimate of $C_k(i-j)$. Instead however, we lose the advantage above of stationarity.

7.(1) When the sample size is n, $\hat{C}_0 \sim N(0, 2\sigma^4/n)$, $\hat{C}_k \sim N(0, \sigma^4/n)$, $\hat{R}_k \sim N(0, n^{-1})$.

(2) For all k, check if $|\hat{R}_k| < \frac{\alpha}{\sqrt{n}}$ holds. For example. α can be set equal to 2.

Chapter 3

1. From the expression $e^{-2\pi ikf} = \cos(2\pi kf) - i\sin(2\pi kf)$, we have $p(f) = \sum_{k=-\infty}^{\infty} C_k \cos(2\pi kf) - i \sum_{k=-\infty}^{\infty} C_k \sin(2\pi kf)$. Here, since C_k is an even function and $\sin(2\pi kf)$ is an odd function, $C_k \sin(2\pi kf)$ becomes an odd function and the second term on the right-hand side of the above equation becomes 0.
2. $p(f) = 1 + C^2 - 2C\cos(2\pi f)$
3.

$$\begin{aligned} p(f) &= \sum_{k=-\infty}^{\infty} C_k e^{-2\pi ikf} = \frac{\sigma^2}{1-a^2} \sum_{k=-\infty}^{\infty} a^{|k|} e^{-2\pi ikf} \\ &= \frac{\sigma^2}{1-a^2}\left(\frac{1}{1-ae^{-2\pi if}} + \frac{1}{1-ae^{2\pi if}} - 1 \right) \\ &= \frac{\sigma^2}{1-a^2} \frac{1-a^2}{|1-ae^{-2\pi if}|^2} = \frac{\sigma^2}{|1-ae^{-2\pi if}|^2} \end{aligned}$$

4.

$$\begin{aligned} &\frac{1}{N}\left| \sum_{n=1}^{N} y_n \exp(-2\pi i(n-1)j/N) \right|^2 \\ &\quad = \frac{1}{N} \sum_{n=1}^{N} \sum_{m=1}^{N} y_n y_m \exp(-2\pi i(n-1)j/N) \exp(2\pi i(m-1)j/N) \\ &\quad = \frac{1}{N}\left\{ \sum_{n=1}^{N} y_n^2 + 2 \sum_{k=1}^{N-1} \sum_{n=k+1}^{N} y_n y_{n-k} \exp(-2\pi ikj/N) \right\} \\ &\quad = \hat{C}_0 + 2 \sum_{k=1}^{N-1} \hat{C}_k \exp(-2\pi ikj/N) \end{aligned}$$

5. By taking the expectation of both sides of (3.9),

$$\begin{aligned} E[\hat{p}(f)] &= \sum_{k=1-N}^{N-1} E[\hat{C}_k] e^{-2\pi ikf} = \sum_{k=1-N}^{N-1} \frac{N-|k|}{N} C_k e^{-2\pi ikf} \\ &= \sum_{k=1-N}^{N-1} C_k e^{-2\pi ikf} - \frac{1}{N} \sum_{k=1-N}^{N} |k| C_k e^{-2\pi ikf} \end{aligned}$$

Chapter 4

1. The log-likelihood is given by $\ell = \sum_{i=1}^{n} \log f(m_i|\lambda) = \sum_{i=1}^{n} \{-\lambda + m_i \log\lambda - \log m_i!\}$. Therefore, from

$$\frac{\partial \ell}{\partial \lambda} = \sum_{i=1}^{n}\left\{-1+\frac{m_i}{\lambda}\right\} = -n + \frac{1}{\lambda}\sum_{i=1}^{n} m_i = 0$$

we have $\hat{\lambda} = n^{-1}\sum_{i=1}^{n} m_i$.

2.(1)

$$\begin{aligned}
\hat{\mu}_0 &= \frac{1}{n+m}\left(\sum_{i=1}^{n} x_i + \sum_{i=1}^{m} y_i\right), \ \hat{\mu}_1 = \frac{1}{n}\sum_{i=1}^{n} x_i, \ \hat{\mu}_2 = \frac{1}{m}\sum_{i=1}^{m} y_i, \\
\hat{\sigma}_0^2 &= \frac{1}{n+m}\left(\sum_{i=1}^{n}(x_i-\hat{\mu}_0)^2 + \sum_{i=1}^{m}(y_i-\hat{\mu}_0)^2\right), \\
\hat{\tau}_0^2 &= \frac{1}{n+m}\left(\sum_{i=1}^{n}(x_i-\hat{\mu}_1)^2 + \sum_{i=1}^{m}(y_i-\hat{\mu}_2)^2\right).
\end{aligned}$$

Then by comparing

$$\mathrm{AIC}_0 = (n+m)(\log 2\pi\hat{\sigma}_0^2 + 1) + 2\times 2$$

$$\mathrm{AIC}_1 = (n+m)(\log 2\pi\hat{\tau}_0^2 + 1) + 2\times 3$$

and if $\mathrm{AIC}_0 < \mathrm{AIC}_1$, then this means that we can consider the two means to be identical.

(2) $\hat{\sigma}_1^2 = \frac{1}{n}\sum_{i=1}^{n}(x_i-\hat{\mu}_0)^2$, $\hat{\sigma}_2^2 = \frac{1}{m}\sum_{i=1}^{m}(y_i-\hat{\mu}_0)^2$, $\mathrm{AIC}_2 = n(\log 2\pi\hat{\sigma}_1^2 + 1) + m(\log 2\pi\hat{\sigma}_2^2 + 1) + 2\times 3$. If $\mathrm{AIC}_0 < \mathrm{AIC}_2$, then the two variances can be considered identical. Here, from $\sum_{k=-\infty}^{\infty}|C_k| < \infty$, for arbitrary $\varepsilon > 0$, there exists an integer m that satisfies $\sum_{k=m+1}^{\infty}|C_k| < \varepsilon/2$. Then, we have

$$\begin{aligned}
\left|\frac{1}{N}\sum_{k=-\infty}^{\infty}|k|C_k e^{-2\pi ikf}\right| &\le \frac{2}{N}\sum_{k=1}^{\infty}k|C_k| \le \frac{2}{N}\sum_{k=1}^{m}kC_0 + 2\sum_{k=m+1}^{\infty}\frac{k}{N}|C_k| \\
&\le \frac{2}{N}\frac{m(m+1)}{2}C_0 + \varepsilon
\end{aligned}$$

Since by taking N sufficiently large, the first term on the right-hand side of the equation can be made arbitrarily small, it follows that $E\left[\hat{p}(f)\right] \to p(f)$.

3. Putting $\hat{\mu} = \dfrac{1}{n}\displaystyle\sum_{i=1}^{n} y_i$, $\hat{\sigma}^2 = \dfrac{1}{n}\displaystyle\sum_{i=1}^{n}(y_i - \hat{\mu})^2$, the value of the AIC for the Gaussian distribution model is obtained by $\mathrm{AIC}_0 = n\log 2\pi\hat{\sigma}^2 + n + 2\times 2$. On the other hand, the AIC value for the Cauchy model is obtained by $\mathrm{AIC}_1 = n\log\hat{\tau}^2 - 2n\log\pi - \sum_{i=1}^{n}\log\{(y_i-\hat{\mu})^2 + \hat{\tau}^2\} + 2\times 2$, where $\hat{\mu}$ and $\hat{\tau}^2$ are obtained by maximizing (4.36). Then, if $\mathrm{AIC}_0 < \mathrm{AIC}_1$, the Gaussian model is considered to be better.

4.(1) For the binomial distribution model $f(m|n,p) = {}_nC_m p^m(1-p)^{n-m}$, the log-likelihood is defined by $\ell(p) = \log{}_nC_m + m\log p + (n-m)\log(1-p)$. Therefore, from $\dfrac{d\ell}{dp} = 0$, $\dfrac{m}{p} - \dfrac{n-m}{1-p} = 0$, we obtain $\hat{p} = m/n$.

(2) The AIC value for the model (1) is obtained by $\mathrm{AIC}_1 = -2\log{}_nC_m - 2m\log\hat{p} - 2(n-m)\log(1-\hat{p}) + 2$. On the other hand, if we assume equal probabilities, taking $p = 1/2$, we obtain $\mathrm{AIC}_0 = -2\log{}_nC_m + 2n\log 2$. Here, if $\mathrm{AIC}_0 < \mathrm{AIC}_1$, we can consider that the equal probability model is better.

5. From $\dfrac{d}{d\theta}\log f(y|\theta) = f(y|\theta)^{-1}\dfrac{df(y|\theta)}{d\theta}$, we have

$$\begin{aligned}
\frac{d^2}{d\theta^2}\log f(y|\theta) &= \frac{d}{d\theta}\left(\frac{d}{d\theta}\log f(y|\theta)\right)\\
&= \frac{d}{d\theta}\left(f(y|\theta)^{-1}\frac{df}{d\theta}\right)\\
&= -f(y|\theta)^{-2}\left(\frac{df}{d\theta}\right)^2 + f(y|\theta)^{-1}\frac{d^2f}{d\theta^2}\\
&= -\left(\frac{d}{d\theta}\log f(y|\theta)\right)^2 + f(y|\theta)^{-1}\frac{d^2f}{d\theta^2}.
\end{aligned}$$

Therefore,

$$\begin{aligned}
J &= -E\left[\frac{d^2}{d\theta^2}\log f(y|\theta)\right]\\
&= E\left(\frac{d}{d\theta}\log f(y|\theta)\right)^2 - E\left[f(y|\theta)^{-1}\frac{d^2f}{d\theta^2}\right]
\end{aligned}$$

$$= \quad I - \int_{-\infty}^{\infty} \frac{d^2 f}{d\theta^2} dy = I - \frac{d^2}{d\theta^2} \int_{-\infty}^{\infty} f(y|\theta) dy = I$$

6. From $z = k(y) = \log y$, $f(z) = (2\pi\sigma^2)^{-1} \exp\{-(z-\mu)^2/2\sigma^2\}$, and we have $\dfrac{dk}{dy} = y^{-1}$. Therefore,
$g(y) = \left|\frac{dk}{dy}\right| f(k(y)) = \frac{1}{y} \frac{1}{\sqrt{2\pi\sigma^2}} e^{-\frac{(\log y - \mu)^2}{2\sigma^2}}$.

Chapter 5

1. Let $\hat{\mu}$ denote the maximum likelihood estimate of μ. Since the number of parameters is 1, the AIC is obtained by

$$\mathrm{AIC} = n \log 2\pi\sigma^2 - \frac{1}{\sigma^2} \sum_{i=1}^{n} (y_i - \hat{\mu})^2 + 2.$$

2.(1) From $S = \sum_{n=1}^{N} (y_n - ax_n^2 - bx_n)^2$,

$$\begin{aligned}
\frac{dS}{da} &= -2 \sum_{n=1}^{N} x_n^2 (y_n - ax_n^2 - bx_n) \\
&= -2 (\sum_{n=1}^{N} x_n^2 y_n - a \sum_{n=1}^{N} x_n^2 - b \sum_{n=1}^{N} x_n^3) = 0 \\
\frac{dS}{db} &= -2 \sum_{n=1}^{N} x_n (y_n - ax_n^2 - bx_n) \\
&= -2 (\sum_{n=1}^{N} x_n y_n - a \sum_{n=1}^{N} x_n^3 - b \sum_{n=1}^{N} x_n^2) = 0.
\end{aligned}$$

Solving these, we have

$$\begin{aligned}
\hat{a} &= \frac{\sum x_n^2 y_n \sum x_n^2 - \sum x_n y_n \sum x_n^3}{\sum x_n^4 \sum x_n^2 - (\sum x_n^3)^2} \\
\hat{b} &= \frac{\sum x_n y_n \sum x_n^4 - \sum x_n^2 y_n \sum x_n^3}{\sum x_n^4 \sum x_n^2 - (\sum x_n^3)^2}.
\end{aligned}$$

(2) $y_n = ax_n(x_n - b) + \varepsilon_n$. By minimizing $S = \sum_{n=1}^{N} (y_n - ax_n^2 - abx_n)^2$ with respect to the two parameters a and b by a numerical optimization procedure, we can obtain the least squares estimates.

Chapter 6

1.(1) Putting $m = 1$ in equation (6.21), the stationarity condition is that the root of $1 - a_1 B = 0$ lies outside the unit circle. Therefore, from $|B| = |a_1^{-1}| > 1$, we have $|a_1| < 1$.

(2) Putting $m = 2$ in equation (6.21), the roots are obtained by $B = (a_1 \pm \sqrt{a_1^2 + 4a_2})/2$. Therefore, the stationarity conditions are that $a_1^2 + 4a_2 \geq 0$, $a_2 < 1 - a_1$ and $a_2 < 1 + a_1$ for $a_1^2 + 4a_2 < 0$, $a_2 > -1$. Therefore, the region satisfying the stationarity condition is a triangle surrounded by three lines $a_2 < 1 - a_1$, $a_2 < 1 + a_1$ and $a_2 > -1$.

2.(1) σ^2

(2) From $y_{n+2} = ay_{n+1} + v_{n+2} = a^2 y_n + av_{n+1} + v_{n+2}$, we have $y_{n+2|n} = a^2 y_n$. Therefore, $E\,(y_{n+2} - y_{n+2|n})^2 = a^2 E v_{n+1}^2 + E v_{n+2}^2 = (1 + a^2)\sigma^2$.

(3) It can be expressed as $y_{n+k} = v_{n+k} + g_1 v_{n+k-1} + g_2 v_{n+k-2} + \cdots$. Here, from the impulse response function of AR(1), $g_i = a^i$. Then, since we can express $y_{n+k|n} = g_k v_n + g_{k+1} v_{n+1} + \cdots$, we have

$$\begin{aligned} E\,(y_{n+k} - y_{n+k|n})^2 &= E\,(v_{n+k} + g_1 v_{n+k-1} + \cdots + g_{k-1} v_{n+1})^2 \\ &= (1 + g_1^2 + \cdots + g_{k-1}^2)\sigma^2 \\ &= (1 + a^2 + \cdots + a^{2(k-1)})\sigma^2 = \frac{1 - a^{2k}}{1 - a^2}\sigma^2. \end{aligned}$$

3.(1) From $C_0 = -0.9C_1 + 1$, $C_1 = -0.9C_0$, we have $C_0 = 0.81C_0 + 1$, $C_0 = 1/0.19 = 5.26$, $C_k = 5.26 \times (-0.9)^k$.

(2) $C_0 = 25/7, C_1 = 75/28, C_3 = 15/14, C_4 = -9/28$.

(3) $C_0 = 1 + b^2, C_1 = -b, C_k = 0\ (k > 1)$.

(4) Putting $E[y_n v_{n-k}] = g_k$, we have $g_0 = 1$, $g_1 = a - b$. Therefore, from $C_0 = aC_1 + g_0 - bg_1$, $C_1 = aC_0 - bg_0$, we have

$$C_0 = \frac{1 - 2ab + b^2}{1 - a^2}, \qquad C_k = \frac{(1 - ab)(a - b)}{1 - a_2} a^{k-1}.$$

4.(1) Substituting $v_n = y_n - ay_{n-1}$ into both sides of $v_n = bv_{n-1} + w_n$, yields

$$y_n = (a + b)y_{n-1} - ab y_{n-2} + w_n,$$

and we obtain an AR model of order 2.

(2) The autocovariance function of y_n is given by $a^k(1-a^2)^{-1}$, $k = 0,1,2,3$. Therefore, $C_0 = (1-a^2)^{-1} + 0.01$, $C_k = a^k(1-a^2)^{-1}$.

5.(1) Substituting $C_0 = 1+b^2$, $C_1 = -b$, $C_k = 0$ and $k > 1$ into $p(f) = \sum_{k=-\infty}^{\infty} C_k e^{-2\pi ikf}$, we have $p(f) = (1+b^2) - be^{-2\pi if} - be^{2\pi if} = |1-be^{-2\pi if}|^2$.

(2) From $dp/df = -4\pi a\sin(2\pi f)/\{1-2a\cos(2\pi f)+a^2\}^2 = 0$, we have $\sin(2\pi f) = 0$. This means that the maximum (or minimum) of the spectrum is attained either at $f = 0$ or $1/2$. If $a > 0$, it has a maximum at $f = 0$ and a minimum at $f = 1/2$. If $a < 0$, they are the other way around.

6. For $y_n = v_n - bv_{n-1} = (1-bB)v_n$, since $(1-bB)^{-1} = 1+bB+b^2B^2+\cdots$, we obtain an AR model of infinite order $y_n = -by_{n-1} - b^2y_{n-1} - \cdots + v_n$.

7.(1) From $y_{n+1|n} = -bv_n$ and $y_{n+k|n} = 0$, we have $E\varepsilon^2_{n+1|n} = 1$, $E(\varepsilon^2_{n+k|n}) = 1+b^2$ $(k \geq 1)$.

(2) $y_n = v_n av_{n-1} + a^2v_{n-2} + \cdots$, $E(\varepsilon^2_{n+k|n}) = 1+a^2+\cdots+a^{2(k-1)}$.

(3) From $y_n = v_n + v_{n-1} + v_{n-2} + \cdots$, we have $E(\varepsilon^2_{n+k|n}) = k$.

8.(1) From $y_{n+1|n} = -bv_n$ and $y_{n+k|n} = 0$, it follws that $E(\varepsilon^2_{n+1|n}) = 1$ and $E(\varepsilon^2_{n+k|n}) = 1+b^2$ $(k \geq 1)$.

(2) Since $y_{n+k} = v_{n+k} + av_{n+k-1} + a^2v_{n+k-2} + \cdots$ and $y_{n+k|n} = a^kv_n + a^{n-1}v_{n-1} + \cdots$, it follows that $\varepsilon_{n+k|n} = v_{n+k} + av_{n+k-1} + \cdots + a^{k-1}v_{n+1}$. Therefore, we have $E(\varepsilon^2_{n+k|n}) = 1+a^2+\cdots+a^{2(k-1)}$.

(3) Since $y_{n+k} = v_{n+k} + v_{n+k-1} + v_{n+k-2} + \cdots$ and $y_{n+k|n} = v_n + v_{n-1} + \cdots$, we have $\varepsilon_{n+k|n} = v_{n+k} + v_{n+k-1} + \cdots + v_{n+1}$. Therefore, $E(\varepsilon^2_{n+k|n}) = k$.

Chapter 7

1.(1) $\mathrm{AIC}_m = N(\log 2\pi\hat{\sigma}^2_{n-1} + \log(1-(a^m_m)^2) + 2(m+1) = \mathrm{AIC}_{m-1} + N\log(1-(a^m_m)^2) + 2$. Therefore, if $N\log(1-(a^m_m)^2)+2 < 0$, i.e., if $(a^m_m)^2 > 1-e^{-2/N}$, then we can conclude that AR(m) is better than AR$(m-1)$.

(2) $\sigma_1^2 = (1-0.9^2)\times 1 = 0.19$, $\sigma_2^2 = 0.1216$, $\sigma_3^2 = 0.1107$, $\sigma_4^2 = 0.1095$, $\sigma_5^2 = 0.1071$ (displayed up to the 4th decimal place)

(3) $\mathrm{AIC}_0 = 100(\log 2\pi \times 1+) + 2\times 1 = 285.78$
$\mathrm{AIC}_1 = 100(\log 2\pi \times 0.19 + 1) + 2\times 2 = 121.71$

$\mathrm{AIC}_2 = 79.09$, $\mathrm{AIC}_3 = 71.65$, $\mathrm{AIC}_4 = 72.65$, $\mathrm{AIC}_5 = 72.37$. Therefore, the third order model is considered best.

2. The Yule-Walker method has the advantage that it always yields a stationary model. On the other hand, it may have large bias, especially for small sample sizes. These properties are due to the implicit assumption that the time series takes a value 0 outside the actually observed interval. The least squares method has the advantage that it provides us with estimates having a small bias and that it is easy to pool additional data and perform various manipulations for fitting a more sophisticated model. On the other hand, it has problems in that stationarity is not guaranteed, and with parameter estimation, the first several observations are used only for conditioning and cannot be directly used for parameter estimation. In AR model estimation, the PARCOR method is very efficient in terms of computation and yields very close estimates as maximum likelihood estimates.
3. Fit a univariate AR model to each time series x_n and y_n, and obtain AIC_x and AIC_y, respectively. On the other hand, fit a 2-variate AR model to $(x_n, y_n)^T$ and compute AIC_0. Then, if $\mathrm{AIC}_x + \mathrm{AIC}_y < \mathrm{AIC}_0$, x_n and y_n are considered independent.

Chapter 8

1. Consider an AR model $y_n = \mu + a_1 y_{n-1} + \cdots + a_m y_{n-m} + v_n$, which has an additional parameter corresponding to the mean of the process.
2. Compare the following two models; the switched model $N(0, \sigma_1^1)$ for $n = 1, \ldots, k$ and $N(0, \sigma_2^1)$, and the stationary model $y_n \sim N(0, \sigma_0^2)$ for $n = 1, \ldots, N$. The AIC values of the models are, respectively, given by

$$\begin{aligned} \mathrm{AIC}_{12} &= N \log 2\pi + k \log \hat{\sigma}^2 + (N-k) \log \hat{\sigma}_2^2 + N + 2 \times 2 \\ \mathrm{AIC}_0 &= N \log 2\pi + N \log \hat{\sigma}_0^2 + N + 2. \end{aligned}$$

   If $\mathrm{AIC}_{12} < \mathrm{AIC}_0$, it is considered that the variance changed at $n = k+1$.
3. Assume that $y_n = a_0 + a_1 x_n + \cdots + a_p x_n^p + \varepsilon_n$ for $n = 1, \ldots, k$, and that $y_n = b_0 + b_1 x_n + \cdots + a_q x_n^q + \delta_n$ for $n = k+1, \ldots, N$, where $\varepsilon_n \sim N(0, \sigma_1^2), \delta_n \sim N(0, \sigma_2^2)$

$$\mathrm{AIC} = N \log 2\pi + k \log \hat{\sigma}_1^2 + (N-k) \log \hat{\sigma}_2^2 + N + 2 \times (p+q+4).$$

4. To ensure continuity of the trend, require the parameters to satisfy

$$a_0 + a_1 k + \cdots + a_p k^p = b_0 + b_1 k + \cdots + b_q k^q.$$

To ensure smoothness of the trend, apply the further restriction

$$a_0 + 2a_1 k + \cdots + p a_p k^p = b_0 + 2b_1 k + \cdots + q b_q k^q.$$

Note that in computing AIC, the number of free parameters is decreased by 1 and 2, respectively.

5. The amount of computation in fitting an ordinary AR model is roughly $Nm^2/2$. On the other hand, the two locally stationary AR models need

$$\frac{1}{2} n_0 m^2 + \frac{n_1 - n_0}{p}\frac{1}{2}(p+1)m^2$$
$$\frac{1}{2}(N - n_1)m^2 + \frac{n_1 - n_0}{p}\frac{1}{2}(p+1)m^2,$$

respectively. Therefore, the total amount of computation required is evaluated as

$$\frac{1}{2}Nm^2 + \frac{1}{2}(n_1 - n_0)m^2 + \frac{n_1 - n_0}{p}m^2.$$

Even for $p = 1$, when the maximum of the sum of the second and third terms is attained with a value of $3/2(n_1 - n_0)m^2$, the increase in the amount of computation is at most three times that of the original AR model.

Chapter 9

1. Multiplying by T from the left on both sides of (9.1), we obtain $Tx_n = TF_n x_n + TG_n v_n = TF_n T^{-1} T x_n + TG_n v_n$. Then, putting $z_n = Tx_n$ and using $y_n = H_n x_n + w_n = H_n T^{-1} T x_n + w_n$, we can verify that we obtain an equivalent representation.

2.(1)

$$\begin{aligned} \text{Initial value} &: \ x_{0|0} = 0, V_{0|0} = 100 \\ \text{Prediction} &: \ x_{n|n-1} = x_{n-1|n-1}, V_{n|n-1} = V_{n-1|n-1} + \tau^2 \\ \text{Filter} &: \ G_n = V_{n|n-1}/(V_{n|n-1} + 1), \\ &\quad\ x_{n|n} = x_{n|n-1} + G_n(y_n - x_{n|n-1}), \\ &\quad\ V_{n|n} = (1 - G_n)V_{n|n-1} = G_n. \end{aligned}$$

(2) $V_{n+1|n} = V_{n|n-1}/(V_{n|n-1} + 1) + \tau^2.$

(3) In (2), put $V_{n+1|n} = V_{n|n-1} = V.$

(4) Denoting the solution of (3) by V, the variance of the filter is obtained by $V' = V/(V+1)$, and

$$x_{n+1|n} = x_{n|n} = x_{n|n-1} + \frac{V}{V+1}(y_n - x_{n|n-1})$$

3. From $V_P = V$, $V_F = G = V/(V+1)$, $A = V/(V+1)/V = 1/(V+1)$ and $V_S = V_F + A^2(V_S - V_P)$, we obtain $V_S = V/(V+2)$.

τ^2	1	0.1	0.01	0.001
V_P	1.1618	0.370	0.105	0.032
V_F	0.618	0.270	0.095	0.031
V_S	0.447	0.156	0.050	0.016

Chapter 10

1. From $x_n = (y_n, y_{n-1}, \ldots, y_{n-m+1})^T$, the (i,j)-element of $Ex_nx_n^T$ is $Ey_{n-i+1}y_{n-j+1} = C_{i-j}$. Therefore, compute the autocovariance functions $C_k,\ k = 0,1,\ldots$ of the AR model of order m and construct the initial matrix by

$$V_{0|0} = \begin{bmatrix} C_0 & C_1 & \cdots & C_{m-1} \\ C_1 & C_0 & \cdots & C_{m-2} \\ \vdots & \vdots & \ddots & \vdots \\ C_{m-1} & C_{m-2} & \cdots & C_0 \end{bmatrix}.$$

2. The change in the log-likelihood for the parameter transformed by (10.9) becomes very small if the absolute value of the parameter is large, and as a result, the optimization procedure may not work at all. Therefore, it is suggested that the range of the transformed parameter be restricted to some appropriately defined interval, say $[-20, 20]$.

Chapter 11

1.(1) For $y_{n+k} = y_{n+k-1} + v_{n+k} = \cdots = y_n + v_{n+1} + \cdots + v_{n+k}$, since $Ev_{n+i} = 0$ and $Ev_{n+i}^2 = \sigma^2$, we have $y_{n+k|n} = y_n$ and $E\varepsilon_{n+k|n}^2 = k\sigma^2$.

(2) From $k\sigma^2 = 4 \times 40{,}000 = 160{,}000$, we have $\sqrt{k}\sigma = 400$. For the normal distribution, the probability of a value larger than 1σ is 0.16.

(3) The variance σ^2 of the random walk changes over time. Therefore, we may consider a model taking into account changes in volatility

$$\begin{aligned} y_n &= y_{n-1} + \sigma_n w_n, \\ \log \sigma_n^2 &= a + b \log \sigma_{n-1}^2 + v_n \quad (\text{or } \log \sigma_n^2 = \log \sigma_{n-1}^2 + v_n). \end{aligned}$$

2. We may, for example, consider a trigonometric model.
3. Omitted.

Chapter 12

1. If a characteristic root of the AR model approaches 1, discrimination between the AR model and the trend model becomes difficult. Therefore, it is recommended to apply some restriction so that the absolute value of the characteristic roots of the estimated AR model does not approach 1.
2. A seasonal component model based on a trigonometric function is obtained by $S_n = \sum_{j=1}^{6}(a_j \cos\frac{\pi jn}{6} + b_j \sin\frac{\pi jn}{6})$.

3.(1) Assuming that $\beta_{n1} = \beta_{n7}$, $\beta_{n2} = \cdots = \beta_{n6}$, we obtain a trading day effect with 2 parameters. In this case, the trading day effect is expressed by $td_n = \beta_{n1}(d'_{n1} + d'_{n7}) + \beta_{n2}(d'_{n2} + \cdots + d'_{n6})$.

(2) Assuming that $\beta_{n2} = \cdots = \beta_{n6}$, we obtain a trading day effect model with 3 parameters.

4. The holiday pattern of Easter or "Golden week" in Japan changes year by year. Therefore, it is necessary to take account of these effects carefully. The effect of a leap year may not be completely removed by the standard trading day adjustment.
5. Omitted.

Chapter 13

1. (Example.) Stock-price data
2. In a time-varying coefficient regression model $y_n = \beta_{0n} + \beta_{1n}x_{n1} + \cdots + \beta_{mn}x_{nm} + \varepsilon_n$, consider, for example, a random walk model $\beta_{jn} = \beta_{j,n-1} + v_n$ for the coefficients $\beta_{0n}, \beta_{1n}, \ldots, \beta_{mn}$. This model can be expressed as a state-space model, so as in the case of time varying coefficient AR model, the parameter can be estimated by the Kalman filter.

Chapter 14

1. Compared with the Gaussian distribution, they have characteristics that the density is concentrated in the center and at the same time, they also have heavy tails. Therefore, they are adequate for handling sudden structural changes or outliers that occur with small probability.
2. For $y \sim N(0,1)$, put $z = y^2$, $x = \log z$. Then the probability that z takes

a smaller value than t is given by

$$F(t) = \text{Prob}(y^2 < t) = \frac{2}{\sqrt{2\pi}} \int_0^{\sqrt{t}} e^{-\frac{y^2}{2}} dy.$$

Differentiating with respect to t yields

$$f(t) = \frac{dF}{dt} = \frac{1}{\sqrt{2\pi}} t^{-\frac{1}{2}} e^{-\frac{t}{2}}$$

(a χ^2 distribution with 1 degree of freedom.) From (4.51), the distribution of the log-transform $x = h(z)$ is given by

$$g(x) = \left| \frac{dh^{-1}}{dx} \right| f(e^x) = e^x \frac{1}{\sqrt{2\pi}} (e^x)^{-\frac{1}{2}} e^{-\frac{e^x}{2}} = \frac{1}{\sqrt{2\pi}} e^{\frac{x}{2} - \frac{e^x}{2}}.$$

3. In the trend model, define the distribution of the system noise by

$$p_v(x) = \begin{cases} \delta(0) & \text{with probability } 1-\alpha \\ N(0,\tau^2) & \text{with probability } \alpha \end{cases},$$

where $\delta(0)$ is the δ function with mass at $x = 0$.

Chapter 15

1. Assuming that y_n is a time series and t_n is a trend, consider the model

$$\begin{aligned} t_n &= t_{n-1} + v_n, \\ \log \sigma_n^2 &= \log \sigma_{n-1}^2 + u_n, \\ y_n &= t_n + \sigma_n w_n, \end{aligned}$$

where $u_n \sim N(0,\tau_1^2)$, $v_n \sim N(0,\tau_2^2)$, $w_n \sim N(0,1)$. Note that in this case, the observation model is nonlinear.

2. In Monte Carlo simulation, in general, we need 100 times as many particles to increase the accuracy by one digit.

3. Without any re-sampling step, the weights of many particles approach to zero and the accuracy of approximation is rapidly reduced.

4. If the number of particles is m, the number of data values is N, the dimension of the state is k and the lag is L, the fixed-interval smoother and the fixed-lag smoother need to store $m \times k \times N$ and $m \times k \times L$ data elements, respectively. Note that $N \gg L$.

Chapter 16

1. Assume that $f(x)$ is the density of a uniform distribution, $f(x) = 1$ for $0 \leq x \leq 1$, and 0 otherwise. Then since
$$g(x) = \int_{-\infty}^{\infty} f(y)f(x-y)dy = \int_{0}^{1} f(x-y)dy = \begin{cases} x & 0 \leq x \leq 1 \\ 2-x & 1 \leq x \leq 2 \\ 0 & \text{otherwise} \end{cases},$$
the density function of W is a triangle.

2. Assume that $y_0 = 1$, $v_n \equiv 0$; then $y_n = a^n$. Therefore, if we take m such that $a^m < c$ (for example, $c = 10^{-3}$), then the effect of the initial value can be ignored. For $a = 0.9, 0.5, 0.1$, m is given by 66, 10, 5, respectively.

3. Using the observed time series, construct the state vector x_n and then by using random numbers, we can generate $x_{n+1}, x_{n+2}, \ldots$. To simulate an AR model using the state given in (9.5), put $x_n = (y_n, y_{n-1}, \ldots, y_{n-m+1})^T$.

Bibliography

[1] Akaike, H. (1968), "On the use of a linear model for the identification of feedback systems", *Ann. Inst. Statist. Math.*, **20**, 425–439.

[2] Akaike, H. (1969), "Fitting autoregressive models for prediction", *Ann. Inst. Statist. Math.*, **21**, 243–247.

[3] Akaike, H. (1971), "Autoregressive model fitting for control", *Ann. Inst. Statist. Math.*, **23**, 163–180.

[4] Akaike, H. (1973), "Information theory and an extension of the maximum likelihood principle", in *Second International Symposium on Information Theory*, eds. B.N. Petrov and F. Caski, Budapest, Akademiai Kiado, 267–281.

[5] Akaike, H. (1974), "A new look at the statistical model identification", *IEEE Trans. Automat. Control*, **AC-19**, 716–723.

[6] Akaike, H. (1977), "On entropy maximization principle", in *Applications of Statistics*, P.R. Krishnaiah, ed. North Holland, The Netherlands, 27–41.

[7] Akaike, H. (1980a), "Likelihood and the Bayes procedure", in *Bayesian Statistics*, J.M. Bernardo, M.H. De Groot, D.V. Lindley and A.F.M. Smith eds., University Press, Valencia, Spain, 143–166.

[8] Akaike, H. (1980b), "Seasonal adjustment by a Bayesian modeling", *J. Time Series Analysis*, **1**, 1–13.

[9] Akaike, H. and Ishiguro, M. (1983), "Comparative study of X-11 and Bayesian procedure of seasonal adjustment," *Applied Time Series Analysis of Economic Data*, U.S. Census Bureau.

[10] Akaike, H. and Nakagawa, T. (1989), *Statistical Analysis and Control of Dynamic Systems*, Kluwer, Dordrecht.

[11] Alspach, D.L. and Sorenson, H.W. (1972), "Nonlinear Bayesian estimation using Gaussian sum approximations", *IEEE Trans, Automat. Control*, **17**, 439–447.

[12] Anderson, B.D.O. and Moore, J.B. (1979), *Optimal Filtering*, Pren-

tice Hall, New Jersey.

[13] Ansley, C.F. (1979), "An algorithm for the exact likelihood of a mixed autoregressive moving average process", *Biometrika*, **66**, 59–65.

[14] Bartlett, M.S. (1946) "On the theoretical specification and sampling properties of autocorrelated time series", *Symposium on Autocorrelation in Time Series*, 27–41.

[15] Bierman G.J. (1977), *Factorization Methods for Discrete Sequential Estimation*, Academic Press, New York.

[16] Blackman, R.B. and Tukey, J.W. (1959), *The Measurement of Power Spectra from the Viewpoint of Communications Engineering*, Dover, New York.

[17] Bloomfield, P. (1976), *Fourier Analysis of Time Series: An Introduction*, Wiley, New York.

[18] Bohlin, T., (1976), "Four cases of identification of changing systems", *System Identification: Advances and Case Studies*, Mehra, P.K. and Lainiotis, D.G., eds., 441–518, Academic Press, New York.

[19] Bolt, B.A. (1987), *Earthquakes*, W.H. Freeman, San Francisco.

[20] Box, G.E.P. and Cox, D.R. (1964), "An analysis of transformations," *J. Royal Statist. Soc.*, **IB-26**, 211–252.

[21] Box, G.E.P., Hillmer, S.C. and Tiao, G.C. (1978) "Analysis and modeling of seasonal time series", in *Seasonal Analysis of Time Seres*, ed.Zellner, A., U.S. Bureau of the Census, *Economic Research Report ER-1*, 309–334.

[22] Box, G.E.P. and Jenkins, G.M. (1970), *Time Series Analysis, Forecasting and Control*, Holden-day, San Francisco.

[23] Box, G. E. P., and Muller, M. E., (1958), "A note on the generation of random normal deviates", *Ann. Math. Statist.*, **29**, 610–611.

[24] Brillinger, D.R (1974), "Fourier analysis of stationary processes", *Proc. IEEE*, **62**, 1628–1643.

[25] Brockwell, P.J. and Davis, R.A., (1991), *Time Series: Theory and Methods*, Second Edition, Springer-Verlag, New York.

[26] Broyden, C. G. (1970), "The convergence of a class of double-rank minimization algorithms", *J. Inst. Math. Its Appl.*, **6**, 76–90

[27] Burg, J.P. (1967), "Maximum entropy spectral analysis", in *Proc. 37th Meeting of the Society of Exploration Geophysicists*,

Peprinted in Modern Spectrum Anglysis, Childers, D.G. ed., IEEE Press, New York(1978), 34–39.

[28] Carlin, B.P., Polson, N.G. and Stoffer, D.S. (1992), "A Monte Carlo approach to nonnormal and nonlinear state space modeling", *J. Amer. Statist. Assoc.*, **75**, 493–500.

[29] Carter, C.K and Kohn, R. (1993), "A comparison of Markov chain Monte Carlo sampling schemes for linear state space models", in *Proceedings American Statistical Association Business and Economic Statistics Section*, 131–136.

[30] Cleveland, W.S. and Devlin, S.J. (1980), "Calendar effects in monthly time series: Detection by spectrum analysis and graphical methods", *J. Amer. Statist. Assoc.*, **75**, 487–496.

[31] Cleveland, W.S., Devlin, S.J. and Terpenning, I. (1982), "The SABL seasonal adjustment and calendar adjustment procedures", *Time Series Analysis: Theory and Practice*, **1**, 539–564.

[32] Doucet, A., de Freitas, N. and Gordon, N. (2001), *Sequential Monte Carlo Methods in Practice*, Springer, New York.

[33] Durbin, J. and Koopman, S.J. (2001), *Time series analysis by state space methods*, Oxford University Press, New York.

[34] Fletcher, R. (1980), *Practical Methods of Optimization*, **1**: Unconstrained optimization, Wiley.

[35] Frühwirth-Schnatter, S. (1994), "Data augmentation and dynamic linear models", *J. Time Series Anal.*, 183–202.

[36] Golub, G. (1965), "Numerical methods for solving linear least-square problems", *Num. Math.*, **7**, 206–216.

[37] Good, L.J. and Gaskins, J.R. (1980), "Density estimation and bump hunting by the penalized likelihood method exemplified by scattering and meteorite data", *J. Amer. Statist. Assoc.*, **75**, 42–73.

[38] Gordon, N.J., Salmond, D.J. and Smith, A.F.M. (1993), "Novel approach to nonlinear/non-Gaussian Bayesian state estimation," *IEE Proceedings–F*, **140**, 107–113.

[39] Harrison, P.J. and Stevens, C.F. (1976), "Bayesian forecasting", (with discussion), *J. Royal Statist. Soc.*, **B 38**, 205–247.

[40] Harvey, A. (1989), *Forecasting, Structural Time Series Models and the Kalman Filter*, Cambridge University Press, Victoria, Australia.

[41] Hillmer, S.C. (1982), "Forecasting time series with trading day variation", *J. Forecasting*, **1**, 385–395.

[42] Huber, P.J. (1967), “The behavior of maximum likelihood estimates under nonstandard conditions”, in *Proc.fifth Berkeley Symp. Statist.*, 221–233.

[43] Jazwinski, A.H. (1970), *Stochastic Processes and Filtering Theory*, Academic Press, New York.

[44] Jenkins, G.M. and Watts, J.G. (1968), *Spectral Analysis and Its Applications*, Holden Day, San Franclsco.

[45] Jiang X.Q, and Kitagawa, G. (1993), “A time varying vector autoregressive modeling of nonstationary time series”, *Signal Processing*, **33**, 315–331.

[46] Jones, R.H. (1980), “Maximum likelihood fitting of ARIMA models to time series with missing observations”, *Technometrics*, **22**, 389–395.

[47] Kalman, R.E. (1960), A new approach to linear filtering and prediction problems”, *Trans. Amer. Soc. Mech. Eng., J. Basic Engineering*, **82**, 35–45.

[48] Kaminski, P.G., Bryson, A.E. and Schmidt, S.F. (1971), “Discrete square root filtering: A survey of current technique”, *IEEE Trans. Auto. Control*, **AC-16**, 727–735.

[49] Kitagawa, G. (1983), “Changing spectrum estimation”, *J. Sound and Vibration*, **89(4)**, 443–445.

[50] Kitagawa, G. (1987), “Non-Gaussian state space modeling of nonstationary time series (with discussion)”, *J. Amer. Statist. Assoc.*, **82**, 1032–1063.

[51] Kitagawa, G. (1989), “Non-Gaussian seasonal adjustment”, *Computers & Mathematics with Applications*, **18**, 503–514.

[52] Kitagawa, G. (1991), “A nonlinear smoothing method for time series analysis”, *Statistica Sinica*, **1**, 371–388.

[53] Kitagawa, G. (1993), “A Monte-Carlo filtering and smoothing method for non-Gaussian nonlinear state space models”, *Proc. 2nd U.S.-Japan Joint Seminar on Statistical Time Series Analysis*, 110–131.

[54] Kitagawa, G. (1996), “Monte Carlo filter and smoother for non-Gaussian nonlinear state space models”, *J. Comp. Graph. Statist.*, **5**, 1–25.

[55] Kitagawa, G., (1998), “A self-organizing state-space model”, *J. Amer. Statist. Assoc.*, **93**, 1203–1215.

[56] Kitagawa, G. and Akaike, H. (1978), "A procedure for the modeling of nonstationary time series", *Ann. Inst. Statist. Math.*, **30-B**, 215–363.

[57] Kitagawa, G. and Gersch, W. (1984), "A smoothness priors-state space modeling of time series with trend and seasonality", *J. Amer. Statist. Assoc.*, **79**, 378–389.

[58] Kitagawa, G. and Gersch, W. (1985), "A smoothness priors time varying AR coefficient modeling of nonstationary time series", *IEEE Trans. on Automat. Control*, **AC-30**, 48–56.

[59] Kitagawa, G. and Gersch, W. (1996), *Smoothness Priors Analysis of Time Series*, *Lecture Notes in Statistics*, **116**, Springer, New York.

[60] Knuth, D.E. (1997), *The Art of Computer Programming*, Third Edition, Addison-Wesley, Massachusetts.

[61] Kohn, R., and Ansley, C. F. (1986), "Fast filtering for seasonal moving average models", *Biometrika*, **73**, 522-524.

[62] Konishi, S. and Kitagawa, G. (2008), *Information Criteria and Statistical Modeling*, Springer, New York.

[63] Kozin, F. and F. Nakajima (1980), "The order determination problem for linear time-varying AR models", *IEEE Trans. Automat. Control*, **AC-25**, 250–257.

[64] Kullback, S. and Leibler, R.A. (1951), "On information and sufficiency", *Ann. Math. Statist.*, **22**, 79–86.

[65] Levinson, N. (1947), "The Wiener RMS error criterion in filter design and prediction", *J. Math. Phys.*, **25**, 261–278

[66] Lewis, T.G. and Payene, W.H. (1973), "Generalized feedback shift register psudorandom number algorithm", *Journal of ACM*, **20**, 456–468.

[67] Matsumoto, M. and Kurita, Y. (1994), "Twisted GFSR Generators II", *ACM Trans. Modeling and Computer Simulation*, **4(3)**, 254–266.

[68] Matsumoto, M. and Nishimura, T. (1998), "Mersenne twister: a 623-dimensionally equidistributed uniform pseudorandom number generator" *ACM Trans. Modeling and Computer Simulation*, **8**, 3–30.

[69] Meinhold, R. J., and Singpurwalla, N. D., (1989), "Introduction to Kalman filtering–A Bayesian view", in *Theory of Reliability*, Serra,

A. and Barlow, R. E., eds., 208–214.

[70] Nocedal, J., and Wright, S. J. (2006), *Numerical Optimization*, Second Edition, Springer, New York.

[71] Ozaki, T. and Tong, H. (1975), "On the fitting of nonstationary autoregressive models in time series analysis", in *Proc. 8th Hawaii Intl. Conf. on System Sciences*, 224–246.

[72] Priestley, M.B. and Subba Rao, T. (1969), "A test for nonstationarity of time-series", *J. Royal Statist. Soc.*, **B-31**, 140–149.

[73] Quenouille, M.H. (1949), "Approximate tests of correlation in time series", *J. Royal Statist. Soc.*, **B-11**, 68–84.

[74] Sage, A.P. and Melsa, J.L. (1971), *Estimation Theory with Applications to Communication and Control*, McGraw-Hill, New York.

[75] Sakamoto, T., Ishiguro M. and Kitagawa, G. (1986), *Akaike Information Criterion Statistics*, D. Reidel, Dordrecht.

[76] Schnatter, S. (1992), "Integration-based Kalman-filtering for a dynamic generalized linear trend model", *Comp. Statist. Data Analysis*, **13**, 447–459.

[77] Shibata, R. (1976), "Selection of the order of an autoregressive model by Akaike's information criterion", *Biometrika*, **63**, 117–126.

[78] Shiskin, J., Young, A.H. and Musgrave, J.C.(1976), "The X-11 variant of the Census method II seasonal adjustment program", *Technical Paper*, **15**, Bureau of the Census, U.S. Dept of Commerce.

[79] Shumway, R.H. and Stoffer, D.S. (2000), *Time Series Analysis and Its Applications*, Springer, New York.

[80] Subba Rao, T. (1970), "The fitting of non-stationary time-series models with time-dependent parameters", *J. Royal Statist. Soc.*, **B-32**, 312–322.

[81] Takanami, T. (1991), "ISM data 43-3-01: Seismograms of foreshocks of 1982 Urakawa-Oki earthquake", *Ann. Inst. Statist. Math.*, **43**, 605.

[82] Takanami, T. and Kitagawa, G. (1991), "Estimation of the arrival times of seismic waves by multivariate time series model", *Ann. Inst. Statist. Math.*, **43**, 407–433.

[83] Tanizaki, H. (1993), *Nonlinear Filters: Estimation and Applications*, Springer-Verlag, New York.

[84] Wahba, G. (1980), "Automatic smoothing of the log periodogram", *J. Amer. Statist. Assoc.*, **75**, 122–132.

[85] West, M. (1981), "Robust sequential approximate Bayesian estimation", *J. Royal Statist. Soc.*, **B, 43**, 157–166.

[86] West, M. and Harrison, P.J. (1989), *Bayesian Forecasting and Dynamic Models, Springer Series in Statistics*, Springer-Verlag, Berlin.

[87] Whittaker, E.T. and Robinson, G. (1924), *Calculus of Observations, A Treasure on Numerical Calculations*, Blackie and Son, Ltd., London, 303–306.

[88] Whittle, P. (1963), "On the fitting of multivariable autoregressions and the approximate canonical factorization of a spectral density matrix", *Biometrika*, **50**, 129–134.

[89] Whittle, P. (1965), "Recursive relations for predictors of non-stationary processes", *J. Royal Statist. Soc.*, **B 27**, 523–532.